Schweizerische Eidgenossenschaft
Confédération suisse
Confederazione Svizzera
Confederaziun svizra

Federal Department of the Environment, Transport, Energy and Communications DETEC

Swiss Federal Office of Energy SFOE
Energy Research and Cleantech Division

Final report dated 05 March 2026

HEATSTORE

De-risking and Optimization of High Temperature Aquifer Thermal Energy Storage in the Swiss Molasse Basin

---

heatstore
High Temperature Underground Thermal Energy Storage

Date: 05 March 2026

Location: Bern

Publisher:
Swiss Federal Office of Energy SFOE
Energy Research and Cleantech
CH-3003 Bern
www.bfe.admin.ch

Subsidy recipients:

Services Industriels de Genève
Chemin du Château-Bloch 21219 Le Lignon
https://ww2.sig-ge.ch/

Energie Wasser Bern (EWB)
Monbijoustrasse 11 Postfach, 3001 Bern
https://www.ewb.ch/

Université de Genève
24, Rue du Général-Dufour 1211 Genève
www.unige.ch

ETH Zürich
Institute of Geochemistry and Petrology
Clausiusstrasse 25 8092 Zürich
www.ethz.ch

University of Neuchâtel
Faubourg de l'Hôpital 41 2000 Neuchâtel
www.unine.ch

University of Bern
Hochschulstrasse 6, 3012 Bern,
www.unibe.ch

Authors:
Luca Guglielmetti, Fleury de Oliveira, Ovie Eruteya, Yasin Makhloufi, Alexandros Daniilidis, Andrea Moscariello, Lorenzo Perozzi (luca.guglielmetti@unige.ch) - UniGe
Carole Nawratil de Bono, Loïc Quiquerez, Frederic Mirjolet, Michel Meyer (carole.nawratildebono@sig-ge.ch) - SIG
Peter Meier, Dieter Ollinger, Andre El-Alfy (p.meier@geo-energie.ch) - EWB
Thomas Driesner, Julian Mindel, Daniel Birdsell, Martin Saar (thomas.driesner@erdw.ethz.ch) - ETHZ
Benoît Valley, Reza Sohrabi. (benoit.valley@unine.ch) - UniNe
Larryn Diamond, Daniela van den Heuvel, Peter Alt-Eppig, Christophe Wanner. (larryn.diamond@geo.unibe.ch) - UniBe
SFOE project coordinators:
Men Wirz, men.wirz@bfe.admin.ch
Florence Bégué, florence.begue@bfe.admin.ch
SFOE contract number: SI/501725-01

Zusammenfassung

Der Einsatz erneuerbarer Energiequellen (EE) für die Strom- und Wärmeerzeugung nimmt in Europa immer mehr zu. Die Schwankungen bei der Verfügbarkeit und Nachfrage von Energie und ihre Integration in die bestehende Energieinfrastruktur stellen jedoch eine Herausforderung dar. Peak Shaving und Wärmespeicherung können dazu beitragen, Angebot und Nachfrage auszugleichen, um die Infrastruktur und die Anlagen besser zu nutzen (z.B. Erhöhung der Vollllaststunden für geothermische Wärmequellen). Thermische Energiespeicher können beispielsweise in Form von unterirdischen Wärmespeichern (Underground Thermal Energy Storage - UTES) in Wärmenetze integriert werden, um die Nutzung von überschüssiger Wärme aus der Industrie und den Einsatz von erneuerbaren Wärmequellen zu unterstützen. UTES bietet eine intelligente und replizierbare Lösung für Regionen mit saisonalen Schwankungen und Spitzen im Wärmebedarf. UTES hat das Potenzial, eine grosse Speicherkapazität (potenziell >10 GWh) pro Standort bereitzustellen, die mit anderen Wärmespeichertechnologien nur schwer zu erreichen ist, und profitiert von einer typischerweise niedrigeren Bandbreite an Speicherkosten.

HEATSTORE ist eines von neun Projekten, die im Rahmen von GEOTHERMICA - ERA-NET im Jahr 2018 für den Zeitraum 2018-2021 finanziert wurden. Das Projekt hatte zum Ziel, die Einführung der Geothermie zu beschleunigen, indem es 1) verschiedene Arten von UTES für das Energiesystem entwickelt und integriert, 2) ein Mittel zur Maximierung der geothermischen Wärmeproduktion bereitstellt und den Business Case von geothermischen Wärmeproduktions-Doubletten optimiert, 3) technische, wirtschaftliche, ökologische, regulatorische und politische Aspekte betrachtet, die notwendig sind, um den effizienten und kostengünstigen Einsatz von UTES-Technologien in Europa zu unterstützen. Das Projekt zielte darauf ab, eine schnelle Markteinführung in Europa anzuregen, die Entwicklung von der Demonstrationsphase bis zum kommerziellen Einsatz innerhalb von 2 bis 5 Jahren zu fördern und einen Ausblick auf das Nutzungspotenzial bis 2030 und 2050 zu geben.

Dreiundzwanzig Partner aus neun Ländern bilden das europäische HEATSTORE-Konsortium, das sich aus einer Mischung aus wissenschaftlichen Forschungsinstituten und privaten Unternehmen zusammensetzt. Die Beteiligung der Industrie wird als ein starker und relevanter Vorteil angesehen, der für den Erfolg entscheidend ist. Die Kombination ausführenden europäischen Forschungsinstituten und kleinen, mittleren und grossen Industrieunternehmen ermöglichte es, Technologien zu testen und zu implementieren, um sie auf den Markt zu bringen und von den relevanten Interessengruppen zu bewerten.

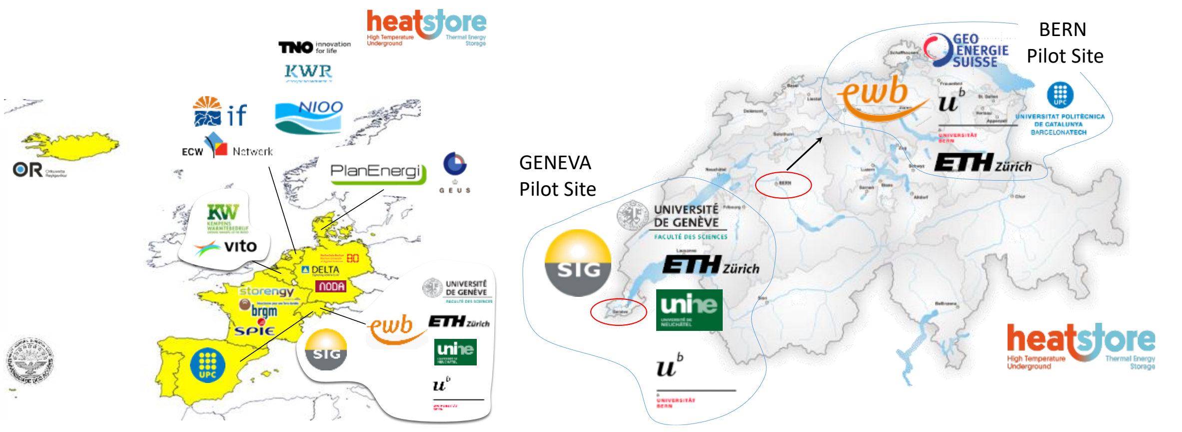

Figure I - Partner des europäischen und schweizerischen Konsortiums

Die Schweizer Partner arbeiteten an zwei Fallstudien in Genf und Bern und standen in enger Verbindung mit europäischen Partnern.

Das Schweizer HEATSTORE-Projekt hatte die folgenden Hauptziele:

- Identifizierung der Möglichkeiten für die Umsetzung der thermischen Hochtemperatur-Aquifer-Energiespeicherung (HT-ATES) in zwei der wirtschaftlichsten Reservoirs im Schweizer Molasseplateau: der känozoischen Molasse und den obermesozoischen Karbonaten
- Implementierung eines multikriteriellen Entscheidungsfindungs-Analyserahmens zur Vorhersage und Bewertung der technisch-wirtschaftlichen Machbarkeit von HT-ATES in der Schweiz
- Identifizierung von Lösungen zur Optimierung der Leistungen von HT-ATES-Technologien und deren Integration in komplexe Energiesystemkonfigurationen
- Vorhersage und Validierung der technisch-wirtschaftlichen Leistung von HT-ATES anhand von Daten, die an zwei Pilotstandorten in Genf und Bern gesammelt wurden
- Identifizierung der Umwelteinflüsse, die mit der Implementierung von HT-ATES-Systemen verbunden sind, und der zu überwindenden Hindernisse im regulatorischen Rahmen.

Diese Ziele tragen zum Endziel von HEATSTORE Switzerland bei, nämlich die kommerzielle Durchführbarkeit von HT-ATES-Technologien voranzutreiben, damit geothermische Energie in Kombination mit einer optimierten unterirdischen Wärmespeicherung ihr maximales Einsatzpotenzial im Rahmen der Schweizer Energiewende erreichen kann.

Das Schweizer Projekt konzentrierte sich auf die Bewertung der Machbarkeit von HT-ATES-Systemen an zwei Standorten in Genf und Bern. Die beiden Standorte weisen unterschiedliche Besonderheiten hinsichtlich der Untergrundbedingungen und der Konfiguration des Energiesystems auf. In Genf ist die überschüssige Wärmequelle eine Müllverbrennungsanlage mit einer Austrittstemperatur von bis zu 120˚C, der angestrebte Speichergrundwasserleiter befindet sich in den zerklüfteten mesozoischen Karbonaten zwischen 450 und 1500 m Tiefe und die Betriebstemperatur des Fernwärmenetzes liegt zwischen 70 und 120˚C. In Bern ist die überschüssige Wärmequelle ein Gaskombikraftwerk, eine Kehrichtverwertungsanlage (KVA)und ein Holzheizkraftwerk mit einer Austrittstemperatur von bis zu 120˚C und der angestrebte Speichergrundwasserleiter ist das känozoische Molassesediment. Die Betriebstemperatur des Fernwärmenetzes liegt bei 90°C.

Die Standorte Genf und Bern spiegeln die meisten der Untergrund- und Energiesystemkonfigurationen wider, die für die Speicherung thermischer Energie in Aquiferen als geeignet angesehen werden und in anderen Städten im gesamten Schweizer Mittelland zu finden sind.

Der Bericht fasst die an den Standorten Genf und Bern durchgeführten Aktivitäten sowie die Endergebnisse und daraus gezogenen Schlussfolgerungen in ihrer Gesamtheit zusammen.

Der Standort Genf

In Genf konzentrierte sich die Fallstudie auf die Machbarkeitsbewertung der Speicherung von überschüssiger Wärme, die von einer Müllverbrennungsanlage bei Temperaturen von bis zu 120˚C (Abschnitt 5.1) in den mesozoischen zerklüfteten Karbonaten in einer Tiefe zwischen 450 und 1500 m abgegeben wird. Der implementierte multikriteriellen Bewertungsrahmen basiert auf techno-ökonomischen Kriterien:

- Bewertung des technischen Potenzials der Wärmespeicherung in der Lagerstätte durch Integration von Oberflächen- und Untergrunddaten
- Identifikation der Umweltauswirkungen, die mit der Speicherung und Produktion verbunden sind
- Bewertung des Zusammenhangs zwischen Speicher-/Rückgewinnungsleistung und wirtschaftlicher Leistung bei verschiedenen technischen Konfigurationen

Der auf einem schrittweisen Ansatz basierende Rahmen kombinierte zunächst die Einschränkungen des Untergrunds und des Energiesystems anhand der zu Beginn des Projekts verfügbaren Daten. Da im Laufe des Projekts neue Daten und Ergebnisse zur Verfügung standen, wurde es schliesslich anhand der Daten kalibriert und validiert, die sich aus der Erkundung des Untergrunds durch die Bohrungen GEo-01 und GEo-02 sowie aus den Entwicklungsszenarien für das Energiesystem 2035 ergaben.

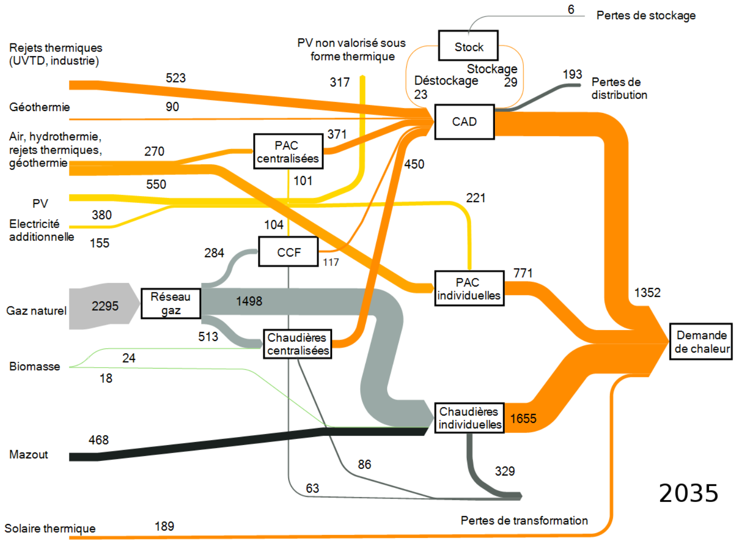

Figure II - Energiesystem in Genf, Szenario 2035

Beide Bohrungen zielten auf die oberen mesozoischen Kalksteine. Die Bohrergebnisse trugen zum Verständnis der Lagerstättenarchitektur und der Verteilung der petrophysikalischen/hydraulischen Eigenschaften bei und verdeutlichten die stark heterogenen hydraulischen Eigenschaften der mesozoischen Karbonate im gesamten Genfer Gebiet. GEo-01, 744 m tief, liefert 34˚C Wasser bei 55 l/s und 8-10 bar Bohrlochdruck, während GEo-02 18˚C Bohrlochtemperatur (~55˚C Temperatur im Bohrloch) bei 0,3 l/s und 10-12 bar Bohrlochdruck liefert.

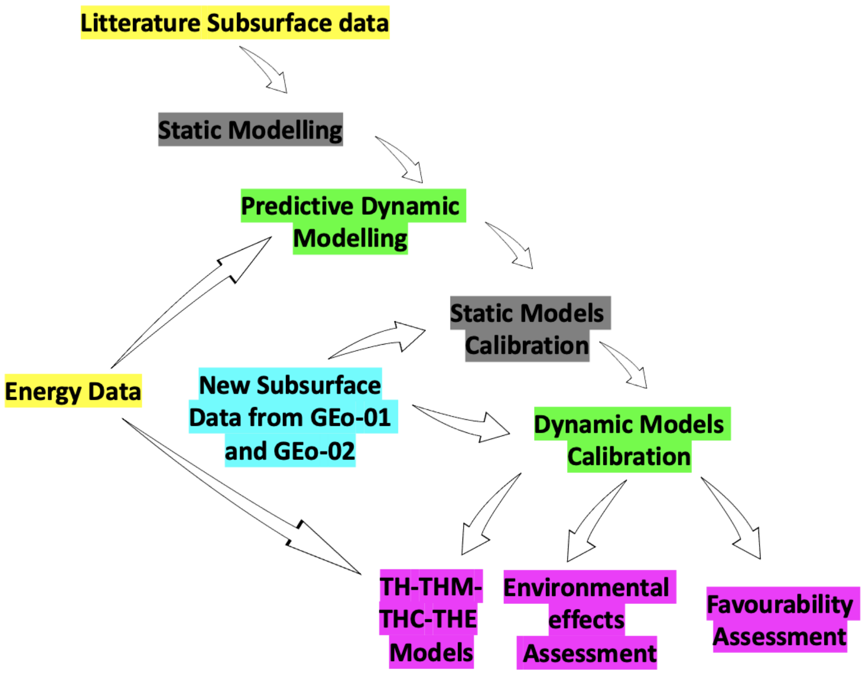

Figure III - Arbeitsablauf des HEATSTORE-Projekts für den Standort Genf

Für die Charakterisierung des Untergrunds wurden ausgehend von statischen Modellen eine Reihe von 3D-Modellen erstellt, die es ermöglichten, die Geometrie und die Verteilung der petrophysikalischen und hydraulischen Eigenschaften der untersuchten Lagerstätten zu erfassen (siehe vollständiger Bericht in den Abschnitten 5.1.2, 5.1.3, 5.1.6). In die berechneten Modelle wurden die verfügbaren geophysikalischen und petrophysikalischen Daten aus den verschiedenen Phasen des Projekts integriert. Der Gesamtansatz basiert auf der Grundlage, dass statische 3D-Modelle in Verbindung mit Informationen über das Energiesystem als Input für die Erstellung dynamischer Modelle (thermohydraulische TH, thermohydraulisch-mechanische THM oder HM, thermohydraulisch-chemische THC und thermohydraulisch-ökonomische THE) dienen, um die Leistung der HT-ATES-Systeme in Genf vorherzusagen. Die Ergebnisse für die statische Modellierung stammen aus der Interpretation mehrerer alter seismischer 2D-Reflexionsdatensätze, Bohrlochprotokolle von GEo-01 und GEo-02, Bohrlochberichten und Aufschlüssen. Die seismische Interpretation zeigt eine gut entwickelte Blumenstruktur, die die mesozoischen und Teile der känozoischen Sedimente im GEo-01-Gebiet deformiert. Die unterirdische strukturelle Situation um den Standort GEo-02 ist anders und umfasst ein System von Überschiebungsstörungen und damit verbundenen normalen Störungen, die die känozoischen und mesozoischen Sedimente deformieren. Die petrophysikalischen Analyse deutet darauf hin, dass die untere Kreideformation im GEo-01-Gebiet dicht ist und sich im Allgemeinen durch niedrige Porositäts- und Permeabilitätswerte auszeichnet. Das Vorhandensein von Bruchnetzen und Verwerfungen, die einen wesentlichen Teil dieser Einheit deformieren, könnte jedoch eine lokale Flüssigkeitszirkulation begünstigen. Im Gebiet GEo-02 deuten die Ergebnisse von Bohrlochtests darauf hin, dass die Formationen innerhalb der mesozoischen Abfolge einen geringen Flüssigkeitsfluss und schwache hydraulische Eigenschaften aufweisen.

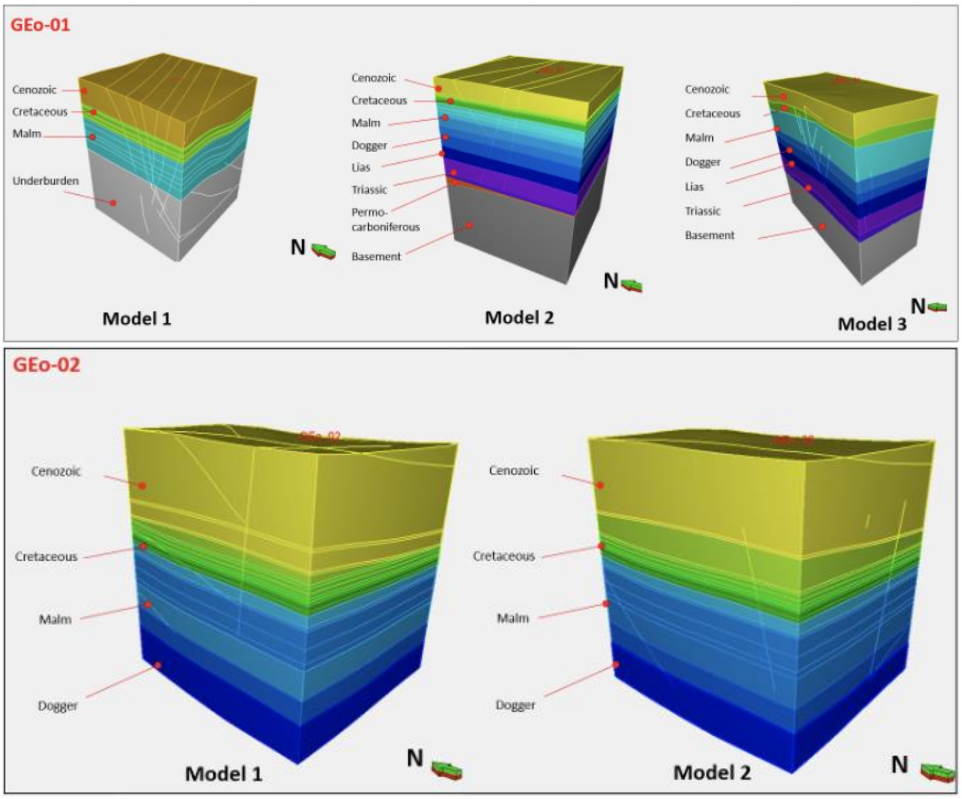

Figure IV- Statische 3D-Modelle für die Gebiete GEo-01 und GEo-02

Anschliessend wurden dynamische thermohydraulische (TH) und hydro-mechanische (HM) Modelle entwickelt, die statische Modelle mit Energiesystemdaten (z.B. Wärmeüberschusstemperatur, Rückgewinnungstemperatur, Nutzung von Wärmepumpen, Wärmeüberschuss und zeitliche Verteilung des Wärmebedarfs) kombinierten, um HT-ATES Betriebsszenarien zu erstellen (siehe Abschnitt 5.1.7). Zunächst basierten alle Modelle auf verfügbaren Literaturdaten, ermöglichten die Einrichtung des gesamten Modellierungsworkflows "von statisch bis dynamisch" und lieferten die erste Reihe von Vorhersagen für das Verhalten des HT-ATES-Systems. Nach der Verfügbarkeit neuer Daten aus den beiden Explorationsbohrungen wurden diese Modelle kalibriert und validiert, um eine Reihe zuverlässigerer und realistischerer Szenarien zu erstellen, die die Vorhersage des Flüssigkeitsstroms in der Lagerstätte und die Quantifizierung der potenziellen bodenmechanischen Auswirkungen (Bodenverformung) aufgrund des Betriebs umfassen. Für die TH-Modelle wurde ein numerischer Diskretisierungsansatz (z.B. Finite Elemente, Finite Volumens) verwendet, um einen Lösungsalgorithmus zu erstellen, der die notwendige diskrete Lösung für unsere Simulationen liefert. Das konzeptionelle Modell befasste sich mit Szenarien von Interesse, die mit den lokalen geologischen und hydrologischen Bedingungen zusammenhängen. Diese Szenarien beinhalten die Modellierung des Einflusses des Grundwasserflusses und der geologischen Heterogenität (d.h. Vorhandensein von Brüchen und Verwerfungen, Riffstrukturen) auf die Speicher- und Gewinnungsmöglichkeiten des Systems.

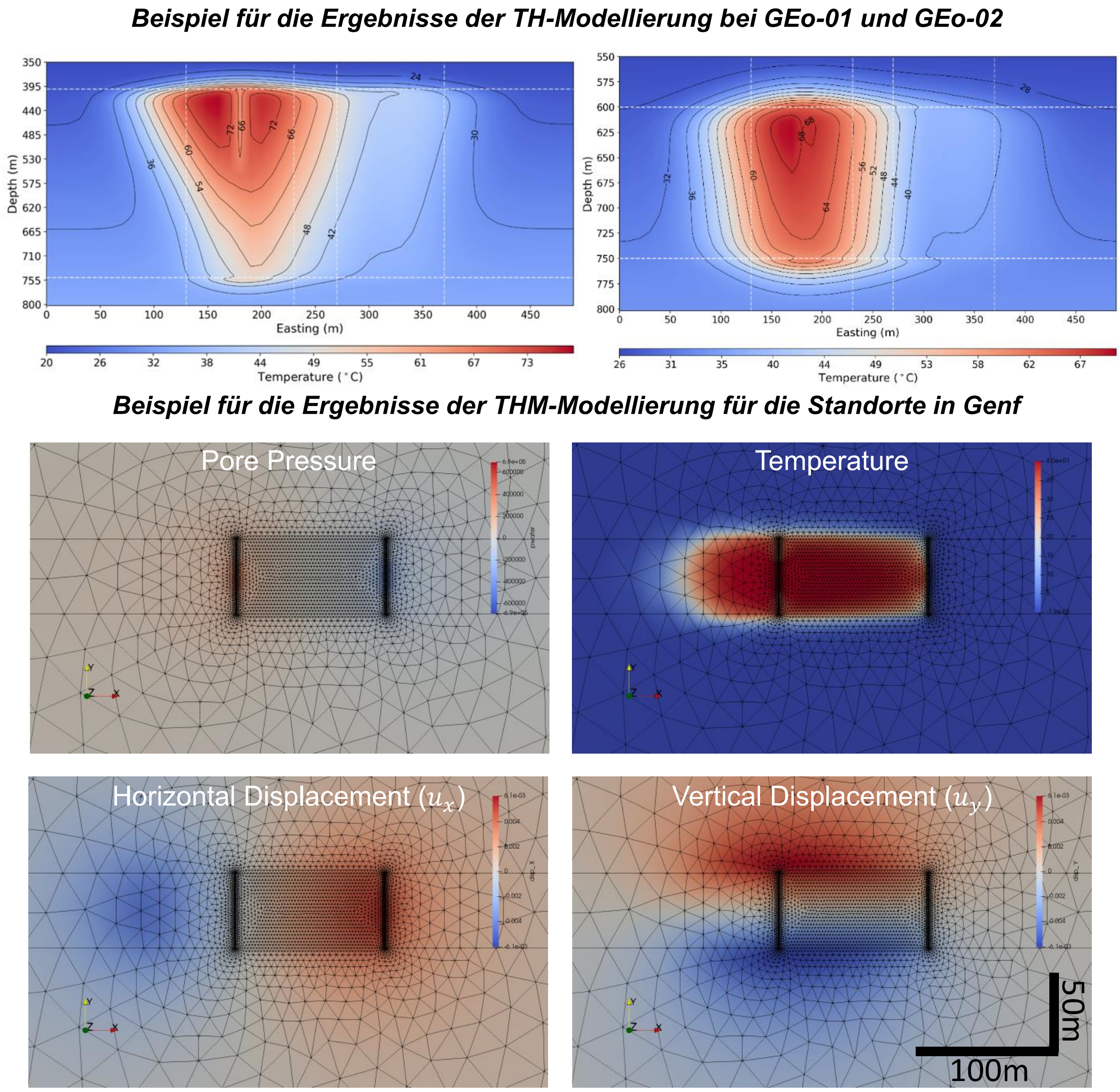

Figure V- Beispiele für Ergebnisse der TH- und THM-Modellierung für den Raum Genf

Geochemische Untersuchungen wurden durchgeführt, um die potenzielle Aktivierung von Wasser-Gestein-Wechselwirkungsmechanismen zu bewerten, die die Eigenschaften der Lagerstätte durch die Auflösung und Ausfällung von Mineralien in den Lagerstätten und das Korrosions-/Kalkungspotenzial an der Oberflächenausrüstung beeinflussen können (siehe Abschnitte 5.1.8 5.1.9.3 und Anhang 7 für einen detaillierten Bericht). Es wurden Wasserproben aus den Lagerstätten entnommen, deren chemische Zusammensetzung analysiert und mit den Ergebnissen der mineralogischen Analyse von Bohrlochabschnitten und Bohrkernen kombiniert. Zusätzlich führten die Projektpartner Laborexperimente und kinetische Modellierungen durch, um die HT-ATES-Bedingungen und die chemischen Auswirkungen auf das Lagerstättenwasser während des HT-ATES-Betriebs zu reproduzieren. Die Ergebnisse zeigen, dass es während des Betriebs zur Auflösung von Karbonat Mineralien und zu Ausfällungen kommen kann. Das Risiko von Ausfällungen in Sektoren des Reservoirs kann zu einer Kompartimentierung führen, die die Leistung der Speichersysteme verringert. Die Schwebstoffbelastung durch GEo-01 wurde ebenfalls analysiert. Dabei zeigte sich, dass eine Kombination aus Sulfatmineralien und einer mikrobiellen Gemeinschaft, insbesondere

Methanobakterien, eine wesentliche Klasse in den Proben bildet. Ausgehend von den Ergebnissen dieser Studie können die folgenden Hauptauswirkungen während des langfristigen Betriebs auftreten:

- Aufgrund ihrer retrograden Löslichkeit (d.h. abnehmende Löslichkeit bei steigender Temperatur) werden Karbonate wie Kalzit wahrscheinlich ausfallen, wenn sich das Wasser während der Lagerungszyklen auf 90°C erhitzt. Die Ausfällung von Karbonat Mineralien könnte den Fluss und den Wärmeaustausch in den Oberflächenanlagen behindern.
- Im Falle des aus GEo-01 geförderten Wassers kann es aufgrund der hohen Sulfid Konzentration zu Korrosion an technischen Anlagen wie Pumpen, Gehäusen und Wärmetauschern kommen. Dies könnte zu Materialversagen und Betriebsproblemen führen.

Um Alternativen für die wirtschaftliche Tragfähigkeit von HT-ATES-Systemen in Genf zu bewerten, haben wir die Ergebnisse der Modellierung mit Daten aus dem Energiesystem kombiniert, um die Speicherszenarien zu bewerten, die für einen technisch-wirtschaftlichen Erfolg relevant(?) sind. Die Ergebnisse zeigen, dass die Nennkapazität je nach Untergrundbeschränkungen zwischen 0,4 MW und 81 MW liegt, wobei die Durchlässigkeit und die Mächtigkeit des Aquifers die wichtigsten Steuerungsvariablen sind. Eine Mindesttransmissivität von 2,5 $\times 10^{-12}$ m^3 ist erforderlich, um die Wärmegestehungskosten (LCOH) unter 200 CHF/MWh zu halten, und eine Kapazität von 25 MW oder mehr ist erforderlich, damit das HT-ATES-System mit anderen grosstechnischen DHN-Wärmequellen konkurrenzfähig wird. Die Kapazität erhöht sich durch die Hinzunahme von Wärmepumpen (HP), die nicht Investitionskosten verursachen und die LCOH erhöhen. Nichtsdestotrotz erhöht die Hinzufügung von Wärmepumpen die Nennkapazität des Systems und führt zu höheren kumulierten vermiedenen CO_2-Emissionen.

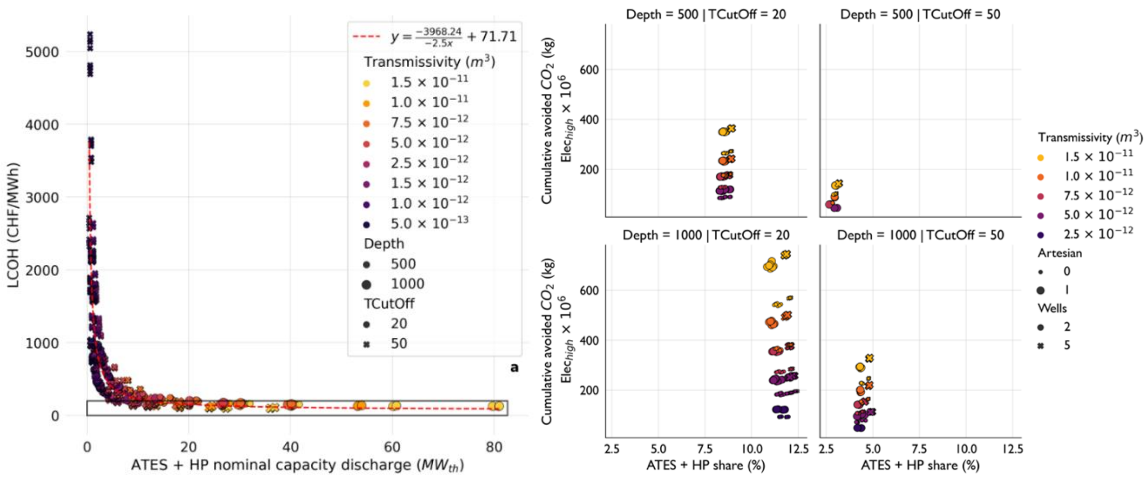

Figure VI: Links: LCOH im Vergleich zur nominalen Produktionskapazität, eingefärbt nach der Transmissivität des Reservoirs, sortiert nach Tiefe und Temperaturgrenzwert Rechts: ATES-Anteil und kumulierte vermiedene CO2-Emissionen für die Simulationen mit einem LCOH unter 200 CHF/MWh

Eine Schnellbewertung der Umweltauswirkungen (Anhang 18) ermöglichte die Identifizierung der Umweltauswirkungen im Zusammenhang mit den Bohrphasen und den HT-ATES-Operationen an den Bohrlöchern GEo-01 und GEo-02. Die Auswirkungen während der Bohrungen wurden anhand der von SIG vor, während und nach den Bohrarbeiten durchgeführten Aktivitäten ermittelt und bewertet. Im Gegensatz dazu wurden die mit den HT-ATES-Operationen verbundenen Auswirkungen durch Datenerfassung, prädiktive Modellierung und Überwachung identifiziert und bewertet. Die Ergebnisse zeigen, dass die Risiken im Zusammenhang mit den Bohrarbeiten gering, bis mittel und zeitlich begrenzt sind. Hohe Risiken, während der HT-ATES-Operationen sind nur mit den Schwankungen der Wasserzusammensetzung des Reservoirs verbunden, ohne dass die oberflächlichen Süssgewässer betroffen sind. Die Einführung von HT-ATES wird die Kohlenstoffintensität des Heizungssektors reduzieren.

GEo-01

Effect \ Phase	Drilling						Operations (predicted)					
	P	A	M	Probability	Consequences	Risk	P	A	M	Probability	Consequences	Risk
Air quality				H	L	M				L	L	L
Noise and vibration				H	L	M				M	L	L
Formation water quality				L	L	L				H	M	H
Formation water temperature										H	L	M
Surface clear water				H	L	M				L	L	L
Soil occupation				H	L	M				H	L	M
Wastes and dangerous substances				H	L	M				M	L	L
Environment				M	L	L				L	L	L
Nature				M	L	L				L	L	L
Soil mechanics										L	L	L
Seismicity				L	H	M				L	H	M
CO2 intensity redyction										H	M	H

GEo-02

Effect \ Phase	Drilling						Operations (predicted)					
	P	A	M	Probability	Consequences	Risk	P	A	M	Probability	Consequences	Risk
Air quality				H	L	M				L	L	L
Noise and vibration				H	L	M				M	L	L
Formation water quality				L	L	L				H	M	H
Formation water temperature										H	L	M
Surface clear water				H	L	M				L	L	L
Soil occupation				H	L	M				H	L	M
Wastes and dangerous substances				H	L	M				M	L	L
Environment				M	L	L				L	L	L
Nature				M	L	L				L	L	L
Soil mechanics										L	L	M
Seismicity				L	H	M				L	H	M
CO2 intensity redyction										H	M	H

Figure VII - Risikobewertung für HT-ATES in Genf im Schnellverfahren

Die schwierigen Untergrundbedingungen für das gewählte Speichersystem in Genf liessen die Durchführung von Injektions-/Rückgewinnungstests bei GEo-01 und GEo-02 nicht zu. Daher wurde ein Feldlabor in Concise (VD) eingerichtet, um zu demonstrieren, ob Wärmespeicherung und -rückgewinnung eine Option für geklüftete Karbonate sein kann (Abschnitt 5.1.5). Drei Bohrungen in 50 m Tiefe erreichten dieselben obermesozoischen Karbonate, die von GEo-01 und GEo-02 erbohrt wurden, und es wurden hydrogeologische, hadrochemische, petrophysikalische, Bohrlochmessungen und thermohydraulische Tests durchgeführt, um die Speicherleistung des untersuchten Reservoirs zu bewerten. Die Entwicklung des Concise-Testgeländes ermöglichte die Anwendung von Methoden zur hydraulischen und thermohydraulischen Charakterisierung von Karst- und geklüfteten Reservoiren, wobei Feldversuche und Modellierung kombiniert wurden.

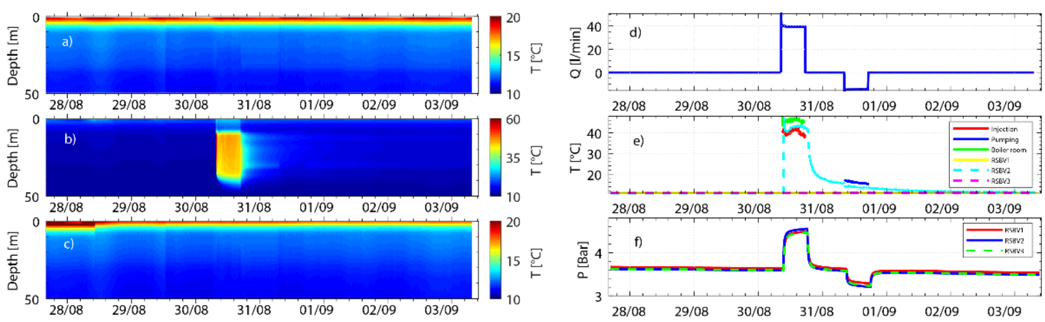

Figure VIII - Temperaturschwankungen, die an den Concise-Bohrungen während der thermohydraulischen Feldtests gemessen wurden, als Funktion der Durchflussraten, der Einspritztemperatur, der Pumptemperatur und des Drucks

Diese Ergebnisse verdeutlichen, wie wichtig die explizite Berücksichtigung der Reservoirstrukturen ist, um robuste thermohydraulische Reaktionen zu erhalten, und bilden die Grundlage für Empfehlungen für die Entwicklung und Charakterisierung von Tiefenwärmespeichern.

Der Standort Bern

In Bern wurden die Möglichkeiten zur Speicherung der überschüssigen Wärme aus der Kehrichtverwertungsanlage (KVA) Forsthaus bis in maximal 500 m Tiefe geplant und getestet (Abschnitt 5.2). Der Standort Bern diente dabei als Pilotanlage in einem typischen Molasse-Sandsteinreservoir („Rinnengürtelsandsteine“ der Unteren Süsswassermolasse), um die Optionen und Eigenschaften eines geothermischen Speichers in diesen - im Schweizer Mittelland weit verbreiteten - Gesteinseinheiten unter realen Bedingungen erstmals zu testen und zu optimieren.

Ziel des Projekts war es, die Machbarkeit und Optionen zur Risikoreduktion für die Nutzung eines Molasse-Sandsteinreservoirs zu untersuchen. Hierfür wurden drei Bohrungen in unmittelbarer Nähe des Kraftwerks erstellt und die Testversuche im Reservoir überwacht. Die Ergebnisse dienen ewb dazu, die für die endgültige Planung notwendigen Informationen zu den Eigenschaften der Rinnengürtel-Sandsteine zu gewinnen und – je nach Ergebnis - nach Projektabschluss den HT-ATES vollständig umzusetzen.

Der konzeptionelle Plan sah vor, saisonal heisses Wasser aus der Anlage einzuspeisen und dann die gespeicherte Wärmeenergie bei erhöhtem Bedarf im Winter wiederzugewinnen und in das Fernwärmenetz einzuspeisen, ohne dass eine Wärmepumpe benötigt wird. Die Einspeisung von heissem Wasser erfolgte über ca. 200 Tage durch den Hauptbrunnen in der Mitte des Systems. Während des Entladezyklus wurde derselbe zentrale Brunnen für die Produktion von warmem Wasser verwendet. Das gleichzeitige Pumpen aus/in die Nebenbrunnen diente dazu, den Durchfluss an den Systemgrenzen zu regulieren und so den Druck im Reservoir während der Injektion und Produktion auszugleichen. Für das angedachte HT-ATES System Geospeicher Forsthaus wurde eine Lebensdauer von 20 Jahren angenommen.

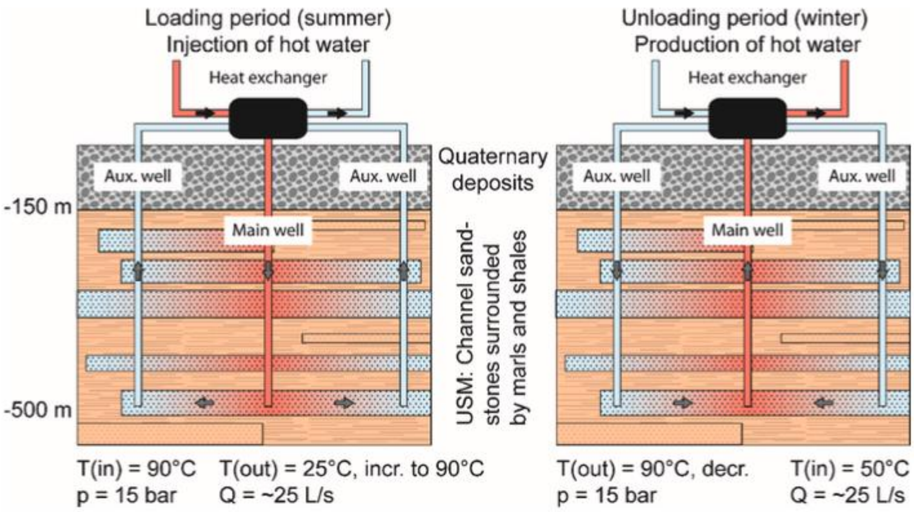

Figure IX – Schematische Darstellung des Betriebskonzepts und der geplanten Betriebsparameter des HT-ATES Pilotprojekts Geospeicher Forsthaus

Es wurden vorab geologische und geochemische Untersuchungen durchgeführt, die potenzielle Ziele in der Unteren Süsswassermolasse in der Abfolge der übereinanderliegenden mittel-bis grobkörnigen Sandsteine der Rinnengürtel aufzeigten. Dabei handelt es sich um die klassischen Sedimente, die sich im zentralen Abschnitt der Rinnengürtel ablagern und kohärente, homogene Sandsteinkörper von mehreren Kilometern Länge, 150-1'500 m Breite und 2-15 m Mächtigkeit bilden können.

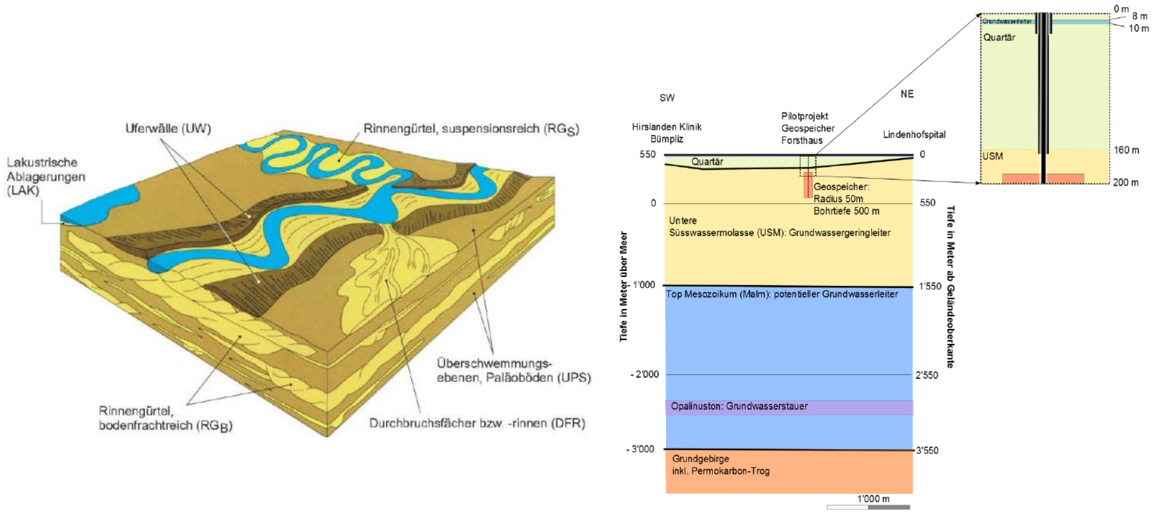

Figure X – Links: Karikatur, die die verschiedenen Fazies für die USM zeigt; Rechts: Geologischer Querschnitt in den tieferen Untergrund des geplanten geologischen Speichers

Diese im Idealfall sehr durchlässigen Sandsteinkörper der Rinnengürtelwechsellagern mit schlecht durchlässigen, feinkörnigen Sedimenten (Figure X). Dadurch ergibt sich eine sehr gute hydraulische Abdichtung der Rinnengürteleinheiten; eine der Grundvoraussetzungen für einen thermischen Speicher. Das eingespeicherte Heisswasser kann damit nicht aus den Sandsteinschichten abfliessen. Da keine standortspezifischen geologischen Daten vorlagen, war es zu Beginn des Projekts nicht möglich, das Speichervolumen und die Tiefe, die Petrophysik und die hydraulischen Eigenschaften sowie das hydrogeologische Regime im Untersuchungsgebiet genau zu bewerten. Die wichtigsten Unbekannten waren:

- Vorhandensein oder Fehlen der Rinnengürtel-Sandsteine in einem bestimmten vertikalen Abschnitt der USM
- 3D-Geometrien und Abmessungen der Rinnengürtel-Sandsteine
- Porosität, Durchlässigkeit, Mineralgehalt und Grad der Calcit-Zementierung in den Rinnengürtel-Sandsteinen
- das Ausmass, in dem einzelne Sandsteinschichten hydraulisch miteinander verbunden sind (im Gegensatz zu einer hydraulischen Abtrennung durch dazwischen liegende Schluff- und Tonsteine);
- Geschwindigkeit und Richtung des Grundwasserflusses sowie Grundwassereigenschaften: Salzgehalt, Zusammensetzung der gelösten Stoffe (insbesondere pCO_2) und mikrobielle Aktivität
- Konzentrationen der korrosionsfördernden Komponenten H_2S, SO_4, Cl und Mikroben im Grundwasser

Es wurden vorab Laborexperimente zu geochemischen Wasser-Gestein-Wechselwirkungen und THC-Modellierungen durchgeführt (Anhang 08).

Es wurden nacheinander drei Bohrlöcher von demselben Bohrkeller aus gebohrt. Der Bohrstart mit der Bohranlage „Marriott Rig 18“ erfolgte am 21. Oktober 2022. Das dritte Bohrloch wurde am 1. April 2023 erfolgreich abgeschlossen.

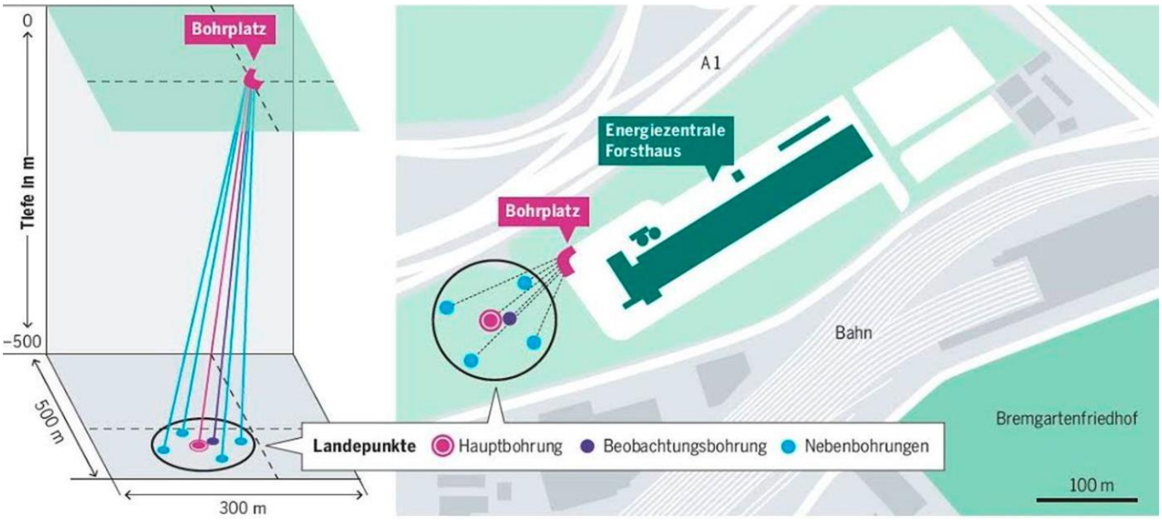

Figure XI - Skizze der 6 geplanten Bohrungen für das Pilotprojekt Geospeicher Forsthaus

Die Bohrungen des Projekts zeigten, dass am Standort eine rund 240 m mächtige quartäre Sedimentbedeckung vorliegt, die damit etwa 80 m mächtiger ist als vor den Bohrungen angenommen. Darunter wurden bis in eine Tiefe von etwa 520 m rund 280 m Sedimente der Unteren Süsswassermolasse (USM) erschlossen. Diese Sedimente dokumentieren ein heterogenes, ehemals mäandrierendes fluviatiles Ablagerungssystem im alpinen Vorland, bestehend aus Sandsteinen, Siltsteinen, Überflutungsablagerungen und Paläoböden. Innerhalb der USM wurden mehrere lateral zusammenhängende Sandsteinintervalle identifiziert, die als potenzielle Reservoirhorizonte für die Wärmespeicherung gelten. Die Sandsteine weisen grundsätzlich geeignete Porositäts- und Permeabilitätseigenschaften auf, auch wenn ihre Durchlässigkeit lokal durch Kalzitzementation reduziert sein kann.

Im Vergleich zu anderen Standorten im zentralen Molassebecken zeigen die Forsthaus-Bohrungen ähnliche sedimentologische und petrophysikalische Eigenschaften, wobei die Durchlässigkeiten teilweise etwas geringer ausfallen.

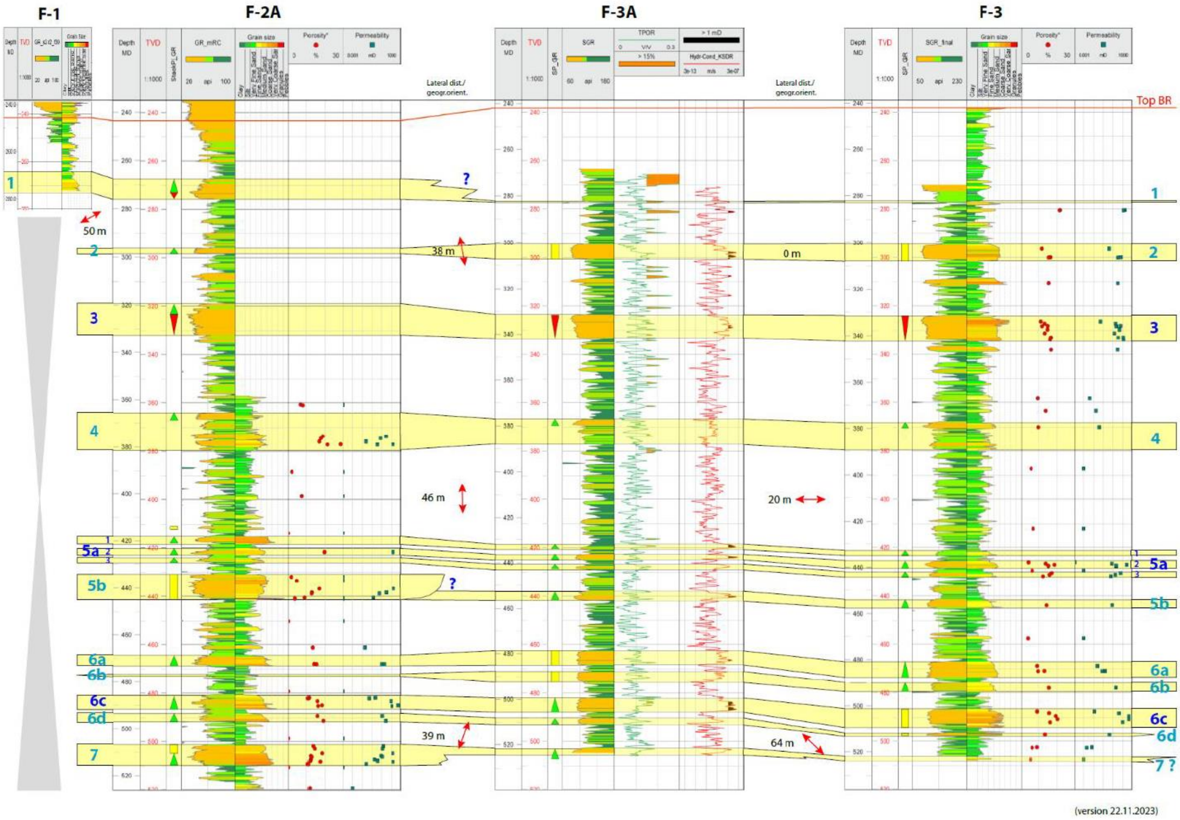

Figure XII - Korrelation der wichtigsten Lagerstätteneinheiten in der untersuchten USM auf der Grundlage von Gammastrahlenmessungen und Korngrössenprofilen.

Für die Anbindung der Bohrungen an das Reservoir und dessen Erschliessung wurde eine repräsentative Sandsteinlage im unteren Abschnitt der Bohrungen ausgewählt. Dadurch sollte sichergestellt werden, dass bei technischen Problemen ohne grössere Schwierigkeiten auf eine höher gelegene Sandsteinlage ausgewichen werden kann. Die Wahl fiel auf die Lage 6c in einer Tiefe von 485 m, da sie unter anderem eine gute horizontale Kontinuität und eine mittlere hydraulische Durchlässigkeit aufweist.

Zunächst wurde die zementierte Verrohrung in der Bohrung F2 mithilfe von Mikro-Sidetracks aufgebohrt, die horizontal bis zu 5 m tief in die Sandsteinlage gebohrt wurden. Dabei musste vermieden werden, dass das Glasfaserkabel beschädigt wird, das entlang der Verrohrung zwischen Casing und Formation einzementiert ist. Nach jedem neuen Mikro-Sidetrack wurde die Injektivität getestet. Anschliessend wurde ein Doppelpackersystem in F2 installiert, um das Testvolumen möglichst gering zu halten und die Mikro-Sidetracks vom übrigen Bohrlochvolumen zu isolieren.

Nach der Installation konnte der Druck in der Sandsteinlage 6c vor und während des Bohrens der Mikro-Sidetracks in Bohrung F3 beobachtet werden. Zunächst fiel der Druck ab, bevor der erste Mikro-Sidetrack in F3 gebohrt und über diesen etwa eine Woche lang Hydrantenwasser mit konstanter Rate injiziert wurde. Durch die Injektion in F3 stieg der Druck in F2 langsam an. Die Auswertung der Druckanstiegskurve ermöglichte es, die hydraulische Verbindung zwischen den beiden Bohrlöchern zu bewerten, repräsentative Werte für die Durchlässigkeit abzuleiten und das Strömungsverhalten zu analysieren. Nachdem alle Mikro-Sidetracks in F3 gebohrt worden waren, wurde ein zweites Doppelpackersystem installiert. Anschliessend wurden in beiden Bohrlöchern Druckstufentests, auch bekannt als „hydraulic jacking tests“, durchgeführt. Bei einem Injektionsdruck oberhalb der vertikalen Gesteinsspannung öffneten sich horizontale, durchlässige Bereiche innerhalb der Sandsteinschichten. Sobald dieser Druck erreicht war, konnte die Injektion mit überproportionalen Injektionsraten durchgeführt werden. Der Datensatz, bestehend aus Drücken im Injektionsbohrloch und im Beobachtungsbohrloch sowie Dehnungsmessungen am Glasfaserkabel entlang der Verrohrung in F2, liess wesentliche Rückschlüsse auf das hydrogeomechanische Verhalten der Sandsteinschicht zu.

Es konnte zudem festgestellt werden, dass sich die Durchlässigkeit der Sandsteinschicht dauerhaft um den Faktor 2 erhöht hat. Diese Erhöhung reichte jedoch nicht aus, um den wirtschaftlichen Betrieb einer Wärmespeicheranlage zu ermöglichen. Während der Druckstufentests wurde die Mikroseismizität mit einem vorübergehend an der Oberfläche installierten Seismometer überwacht, und mögliche Hebungen und Setzungen wurden mit dem permanenten Überwachungssystem erfasst.

Trotz der geringen Transmissivität konnte zwischen den Bohrungen ein Dipol-Strömungsfeld aufgebaut und über mehr als zwei Monate aufrechterhalten werden. Dazu wurde Hydrantenwasser mit einer Rate von 8 l/min in F3 injiziert, während in F2 2 l/min frei ausliefen. Es konnten hydrogeochemische Parameter online gemessen und Wasserproben für Laboranalysen an der Universität Bern entnommen werden.

Nachdem die, während der Bohrung eingebrachte Bohrspülung vollständig aus der Formation gefördert wurde, wurde natürliches Formationswasser nachgewiesen. Nach etwa zwei Monaten wurde erstmals die chemische Signatur des in F3 injizierten Hydrantenwassers festgestellt. Der Langzeit-Zirkulationstest konnte daher auch als Tracertest ausgewertet werden. Noch bevor das Hydrantenwasser geringfügig durchbrach, führte die Firma Hydroisotop eine Wasserprobenahme für eine ^{81}Kr-Analyse durch, um ein Modellalter des Formationswassers zu bestimmen.

Nach Abschluss der hydrogeochemischen Charakterisierung wurde ein Experiment begonnen, bei dem die durchlässigsten Strömungspfade mithilfe von in Wasser gelöstem CO_2 angesäuert werden sollten, um die Transmissivität zu erhöhen. Über mehrere Wochen wurden bei geschlossener Bohrung F2 rund 5,5 t CO_2 in F3 injiziert. Anschliessend wurde das gelöste Kalzit durch Injektion von Hydrantenwasser in F2 ausgespült. Das in F3 austretende Wasser wurde in regelmässigen Abständen von der Universität Bern beprobt.

Nachdem bis Ende 2024 der Grossteil des Kalzits ausgetragen worden war, wurden nochmals hydraulische Tests durchgeführt, um die Veränderung der Transmissivität zu bestimmen. Der umfangreiche hydrogeochemische Datensatz wurde von der Universität Bern mithilfe eines numerischen hydrogeochemisch-hydraulischen Modells ausgewertet. Das aufwendig kalibrierte Modell stimmt konzeptionell gut mit den bisher erhobenen Daten zur Sandsteinlage sowie zur Geometrie der Reservoiranbindung an die Mikro-Sidetracks überein.

Die Untersuchungen, die während des Projekts durchgeführt wurden, zeigen, dass grundsätzlich die Voraussetzungen für ein geothermisches Speichersystem im Forsthaus Bern grösstenteils erfüllt werden. Jedoch stellt die unzureichende Durchlässigkeit das grösste Hindernis für einen wirtschaftlichen Betrieb eines Speichers dar.

Räumliche multikriteriellen Analyse der HT-ATES-Günstigkeit in der Schweiz

Da es sich um ein mehrdimensionales Konzept handelt, basierte die in HEATSTORE durchgeführte Bewertung der Günstigkeit von HT-ATES auf der Aggregation einer Reihe von techno-ökonomischen Kriterien mittels räumlicher Multikriterienanalyse (SMCA). Die techno-ökonomischen Leistungen von HT-ATES sind jedoch durch geologische (Play-Elemente) und geografische Merkmale gekennzeichnet, die im gesamten Schweizer Mittelland unterschiedlich sind. Der Fokus auf das Schweizer Mittelland wurde durch die Verfügbarkeit öffentlicher Daten und die Tatsache, dass sich der Grossteil des Wärmeüberschusses und des Wärmebedarfs in dieser Region konzentriert, bestimmt. Die im Rahmen dieser Aufgabe durchgeführten Arbeiten umfassen die Implementierung eines räumlichen multikriteriellen Play-Fairway-Rahmens, der sich auf das Potenzial der Implementierung von HT-ATES-Systemen in zwei geologischen Haupteinheiten konzentriert: die känozoischen Sedimente (d.h. das Ziel des Berner Projekts) und die geklüfteten obermesozoischen Karbonate (d.h. das Ziel des Genfer Projekts). Zu den unterirdischen Daten gehören die Geometrie der geologischen Zieleinheiten in einer Tiefe von bis zu 2000 Metern, ihre Dichte, Porosität, Permeabilität, Verwerfungen und regionalen Spannungen. Oberflächliche Randbedingungen, einschliesslich der geografischen Verteilung von Wärmeüberschuss, Wärmebedarf, Fernwärmenetzen und Müllverbrennungsanlagen, wurden in den Analyserahmen einbezogen, um Karten zu erstellen, die verschiedene HT-ATES-Günstigkeitsszenarien darstellen. In dieser Phase wurde bei den wirtschaftlichen Zwängen das Konzept der minimalen, wirtschaftlich vertretbaren Transmissivität des Zielreservoirs berücksichtigt, wobei der auf 5x10-13m3 festgelegte Schwellenwert dazu beitrug, die günstigsten Gebiete zu identifizieren.

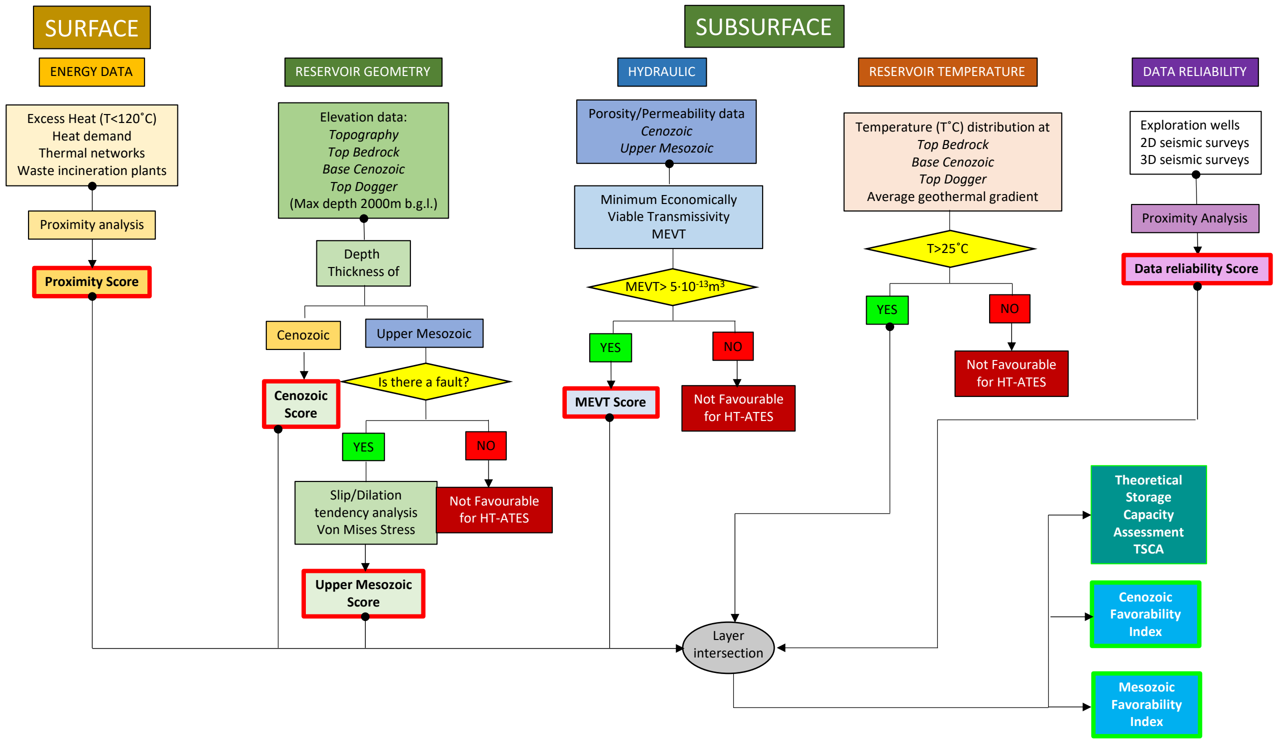

Figure XIII – Rahmen für HT-ATES SMCA in der Schweiz implementiert

Die Ergebnisse zeigen, dass das Känozoikum in den zentralen und südlichen Teilen des Molasseplateau, wo sich einige Grossstädte befinden (Zürich, Bern, Lausanne), ein hohes Speicherpotenzial besitzt, wenn eine Durchlässigkeit von mehr als 300 mD festgestellt wird. Darüber hinaus sind diese Teile des Plateaus auch durch die grosse Mächtigkeit des Känozoikums und damit durch ihre hydraulische Durchlässigkeit gekennzeichnet. Es muss darauf hingewiesen werden, dass wir in dieser Studie die gesamte Mächtigkeit der känozoischen Sedimente als potenzielles Reservoir betrachtet haben. Wir wissen jedoch, dass diese Einheit durch grosse vertikale und laterale lithologische Heterogenität gekennzeichnet ist und nur ein Teil der gesamten känozoischen Abfolge für die Speicherung geeignet ist. Daher wird eine detailliertere Netto-zu-Brutto-Bewertung ein genaues Screening der tatsächlichen Volumina mit effektiver Porosität und angemessener Permeabilität auf standortspezifischer Ebene ermöglichen.

Die Bewertung des oberen Mesozoikums konzentrierte sich nur auf die Verwerfungskorridore, die das Schweizer Plateau durchschneiden, da die Matrixporosität und Permeabilität der Karbonate bekanntlich sehr gering sind. Daher wurde eine Analyse der Gleit- und Dilatationstendenzen und der Von-Mises-Spannung auf der Grundlage der verfügbaren regionalen Spannungsdaten berechnet. Nach den Ergebnissen der Szenario Modellierung, die auf die Karbonate des oberen Mesozoikums angewandt wurde, können nur die Szenarien, die sich aus Permeabilitätsverteilungen der Verwerfungen zwischen 3,5 und 350 mD ergeben, als vielversprechende Ziele angesehen werden. Nach den vorliegenden Daten können Verwerfungsstrukturen in Aarau, Biel und Genf als Ziele geeignet sein. Wie die Bohrung GEo-01 in Genf jedoch gezeigt hat, führen hohe Permeabilität, die für

Verwerfungskorridore charakteristisch sind, zu einem hohen Bohrlochdruck und einem natürlichen artesischen Fluss, also zu einem begrenzenden Faktor für die Speicherung. Eine detailliertere Charakterisierung der hydraulischen Eigenschaften der Verwerfungsstrukturen ist für künftige Studien erforderlich, um diese Art der Bewertung zu verbessern.

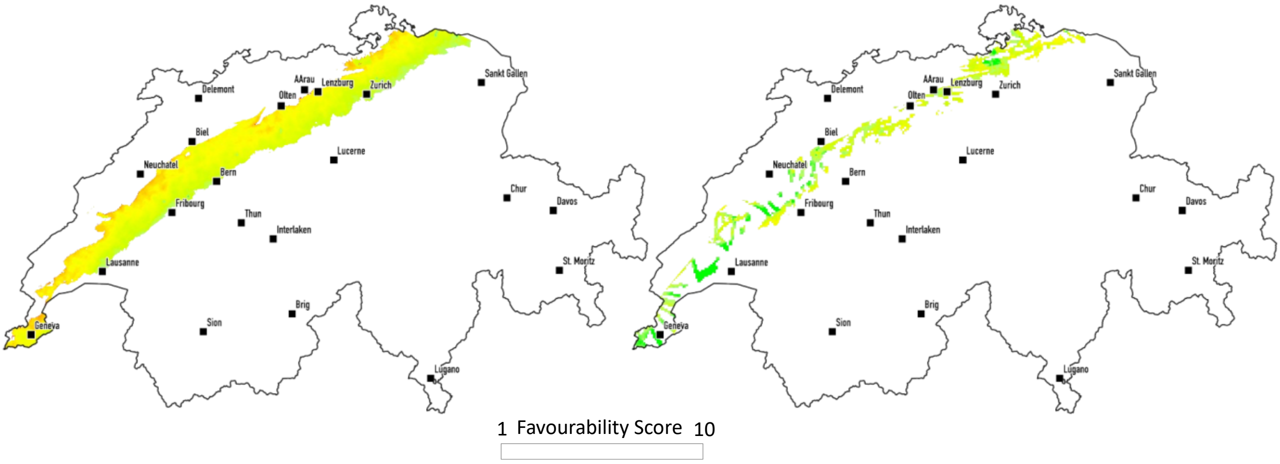

Figure XIV- Beispiel für HT-ATES-Günstigkeitsverteilungen für das Känozoikum (links) und das obere Mesozoikum (rechts)

Regulatorischer Rahmen für HT-ATES in der Schweiz

Der schweizerische Rechtsrahmen wurde mit dem Ziel analysiert, das Potenzial und die Grenzen seiner Anwendung auf HT-ATES-Systeme zu ermitteln. In der Schweiz gibt es keinen spezifischen Rechtsrahmen für HT-ATES-Systeme. Die Schweizer Gesetzgebung, die auf geothermische Projekte angewendet wird, basiert auf der Eidgenössischen Gewässerschutzverordnung, die darauf abzielt, Oberflächen- und Grundwasser zu schützen und sicherzustellen, dass die verschiedenen Nutzungen von Wasser nachhaltig sind. Die energetische Nutzung von Wasser kann sich negativ auf die unmittelbare Umwelt auswirken, ermöglicht aber gleichzeitig die Substitution fossiler Brennstoffe und wirkt damit der globalen Erwärmung entgegen.

In diesem Rahmen und um die Entwicklung von Tiefengeothermie Projekten zu ermöglichen, wurden einige Empfehlungen vorgeschlagen. Ein gewisses Mass an Flexibilität, um von bestimmten, derzeit festgelegten Grenzen abzuweichen, könnte wünschenswert sein. Im Falle von mittel- bis tiefreichenden Projekten in der Schweiz könnte es interessant sein, eine Arbeitsgruppe mit den Projektleitern, den beteiligten Ingenieurbüros, den Kantonen und dem Bund einzurichten, um die Grenzen des Systems zu definieren und Lösungen für das Management, den Betrieb und die Überwachung neuer Projekte vorzuschlagen. Letztlich könnten die in diesem Rahmen analysierten Elemente die Ausarbeitung von Richtlinien für Projekte mit mittlerer/grosser Wärmenutzung ermöglichen.

Der Vergleich der bestehenden rechtlichen Rahmenbedingungen für HT-ATES-Systeme in mehreren europäischen Ländern dank des HEATSTORE-Projekts hat gezeigt, dass die folgenden Schlüsselelemente für eine effiziente Entwicklung von HT-ATES-Projekten notwendig sind:

- Klar und deutlich definierte Arbeitsabläufe zwischen Projektentwicklern und Behörden
- Bestehender rechtlicher Rahmen auf nationaler Ebene, der jedoch auf regionaler Ebene durch die zuständigen lokalen Behörden umgesetzt und angepasst wird
- Gut dokumentierte, aktuelle und leicht zugängliche öffentliche Datenbanken
- Langfristige Entwicklungspläne (Masterpläne) auf regionaler Ebene, die auf einer globalen Vision basieren, die sowohl von den Behörden als auch von den Projektentwicklern geteilt und vorangetrieben wird

- Obligatorische Überwachung der Produktionsdaten (Temperatur, Druck, pH-Wert, Wasseranalysen usw.) in Verbindung mit einem angemessenen Historienabgleich auf der Grundlage eines iterativ aktualisierten thermohydraulischen 3D-Modells

Résumé

Le déploiement des sources d'énergie renouvelables (SER) pour la production d'électricité et de chaleur s'accélère en Europe. Cependant, les variations de la disponibilité et de la demande d'énergie et leur intégration dans l'infrastructure énergétique existante posent des problèmes de variabilité et d'équilibrage opérationnels. L'écrêtement des pointes et le stockage de la chaleur peuvent contribuer à équilibrer l'offre et la demande afin de mieux utiliser les infrastructures et les actifs (par exemple, augmenter les heures de pleine charge pour les sources de chaleur géothermiques). Le stockage d'énergie thermique peut, par exemple, être mis en œuvre dans les réseaux de chauffage sous la forme d'un stockage souterrain d'énergie thermique (UTES) pour soutenir l'utilisation de la chaleur excédentaire de l'industrie et la mise en œuvre de sources de chaleur renouvelables. L'UTES offre une solution intelligente et reproductible pour les régions présentant une baisse et un pic saisonniers de la demande de chauffage. L'UTES a le potentiel de fournir une capacité de stockage à grande échelle (potentiellement >10 GWh) par site, ce qui est difficile à réaliser avec d'autres technologies de stockage de la chaleur et bénéficie d'une gamme de coûts de stockage généralement plus faible.

HEATSTORE est l'un des neuf projets GEOTHERMICA - ERA-NET financés en 2018 pour la période 2018-2021 et avait pour objectif d'accélérer l'adoption de l'énergie géothermique en 1) faisant progresser et en intégrant différents types d'UTES dans le système énergétique, 2) fournissant un moyen de maximiser la production de chaleur géothermique et d'optimiser l'analyse de rentabilité des doublets de production de chaleur géothermique, 3) abordant les aspects techniques, économiques, environnementaux, réglementaires et politiques qui sont nécessaires pour soutenir le déploiement efficace et rentable des technologies UTES en Europe. Le projet visait à stimuler une adoption rapide du marché en Europe, à promouvoir le développement de la phase de démonstration jusqu'au déploiement commercial dans un délai de 2 à 5 ans et à fournir une perspective du potentiel d'utilisation vers 2030 et 2050.

Vingt-trois partenaires contributeurs de 9 pays forment le consortium européen HEATSTORE, composé d'un mélange d'instituts de recherche scientifique et de sociétés privées. La participation industrielle est considérée comme un avantage puissant et pertinent, qui est déterminant pour le succès. La combinaison d'instituts de recherche européens de premier plan et de petites, moyennes et grandes entreprises industrielles a permis de tester et de mettre en œuvre des technologies qui ont été mises sur le marché et valorisées par les parties prenantes concernées.

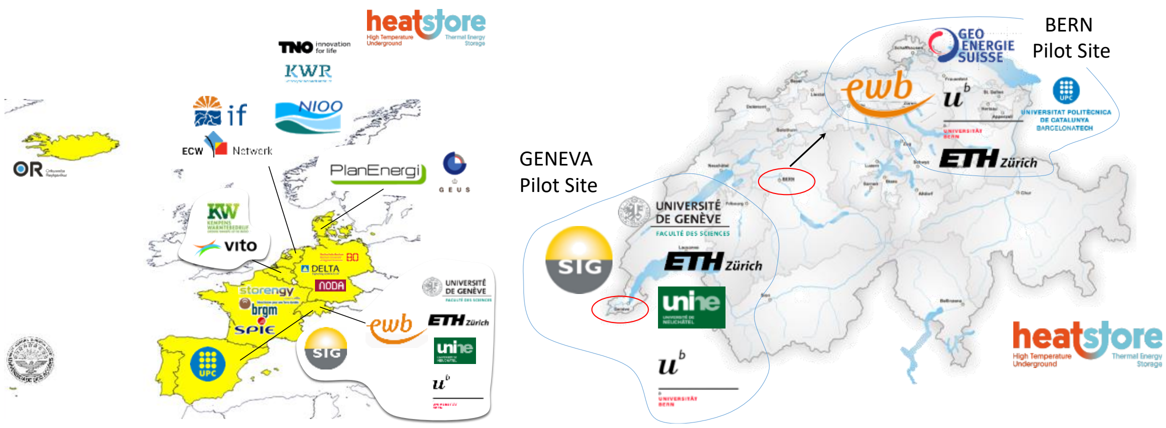

Figure I - Partenaires des Consortiums européen et suisse

Les partenaires suisses ont collaboré à deux études de cas à Genève et à Berne et ont travaillé en étroite collaboration avec des partenaires européens.

Le projet suisse HEATSTORE avait les objectifs principaux suivants :

- Identifier les opportunités de mise en œuvre du stockage d'énergie thermique en aquifère à haute température (HT-ATES) dans deux des réservoirs les plus commercialement viables du plateau molassique suisse : la Molasse cénozoïque et les carbonates du Mésozoïque supérieur.
- Mettre en œuvre un cadre d'analyse décisionnel multicritères pour prédire et évaluer la faisabilité technico-économique du HT-ATES en Suisse
- Identifier des solutions pour optimiser les performances des technologies HT-ATES et les intégrer dans des configurations de systèmes énergétiques complexes
- Prédire et valider les performances technico-économiques des HT-ATES grâce aux données recueillies sur deux sites pilotes à Genève et à Berne
- Identifier les effets environnementaux associés à la mise en œuvre des systèmes HT-ATES et les obstacles du cadre réglementaire à surmonter.

Ces objectifs contribuent à l'objectif final de HEATSTORE Switzerland, à savoir faire progresser la viabilité commerciale des technologies HT-ATES afin que l'énergie géothermique, combinée à un stockage de chaleur souterrain optimisé, puisse atteindre son potentiel de déploiement maximal dans la transition énergétique suisse.

Le projet suisse s'est concentré sur l'évaluation de la faisabilité des systèmes HT-ATES sur deux sites à Genève et à Berne. Les deux sites présentent des particularités différentes en ce qui concerne les conditions du sous-sol et la configuration du système énergétique. À Genève, la source de chaleur excédentaire est une usine d'incinération des déchets dont la température de rejet peut atteindre 120˚C, l'aquifère de stockage ciblé se trouve dans les carbonates mésozoïques fracturés entre 450 et 1500m de profondeur, et la température de fonctionnement du réseau de chauffage urbain se situe entre 70 et 120˚C. À Berne, la source de chaleur excédentaire est une centrale à cycle combiné, une centrale de valorisation des déchets, une centrale à bois dont la température de rejet peut atteindre 120˚C, et l'aquifère de stockage ciblé, les sédiments molassiques cénozoïques. La température de fonctionnement du réseau de chauffage urbain est d'environ 90˚C.

Les sites de Genève et de Berne reflètent la plupart des configurations du sous-sol et des systèmes énergétiques considérés comme adaptés au stockage d'énergie thermique en aquifère que l'on peut trouver dans d'autres villes sur l'ensemble du plateau molassique suisse.

Le raport présente l'ensemble des activités menées sur les sites de Genève et de Berne. Ces deux projets peuvent être considérés comme achevés.

Le site de Genève

A Genève, l'étude de cas s'est concentrée sur l'évaluation de la faisabilité du stockage de la chaleur excédentaire rejetée par une usine d'incinération des déchets à des températures allant jusqu'à 120˚C (section 5.1) dans les carbonates fracturés du Mésozoïque à une profondeur comprise entre 450 et 1500m. Le cadre d'évaluation multicritères mis en place est basé sur des critères technico-économiques afin de :

- Évaluer le potentiel technique de stockage de la chaleur dans le réservoir en intégrant les données de surface et de subsurface.
- Identifier les effets environnementaux liés aux opérations de stockage et de production
- Évaluer le lien entre les résultats de stockage/récupération et les performances économiques dans différentes configurations techniques.

Le cadre basé sur une approche progressive a initialement combiné les contraintes de la subsurface et du système énergétique en utilisant les données disponibles au début du projet. Au fur et à mesure que de nouvelles données et de nouveaux résultats sont devenus disponibles au cours du projet, il a finalement été calibré et validé en fonction des données résultant des activités d'exploration du sous-sol réalisées par le forage des puits GEo-01 et GEo-02 et des scénarios de développement du système énergétique de 2035.

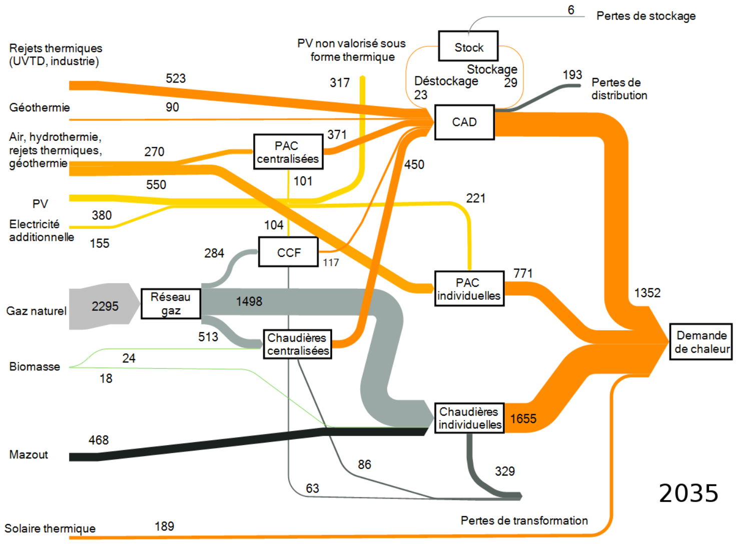

Figure II – Système Énergétique a Geneve, scenario 2035

Les deux puits ont ciblé les calcaires du Mésozoïque supérieur. Les résultats du forage ont contribué à la compréhension de l'architecture du réservoir et de la distribution des propriétés pétrophysiques/hydrauliques et ont mis en évidence les propriétés hydrauliques fortement hétérogènes des carbonates mésozoïques dans toute la région de Genève. GEo-01, d'une profondeur de 744 m, délivre une eau de 34˚C à 55l/s et une pression de tête de puits de 8-10 bars, tandis que GEo-02 délivre une température de tête de puits de 18˚C (~55˚C de température de fond de puits) à 0,3 l/s et une pression de tête de puits de 10-12 bars.

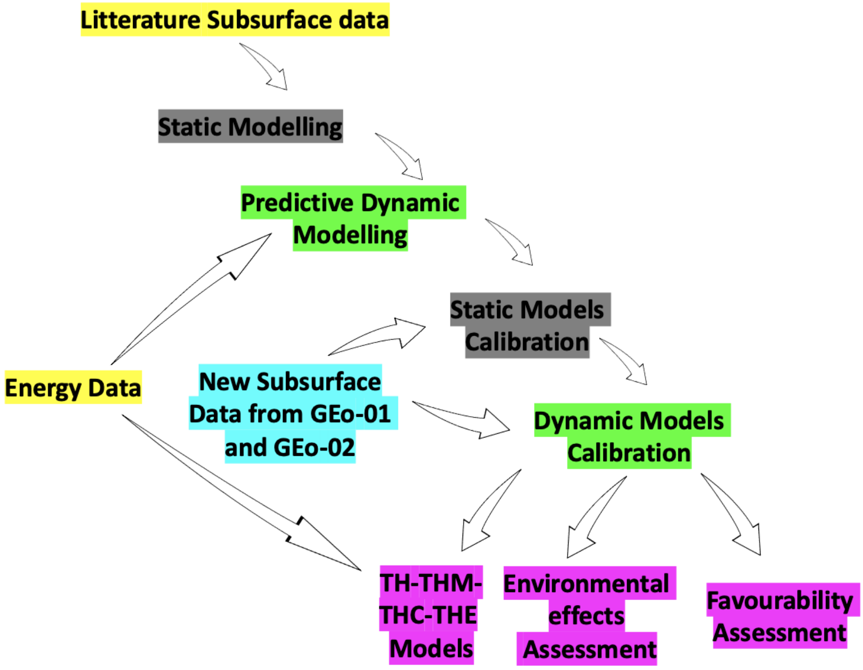

Figure III - Flux de travail du projet HEATSTORE appliqué au site de Genève

En termes de caractérisation de la subsurface, un ensemble de modèles 3D a été produit à partir de modèles statiques, qui ont permis de capturer la géométrie et la distribution des propriétés pétrophysiques et hydrauliques des réservoirs étudiés (voir rapport complet sections 5.1.2, 5.1.3, 5.1.6). Les modèles calculés ont intégré les données géophysiques et pétrophysiques disponibles au cours des différentes phases du projet. L'approche globale est basée sur le principe que les modèles statiques 3D servent d'entrées, en intégration avec les informations du système énergétique, pour produire des modèles dynamiques (thermo-hydraulique TH, thermo-hydraulique-mécanique THM, ou HM, thermo-hydraulique-chimique THC, et thermo-hydraulique-économique THE) afin de prédire la performance des systèmes HT-ATES à Genève. Les résultats de la modélisation statique découlent de l'interprétation de plusieurs ensembles de données de réflexion sismique 2D d'époque, des diagraphies de puits de GEo-01 et GEo-02, des rapports de puits et des analogues d'affleurement. L'interprétation sismique révèle une structure florale bien développée déformant les sédiments mésozoïques et certaines parties du cénozoïque dans la zone GEo-01. La situation structurelle de subsurface autour du site GEo-02 est différente, comprenant un système de failles de chevauchement et des failles normales associées déformant les sédiments du Cénozoïque et du Mésozoïque. L'analyse pétrophysique suggère que la formation du Crétacé inférieur dans la zone GEo-01 est serrée, généralement caractérisée par de faibles valeurs de porosité et de perméabilité. Cependant, la présence de réseaux de fractures et de failles déformant une partie importante de cette unité peut favoriser une circulation localisée des fluides. Dans la zone GEo-02, les résultats des tests de puits suggèrent que les formations de la succession mésozoïque ont une faible circulation de fluide et de faibles propriétés hydrauliques.

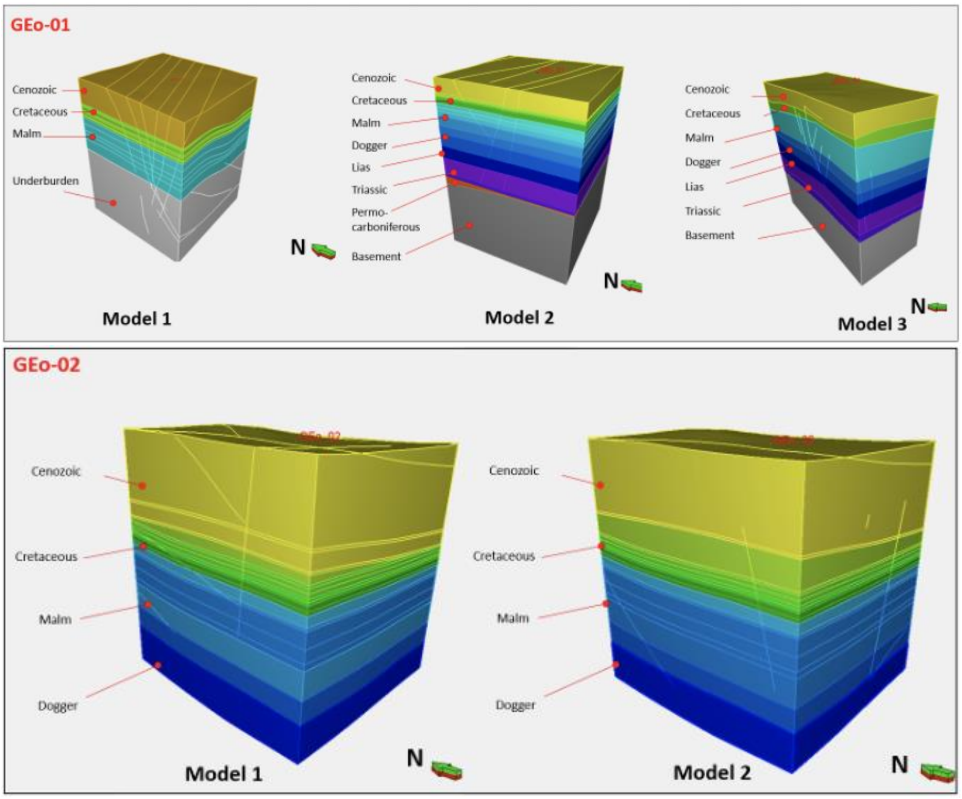

Figure IV- Modelés statique 3D pour les zones des forages géothermiques GEo-01 and GEo-02

Par la suite, les modèles dynamiques Thermo-Hydraulique (TH) et Hydro-Mécanique (HM) développés en intégrant les modèles statiques aux données du système énergétique (par exemple, la température de la chaleur excédentaire, la température de récupération, l'utilisation des pompes à chaleur, la chaleur excédentaire et la distribution temporelle de la demande de chaleur) ont permis de produire des scénarios opérationnels HT-ATES (voir section 5.1.7). Initialement, tous les modèles étaient basés sur les données disponibles dans la littérature, permettaient de configurer l'ensemble du flux de travail de modélisation "de la statique à la dynamique" et fournissaient la première série de prédictions sur le comportement du système HT-ATES. À la suite de la disponibilité de nouvelles données provenant des deux puits d'exploration, ces modèles ont été calibrés et validés pour produire un ensemble de scénarios plus fiables et plus réalistes capturant la prédiction de l'écoulement des fluides dans le réservoir et la quantification des effets potentiels de la mécanique des sols (déformation du sol) dus aux opérations. Une approche de discrétisation numérique (par exemple, éléments finis, volumes finis) a été utilisée pour les modèles TH afin de créer un algorithme de solution qui fournira la solution discrète nécessaire à nos simulations. Le modèle conceptuel a abordé des scénarios d'intérêt liés aux conditions géologiques et hydrologiques locales. Ces scénarios comprennent la modélisation de l'influence de l'écoulement des eaux souterraines et de l'hétérogénéité géologique (c'est-à-dire la présence de fractures et de failles, de structures récifales) sur les capacités de stockage et de récupération du système de stockage.

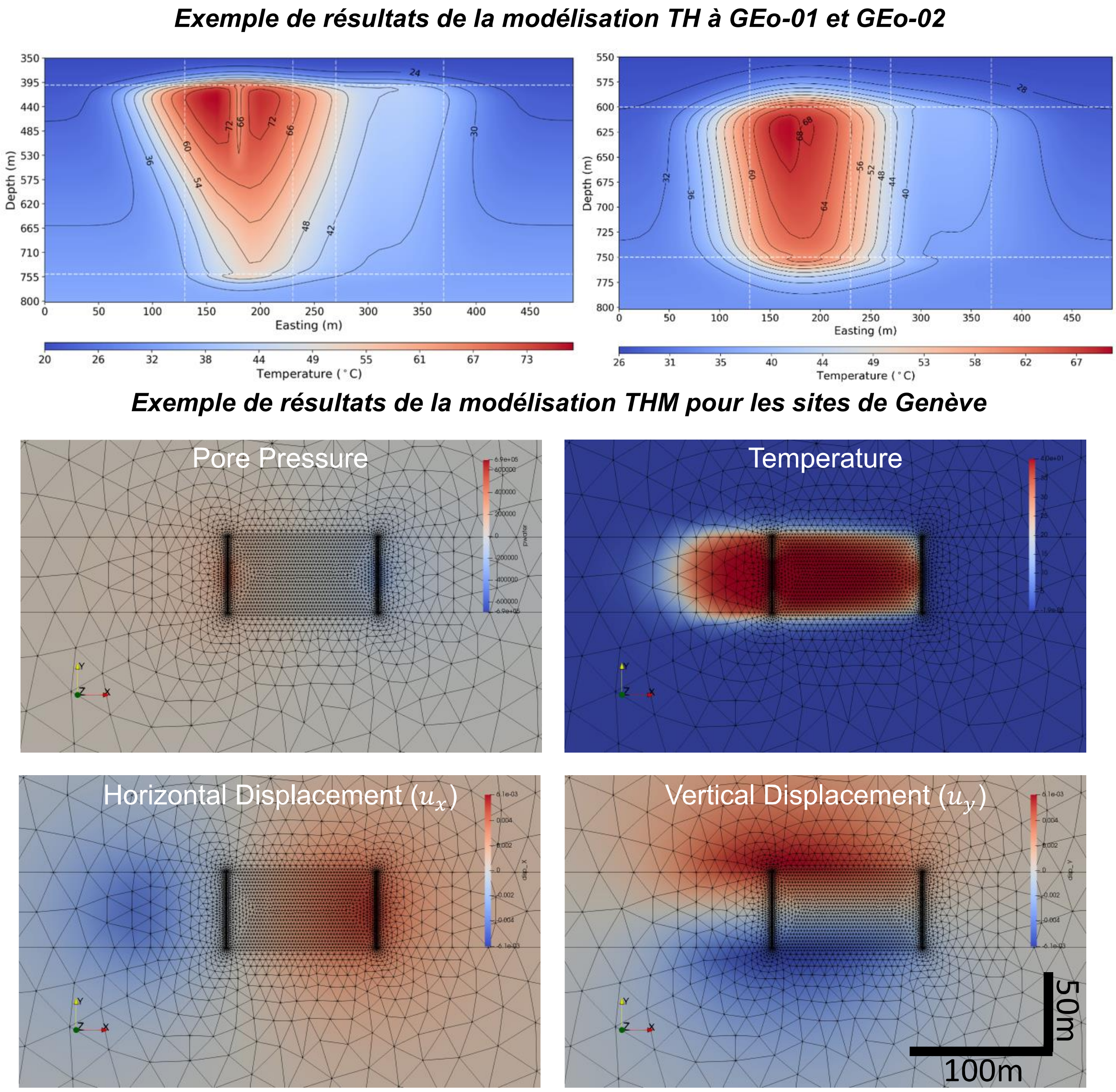

Figure V- Exemples des résultats de la modélisation TH et THM pour la région de Genève

Des études géochimiques ont été réalisées afin d'évaluer l'activation potentielle des mécanismes d'interaction eau-roche qui peuvent affecter les propriétés du réservoir en raison de la dissolution et de la précipitation des minéraux dans les réservoirs et du potentiel de corrosion/écaillage sur l'équipement de surface (voir les sections 5.1.8 5.1.9.3 et l'annexe 7 pour un rapport détaillé). Des échantillons d'eau de réservoir ont été prélevés, et leur composition chimique a été analysée et combinée aux résultats de l'analyse minéralogique effectuée sur les déblais et les carottes de forage. En outre, les partenaires du projet ont réalisé des expériences en laboratoire et une modélisation cinétique pour reproduire les conditions HT-ATES et les effets chimiques sur les variations de l'eau du réservoir pendant les opérations HT-ATES. Les résultats révèlent que la dissolution et la précipitation des minéraux carbonatés peuvent se produire pendant l'exploitation. Un risque de précipitation dans des secteurs du réservoir peut conduire à sa compartimentation réduisant les performances des systèmes de stockage. La charge en suspension déversée par le GEo-01 a également été analysée, révélant qu'une combinaison de minéraux sulfatés et de communauté microbienne, en particulier des

Methanobacteria, forme une classe essentielle dans les échantillons. D'après les résultats de cette étude, les principaux effets suivants peuvent se produire pendant les opérations à long terme :

- En raison de leur solubilité rétrograde (c'est-à-dire une solubilité décroissante avec l'augmentation de la température), les carbonates tels que la calcite risquent de précipiter lorsque les eaux se réchauffent à 90°C pendant les cycles de stockage. La précipitation des minéraux carbonatés pourrait entraver l'écoulement et l'échange de chaleur dans les installations de surface.
- Dans le cas de l'eau produite à partir de GEo-01, la corrosion des installations techniques telles que les pompes, les boîtiers et les échangeurs de chaleur pourrait se produire en raison de la concentration élevée de sulfure. Cela pourrait entraîner une défaillance des matériaux et des problèmes opérationnels.

Afin d'évaluer les alternatives concernant la viabilité économique des systèmes HT-ATES à Genève, nous avons combiné les résultats de la modélisation avec les données du système énergétique pour évaluer les scénarios de stockage susceptibles de réussir sur le plan technico-économique. Les résultats montrent que, sous réserve des contraintes du sous-sol, la capacité nominale varie de 0,4 MW à 81 MW, la perméabilité et l'épaisseur de l'aquifère étant les principales variables de contrôle. Une transmissivité minimale de $2{,}5 \times 10^{-12}$ m^3 est nécessaire pour maintenir le coût nivelé de la chaleur (LCOH) en dessous de 200 CHF/MWh, et une capacité de 25 MW ou plus est nécessaire pour que le système HT-ATES devienne compétitif par rapport aux autres sources de chaleur DHN à grande échelle. La capacité augmente grâce à l'ajout de pompes à chaleur (HP), ce qui entraîne des coûts non récupérables et augmente le LCOH. Néanmoins, l'ajout de HP augmente la capacité nominale du système et entraîne des émissions de CO_2 cumulées évitées plus élevées.

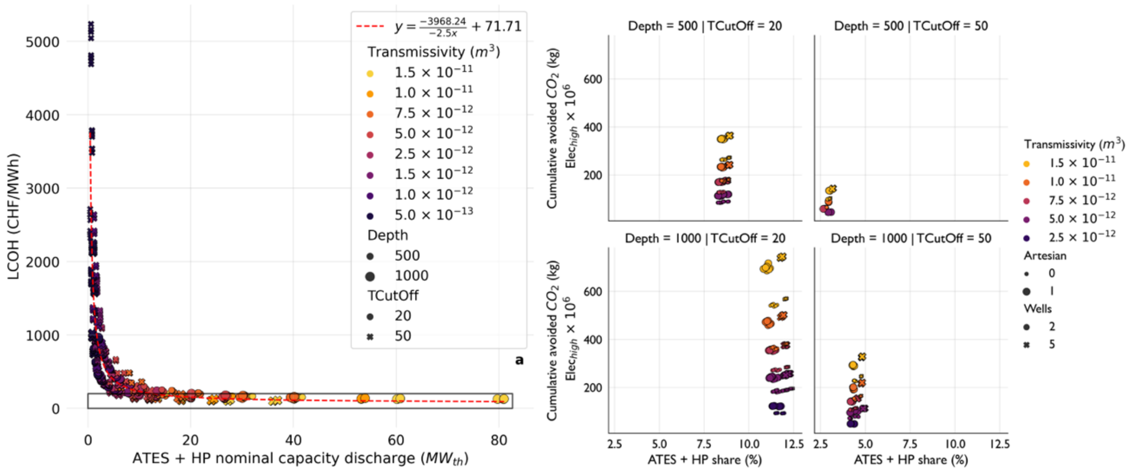

Figure VI: Gauche : LCOH contre la capacité de production nominale colorée par la transmissivité du réservoir, dimensionnée par la profondeur et la température de coupure Droite : Part de l'ATES et émissions de CO_2 évitées cumulées pour les simulations avec un LCOH inférieur à 200 CHF/MWh

Une évaluation accélérée des effets sur l'environnement (annexe 18) a permis d'identifier les effets sur l'environnement associés aux phases de forage et aux opérations HT-ATES sur les sites des puits GEo-01 et GEo-02. Les effets pendant le forage ont été identifiés et évalués en fonction des activités réalisées par SIG avant, pendant et après les opérations de forage. En revanche, les effets associés aux opérations HT-ATES ont été identifiés et évalués via l'acquisition de données, la modélisation prédictive et la surveillance. Les résultats révèlent que les risques associés aux opérations de forage sont faibles à moyens et limités dans le temps. Les risques élevés pendant les opérations HT-ATES sont uniquement associés aux variations de la composition de l'eau des réservoirs sans affecter les eaux douces peu profondes. La mise en œuvre du HT-ATES permettra de réduire l'intensité carbonique du secteur du chauffage.

GEo-01

Effect \ Phase	Drilling						Operations (predicted)					
	P	A	M	Probability	Consequences	Risk	P	A	M	Probability	Consequences	Risk
Air quality				H	L	M				L	L	L
Noise and vibration				H	L	M				M	L	L
Formation water quality				L	L	L				H	M	H
Formation water temperature										H	L	M
Surface clear water				H	L	M				L	L	L
Soil occupation				H	L	M				H	L	M
Wastes and dangerous substances				H	L	M				M	L	L
Environment				M	L	L				L	L	L
Nature				M	L	L				L	L	L
Soil mechanics										L	L	L
Seismicity				L	H	M				L	H	M
CO2 intensity redyction										H	M	H

GEo-02

Effect \ Phase	Drilling						Operations (predicted)					
	P	A	M	Probability	Consequences	Risk	P	A	M	Probability	Consequences	Risk
Air quality				H	L	M				L	L	L
Noise and vibration				H	L	M				M	L	L
Formation water quality				L	L	L				H	M	H
Formation water temperature										H	L	M
Surface clear water				H	L	M				L	L	L
Soil occupation				H	L	M				H	L	M
Wastes and dangerous substances				H	L	M				M	L	L
Environment				M	L	L				L	L	L
Nature				M	L	L				L	L	L
Soil mechanics										L	L	M
Seismicity				L	H	M				L	H	M
CO2 intensity redyction										H	M	H

Figure VII - Fast-track analyse des risques pour HT-ATES a Geneva

Les conditions de subsurface difficiles pour le système de stockage sélectionné à Genève n'ont pas permis d'effectuer des tests d'injection/récupération à GEo-01 et GEo-02. Par conséquent, un laboratoire de terrain à Concise (VD) a été mis en place pour démontrer si le stockage et la récupération de chaleur peuvent être une option pour les carbonates fracturés (section 5.1.5). Trois puits forés à 50 m de profondeur ont atteint les mêmes carbonates du Mésozoïque supérieur que ceux forés par GEo-01 et GEo-02, et des opérations hydrogéologiques, hydrochimiques, pétrophysiques, de diagraphie des sondages, de tests thermo-hydrauliques ont été réalisées pour évaluer les performances de stockage du réservoir étudié. Le développement du site d'essai Concise a permis d'appliquer des méthodes de caractérisation hydraulique et thermohydraulique des réservoirs karstiques et fracturés, combinant essais sur le terrain et modélisation.

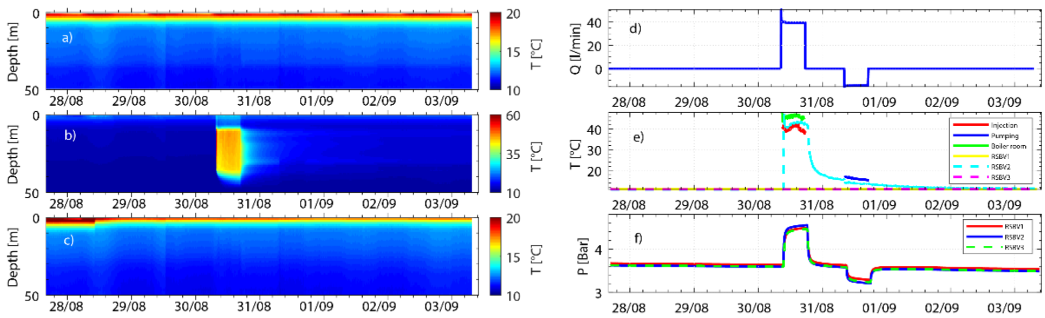

Figure VIII - Variations de température mesurées dans les puits de Concise lors des essais thermo-hydrauliques sur le terrain en fonction des débits, de la température d'injection, de la température de pompage et de la pression.

Ces résultats soulignent l'importance de la prise en compte explicite des structures du réservoir pour obtenir des réponses thermo-hydrauliques robustes et fournissent la base de recommandations pour le développement et la caractérisation des systèmes de stockage de chaleur en profondeur.

Le site de Berne

À Berne, les possibilités de stockage de la chaleur excédentaire provenant de l'usine d'incinération des déchets (UID) de Forsthaus ont été étudiées et testées jusqu'à une profondeur maximale de 500 m (section 5.2). Le site de Berne a servi de site pilote dans un réservoir typique de grès molassique (« grès des ceintures de chenaux » de la Molasse inférieure d'eau douce) afin de tester et d'optimiser pour la première fois, dans des conditions réelles, les options et les propriétés d'un réservoir géothermique dans ces formations rocheuses largement répandues dans le Plateau suisse.

L'objectif du projet était d'étudier la faisabilité et les options de réduction des risques liés à l'exploitation d'un réservoir de grès molassique. À cette fin, trois forages ont été réalisés à proximité immédiate de la centrale et les essais dans le réservoir ont été surveillés. Les résultats serviront à l'ewb pour obtenir les informations nécessaires à la planification définitive concernant les propriétés des grès de la ceinture de Rinne et, en fonction des résultats, pour mettre pleinement en œuvre le HT-ATES une fois le projet achevé.

Le plan conceptuel prévoyait d'injecter de l'eau chaude provenant de l'installation en fonction des saisons, puis de récupérer l'énergie thermique stockée en cas de demande accrue en hiver et de l'injecter dans le réseau de chauffage urbain, sans avoir recours à une pompe à chaleur. L'injection d'eau chaude s'est effectuée pendant environ 200 jours via le puits principal situé au centre du système. Pendant le cycle de décharge, ce même puits central a été utilisé pour la production d'eau chaude. Le pompage simultané depuis/vers les puits secondaires a servi à réguler le débit aux limites du système et ainsi à équilibrer la pression dans le réservoir pendant l'injection et la production. Une durée de vie de 20 ans a été retenue pour le système HT-ATES « Geospeicher Forsthaus » envisagé.

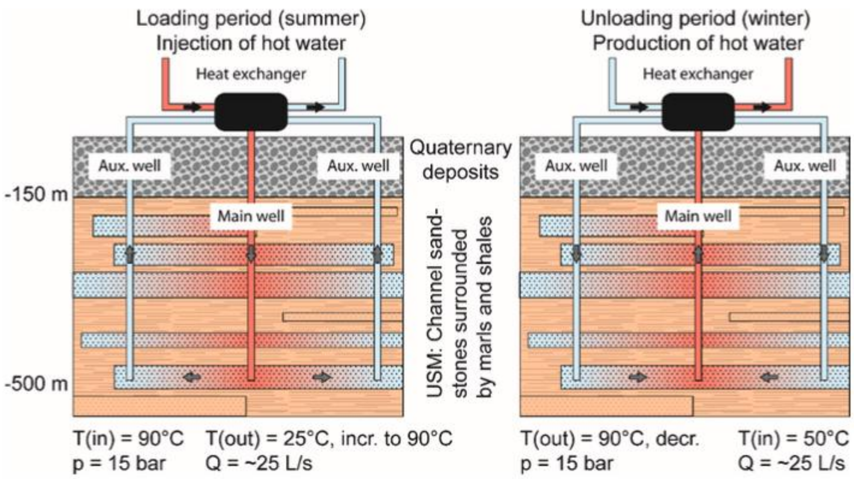

Figure IX – Représentation schématique de la conception opérationnelle et des paramètres opérationnels prévus du projet pilote HT-ATES Geospeicher Forsthaus

Des études géologiques et géochimiques préalables ont été menées, qui ont mis en évidence des cibles potentielles dans la Molasse inférieure d'eau douce, au sein de la succession de grès à grains moyens à grossiers superposés des ceintures de chenaux. Il s'agit là des sédiments classiques qui se déposent dans la partie centrale des ceintures de chenaux et peuvent former des corps de grès cohérents et homogènes de plusieurs kilomètres de long, de 150 à 1 500 m de large et de 2 à 15 m d'épaisseur.

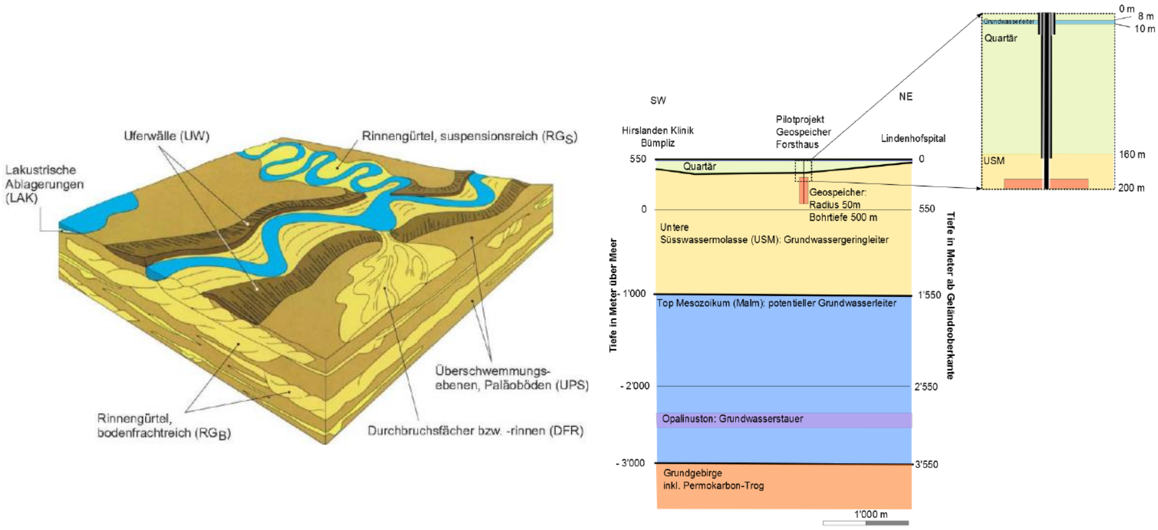

Figure X – Gauche : Dessin humoristique montrant les différents faciès de l'USM ; Droite : Coupe géologique jusqu'à la subsurface profonde de l'installation de stockage géologique prévue.

Ces formations de grès, idéalement très perméables, des ceintures de chenaux alternent avec des sédiments à grains fins peu perméables (figure X). Il en résulte une très bonne étanchéité hydraulique des unités des ceintures de chenaux, l'une des conditions fondamentales pour un stockage thermique. L'eau chaude stockée ne peut donc pas s'écouler hors des couches de grès. En l'absence de données géologiques spécifiques au site, il n'était pas possible, au début du projet, d'évaluer avec précision le volume de stockage et la profondeur, la pétrophysique et les propriétés hydrauliques, ainsi que le régime hydrogéologique dans la zone d'étude. Les principales inconnues étaient les suivantes :

- Présence ou absence des grès dans une section verticale donnée de l'USM
- Les géométries et dimensions 3D des grès
- La porosité, la perméabilité, la teneur en minéraux et le degré de cimentation de la calcite dans les grès
- La mesure dans laquelle les couches individuelles de grès sont hydrauliquement connectées (par opposition à une compartimentation hydraulique par des silts et des argiles intercalés) ;
- La vitesse et la direction de l'écoulement des eaux souterraines les propriétés des eaux souterraines: salinité, composition des solutés (en particulier pCO_2) et activité microbienne
- Concentrations dans les eaux souterraines des composants induisant la corrosion : H2S, SO4, Cl, et microbes

Des expériences en laboratoire ont été menées au préalable sur les interactions géochimiques entre l'eau et la roche ainsi que sur la modélisation du THC (annexe 08).

Trois forages ont été réalisés successivement à partir de la même plate-forme de forage. La plate-forme « Marriott Rig 18 » a été mise en place sur le site et le premier forage a débuté le 21 octobre 2022. Le troisième forage s'est achevé avec succès le 1er avril 2023.

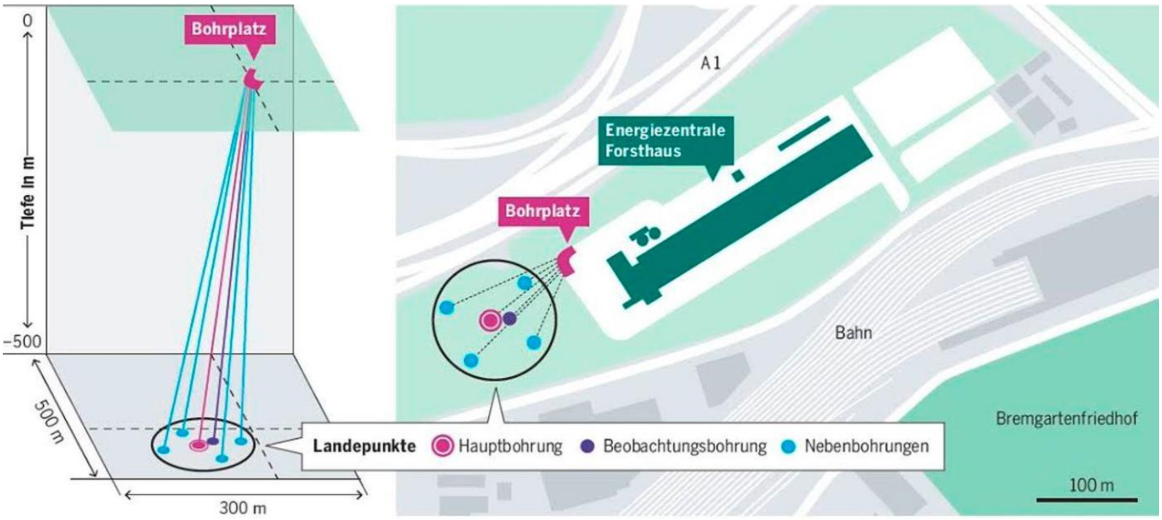

Figure XI – Croquis des 6 forages prévus pour le projet pilote de stockage géologique de Forsthaus

Les forages réalisés dans le cadre du projet ont montré que le site recèle une couche de sédiments quaternaires d'une épaisseur d'environ 240 m, soit environ 80 m de plus que ce qui avait été supposé avant les forages. En dessous, jusqu'à une profondeur d'environ 520 m, environ 280 m de sédiments de la Molasse d'eau douce inférieure (USM) ont été mis au jour. Ces sédiments témoignent d'un système de dépôt fluvial hétérogène, autrefois sinueux, dans les contreforts alpins, composé de grès, de siltites, de dépôts de crue et de paléosols. Au sein de l'USM, plusieurs intervalles de grès contigus latéralement ont été identifiés, qui sont considérés comme des horizons réservoirs potentiels pour le stockage de chaleur. Les grès présentent généralement des propriétés de porosité et de perméabilité appropriées, même si leur perméabilité peut être localement réduite par la cimentation calcaire.

Par rapport à d'autres sites du bassin molassique central, les forages de Forsthaus présentent des caractéristiques sédimentologiques et pétrophysiques similaires, même si les perméabilités sont parfois légèrement inférieures.

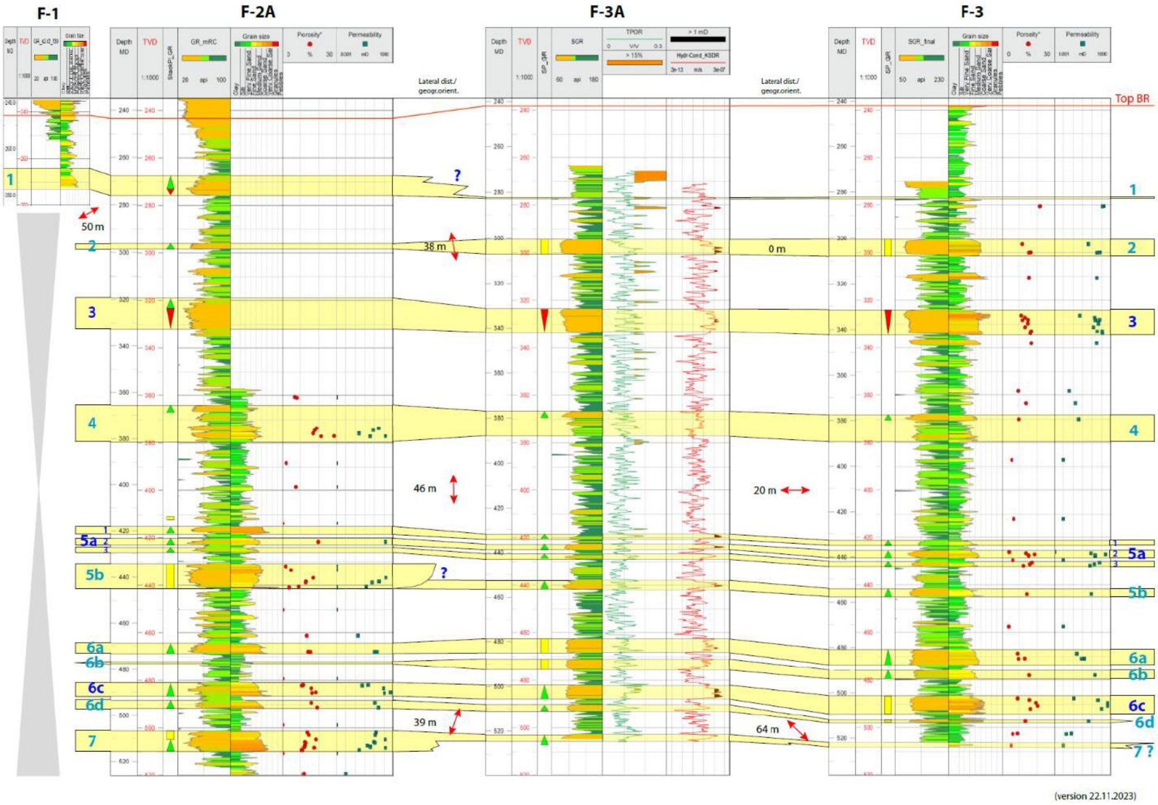

Figure XII - Corrélation des principales unités de gisement dans l'USM étudiée, sur la base de mesures gamma et de profils granulométriques.

Pour raccorder les forages au réservoir et permettre son exploitation, une couche de grès représentative située dans la partie inférieure des forages a été choisie. Cette décision visait à garantir qu'en cas de problèmes techniques, il serait possible de se rabattre sans trop de difficultés sur une couche de grès située plus haut. Le choix s'est porté sur la couche 6c, située à une profondeur de 485 m, car elle présente notamment une bonne continuité horizontale et une perméabilité hydraulique moyenne.

Dans un premier temps, le tubage cimenté dans F2 a été percé à l'aide de micro-dérivations forées horizontalement jusqu'à 5 m de profondeur dans la couche de grès. Il fallait veiller à ne pas endommager le câble en fibre de verre cimenté le long du tubage, entre le tubage et la formation. Après chaque nouveau micro-dérivation, l'injectivité a été testée. Un système à double packer a ensuite été installé dans F2 afin de réduire au maximum le volume d'essai et d'isoler les micro-dérivations du reste du volume du puits.

Après l'installation, la pression dans la couche de grès 6c a pu être observée avant et pendant le forage des micro-dérivations dans F3. La pression a d'abord baissé, puis la première micro-dérivation a été forée dans F3 et de l'eau de bouche d'incendie y a été injectée à débit constant pendant environ une semaine. L'injection dans F3 a entraîné une augmentation progressive de la pression dans F2. L'analyse de la courbe d'augmentation de la pression a permis d'évaluer la connexion hydraulique entre les deux puits, d'en déduire des valeurs représentatives de la perméabilité et d'analyser le comportement de l'écoulement. Une fois tous les micro-dérivations forées dans F3, un deuxième système à double packer a été installé. Des essais de pression par paliers, également appelés « essais de levage hydraulique », ont ensuite été réalisés dans les deux puits. À une pression d'injection supérieure à la contrainte verticale de la roche, des zones horizontales perméables se sont ouvertes au sein des couches de grès. Dès que cette pression a été atteinte, l'injection a pu être effectuée à des débits disproportionnés. L'ensemble des données, comprenant les mesures de pression dans le puits d'injection et dans le puits d'observation ainsi que les mesures de déformation sur le câble à fibre optique le long du tubage dans F2, a permis de tirer des conclusions importantes sur le comportement hydromécanique de la couche de grès.

Il a en outre été constaté que la perméabilité de la couche de grès avait augmenté de manière durable d'un facteur 2. Cette augmentation n'a toutefois pas suffi à permettre l'exploitation rentable d'une installation de stockage thermique. Pendant les essais de mise en pression, la microsismicité a été surveillée à l'aide d'un sismomètre installé temporairement en surface, et les éventuels soulèvements et tassements ont été enregistrés par le système de surveillance permanent.

Malgré la faible transmissivité, un champ d'écoulement dipolaire a pu être établi entre les forages et maintenu pendant plus de deux mois. Pour ce faire, de l'eau de bouche d'incendie a été injectée à un débit de 8 l/min dans le forage F3, tandis que 2 l/min s'écoulaient librement dans le forage F2. Des paramètres hydrogéochimiques ont pu être mesurés en temps réel et des échantillons d'eau ont été prélevés pour des analyses en laboratoire à l'Université de Berne.

Une fois que la boue de forage introduite pendant le forage a été entièrement extraite de la formation, de l'eau de formation naturelle a été détectée. Après environ deux mois, la signature chimique de l'eau de bouche d'incendie injectée dans F3 a été identifiée pour la première fois. Le test de circulation à long terme a donc également pu être évalué comme un test de traçage. Avant même que l'eau de bouche d'incendie ne perce légèrement, la société Hydroisotop a prélevé un échantillon d'eau pour une analyse au ^{81}Kr afin de déterminer l'âge modélisé de l'eau de formation.

Une fois la caractérisation hydrogéochimique achevée, une expérience a été lancée dans le but d'acidifier les voies d'écoulement les plus perméables à l'aide de CO_2 dissous dans l'eau, afin d'augmenter la transmissivité. Pendant plusieurs semaines, environ 5,5 tonnes de CO_2 ont été injectées dans F3 alors que le forage F2 était obturé. La calcite dissoute a ensuite été éliminée par rinçage à l'aide d'eau provenant de bouches d'incendie injectée dans F2. L'eau s'écoulant de F3 a été prélevée à intervalles réguliers par l'Université de Berne.

Une fois la majeure partie de la calcite éliminée d'ici fin 2024, de nouveaux essais hydrauliques ont été réalisés afin de déterminer l'évolution de la transmissivité. L'ensemble complet de données hydrogéochimiques a été analysé par l'Université de Berne à l'aide d'un modèle numérique hydrogéochimique et hydraulique. Ce modèle, calibré avec soin, correspond bien, sur le plan conceptuel, aux données recueillies jusqu'à présent concernant la formation de grès ainsi que la géométrie de la connexion du réservoir aux micro-dérivations.

Les études menées au cours du projet montrent que les conditions requises pour un système de stockage géothermique à Forsthaus Bern sont globalement remplies. Cependant, la perméabilité insuffisante constitue le principal obstacle à l'exploitation rentable d'un réservoir.

Analyse spatiale multicritères pour la favorabilité des HT-ATES en Suisse

S'agissant d'un concept multidimensionnel, l'évaluation de la favorabilité des HT-ATES réalisée dans HEATSTORE a été basée sur l'agrégation d'un ensemble de critères technico-économiques via l'Analyse Spatiale Multicritères (ASMC). Or, les performances technico-économiques des HT-ATES sont caractérisées par des caractéristiques géologiques (éléments Play) et géographiques, qui sont variables sur le Plateau suisse. L'accent mis sur le Plateau suisse a été motivé par la disponibilité de données publiques et par le fait que la grande majorité de la chaleur excédentaire et de la demande de chaleur est concentrée dans cette région. Le travail effectué dans cette tâche comprend la mise en œuvre d'un cadre spatial multicritères de type Play-fairway se concentrant sur le potentiel de mise en œuvre de systèmes HT-ATES dans deux unités géologiques principales : les sédiments du Cénozoïque (c'est-à-dire la cible du projet de Berne) et les carbonates fracturés du Mésozoïque supérieur (c'est-à-dire la cible du projet de Genève). Les données de subsurface comprennent la géométrie des unités géologiques cibles jusqu'à 2000 m de profondeur, leur gamme de valeurs de densité, de porosité, de perméabilité, la distribution des failles et les contraintes régionales. Les contraintes de surface, notamment la répartition géographique de l'excès de chaleur, la demande de chaleur, les réseaux de chauffage urbain et les usines d'incinération des déchets, ont été intégrées au cadre d'analyse pour produire des cartes représentant différents scénarios de favorabilité HT-ATES. À ce stade, les contraintes économiques ont pris en compte le concept de transmissivité minimale économiquement viable du réservoir cible, dont la valeur seuil fixée à $5x10^{-13}m^3$ a contribué à identifier les zones les plus favorables.

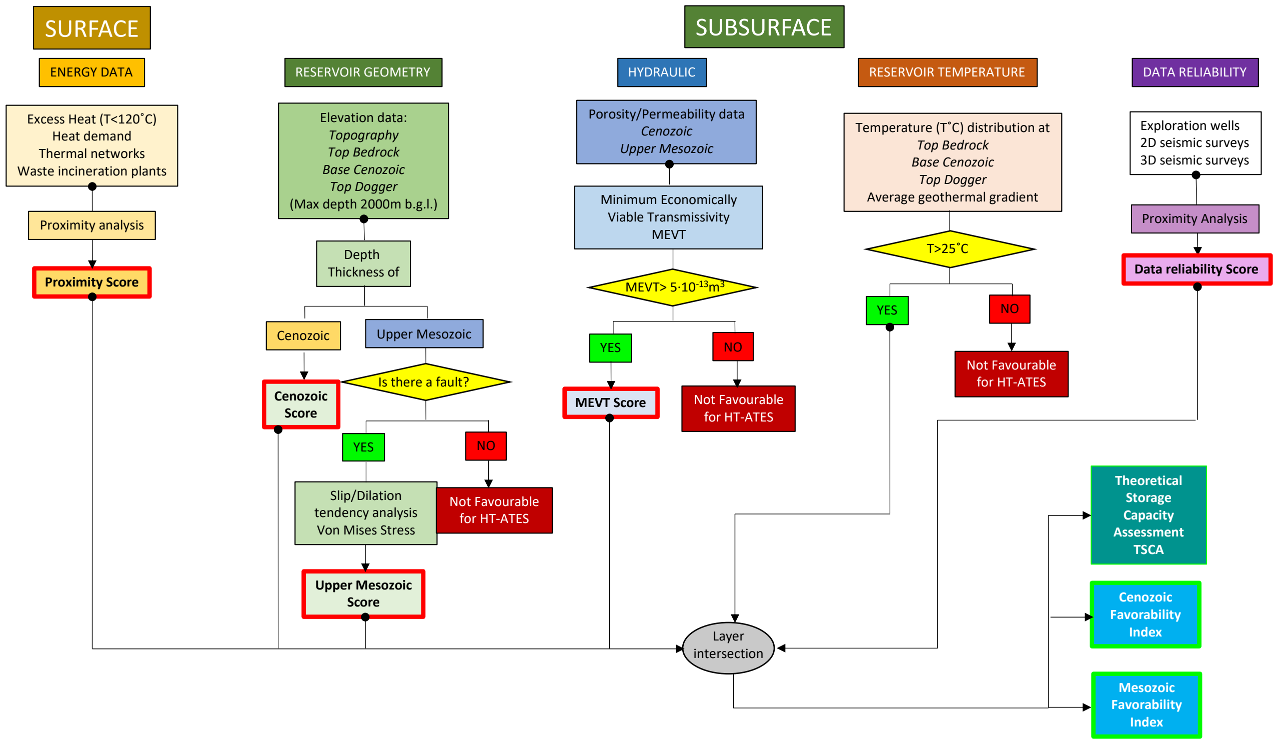

Figure XIII – Cadre mis en place pour le SMCA HT-ATES en Suisse

Les résultats montrent que le Cénozoïque présente un fort potentiel de stockage dans les parties centrales et méridionales de la zone du Plateau de la Molasse, où se trouvent certaines grandes villes (Zurich, Berne, Lausanne) si une perméabilité supérieure à 300mD est identifiée. De plus, ces portions du Plateau sont également caractérisées par la grande épaisseur du Cénozoïque, d'où leur transmissivité hydraulique. Il faut souligner que dans cette étude, nous avons considéré comme réservoir potentiel toute l'épaisseur des sédiments du Cénozoïque. Cependant, nous savons que de grandes hétérogénéités lithologiques verticales et latérales caractérisent cette unité, et que seule une partie de l'ensemble de la séquence cénozoïque convient au stockage. Par conséquent, une évaluation plus détaillée du net au brut permettra une sélection précise à l'échelle d'un site spécifique des volumes réels ayant une porosité efficace et une perméabilité adéquate.

L'évaluation du Mésozoïque supérieur s'est concentrée uniquement sur les couloirs de failles qui traversent le Plateau suisse, car il est bien connu que la porosité et la perméabilité de la matrice des carbonates sont très faibles. Par conséquent, une analyse des tendances au glissement et à la dilatation ainsi que de la contrainte de Von Misses a été calculée sur la base des données de contrainte régionales disponibles. D'après les résultats de la modélisation de scénarios appliquée aux carbonates du Mésozoïque supérieur, seuls les scénarios résultant de distributions de perméabilités de failles entre 3,5 et 350 mD peuvent être considérés comme des cibles prometteuses. D'après les données disponibles, les structures de failles peuvent convenir comme cibles à Aarau, Bienne et Genève. Cependant, comme l'a démontré le puits GEo-01 à Genève, les perméabilités élevées caractérisant les couloirs de faille entraînent une pression élevée en tête de puits et un écoulement artésien naturel, donc un facteur limitant pour le stockage. Une caractérisation plus détaillée des propriétés hydrauliques des structures de faille sera nécessaire pour les études futures afin d'améliorer ce type d'évaluation.

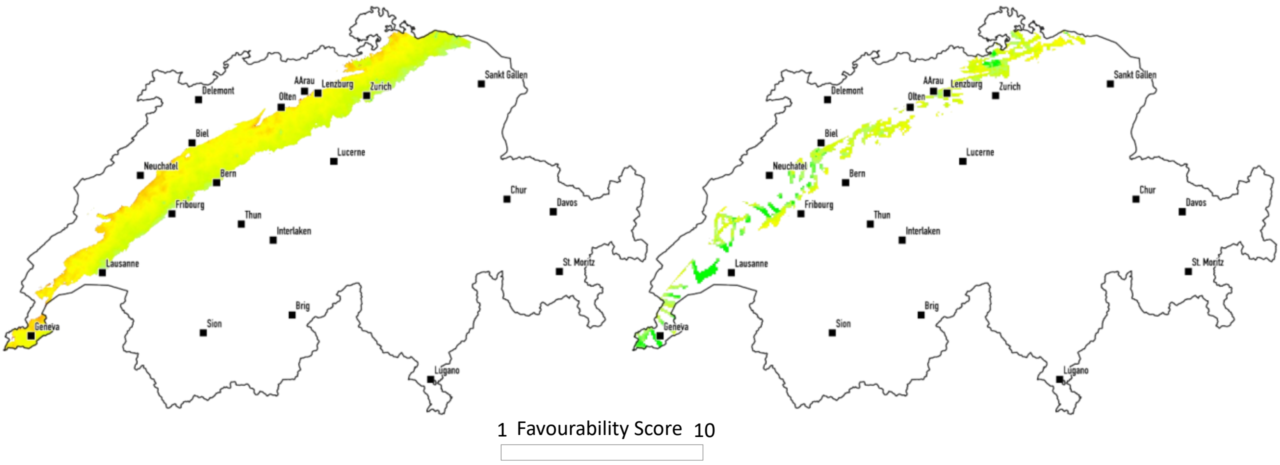

Figure XIV- Exemple de distributions de favorabilité HT-ATES pour le Cénozoïque (à gauche) et le Mésozoïque supérieur (à droite)

Cadre réglementaire pour les HT-ATES en Suisse

Le cadre réglementaire suisse a été analysé dans le but d'identifier le potentiel et les limites de son application aux systèmes HT-ATES. En Suisse, il n'existe pas de cadre réglementaire spécifique pour les systèmes HT-ATES et la législation suisse appliquée aux projets géothermiques est basée sur l'Ordonnance fédérale sur la protection des eaux, qui vise à protéger les eaux de surface et souterraines et à garantir que les différentes utilisations de l'eau sont durables. L'utilisation énergétique de l'eau peut avoir un impact négatif sur l'environnement immédiat, mais elle permet en même temps de substituer les énergies fossiles et agit ainsi contre le réchauffement climatique.

Dans ce cadre et pour permettre le développement de projets de géothermie profonde, quelques recommandations ont été proposées. Il pourrait être souhaitable de disposer d'une certaine souplesse pour déroger à certaines limites actuellement fixées et, dans le cas de projets de moyenne et grande profondeur en Suisse, il pourrait être intéressant de mettre en place un groupe de travail avec les porteurs de projets, les bureaux d'ingénieurs concernés, les cantons et la Confédération pour définir les limites du système et proposer des solutions de gestion, d'exploitation et de surveillance pour les nouveaux projets. A terme, les éléments analysés dans ce cadre pourraient permettre d'élaborer des directives pour les projets de moyenne/grande profondeur d'utilisation de la chaleur.

La comparaison des cadres réglementaires existants pour les systèmes HT-ATES dans plusieurs pays européens grâce au projet HEATSTORE a montré que les éléments clés suivants sont nécessaires pour un développement efficace des projets HT-ATES :

- Flux de travail clairs et bien définis entre les développeurs de projets et les autorités
- Cadre juridique existant au niveau national mais mis en œuvre et adapté au niveau régional par les autorités locales compétentes
- Bases de données publiques bien documentées, à jour et facilement accessibles
- Schémas de développement à long terme (master plans) au niveau régional basés sur une vision globale partagée et conduite par les autorités et les développeurs de projets
- Un suivi obligatoire des données de production (température, pression, pH, analyses d'eau, etc.) couplé à un processus approprié d'historisation basé sur un modèle thermo-hydraulique 3D du sous-sol mis à jour de manière itérative

Executive summary

The deployment of renewable energy sources (RES) for power and heat production is accelerating in Europe. However, the variations in both the availability and demand of energy and their integration into the existing energy infrastructure raise operational variability and balancing challenges. Peak shaving and heat storage can help balance demand and supply to make better use of infrastructure and assets (e.g., increase full load hours for geothermal heat sources). Thermal energy storage can, for example, be implemented in heating networks in the form of Underground Thermal Energy Storage (UTES) to support the use of surplus heat from industry and the implementation of renewable heat sources. UTES provides an intelligent and replicable solution for regions having a seasonal dip and peak in heating demand. UTES has the potential to provide large-scale (potentially >10 GWh) storage capacity per site that is difficult to achieve with other heat storage technologies and benefits from a typically lower range of storage costs.

HEATSTORE is one of nine projects under GEOTHERMICA - ERA-NET funded in 2018 for the period 2018-2021 and had the objective of accelerating the uptake of geothermal energy by 1) advancing and integrating different types of UTES in the energy system, 2) providing a means to maximize geothermal heat production and optimize the business case of geothermal heat production doublets, 3) addressing technical, economic, environmental, regulatory and policy aspects that are necessary to support the efficient and cost-effective deployment of UTES technologies in Europe. The project aimed to stimulate a fast-track market uptake in Europe, promote development from the demonstration phase to commercial deployment within 2 to 5 years and provide an outlook for utilization potential towards 2030 and 2050.

Twenty-three contributing partners from 9 countries form the HEATSTORE European consortium, composed of a mix of scientific research institutes and private companies. Industrial participation is considered a powerful and relevant advantage, which is instrumental for success. The combination of leading European research institutes and small, medium, and large industrial enterprises allowed testing and implementing technologies to be brought to market and valorized by the relevant stakeholders.

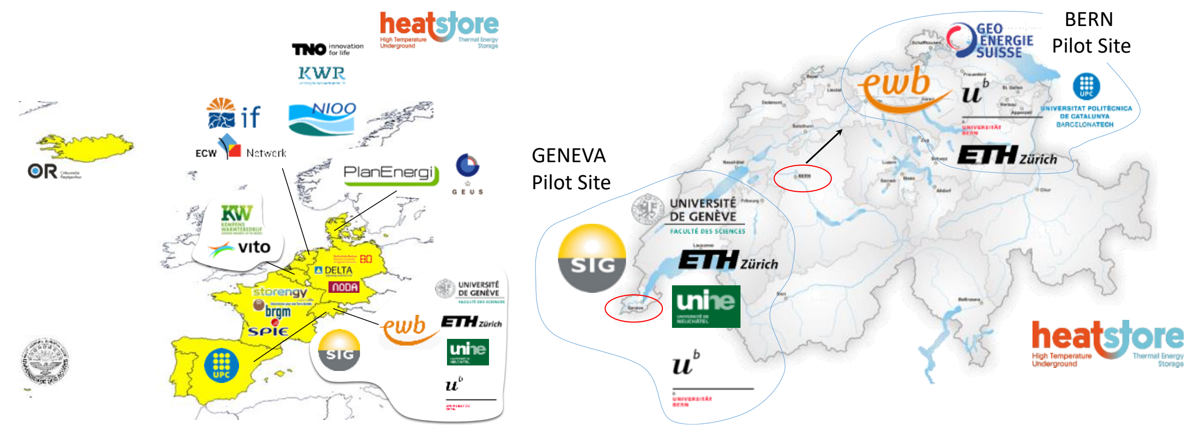

Figure I - Partners of the European and Swiss Consortiums

The Swiss partners collaborated on two case studies in Geneva and Bern and worked in close connection with European partners.

The Swiss HEATSTORE project had the following primary goals:

- Identifying the opportunities for implementation of high-temperature aquifer thermal energy storage (HT-ATES) in two of the most commercially viable reservoirs in the Swiss Molasse Plateau: the Cenozoic Molasse and the Upper Mesozoic carbonates

- Implementing a multi-criteria decision-making analysis framework to predict and assess the techno-economic feasibility of HT-ATES in Switzerland
- Identifying solutions for optimizing the performances of HT-ATES technologies and integrating them within complex energy systems configurations
- Predict and validate HT-ATES techno-economic performance via data collected at two pilot sites in Geneva and Bern
- Identifying the environmental effects associated with the implementation of HT-ATES systems and the regulatory framework barriers to be overcome.

These objectives contribute to the final goal of HEATSTORE Switzerland, to advance the commercial viability of HT-ATES technologies so that geothermal energy, combined with an optimized through underground heat storage, can reach its maximum deployment potential in the Swiss energy transition.

The Swiss project focused on assessing the feasibility of HT-ATES systems at two sites in Geneva and Bern. The two sites present different peculiarities regarding subsurface conditions and energy system configuration. In Geneva, the excess heat source is a waste incineration plant with discharge temperature up to 120˚C, the targeted storage aquifer is in the fractured Mesozoic carbonates between 450 and 1500m at depth, and the operating temperature of the district heating network is between 70 and 120˚C. In Bern, the excess heat source is a combined-cycle plant, waste-to-energy plant, wood-fired power station plant with discharge temperature up to 120˚C, and the targeted storage aquifer, the Cenozoic Molasse sediments. The operating temperature of the district heating network is around 90˚C.

The Geneva and Bern sites reflect most of the subsurface and energy system configurations considered suitable for aquifer thermal energy storage that can be found in other cities over the entire Swiss Molasse Plateau.

The report provides a comprehensive overview of the activities carried out at the Geneva and Bern sites. Both projects can be considered completed.

The Geneva site

In Geneva, the case study focused on the feasibility assessment of excess heat storage discharged from a waste incineration plant at temperatures up to 120˚C (section 5.1) in the Mesozoic fractured carbonates at a depth between 450 and 1500m. The multi-criteria assessment framework implemented is based on techno-economic criteria in order to:

- Assess the technical potential of storing heat in the reservoir by integrating surface and subsurface data
- Identify the environmental effects associated with storage and production operations
- Assess the link between storage/recovery outputs with economic performances under different technical configurations

The framework based on a stepwise approach initially combined subsurface and energy system constraints using the data available at the beginning of the project. As new data and results become available during the project, it has eventually been calibrated and validated according to the data resulting from the subsurface exploration activities carried out by drilling the GEo-01 and GEo-02 wells and the 2035 energy system development scenarios.

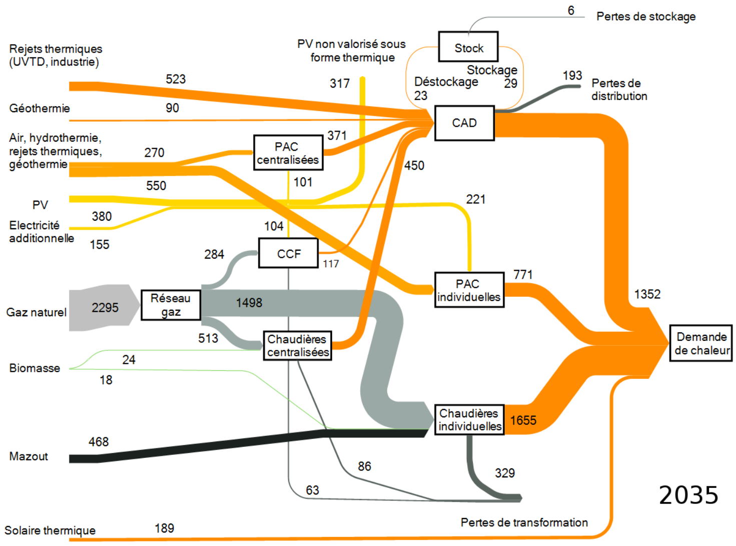

Figure II - Energy system in Geneva, scenario 2035

Both wells targeted the upper Mesozoic limestones. The drilling results contributed to understanding reservoir architecture and petrophysical/hydraulic properties distribution and highlighted the strongly heterogeneous hydraulic properties of the Mesozoic carbonates across the Geneva area. GEo-01, 744 m deep, delivers 34˚C water at 55l/s at 8-10 bars wellhead pressure, whereas GEo-02 delivers 18˚C wellhead temperature (~55˚C bottomhole temperature) at 0.3 l/s and 10-12 bars wellhead pressure.

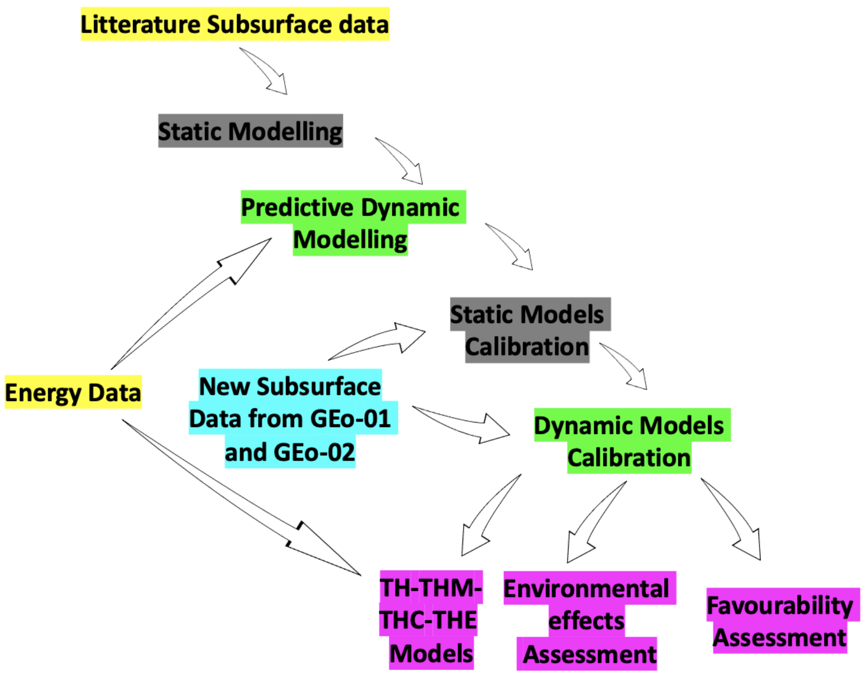

Figure III - Workflow of the HEATSTORE project applied to the Geneva site

In terms of subsurface characterization, a set of 3D models were produced starting from static models, which allowed capturing the geometry and the distribution of the petrophysical and hydraulic properties of the investigated reservoirs (see full report sections 5.1.2, 5.1.3, 5.1.6). The computed models integrated the available geophysical and petrophysical during the different phases of the project. The overall approach is based on the baseline that 3D static models serve as inputs, in integration with energy system information, to produce dynamic models (thermo-hydraulic TH, Thermo-hydraulic-mechanic THM, or HM, thermo-hydraulic-chemical THC, and Thermo-hydraulic- economic THE) to predict the performance of HT-ATES systems in Geneva. The results for the static modeling derive from the interpretation of several vintage 2D seismic reflection datasets, well logs from GEo-01 and GEo-02, well reports, and outcrop analogs. Seismic interpretation reveals a well-developed flower structure deforming the Mesozoic and parts of the Cenozoic sediments in the GEo-01 area. The subsurface structural situation around the GEo-02 site is different, comprising a thrust faults system and associated normal faults deforming the Cenozoic and Mesozoic sediments. Petrophysical analysis suggests the Lower Cretaceous Formation in the GEo-01 area is tight, generally characterized by low porosity and permeability values. However, the presence of fracture networks and faults deforming a substantial part of this unit may promote localized fluid circulation. In the GEo-02, well test results suggest that the formations within the Mesozoic succession have low fluid flow and weak hydraulic properties.

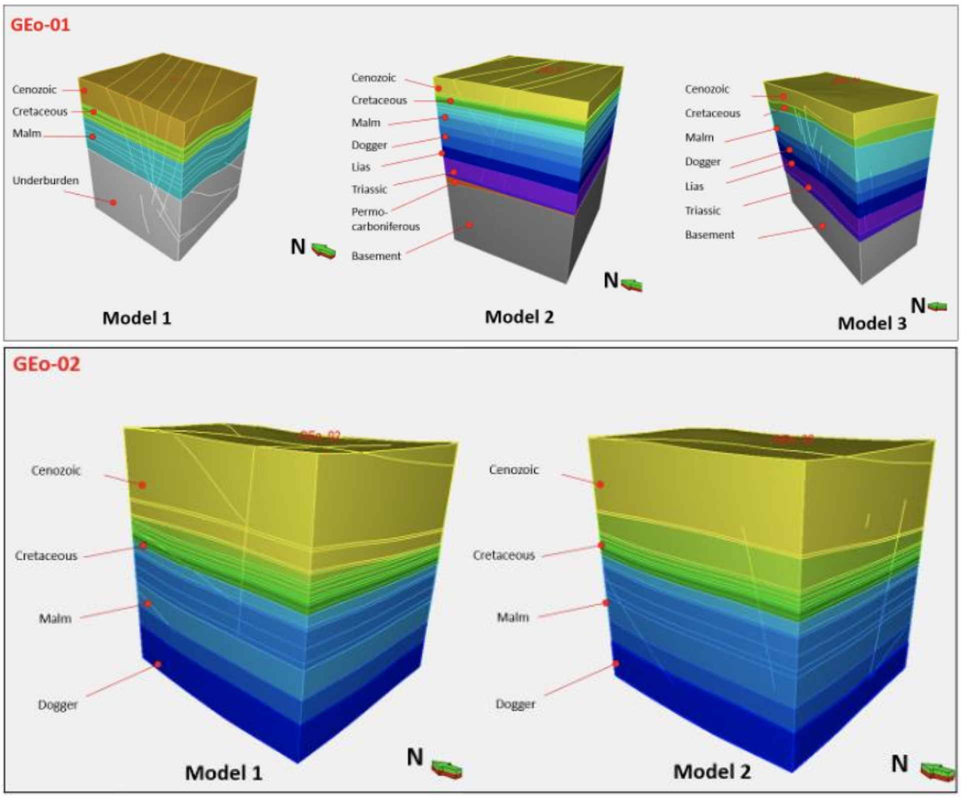

Figure IV- 3D static models for the GEo-01 and GEo-02 areas

Subsequently, dynamic Thermo-Hydraulic (TH) and Hydro-Mechanic (HM) developed integrating static models to energy system data (e.g., excess heat temperature, recovery temperature, utilization of heat pumps, excess heat, and heat demand temporal distribution) allowed producing HT-ATES operational scenarios (see section 5.1.7). Initially, all models were based on available literature data, allowed for the set-up of the entire modeling workflow "from static to dynamic" and provided the first set of predictions for the behavior of the HT-ATES system. Following the availability of new data from the two exploration wells, these models were calibrated and validated to produce a set of more reliable and realistic scenarios capturing the prediction of the fluid flow in the reservoir and the quantification of the potential soil mechanics effects (ground deformation) due to operations. A numerical discretization approach (e.g., Finite Elements, Finite Volumes) was used for TH models to create a solution algorithm that will provide the necessary discrete solution for our simulations. The conceptual model addressed scenarios of interest linked to local geological and hydrological conditions. These scenarios include modeling the influence of groundwater flow and geologic heterogeneity (i.e., presence of fractures and faults, reef structures) on the storage and recovery capabilities of the system.

Example of the results from TH modeling at GEo-01 and GEo-02

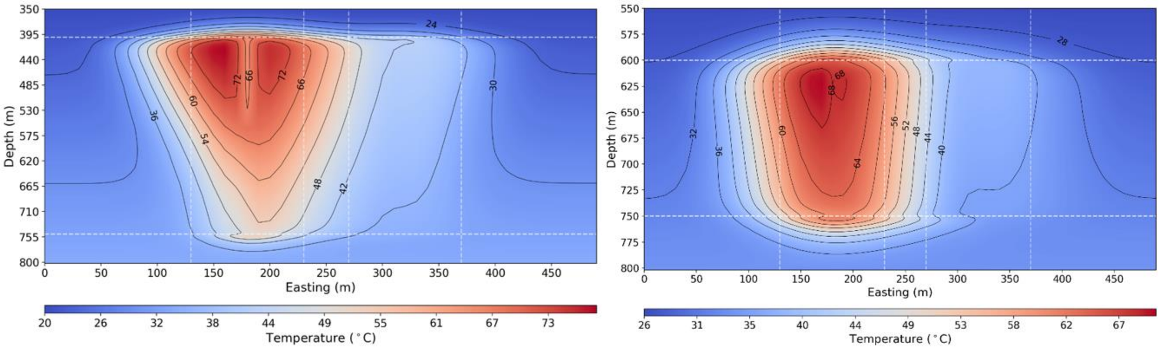

Example of the results from THM modeling for the Geneva sites

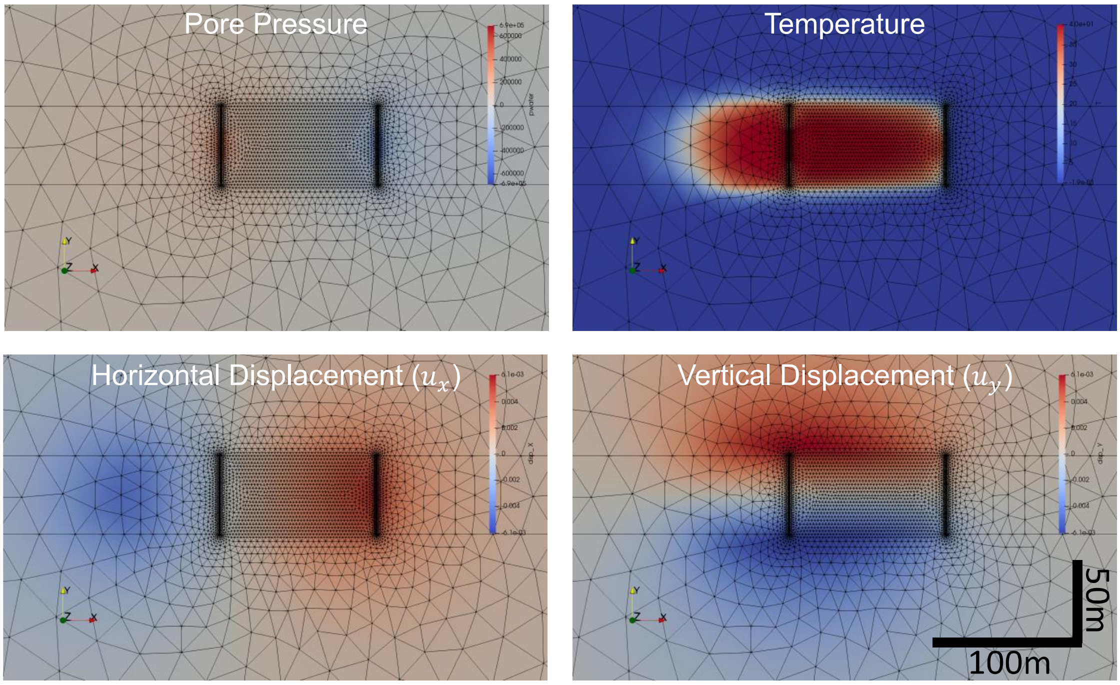

Figure V- Examples of results from TH and THM modelling for the Geneva area

Geochemical investigations were performed to assess the potential activation of water-rock interaction mechanisms that can affect the reservoir properties due to dissolution and precipitation of minerals across the reservoirs and the corrosion/scaling potential on surface equipment (see sections 5.1.8 5.1.9.3 and Appendix 7 for a detailed report). Reservoir water samples were collected, and their chemical composition was analyzed and combined with the results of the mineralogical analysis performed on wellbore cuttings and cores. Additionally, the project partners conducted laboratory experiments and kinetic modeling to reproduce the HT-ATES conditions and the chemical effects on reservoir water variations during HT-ATES operations. The results reveal that carbonate mineral dissolution and precipitation can occur during operation. A risk of precipitation in sectors of the reservoir can lead to its compartmentalization reducing the storage systems' performances. The suspended load discharged by GEo-01 was also analyzed, revealing that a combination of sulfate minerals and microbial community, in particular Methanobacteria, forms an essential class in the samples. Based on the results of this study, the following main effects can occur during long-term operations:

- Owing to their retrograde solubility (i.e., decreasing solubility with increasing temperature), carbonates such as calcite will likely precipitate when the waters heat up to 90°C during storage cycles. The carbonate mineral precipitation could impede flow and heat exchange in the surface installations.
- In the case of the water produced from GEo-01, corrosion of technical installations such as pumps, casings, and heat exchangers may occur due to the high sulfide concentration. This could lead to material failure and operational problems.

To evaluate alternatives regarding the economic viability of HT-ATES systems in Geneva, we combined the results from modeling with energy system data to evaluate the storage scenarios prone to techno-economic success. The results show that subject to subsurface constraints, the nominal capacity ranges from 0.4 MW to 81 MW, with aquifer permeability and thickness being the significant control variables. A minimum transmissivity of 2.5 $\times 10^{-12}$ m^3 is required to keep the Levelized Cost of Heat (LCOH) below 200 CHF/MWh, and a capacity of 25 MW or higher is needed for the HT-ATES system to become competitive with other large-scale DHN heat sources. The capacity increases from the addition of Heat Pumps (HP), which incurs non-recoverable costs and increases the LCOH. Nonetheless, the addition of HP increases the nominal capacity of the system and results in higher cumulative avoided CO_2 emissions.

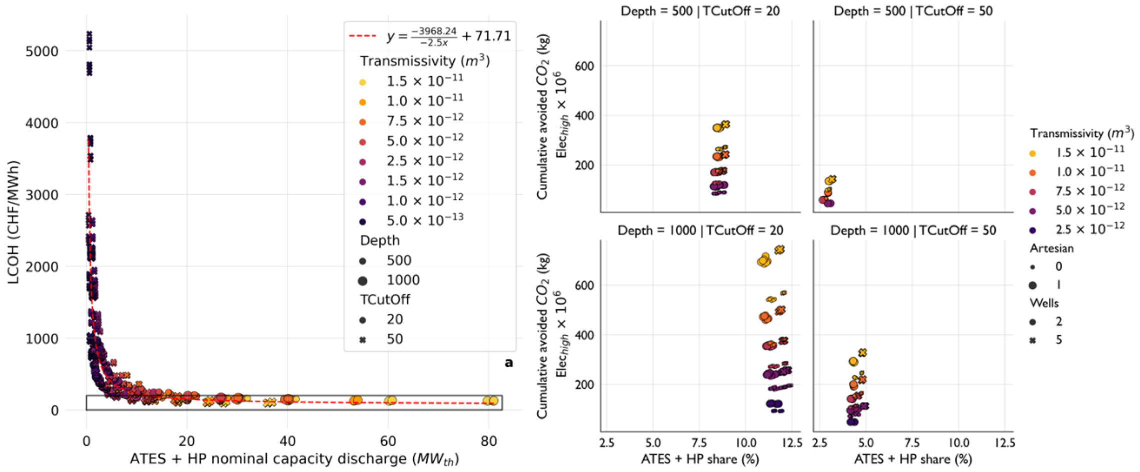

Figure VI: Left: LCOH against nominal production capacity colored by reservoir transmissivity, sized by depth and temperature cut-off Right: ATES share and cumulative avoided CO2 emissions for the simulations with an LCOH below 200 CHF/MWh

A fast-track environmental effects assessment (Appendix 18) allowed identifying the environmental effects associated with the drilling phases and the HT-ATES operations at the GEo-01 and GEo-02 well sites. The effects during drilling were identified and assessed according to the activities carried out by SIG before, during, and after drilling operations. In contrast, the effects associated with HT-ATES operations have been identified and assessed via data acquisition, predictive modeling, and monitoring. The results reveal that risks associated with drilling operations are low to medium and limited in time. High risks during HT-ATES operations are only associated with the variations of reservoir water compositions without affecting shallow freshwaters. The implementation of HT-ATES will reduce the heating sector's carbon intensity.

GEo-01												
Phase / Effect	Drilling						Operations (predicted)					
	P	A	M	Probability	Consequences	Risk	P	A	M	Probability	Consequences	Risk
Air quality				H	L	M				L	L	L
Noise and vibration				H	L	M				M	L	L
Formation water quality				L	L	L				H	M	H
Formation water temperature										H	L	M
Surface clear water				H	L	M				L	L	L
Soil occupation				H	L	M				H	L	M
Wastes and dangerous substances				H	L	M				M	L	L
Environment				M	L	L				L	L	L
Nature				M	L	L				L	L	L
Soil mechanics										L	L	L
Seismicity				L	H	M				L	H	M
CO2 intensity redyction										H	M	H

GEo-02												
Phase / Effect	Drilling						Operations (predicted)					
	P	A	M	Probability	Consequences	Risk	P	A	M	Probability	Consequences	Risk
Air quality				H	L	M				L	L	L
Noise and vibration				H	L	M				M	L	L
Formation water quality				L	L	L				H	M	H
Formation water temperature										H	L	M
Surface clear water				H	L	M				L	L	L
Soil occupation				H	L	M				H	L	M
Wastes and dangerous substances				H	L	M				M	L	L
Environment				M	L	L				L	L	L
Nature				M	L	L				L	L	L
Soil mechanics										L	L	M
Seismicity				L	H	M				L	H	M
CO2 intensity redyction										H	M	H

Figure VII - Fast-track risk assessment for HT-ATES in Geneva

The challenging subsurface conditions for the selected storage system in Geneva did not allow carrying out injection/recovery tests at GEo-01 and GEo-02. Therefore, a field lab in Concise (VD) has been implemented to demonstrate whether heat storage and recovery can be an option for fractured carbonates (Section 5.1.5). Three wells drilled at 50m at depth reached the same Upper Mesozoic carbonates drilled by GEo-01 and GEo-02, and hydrogeological, hadrochemical, petrophysical, borehole logging, thermo-hydraulic testing operations were performed to assess the storage performances of the investigated reservoir. The development of the Concise test site has enabled the application of methods for hydraulic and thermohydraulic characterization of karst and fractured reservoirs, combining field testing and modeling.

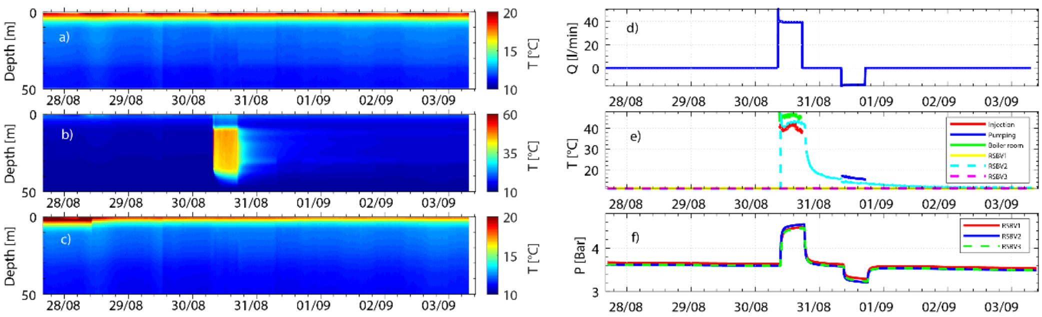

Figure VIII - Temperature variations measured at the Concise wells during field thermo-hydraulic tests as a function of flow rates, injection temperature, pumping temperature, and pressure

These results highlight the importance of explicit consideration of reservoir structures to obtain robust thermal-hydraulic responses and provide the basis for recommendations for the development and characterization of deep heat storage systems.

The Bern site

In Bern, options for storing excess heat from the Forsthaus waste-to-energy plant (WTP) at depths of up to 500 meters were planned and tested (Section 5.2). The Bern site served as a pilot facility in a typical molasse sandstone reservoir (“Rinnengürtel sandstones” of the Lower Freshwater Molasse) to test and optimize, for the first time under real-world conditions, the options and characteristics of a geothermal storage facility in these rock formations—which are widespread across the Swiss Plateau.

The aim of the project was to investigate the feasibility and risk-reduction options for utilizing a Molasse sandstone reservoir. To this end, three boreholes were drilled in the immediate vicinity of the power plant, and the test operations in the reservoir were monitored. The results will help ewb obtain the information on the properties of the Rinnengürtel sandstones necessary for final planning and—depending on the results—fully implement the HT-ATES after project completion.

The conceptual plan called for feeding hot water from the plant into the system seasonally and then, during periods of increased demand in winter, recovering the stored thermal energy and feeding it into the district heating network without the need for a heat pump. Hot water was fed into the system for approximately 200 days via the main well located at the center of the system. During the discharge cycle, the same central well was used for hot water production. Simultaneous pumping to and from the auxiliary wells served to regulate the flow at the system boundaries, thereby balancing the pressure in the reservoir during injection and production. A 20-year lifespan is assumed for the HT-ATES system *Geospeicher Forsthaus*.

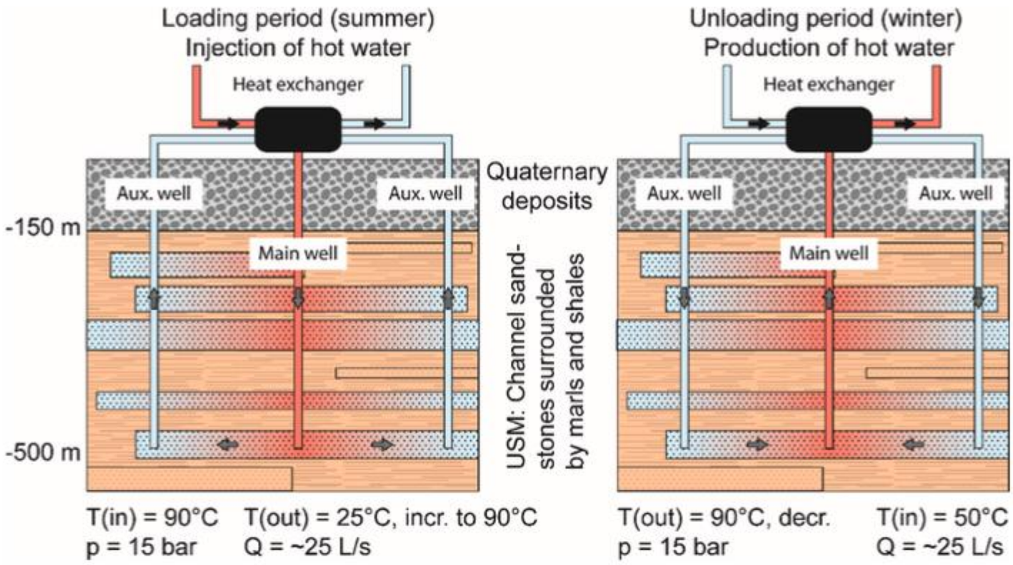

Figure IX – Schematic depiction of the operational design and planned operational parameters of the HT-ATES pilot project Geospeicher Forsthaus

Preliminary geological and geochemical studies were conducted, which identified potential targets in the Lower Freshwater Molasse within the sequence of overlying medium- to coarse-grained sandstones of the channel belts. These are the classic sediments deposited in the central section of the channel belts, capable of forming coherent, homogeneous sandstone bodies several kilometers long, 150–1,500 m wide, and 2–15 m thick.

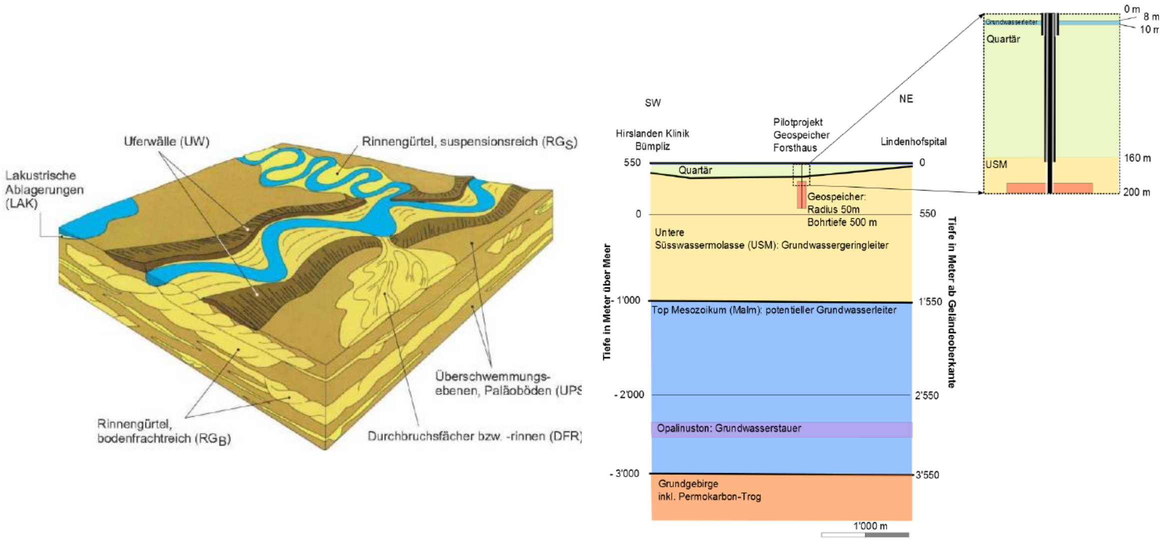

Figure X – Left: Cartoon showing the different facies for the USM; Right: Geological cross-section down to the deeper subsurface of the planned geothermal storage facility

These sandstone bodies, which are ideally highly permeable, alternate with poorly permeable, fine-grained sediments in the channel belt (Figure X). This results in very good hydraulic sealing of the channel belt units—one of the basic prerequisites for a thermal storage facility. The stored hot water cannot therefore flow out of the sandstone layers. Since no site-specific geological data was available, it was not possible at the start of the project to accurately assess the storage volume and depth, the petrophysics and hydraulic properties, or the hydrogeological regime in the study area. The most significant unknowns were:

- presence or absence of the sandstones in any given vertical section of the USM
- 3D geometries and dimensions of the sandstones
- porosity, permeability, mineral content, and degree of calcite cementation in the sandstones
- the extent to which individual sandstone layers are hydraulically connected (versus hydraulically compartmentalized by interlayered silt- and claystone).
- velocity and direction of groundwater flow groundwater properties: salinity, solute composition (especially pCO_2), and microbial activity
- concentrations in the groundwater of the corrosion-inducing components H_2S, SO_4, Cl, and microbes

Preliminary laboratory experiments on geochemical water-rock interactions and THC modeling were conducted (Appendix 08).

Three boreholes were drilled consecutively from the same drilling pad. The “Marriott Rig 18” drilling rig was transported to the site, and drilling began on October 21, 2022. The third borehole was successfully completed on April 1, 2023.

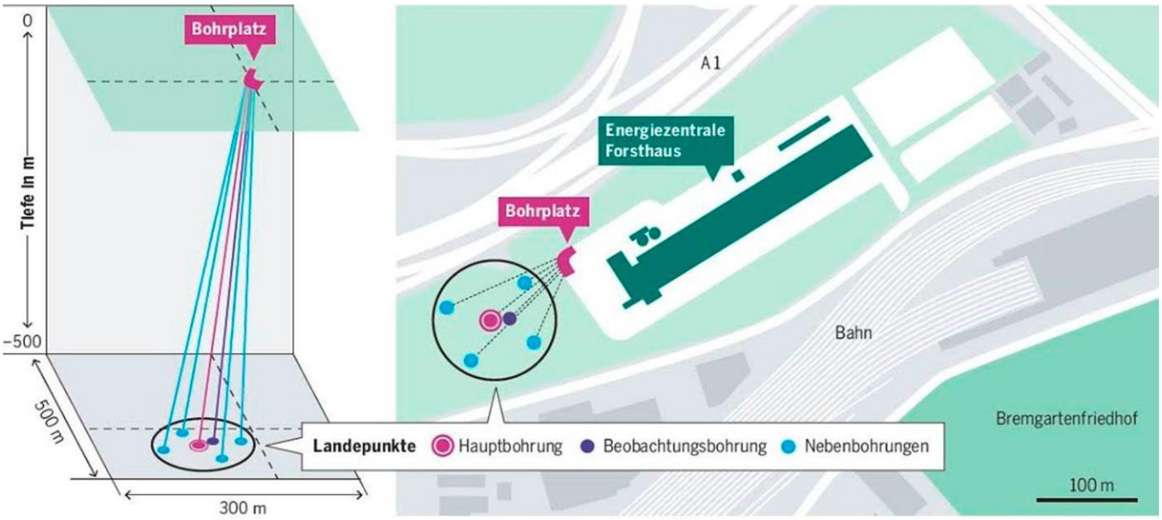

Figure XI - Sketch of the 6 planned boreholes for the pilot project Geospeicher Forsthaus

Drilling conducted as part of the project revealed that the site is covered by a Quaternary sediment layer approximately 240 m thick, which is about 80 m thicker than previously assumed. Beneath this, sediments of the Lower Freshwater Molasse (USM) were encountered to a depth of approximately 520 m, with a thickness of about 280 m. These sediments document a heterogeneous, formerly meandering fluvial depositional system in the Alpine foreland, consisting of sandstones, siltstones, flood deposits, and paleosols. Within the USM, several laterally continuous sandstone intervals were identified that are considered potential reservoir horizons for thermal storage. The sandstones generally exhibit suitable porosity and permeability properties, although their permeability may be locally reduced by calcite cementation.

Compared to other sites in the central Molasse Basin, the Forsthaus boreholes show similar sedimentological and petrophysical properties, although the permeabilities are in some cases slightly lower.

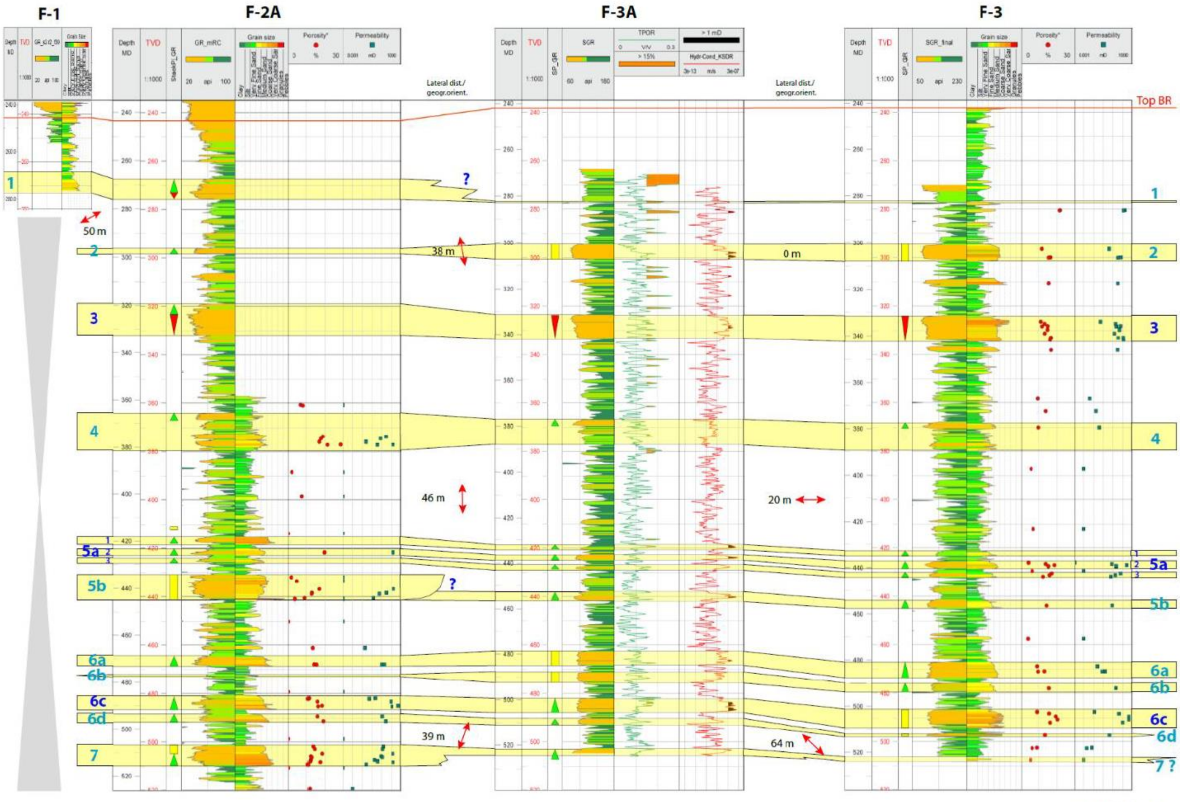

Figure XII - Correlation of the most important reservoir units in the studied USM based on gamma-ray measurements and grain-size profiles.

A representative sandstone layer in the lower section of the wells was selected to connect the wells to the reservoir and for its development. This was intended to ensure that, in the event of technical problems, it would be possible to switch to a higher-lying sandstone layer without major difficulties. The choice fell on zone 6c at a depth of 485 m, as it exhibits, among other things, good horizontal continuity and moderate hydraulic permeability.

First, the cemented casing in F2 was drilled open using micro-sidetracks, which were drilled horizontally up to 5 m deep into the sandstone zone. Care had to be taken to avoid damaging the fiber-optic cable, which is cemented in place along the casing between the casing and the formation. Injectivity was tested after each new micro-sidetrack. Subsequently, a double-packer system was installed in F2 to keep the test volume as small as possible and to isolate the micro-sidetracks from the rest of the wellbore volume.

After installation, the pressure in sandstone layer 6c was monitored before and during the drilling of the micro-sidetracks in F3. Initially, the pressure dropped before the first micro-sidetrack was drilled in F3 and hydrant water was injected through it at a constant rate for about a week. As a result of the injection into F3, the pressure in F2 rose slowly. Analysis of the pressure rise curve made it possible to evaluate the hydraulic connection between the two boreholes, derive representative values for permeability, and analyze the flow behavior. After all micro-sidetracks had been drilled in F3, a second double-packer system was installed. Subsequently, pressure step tests, also known as “hydraulic jacking tests,” were conducted in both boreholes. At an injection pressure above the vertical rock stress, horizontal, permeable zones opened up within the sandstone layers. Once this pressure was reached, injection could be carried out at disproportionately high injection rates. The dataset, consisting of pressures in the injection borehole and the observation borehole as well as strain measurements on the fiber-optic cable along the casing in F2, allowed for significant conclusions to be drawn regarding the hydrogeomechanical behavior of the sandstone layer.

It was also found that the permeability of the sandstone layer had permanently increased by a factor of 2. However, this increase was not sufficient to enable the economical operation of a thermal storage facility. During the pressure-step tests, microseismicity was monitored using a seismometer temporarily installed at the surface, and any potential uplift and subsidence were recorded by the permanent monitoring system.

Despite the low transmissivity, a dipole flow field was established between the boreholes and maintained for more than two months. To achieve this, hydrant water was injected into F3 at a rate of 8 l/min, while 2 l/min flowed freely out of F2. Hydrogeochemical parameters were measured online, and water samples were collected for laboratory analysis at the University of Bern.

After the drilling fluid introduced during drilling was completely extracted from the formation, natural formation water was detected. After about two months, the chemical signature of the hydrant water injected into F3 was detected for the first time. The long-term circulation test could therefore also be evaluated as a tracer test. Even before the hydrant water began to seep through slightly, the company Hydroisotop conducted water sampling for ^{81}Kr analysis to determine a model age for the formation water.

After completing the hydrogeochemical characterization, an experiment was initiated to acidify the most permeable flow paths using CO_2 dissolved in water, with the aim of increasing transmissivity. Over several weeks, approximately 5.5 tons of CO_2 were injected into F3 while borehole F2 remained closed. Subsequently, the dissolved calcite was flushed out by injecting hydrant water into F2. The water emerging from F3 was sampled at regular intervals by the University of Bern.

After the majority of the calcite had been flushed out by the end of 2024, hydraulic tests were conducted again to determine the change in transmissivity. The extensive hydrogeochemical dataset was analyzed by the University of Bern using a numerical hydrogeochemical-hydraulic model. The carefully calibrated model conceptually aligns well with the data collected to date regarding the sandstone formation and the geometry of the reservoir connection to the micro-sidetracks.

The investigations conducted during the project show that, in principle, the requirements for a geothermal storage system at Forsthaus Bern are largely met. However, insufficient permeability represents the greatest obstacle to the economic operation of a storage facility.

Spatial Multi-Criteria Analysis for HT-ATES favorability in Switzerland

Being a multi-dimensional concept, the assessment of favorability of HT-ATES performed in HEATSTORE was based on the aggregation of a set of techno-economic criteria via Spatial Multi-Criteria Analysis (SMCA). However, the techno-economic performances of HT-ATES are characterized by geologic (Play elements) and geographic characteristics, which are variable across the Swiss Plateau. The focus on the Swiss Plateau was driven by the public data availability and the fact that the vast majority of the excess heat and heat demand is concentrated in this region. The work carried out in this task comprises the implementation of a spatial multi-criteria play-fairway framework focusing on the potential of implementation of HT-ATES systems in two main geologic units: the Cenozoic sediments (i.e., the target of the Bern project) and the fractured Upper Mesozoic carbonates (i.e., the target of the Geneva project). Subsurface data include the geometry of the target geologic units down to 2000m at depth, their range of density, porosity, permeability values, fault distribution, and regional stress. Surface constraints, including the geographical distribution of excess heat, heat demand, district-heating networks, and waste-incineration plants, have been incorporated into the analysis framework to produce maps portraying different HT-ATES favorability scenarios. At this stage, economic constraints considered the concept of minimal economically viable transmissivity of the target reservoir, which threshold value set to 5x10-13m3 contributed to identifying the most favorable areas.

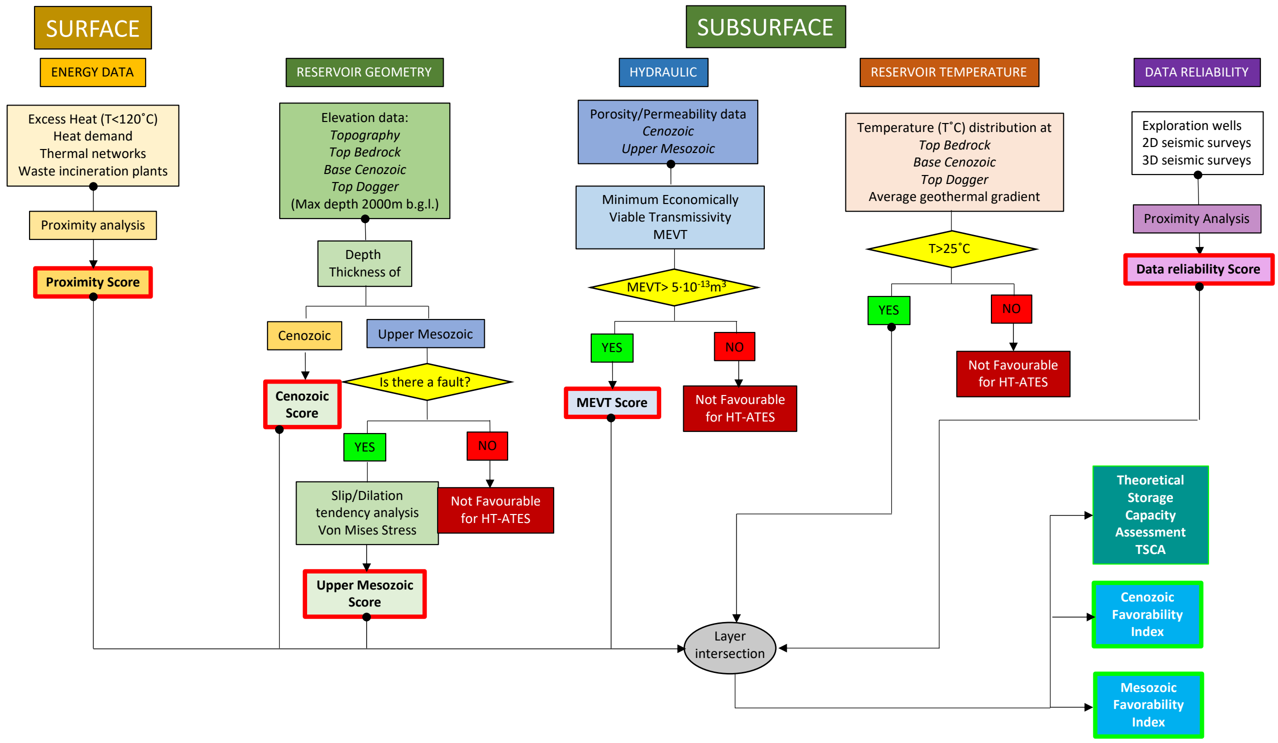

Figure XIII – Framework implemented for HT-ATES SMCA in Switzerland

The results show that the Cenozoic has some high storage potential in the central and southern portions of the Molasse Plateau area, where some major cities are located (Zurich, Bern, Lausanne) if permeability higher than 300mD will be identified. Additionally, these portions of the Plateau are also characterized by the large thickness of the Cenozoic, hence their hydraulic transmissivity. It must be pointed out that in this study, we considered as a potential reservoir the entire thickness of the Cenozoic sediments. However, we know large vertical and lateral lithological heterogeneities characterize this Unit, and only part of the entire Cenozoic sequence is suitable for storage. Therefore, a more detailed net-to-gross assessment will allow accurate screening at a site-specific scale of the actual volumes having effective porosity and adequate permeability.

The Upper Mesozoic assessment focused only on the fault corridors cutting the Swiss Plateau as it is well known that the matrix porosity and permeability of the carbonates are very low. Therefore, an analysis of the Slip and Dilation tendencies and the Von Misses Stress was computed based on the regional stress data available. According to the results from the scenario modelling applied to the upper Mesozoic carbonates, only the scenarios resulting from faults' permeabilities distributions between 3.5 and 350 mD can be considered promising targets. According to the data available, fault structures can be suitable as targets in Aarau, Biel, and Geneva. However, as demonstrated by the GEo-01 well in Geneva, high permeabilities characterizing fault corridors lead to high wellhead pressure and natural artesian flow, therefore, a limiting factor for storage. A more detailed characterization of the hydraulic properties of the fault structures will be necessary for future studies to improve such type of assessment.

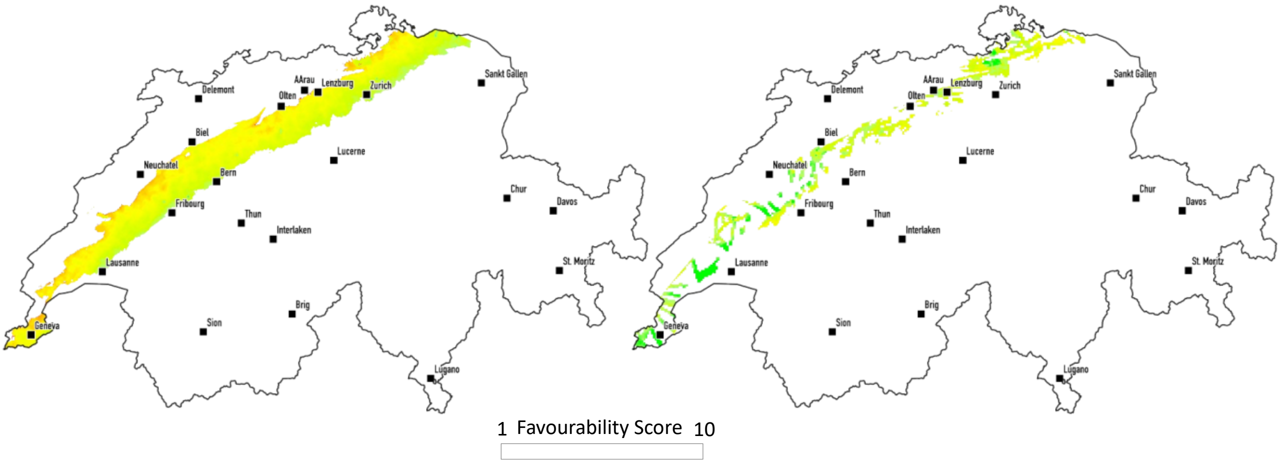

Figure XIV- Example of HT-ATES favorability distributions for the Cenozoic (left) and the Upper Mesozoic (right)

Regulatory framework for HT-ATES in Switzerland

The Swiss regulatory framework was analyzed with the goal to identify the potential and the limitation of its application to HT-ATES systems. In Switzerland there is not a specific regulatory framework for HT-ATES systems and the Swiss legislation applied to geothermal project is based on the Federal Ordinance on Water Protection, which aims at protecting surface and ground water and to ensure that the various uses of water are sustainable. The energetic use of water can have a negative impact on the immediate environment, but at the same time it allows the substitution of fossil fuels and thus acts against global warming.

Within this framework and to enable the development of deep geothermal projects, some recommendations have been proposed. It might be desirable a certain degree of flexibility to derogate from certain current limits set, and in the case of medium to deep projects in Switzerland, it might be interesting to set up a working group with project leaders, the engineering offices involved, cantons and the Confederation to define the limits of the system and to propose management, operating and monitoring solutions for new projects. Ultimately, the elements analyzed in this framework could make it possible to draw up guidelines for projects with medium/large depths of heat use.

The comparison of existing regulatory frameworks for HT-ATES systems across several European countries thanks the HEATSTORE project has shown that the following key elements are necessary for an efficient development of HT-ATES projects:

- Clearly and well-defined workflows between project developers and authorities
- Existing legal framework on national level but implemented and adapted on a regional level through local competent authorities
- Well documented, up to date, and easily accessible public databases
- Long term development schemes (masterplans) on a regional level based on a global vision shared and driven by both the authorities and project developers
- Compulsory monitoring of production data (temperature, pressure, pH, water analyses, etc.) coupled to an appropriate history-matching process based on an iteratively updated 3D thermo-hydraulic model of the underground

Contents

Abbreviations

ALT: Advanced Logic Technology

APW: Artificial Pore Water

ATES: Aquifer Thermal Energy Storage

BTES: Borehole Thermal Energy Storage

COP: Coefficient Of Performance

DHN: District Heating Network

HEx: Heat Exchangers

HT: High Temperature

LCOH: Levelized Cost Of Heat

MD: Measured Depth

MTES: Mine Thermal Energy Storage

PTES: Pit Thermal Energy Storage

TH: Thermo-Hydraulic

THC: Thermo-Hydraulic-Chemical

THE: Thermo-Hydraulic-Economic

THM: Thermo-Hydraulic-Mechanical

TVD: True Vertical Depth

UTES: Underground Thermal Energy Storage

1 Introduction

HEATSTORE is one of nine projects under GEOTHERMICA - ERA NET funded in 2018 for the period 2018-2021 and had the objective of accelerating the uptake of geothermal energy by 1) advancing and integrating different types of underground thermal energy storage (UTES) in the energy system, 2) providing a means to maximize geothermal heat production and optimize the business case of geothermal heat production doublets, 3) addressing technical, economic, environmental, regulatory and policy aspects that are necessary to support efficient and cost-effective deployment of UTES technologies in Europe. The project aimed at stimulating a fast-track market uptake in Europe, promoting development from demonstration phase to commercial deployment within 2 to 5 years, and provide an outlook for utilization potential towards 2030 and 2050.

23 contributing partners from 9 countries form the HEATSTORE European consortium which is composed of a mix of scientific research institutes and private companies (Figure 1). The industrial participation is considered a very strong and relevant advantage, which is instrumental for success. The combination of leading European research institutes together with small, medium, and large industrial enterprises, allowed testing and implementing technologies to be brought to market and valorized by the relevant stakeholders.

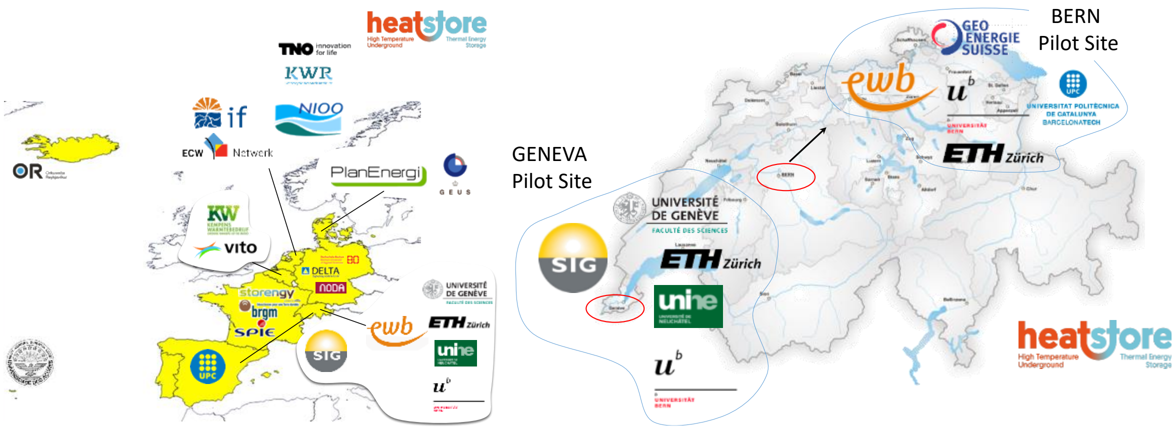

Figure 1 - Partners of the European (left) and Swiss (right) consortia

The Swiss partners collaborated on the two Swiss case-studies in Geneva and Bern and worked in close connection with European partners (Figure 1). The two Swiss case studies focused on High-Temperature Aquifer Thermal Energy storage.

1.1 Background information and current situation

The deployment of renewable energy sources (RES) for both power and heat production is accelerating in Europe, a trend that will continue. However, the variations in both the availability and demand of energy and their integration into the existing energy infrastructure raise challenges in terms of operational variability and balancing. Peak shaving and heat storage can help to balance demand and supply to make better use of infrastructure and assets (e.g., increase full load hours for geothermal heat sources). Thermal energy storage can, for example, be implemented in heating networks in the form of Underground Thermal Energy Storage (UTES) to support the use of surplus heat from industry and the implementation of renewable heat sources such as bio-Combined Heat and Power (CHP), geothermal, and solar energy. UTES provides a smart and replicable solution for the 'bathtub challenge' (Fig. 1) for regions that have a seasonal dip and peak in heating demand.

Underground thermal energy storage (UTES) provides large scale (potentially >10 GWh) storage capacity per site that is difficult to achieve with other heat storage technologies, and benefits from a typically lower range of storage costs.

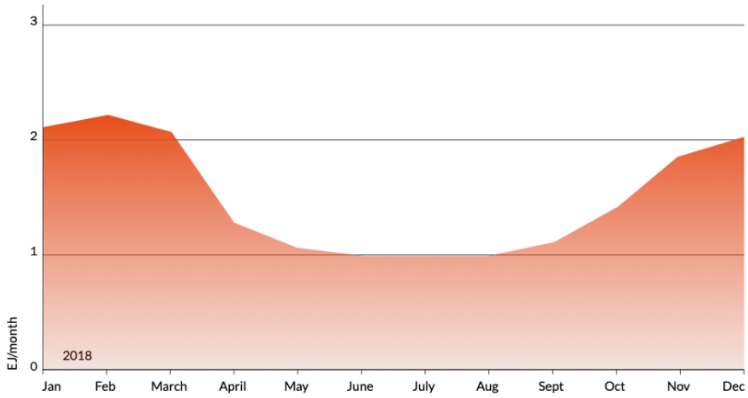

Figure 2 - The ‘bathtub’ challenge: how are we going to meet the heating demand with a distinct seasonal profile without fossil fuels but with the same security of supply? Here the bathtub is represented by the Natural gas demand in Europe (Source Eurostat, 2019)

Challenges highlighted for UTES technologies defined in the EASE-EERA energy storage technology roadmap towards 2030 (EASE/EERA, 2017) include the need to assess the potential and suitability of the subsurface in Europe. This includes research and demonstration regarding high temperature storage systems and hybrid UTES systems to increase capacity, efficiency, and alignment with renewable heat production technologies (solar heat, geothermal heat, biomass heat). Optimized control of heat networks with UTES can lead to energy savings and reduce the use of back-up systems. The Horizon 2020 STORM project indicates that the employment of a smart heat network controller can reduce peak demand with 20 to 30% (Mijnwater, 2015). In combination with thermal storage capacity, demand side management in heating networks is an enabling technology for many renewable heat sources, including geothermal.

A review of experiences and lessons learned on Underground Thermal Energy Storage (UTES) systems from the participating EU project partners is provided in ***D1.1 Underground Thermal Energy Storage (UTES) – state-of-the-art, example cases and lessons learned*** of the HEATSTORE European project in ANNEX1.

Currently known UTES concepts include ATES (Aquifer Thermal Energy Storage), BTES (Borehole Thermal Energy Storage), PTES (Pit Thermal Energy Storage), and MTES (Mine Thermal Energy Storage) (Lee, 2013).

1.1.1 Aquifer Thermal Energy Storage ATES

ATES can take place by injection and later re-production of hot water in reservoirs in both deep and shallow geological formations and the reservoirs can be both unconsolidated sand units, porous rocks like sandstones or limestone or e.g., fractured rock formations. Deep reservoirs provide an option for high temperature storage (HT), while the injection temperature in shallow aquifer units in the upper few hundred meters of the subsurface in most countries will be restricted to a few tens of degrees Celsius (Danish Energy Agency, 2014).

Known technical challenges mainly include high return temperatures on the surface site and hydrogeochemical challenges such as precipitation of scales as well as increased weathering of the geological formation and other geochemical and rock mechanical effects resulting in formation damage. On the other hand, some of the advantages of ATES systems include very large storage potential and low operation costs and high long-term profitability.

While there are more than 2000 low temperature (< 30°C) heat and cold ATES plants in the Netherlands (Bakema et al, 206), the number of medium temperature (30-60°C) systems is very limited and there are no high temperature (> 60 °C) systems in operation (Schout et al. 2014). For comparison the number of low temperature (< 22°C) ATES plants in Denmark is about ten (Danish Energy Agency, 2014). Both technical issues (Rosenbrand et al, 2014) and legal aspects (Vangkilde-Pedersen et al, 2012) is currently regarded as barriers for HT ATES deployment in Denmark and the Netherlands. Existing HT ATES projects in Germany include:

- The Neubrandenburg plant with storage of 80°C hot water in a depth of 1250 m (Kabus et al, 2009).
- The energy concept Spreebogen at the German Reichstag building with storage of 60°C hot water in a depth of 300 m (and storage of cold in shallow aquifers) (Sanner et al, 2005).

In Switzerland, high-temperature storage systems are not implemented yet, to our knowledge despite a few storage systems have been tested and implemented in the past.

The most successful ATES project, which was developed in the eighties is SPEOS. The principle of SPEOS is based on a central well, 27 m deep and 2.2 m in diameter from which two levels of 6 horizontal drains, 25 m long and 25 cm in diameter, served both for injection and pumping in two stratified aquifers. These aquifers are separated from each other by about ten meters of a silty layer, which acts as impermeable barriers. The upper aquifer is separated from the surface by another silty bank and the unsaturated zone. The supply of hot water came from the Lausanne-Vidy wastewater treatment plant (STEP), and the facility was used to heat the University Sports Center. The storage was first tested in the upper aquifer aiming at verifying the potential interference with the natural groundwater flow and the thermal efficiency of the system. The losses, especially by diffusion, revealed to be important, therefore the injection of hot water at 90˚C was then moved into the lower layers. The stored thermal power is of about 1MW, and the storage volume is 100'000 m3. The ATES system is now able to provide temperatures between 50˚C and 70˚C, having an overall efficiency performance of 50%. The generalization of the concept never developed, despite the large number of potentially suitable sites such as deltas of rivers and lakes. The main reasons for the failure of this concept are probably related to the cut of the financial support, the difficulty to promote the advantages of the system and the lack of the necessary proximity of favorable subsurface conditions, a waste heat source and final users.

1.1.2 Borehole Thermal Energy Storage BTES

The principle of BTES is to heat up soil and cool it down again by circulating a brine in many closely spaced so-called closed loop boreholes installed with plastic pipes and a grouting. The distance between the boreholes must be 2-5 m and BTES is normally limited to boreholes of c. 20-200 m depth. The thermal losses depend on the thermal and hydraulic properties of the subsurface (heat losses by conduction and density driven flow) and regional groundwater flow (heat losses by advection).

Temperatures up to c. 90°C can be stored (Sibbit et al. 2015) and BTES can be used to store excess heat from industries, incineration plants and heat from renewable energy sources such as solar thermal for use in district heating. BTES is ideal for integrating heat from various sources, e.g., heat pumps, solar thermal and CHP plants in combined energy systems utilizing power to heat (heat pumps) in periods with excess electricity production and store heat from periods with need for electricity production from CHP.

A relatively large number of low-temperature BTES plant exists worldwide for local heating and cooling of large office buildings etc., but the number of high-temperature BTES plants for heat storage is still small. In Denmark there is one (Soerensen et al. 2013), and in Germany three (Mangold et al, 2005) BTES plants that are connected to district heating networks, while in the Netherlands one, and in Sweden two large scale BTES plants are storing high temperatures for industrial purposes/building heating. For example, the Emmabodda HT-BTES (Sweden) stores c.a. 3,800 MWh/y of industrial waste heat into 322,500 m^3 of ground, with a recovery rate of c.a. 70 %. 750 MWh/y of solar thermal energy is stored into a 24,000 m3 BTES in Solar Drake Landing (Okotoks, Canada) which has been monitored since 2004, the recovery rate being c.a. 50% (Sibbitt et al. 2012).

Switzerland is known to be a European leader in shallow ground source heat pumps (GSHP), with 3'103'500 MWh/y of heat produced by GSHP, which represents the 80% of the current Swiss geothermal heat production. Several solutions have been studied in terms of potential application of seasonal storage in these systems, mainly to overcome the gradual cooling of the subsurface where extensive GSHP have been installed. Some examples of BTES can be identified in Wollerau where 36 probes 120m in depth, was implemented in 1998, the Technopark buildings in Root (Lucerne) developed by SUVA, which was built in 2001 drilling 49 probes, 160m deep, over a volume of approximately 360'000 m3 and is operating since 2003. In Suurtoffi (Zug), another heat storage system consists of 220 geothermal probes, 150 m deep. The main goal of this project is to operate a new district, renewable and at zero emissions. The waste heat source is generated by cooling the buildings during summer season and is transported via the local network to the geothermal boreholes where it is stored. In winter, the stored heat is then used by means of heat pumps. PV panels generate the electric power needed to run the heat pumps. The temperature of the water varies between 5 ° C in winter and about 25 ° C in summer. The project of the holiday park in Blatten-Belalp (Valais) was inaugurated in 2014, demonstrates that the concept of a combination between solar thermal and geothermal underground storage composed by a series of 120m deep boreholes is a stable and working solution even in Alpine regions. The magazine "Wohnen" reported in October 2013 an original concept set up in 2012 based on a floor heating system at very low temperature (30˚C). A set of five residential houses with 100 apartments are equipped with photovoltaic hybrid solar panels and thermal, which are connected 40 geothermal boreholes, 125m deep, also serving as seasonal storage. The originality of the concept is that properly glazed stairwells act as buffers of thermal energy.

1.1.3 Pit Thermal Energy Storage PTES

The principle of PTES is very simple and works by storing hot water in very large, excavated basins with an insulated lid. Temperatures up to c. 90°C can be stored and PTES offers the same flexibility to e.g., district heating energy systems as BTES. Among current and needed research topics are lifetime of HDPE-liners and lifetime and ventilation of insulating lid constructions. In Denmark there are 5 plants connected to district heating networks (Danish Energy Agency, 2014) and in Germany there are three. (Mangold et al., 2009)

1.1.4 Mine Thermal Energy Storage MTES

Mine water of abandoned and flooded mines is used as a low-temperature energy source for heating buildings and a few plants exist in Germany and the Netherlands. Up to this point a pilot plant has not been established, in which the possibility of thermal energy storage in a former coal mine has been considered. Well-known executed projects concerning the utilization of mine water include:

- The Mijnwater-project in Heerlen (Netherlands), where a flooded mine structure was accessed by 5 wells of variable depth in a depth range from 250 to 700 m (Verhoeven et al. 2016).
- The School of Design at the Zeche Zollverein in Essen (Germany), which is heated by 28°C mine water from a depth of about 1.000 m (Bleicher et al, 2007).
- Water from Robert Müser coal mine in Bochum supplying two schools and the main fire station with heat from 20°C mine water from a depth of 570 m (Willmes et al, 2014).

1.2 Purpose of the project

The GEOTHERMICA HEATSTORE project aligns with these research and development needs described in energy storage and heat network roadmaps (http://www.heatroadmap.eu/). The project had three primary goals

- optimizing the performance of high temperature (~25 to ~90°C) underground thermal energy storage (HT-UTES) technologies
- lowering exploration and operational cost
- reducing techno-economic risks

These three contribute to the final goal of HEATSTORE, to advance the commercial viability HT-UTES technologies, so that geothermal energy, combined with and optimized through underground heat storage, can reach its maximum deployment potential in the European energy transition.

The Swiss project focused on the assessment of the feasibility of HT-ATES systems at two sites in Geneva and in Bern. The two sites present different challenges in terms of subsurface conditions and energy system configuration but are rather representative of most of the suitable sites over the entire Swiss Molasse Plateau where most of the excess heat and heat demand are identified.

The characterization and integration of both elements via the implementation and validation of a multi-criteria framework able to assess the favorable techno-economic conditions for HT-ATES implementations as well as the effects on the environment and the identification of the regulatory framework barriers to be overcome has been the main purposes of the Swiss project.

In Geneva the case-study focused on the storage of excess heat from a waste incineration plant in the Mesozoic fractured carbonates at depth between 450 and 1500m. The proposed framework has been calibrated and validated according to the data resulting from the exploration activities carried out. The goal of implementing a HT-ATES systems has not been achieved because of unsuitable subsurface conditions for the selected storage system but heat storage and recovery tests at the field lab in Concise (VD) have been performed and demonstrated that storage and recovery of heat can be an option for the fractured carbonates.

In Bern the storage of excess heat from the Forsthaus waste-to energy and wood fired plant has been planned to take place in the Molasse sediments at 500m in depth. The project purpose is to drill a set of wells in the vicinities of the plant and perform and monitor heat injection operations to design and implementation of the full HT-ATES. Now drilling operations are set-up and the project will continue in the coming years.

1.3 Objectives

The specific research and demonstration objectives of the Swiss project have been:

- Characterize the (local) geological, hydrogeological, and hydro-chemical settings necessary to allow ATES technologies to perform under different geological settings, heating demands and heat sources.

- Compose, improve, and validate a framework that can be used to predict subsurface dynamics, system performance and economically optimize the integration of the geothermal energy storage project within the local heat distribution networks and power infrastructures.
- Design and potentially implement pilot demonstration projects integrating HT-ATES and demand side management in various heat system configurations.
- Monitor the two sites focusing on thermal/hydraulic/mechanical/chemical effects in the environment to understand the technical impacts of heat storage.
- Validate and improve existing process models to enhance prediction of site performance to optimize performance and longevity for HT-ATES facilities.
- Determine the current and required stakeholder engagement and regulatory conditions necessary to allow HT-ATES to take place in Switzerland.

2 Description of facilities

2.1 Geneva Site

The Geneva case study is based on the results of two exploration wells (GEo-01 and GEo-02) drilled by the Services Industriels de Geneve (local energy provider) in the framework of the GEothermies program (https://www.geothermies.ch). The geothermal target of the two wells is the Upper Mesozoic carbonates which petrophysical and hydraulic properties are predominantly controlled by fractures conditions along fault corridors, and by karstification at the transition between the low permeability Cenozoic sediments and the Lower Cretaceous carbonates.

The heterogenous distribution of both fault corridors and karst structures has been a clear challenge to properly identify and characterize suitable targets for thermal energy storage in the Mesozoic units. Noticing that the hydraulic properties of potential reservoir play a major role in defining the technical and economic viability of HT-ATES in such complex carbonate reservoirs.

The GEo-01 is 744m deep and is characterized by a natural artesian flow (55l/s at 34˚C and 8 bars wellhead pressure). These conditions represent an extremely interesting geothermal resource which optimal utilisation is now under evaluation by SIG. The reservoir produces from a set of fractures mostly from the Lower Cretaceous (~70%) and partially from the Upper Jurassic (~30%). The permeability has been estimated to be up to 300 mD, which, coupled to the high wellhead pressure (8-10 bars) and the artesian flow make the GEo-01 site challenging for an effective thermal storage implementation. The GEo-02, 1456m deep, is characterized by an extremely low natural artesian flow (0.3l/s at 18˚C and 12 bars wellhead pressure) suggesting low reservoir transmissivity for thermal storage implementation.

To overcome the technical challenges related to testing hot water injection in the target formations, a shallow field laboratory has been implemented in Concise (VD) by the University of Neuchatel: three wells reaching a depth between 50-60m drilled into the Upper Mesozoic where different types of geomechanical and hydraulic tests were performed in the 3rd year of the project. Geo-02 was drilled in 2021 and targets the Base of the Upper Jurassic at about 1300-1400m in depth, which is considered a potential geothermal reservoir, possibly suitable for storage as well. Surface constraints for the project are provided by the proximity of the District Heating and Cooling network and the heat demand, which provide input for defining the optimal operational conditions. Now the district heating and cooling network is located on the central part of the Canton and is operating at rather high temperatures (up to 120˚C in supply and 70˚ in return) for heating purposes but a lower temperature DHN is planned on the southern part of the canton in the future. Most of the heat demand is in the Geneva city but only 15% of it is covered by the DHN (Figure 3).

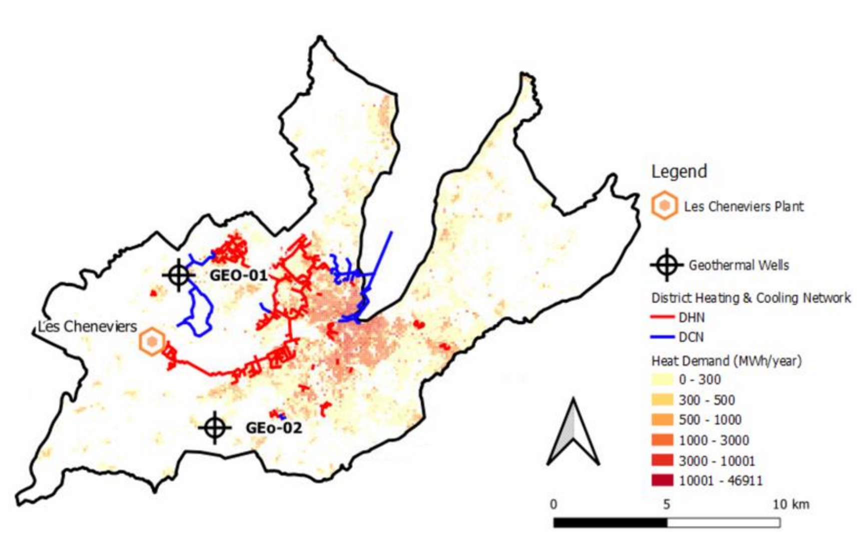

Figure 3 – Map of the main elements composing the Geneva project.

2.2 Concise (VD) – analog test site in fractured and karstified limestones

In complement to the Geneva exploration boreholes, the Centre for Hydrogeology and Geothermics (CHYN) has developed an analogue test site with 3 boreholes in fractured and karstified limestones. The aim of this site is to study thermo-hydraulic processes in fractured and karstified limestones under various hydrogeological conditions. The site allows to performed tests in-situ with a much simpler logistic than in deep boreholes and thus is ideal to develop our knowledge of thermo-hydraulic processes in fractured and karstified limestone. The site has been developed in the framework of the "HEATSTORE" project with the objective of testing well test protocols to estimate the hydrodynamic and thermal characteristics of the aquifer.

The site is located at the southern foot of the Jura Mountains near Lake Neuchâtel. The regional stratigraphy is well known. For formation names, we will use here the new nomenclature (Strasser et al., 2016) and indicate in brackets the old local nomenclature still widely used in practice. Near the drill site, limestones of the Gorges de l'Orbe Formation (Lower Urgonian/Yellow) of Barremian age are in outcrop (estimated thickness: 0-50m). These limestones are superimposed on the limestones of the upper part of the Grand Essert Formation (Pierre Jaune de Neuchâtel) of Hauterivian age (thickness: 35-37m). The underlying formation is the more marly Hauterive Member (Marnes Bleues) of early Hauterivian or late Valanginian age (thickness: 31m). The rest of the series, not perforated by our drilling, is typical of the Neuchâtel Jura. At the study site, the limestones form the southern flank of the first Jura fold and have an average orientation of 135/15. The site is located 1.6 km northeast of the Lance Fault. The Lance Fault is a 10 km dextral structure with a horizontal throw of about 3 km.

Site location along with a simplified geological cross section and borehole technical section is provided in Figure 4. One important characteristic of the site is to give access to saturated fractured and karstified limestone at shallow depth in formation comparable to those penetrated by the GEo-01 and GEo-02 wells in Geneva. More details are given in Section 4.1.5. A description of tests performed to date in the RSBV boreholes is also provided. The site development, characterization and thermo-hydraulic testing has been the subject of three M.Sc. thesis at the CHYN. Refer to the complete thesis for full details on the site development and characterization (cf. André, 2021; Milo, 2021; Jaquet, 2021)

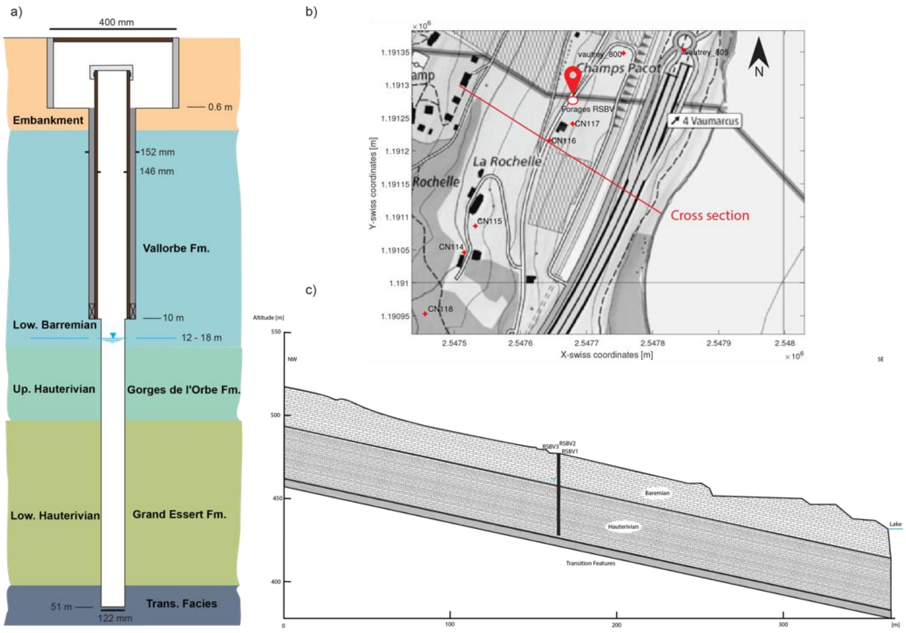

Figure 4 - a) Completion of boreholes RSBV1, RSBV2 and RSBV3 (not to scale), b) location of the drill holes in the area (red crosses) and the RSBV drill holes (red pointer) and the location of the geological section, c) local NW-SE geological section passing near the drilling site.

2.3 Bern Forsthaus Site

The pilot project in Bern aimed to store waste heat from the nearby power generation site Bern-Forsthaus. The power generation site is operated by the local utility company Energie Wasser Bern (EWB) and contains a combined-cycle plant, waste-to-energy plant and wood-fired power station for electricity and heat production (Figure 5).

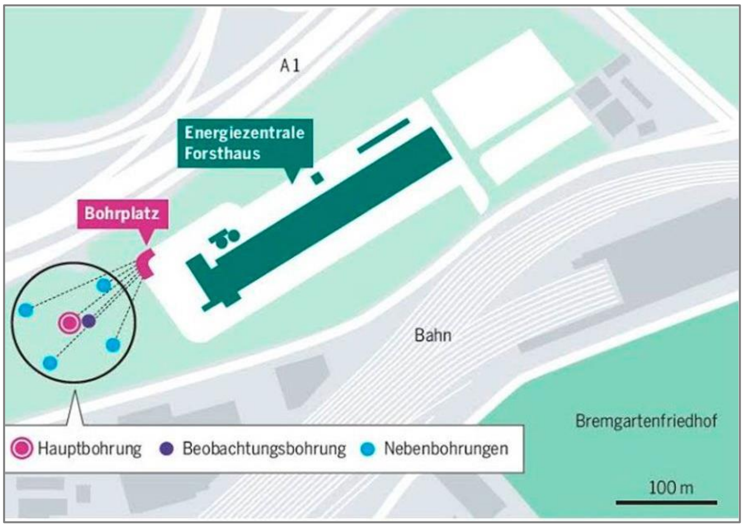

Figure 5 – Map of the Bern Forsthaus site.

The heat user is an existing district network, which presents an increasing heat demand and a planned expansion in the city of Bern. The project consists in storing waste heat during the low-demand season, and in delivering it during heating seasons, thus replacing the standard gas heat production (Figure 6).

For the pilot heat storage system, three exploration wells ~ 500 m deep were drilled to reach the sandstone layers (“Rinnengürtel”) of the Lower Freshwater Molasse (USM). The goal was to assess the feasibility and options of de-risking of an HT-ATES system and, possibly realize a fully functional heat storage system with an injection temperature of max. 120 °C and an expected output of 7 – 10 MW_{th}.

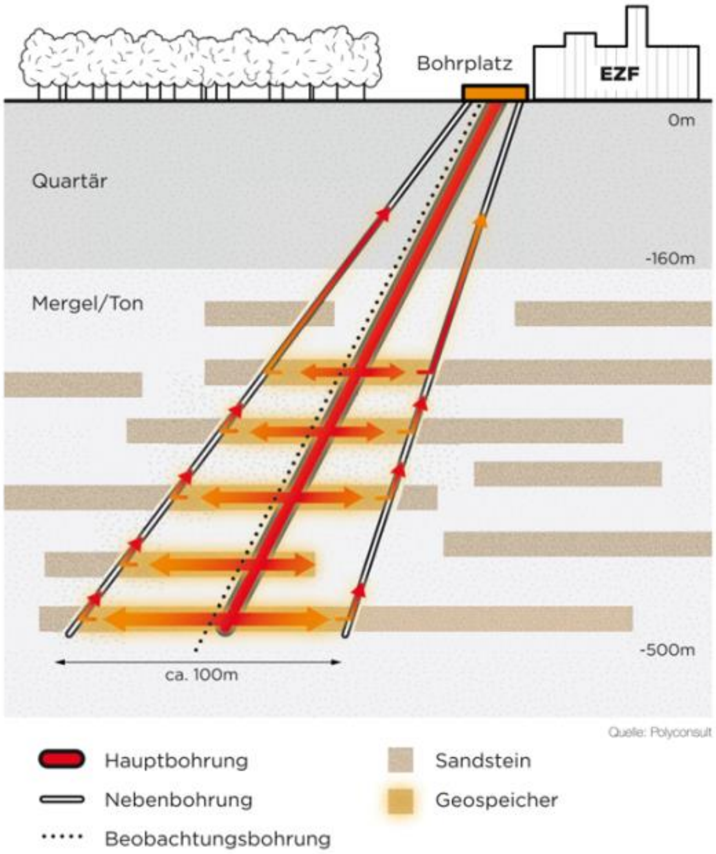

Figure 6 – Schematic representation of the Bern Forsthaus project

Different pre-investigation studies have been carried out:

- Survey on ground level to anticipate/measure any ground movement due to production and reinjection (however there is an equilibrium of produced and injected volumes) with HM modelling,
- Testing of each layer of the sandy reservoir (multi-layered reservoir with different transmissivity) in order to avoid thermal shortcuts or interferences,
- TH and THC modelling to assess the efficiency of the storage and possible geochemical reactions (precipitations) close to or in the wells or in the heat exchangers at the surface

Additionally, a long-term injection/production test was conducted at the pilot site, including ground level measurements (which is a sensible subject because of surrounding infrastructures). This ground level surveillance has been proposed by Geo-Energie Suisse AG at the beginning of the project, the authority and site owner have been very interested by this.

The ideal design of the Bern ATES consists of one central hot well for heat storage and heat recovery, and up to 5 lateral cold auxiliary wells to close the subsurface circulation loop. Depending on the operational regime — heat injection or heat extraction — the direction of subsurface circulation would be reversed, implying that each well alternates between production and reinjection Due to the high degree of uncertainty in the aquifer hydraulic properties, a flowchart for a step-by-step drilling was conceived, allowing to go to the next step only if the hydraulic conductivity was satisfying, and providing fallback solutions.

The ~ 500 m deep wells target the upper part of the Lower Freshwater Molasse formation (USM) which is composed of sandstones and clayey levels . The wells are deviated (16° at 180 m), with the top of reservoir at 350 TVD.

The wells were equipped with glass fiber casings. To avoid warming up the shallow groundwater, a 6'' diameter tubing was inserted into the casing. The air gap provided sufficient thermal insulation. This tubing was installed down to a depth of250 m (depending on the reservoir pressure). This tube also allowed to avoid injecting chemical to mitigate the corrosion. The excess heat is only available in summertime (excess heat from the EWB power plant) as is used in the winter through the municipal heating network. The amount of excess heat is correlated with electricity demand and is overall constant through the years.

3 Procedures and methodology

The overall workflow for the HEATSTORE project is to define the optimal operational conditions for storing excess heat in fractured carbonates. The two main pillars driving the technical feasibility of an HT-ATES system are 1) the definition of the excess heat availability and heat demand fluctuations over time, and 2) the subsurface characterization to predict the performances of the system. Once these two elements are combined, the resulting output fed into a techno-economic assessment framework. Additionally, potential effects on the environment have been identified and quantified where possible, limitations and potential adaptations to the current regulatory framework have been proposed to support improvements to enable future implementations (Figure 7).

For Geneva, the subsurface characterization has been performed in a first stage using literature data that provided constraints to create an initial set of 3D static models able to capture the information from geophysical, borehole to populate the 3D models at GEo-01 and GEo-02 with petrophysical and hydraulic properties. To predict the performances oh HT-ATES systems the excess heat and heat demand configurations over time have been included as inputs parameters to those coming from static models and a set of TH, THM and THC models have been produced.

The availability of new subsurface data generated by the drilling and logging results at GEo-02 and by the hydraulic testing as GEo-01 provided further constraints to calibrate the static models and, consequently, the dynamic models. The results of the final dynamic models have been used for assessing the economic viability of HT-ATES based on the impact of subsurface performances on the Levelized Cost of Heat (LCOH). Additionally, environmental effects on soil mechanics, groundwater quality, and carbon intensity have been assessed to highlight the potential risks but also the benefits of integrating HT-ATES in the Geneva energy system.

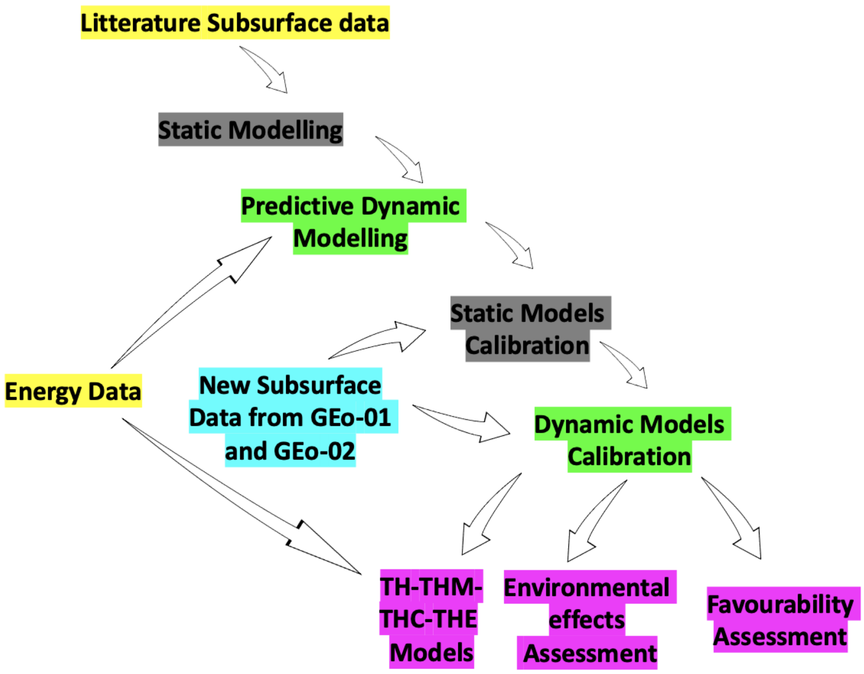

Figure 7 – Workflow of the HEATSTORE project.

The potential of HT-ATES implementations over the entire Swiss Molasse Plateau has been assessed using Spatial Multi-Criteria analysis based on Play-Analysis evaluation of the two main geologic Plays studied in this project, the Molasse and the Upper Mesozoic carbonates. Public subsurface data have been coupled to excess heat data, heat demand and other surface constraints (such as waste incineration plant and district heating locations) to assess the storability potential of the two reservoirs and therefore their potential to deliver heat to supply the heat demand. These results eventually define the favorability of HT-ATES implementation over the Swiss Plateau

For Bern, predictive dynamic models have been performed to assess the storage potential at the study site and support the design of the boreholes. Geochemical studies have been performed to assess the potential geochemical impacts of storing high temperature water in a relatively cold aquifer (~25˚C) and identify the effects in terms of mineral dissolution/precipitation at the reservoir scale as well as the risks for scaling and corrosion at the surface equipment. At present, the operations related to the set-up of the drilling operations are ongoing and the Bern project will be extended furthermore with the goal to drill exploration wells and perform hydraulic and storage tests and eventually evaluate the feasibility of the system.

4 Synthesis of demonstrators and case studies

This chapter aims at summarizing the results of the two case-study sites in Geneva and Bern as report in the full deliverable **D1.4-4.2-.4.3** of the European Project ***Synthesis of demonstrators and case studies - Best practice guidelines for UTES*** development available in Annex 19.

4.1 The Geneva Site

The Geneva case study is based on the results of two exploration wells (GEo-01 and GEo-02) drilled by the Services Industriels de Geneve (local energy provider) in the framework of the GEothermies program (https://www.geothermies.ch). The geothermal target of the two wells is the Upper Mesozoic carbonates which petrophysical and hydraulic properties are predominantly controlled by fractures conditions along fault corridors, and by karstification at the transition between the low permeability Cenozoic sediments and the Lower Cretaceous carbonates. The heterogenous distribution of both fault corridors and karst structures has been a clear challenge to properly identify and characterize suitable targets for thermal energy storage in the Mesozoic units. Noticing that the hydraulic properties of potential reservoir play a major role in defining the technical and economic viability of HT-ATES in such complex carbonate reservoirs (Figure 2).

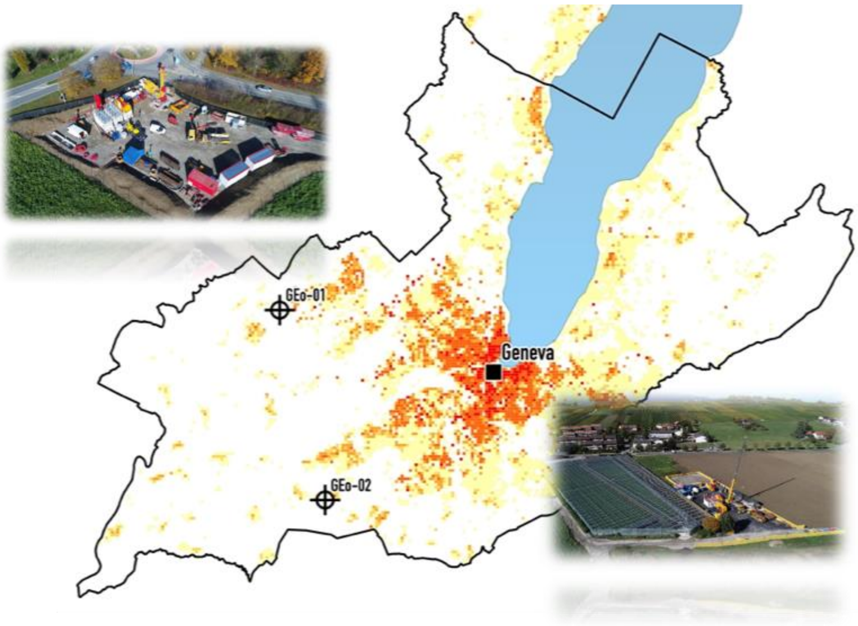

Figure 8 – Map of the Geneva project with indication of the two exploration wells superposed on the heat demand over the Geneva Canton

In the Geneva demo site two deep explorations wells (GEo-1 and GEo-2) have been drilled at 744 MD for GEo-1 and 1456 MD for GEo-2 into the fractured Mesozoic limestones. The characteristics of the wells are:

- GEo-1: artesian flow of 55 l/s, temperature of 34°C, 8 bar wellhead pressure.
- GEo-2: no productive well (0,6 l/s), temperature of 55°C and 12 bar wellhead pressure.

The reservoir produces from a set of fractures mostly from the Lower Cretaceous (~70%) and partially from the Upper Jurassic (~30%). The permeability has been estimated to be up to 300 mD (GEo-1), which, coupled to the rather high wellhead pressure (8-10 bars) and the natural artesian flow (50l/s) constitute reservoir challenging conditions for an effective thermal storage implementation. The GEo-

02 well characterized by an extremely low natural artesian flow suggests low reservoir transmissivity for thermal storage implementation.

GEo-1 and GEo-2 wells will not be used at the end of the project for an ATES (possibly in a later stage for GEo-1 or will be kept as a monitoring well). Future operations are planned for further subsurface characterization like the acquisition of a 3D seismic survey (2021) and the drilling of two additional exploration wells between 1500 and 2000 m (GEo-03 and GEo-04, in 2022-2023) for testing different geological contexts and characterizing the geothermal potential at the basin's scale.

For the design of a future HT-ATES, numerical thermo-hydraulic simulations based on different scenarios and their integration in the energy system were made (see D3.3, and Mindel and Driesner, 2021). Based on existing DH temperature regimes in Bern, the ATES system is charged during summertime with 90°C (DH supply temperature) and that direct discharge is possible down to 50°C (discharge cut-off, corresponding to the DH return temperature). For extracting more energy from the storage and reduction of the re-injection temperature down to 20°C, the use of heat pumps was also analyzed. Based on the detailed geological study carried out by the University of Geneva (UniGe) and Services Industriels de Genève (SIG), a cube-shaped 1km3 block was constructed by UniGe using the analysis of a collection of subsurface datasets. The modelling scenarios analyzed concern variations in aquifer permeability, thickness, inclination, presence of fractured upstream and downstream the hot well, wells' configuration (single, doublet, 5 spot) and the presence of groundwater flow. Those preliminary simulations confirm observations already pinpointed in §2.1.1.4 like the effect of buoyancy driven force on recovery efficiency and the necessity of auxiliary cold wells (at least one well) to reduce well injection pressure and mitigate the drift of the" hot bubble" due to the groundwater flow.

To complement the deep-seated boreholes in the Geneva basin and to be able to perform heat storage experiments, a field lab was developed by the University of Neuchâtel at Concise (VD - Switzerland) in analog limestone formation. Three 50 m deep boreholes target Lower Cretaceous and Upper Jurassic fractured and karstified limestones, which are analogues to the target units in Geneva. The objectives of the tests performed at the Concise test site were to characterize the thermo-hydraulic response of the fracture and karstified limestone rock mass to heat storage. A series of hydraulic and thermal tests have been carried out in the boreholes: (i) standard open-hole hydraulic tests and tests between packers (shallower part artesian can hide more productive layer above) and (ii) tracer and heat transfer tests by using "push-pull" tests (using one well) with different duration of injection period and complemented by image and flow logs. Tracer dilution tests were performed for assessing natural flow conditions and were monitored in-situ with pressure and temperature gauge as well as with fiber optic based distributed temperature sensing.

4.1.1 Challenges

The Geneva project allowed to implement for the first time a HT-ATES performance prediction modelling framework based on fully coupled techno-economic assessment combining subsurface, energy system, operational CO_2 emissions, and economic modelling based on a scaled DHN demand. The results show that, subject to subsurface constraints, the nominal capacity ranges from 0.4 MW to 81 MW, with aquifer permeability and thickness being the major control variables. A minimum transmissivity of 2.5 ×10-12 m3 is required to keep the Levelized Cost Of Heat (LCOH) below 200 CHF/MWh and a capacity of 25 MW or higher is needed for the HT-ATES system to become competitive with other large-scale DHN heat sources. The capacity increase from the addition of Heat Pumps (HP) incurs non-recoverable costs and in turn increases the LCOH. Nonetheless, the addition of HP increases the nominal capacity of the system and results in higher cumulative avoided CO_2 emissions.

To complement deep seated borehole in the Geneva basin and to be able to perform heat storage experiments, a field lab was developed by the University of Neuchâtel at Concise (VD - Switzerland) in analog limestone formation (see § 2.2.4.2).

Appropriate geological conditions to build an ATES system in Geneva were not encountered (either too high permeability in Geo-01 or too low at GEo-02). Eventually, the field laboratory resulted in a partial recovery of the hot water and tracer injected demonstrating that the Mesozoic carbonates could be suited for ATES system

4.1.2 Lesson Learned

The results of the project clearly reveal the main subsurface challenges related to such fractured reservoirs, which are the hydraulic heterogeneity and reservoir compartmentalization, requiring more detailed exploration surveys (i.e., 3D seismic) to properly identify those targets potentially suitable for storage. Additionally, potential storage targets in Geneva should not be limited to the Mesozoic carbonates but could be in the Cenozoic sediments as well.

For the moment the Geneva project did not enter into the implementation phase but the field laboratory from University of Neuchatel could be useful to further test different storage set-ups in terms of charging/discharging temperature, duration, pressure and get a better understanding about the recovery efficiency and petrophysical-hydrochemical effects that could activate consequentially.

HT-ATES are a concrete opportunity to decarbonize the Geneva energy system but, in addition to subsurface challenge, the energy system needs to be suitable for an optimal integration in terms of operating temperatures and flexibility of the energy supply.

4.1.3 Recommendations

- Further explore the Mesozoic fault structures and the Karstified Upper Cretaceous with high resolution geophysical methods and field lab tests,
- Consider the Cenozoic sedimentary cover as a potential target for both ATES and BTES solutions,
- In situ tests of different smart control set-ups to define the charge/discharge/rest periods and the impact on energy efficiency,
- Site analysis during drilling of the well to define well deviation to reach favorable geological conditions,
- Compare geochemical site samples with previous laboratory analysis to establish at first order mineral precipitation and their impacts on borehole and surface installations,
- Test different well configurations and see the impact on energy efficiency and analyze the impacts on the financial sustainability of the different solutions

4.2 The Bern site

The pilot project in Bern aims to store waste heat from the nearby power generation site Bern-Forsthaus. The power generation site is operated by the local utility company Energie Wasser Bern (EWB) and contains a combined-cycle plant, waste-to-energy plant and wood-fired power station for electricity and heat production. The heat user is an existing district network, which presents an increasing heat demand and a planned expansion in the city of Bern. The project consists in storing waste heat during the low-demand season, and in delivering it during heating seasons, thus replacing the standard gas heat production (Figure 3).

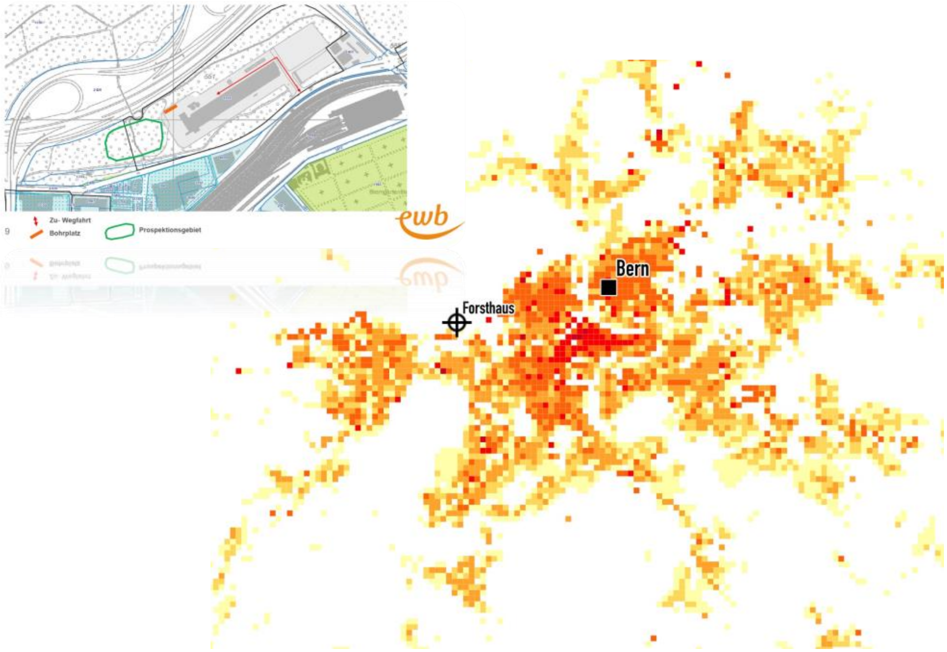

Figure 9 – Map of the Bern project with indication of the Forsthaus project superposed on the heat demand over the Geneva Canton

Different pre-investigation studies were carried out:

- Survey on ground level to anticipate/measure any ground movement due to production and reinjection (however there is an equilibrium of produced and injected volumes).
- Modelling of the thermal development in an anticipated sand layer over several storage cycles.
- Evaluation of a recovered core from an offset well to determine permeability, porosity, mineralogy, and the sanding behavior.
- Modelling of the thermal influence on the ground water layer and the heat transfer.
- TH and THC modelling to assess the efficiency of the storage and possible geochemical reactions (precipitations and solution) in the reservoir, in the wells or in the heat exchangers at the surface.
- With the input of the geological and hydraulic data a detailed well engineering was conducted, including Casing Design, Wellpath Design with Anti Collision Criteria, Mud Design with laboratory testing, Cement Design with laboratory testing, BHA design, tool, and packer design for the hydraulic testing with a trial run on site.

Thorough THC modelling and experimental laboratory tests using drill core and formation waters from shallow wells 2 km from the site were carried out to assess the chemical processes and impacts of heat storage and unloading cycles at the reservoir scale. The results of the experimental tests and modelling study showed no critical issues that would imply a different storage strategy from a geo-chemical point of view.

Nevertheless, the following risks and possible complications were identified, they are viewed as non-critical, but they require consideration:

- Preferential flow paths may develop between the main and supporting wells due to heterogeneous permeability of the sandstones. This could reduce the volume of rock swept by the injected hot water, lowering the efficiency of heat storage below previous expectations.
- Calcite is predicted to precipitate in some regions of the reservoir and to dissolve in others during the water injection/extraction cycles. Regions clogged by calcite may become barriers to the injection/extraction flow regimes. Regions of moderate calcite depletion may focus flow and thereby leave other regions of the reservoir unswept by the injected hot water. Thus, both calcite clogging and dissolution may contribute to lowering the heat-storage efficiency of the reservoir.
- Extreme dissolution of calcite cement may induce local mechanical disintegration and compaction of the sandstones, and mobilize fines that clog pore throats, reducing permeability and hence further lowering the efficiency of the water injection/extraction cycles.
- Microbes may form biofilms and clog the casings of the supporting wells, where temperatures are < 50 °C. Microbial activity is expected to diminish as the reservoir heats up to 90 °C.
- The evolving thermal plume and the water–rock reaction zone around the main well are predicted to remain within a 50 m radius from the well. However, the influence of the entire heat storage reservoir, if defined by the distance to which non-reactive solutes injected or released from the rock can travel in the USM (Lower Freshwater Molasse) groundwater system, is much larger. There is therefore a possibility that unwanted chemical compounds are transported over large distances.
- Significant carbonate scaling is expected in the surface installations during the heat-loading cycle. This could impede flow and exchange of heat in the surface installations.

The full description of the design and construction activities planned for the Bern site is available in Section 5.2 of this report.

5 Results and discussion

5.1 Geneva study site

Currently, about 60-70 GWh/year of heat are wasted during summertime at Cheneviers, the urban solid waste incineration plant of Geneva and main non-fossil source of the existing DH. To maximize heat recovery energy from the plant, preliminary studies were done by the Swiss consortium of HEATSTORE to evaluate the feasibility to integrate an ATES into the DH network (see Deliverable 3.3 of the European project in Appendix 16).

Energy scenarios were constructed based on the evolution of the district heating network (temperature levels, demand profile and supply sources), while ATES thermo-hydraulic responses were simulated numerically to estimate its energy efficiency and the impact of the integration ATES into the DH. Noticing that thermo-hydraulic conditions used on numerical analysis are based on in situ data (drilling results, cuttings and geomechanical characterization).

5.1.1 Energy system context and system modelling

Currently, more than 50% of total final energy in Geneva is used to cover space heating (SH) and domestic hot water (DHW) demand. Despite the importance of the heating sector and the high heat demand density (Quiquerez et al, 2016), less than 15% of total thermal demand is covered by district heating networks (DH) (Figure 10 - top).

By 2035, the DH coverage is bound to supply 35% of the total heat demand, with at least 80% of it supplied by renewable energy and waste heat recovery. A prospective scenario for 2035 is shown in Figure 10 (bottom), where one can easily see the increasing importance of renewable resources into the cantonal heating energy system, as well as the development of district heating (DH - “CAD” in French) (De Oliveira Filho et al., 2020).

In this context, subsurface formations will have a double importance in near future. They will be used: i) as a heat source injected directly or indirectly (temperature upgrade by heat pump) into the DH system; ii) as a storage medium for summer DH heat surplus (Moscariello et al., 2020).

To integrate geothermal energy massively into Geneva’s heating system, reducing of current DH temperature levels remains the main constraint to overcome. Existing DH operates at a 120°C/70°C temperature regime (supply/return), which imposes a geothermal exploitation at a depth of 2’000 m or deeper (average geothermal gradient 33 K/km – Chelle-Michou et al., 2017)) to ensure the direct use of underground heat in the DH. Obviously, lower depth geothermal units can also be used, in conjunction with heat pumps (HP), which however entails additional electricity consumption.

Apart from temperature compatibility between geothermal resources and DH, the use of geothermal heat is constrained by the DH demand, and in the case of underground thermal energy storage (UTES) systems, also by the amount of excess heat available to charge the storage. For the latter, charging energy must be available at relatively low cost and DH must be able to accept the extra energy from the UTES. Theses aspects are very important to ensure the economic feasibility of the project and must be analyzed during the project phase, alike energy losses and storage efficiency.

In this study, the evaluation of the DH heat demand and supply is carried out by way of an input-output model inspired from EnergyPLAN (Østergaard, 2015) which is validated at cantonal level (Quiquerez, 2017). In 2019, the model was adapted, and temperature constraints were implemented to guarantee a more precise source to sink matching, especially concerning low-temperature renewable resources and geothermal energy (Quiquerez et al, 2020).

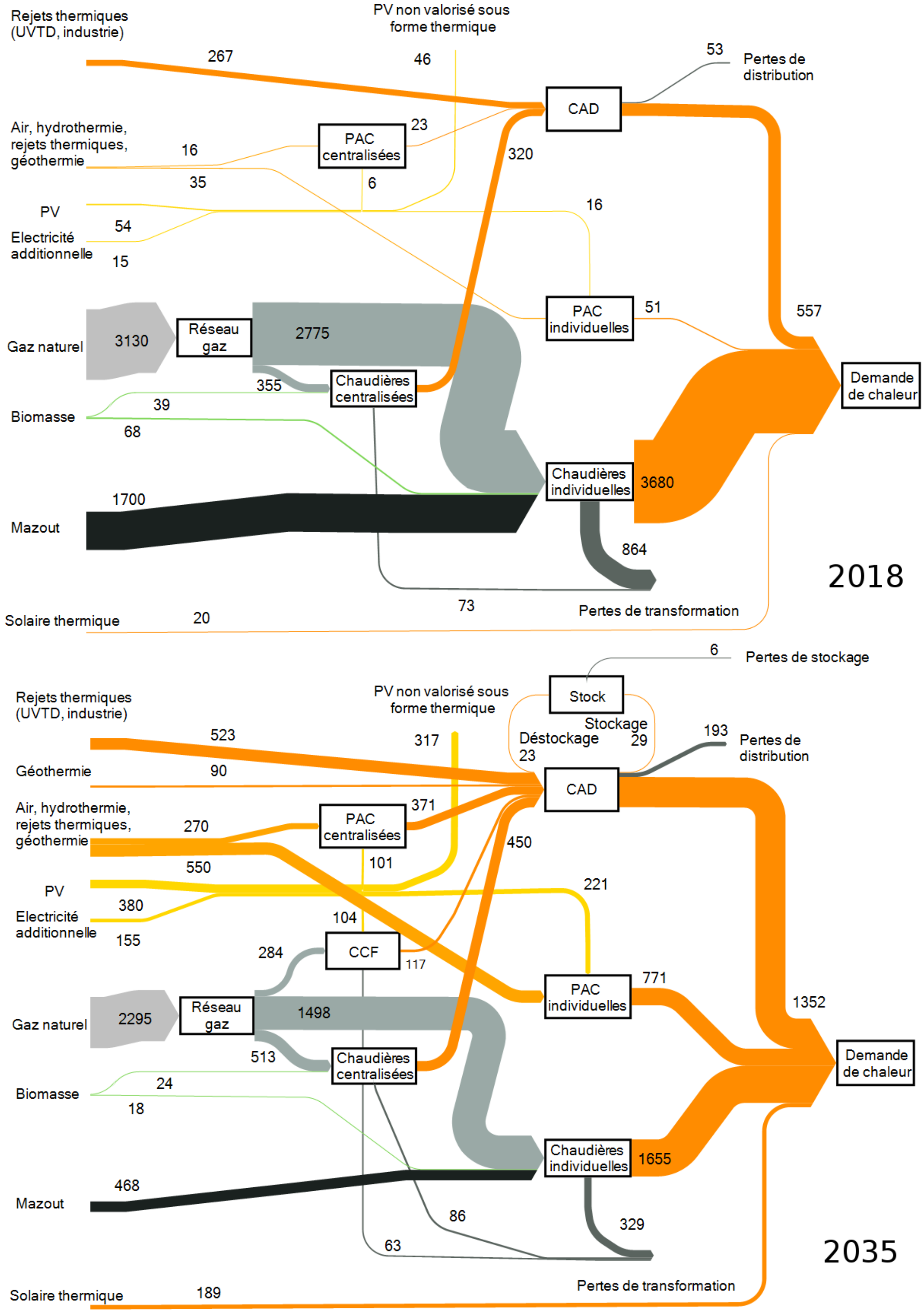

Figure 10 - Current heat demand and thermal energy scenario for 2035 (values in GWh/yr.

In the model, hourly profiles are used to ensure the matching between fluctuating renewable energy sources and weather-dependent heat demand. Space heating (SH) and domestic hot water production (DHW) dynamics are based on measured load curves of existing DH network, which are up/down scaled for considering the evolution of the heat demand related to improvements on the thermal performance of retrofitted buildings (SH reduction), climate change (SH reduction) and the increasing share of DHW on new buildings. Production profiles also come from in situ measurements, those related to solar thermal and solar PV production and are up/down scaled in relation with the installed capacity.

Balance between heat supply and demand considers the diverse source and sink dynamics (hourly time-step) and the corresponding temperature profiles; the efficiency and capacity of the production plants; transport heat losses; as well as the merit-order for the activation of the diverse resources and production plants.

Optimization is based on a *"what... if..."* analyses, by changing some parameters like the DH coverage, the retrofit rate and quality, the heat production capacity and efficiency, the merit-order for activation of the diverse DH resources and supply plants, as well as the combined heat and power (CHP) production strategy (driven by electric or by heating markets). Scenarios are compared by way of the annual production mix, the full load capacity for each production plant, and the corresponding CO_2 emissions for the entire thermal sector.

5.1.1.1. Charging the storage

UTES efficiencies are highly dependent on geological conditions, but also on charging / discharging profiles over the system lifetime (Flechaus et al., 2020). In the Geneva case study, available energy for charging a UTES essentially comes from the urban waste CHP plant and from future geothermal units. The use of wood, which is a scare resource and is already a stored form of energy, is limited to the heating season (Quiquerez et al, 2020). The evolution of the theoretical available energy to charge the UTES is shown in Figure 11, in hourly and weekly values. As can be seen, excess heat is mainly present during June – September, when heat demand is limited to DHW, except for August, when the urban waste CHP plant is in maintenance. Furthermore, the available excess heat reduces over the years, due to DH extension and related increase of heat demand to cover DHW needs during summer. The evolution of the annual available excess heat is further shown in Figure 12, in integrated values over the entire year as well as over the 3 summer months (June– August), which confirms that most of the heat available for storage is concentrated on the 3 summer months.

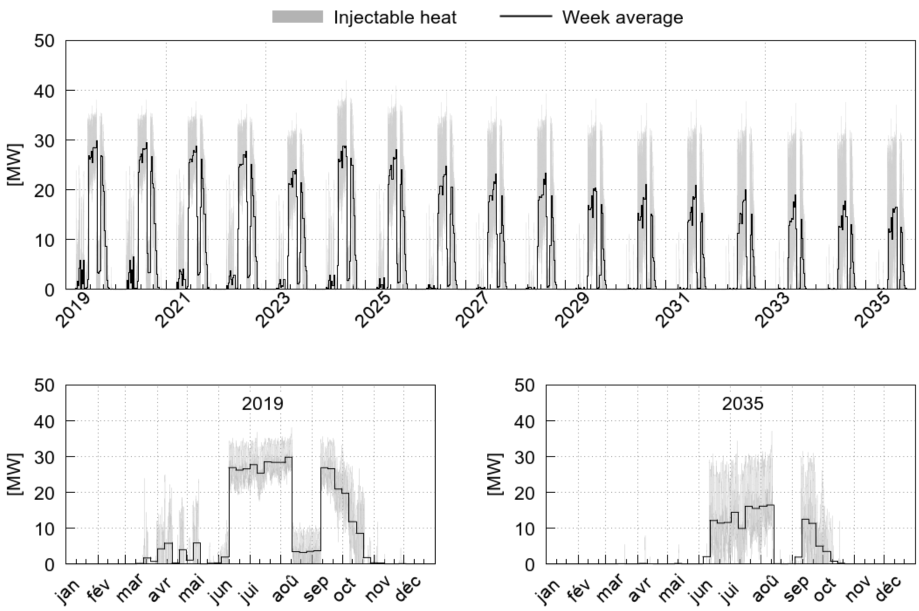

Figure 11 - Available excess heat for charging of a UTES, in hourly and weekly values: evolution over the entire period (top) and focus on first and last years (bottom).

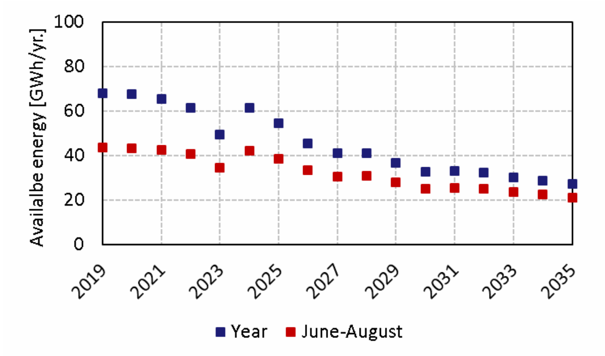

Figure 12 - Evolution of annual available heat for charging of a UTES: integrated values over the entire year and over the 3 summer months (June – August).

As a complement to the available annual energy, the maximum heat load plays a fundamental role in the design of the underground thermal energy storage (UTES), as it is related with investments in heat transfer technologies (number of boreholes for boreholes thermal energy storage (BTES) systems, flowrate and number of wells for aquifer thermal energy storage (ATES) systems). An option to reduce such investment costs is to integrate a buffer between the UTES and the DH. The buffer is designed to absorb high-frequency power fluctuation (short-term storage), while UTES is used as long-term storage for huge amounts of energy, at a more or less constant power (Mesquita et al., 2019. As an example, in the Danish thermal district heating network Braedstrup Fjernvarme (total heat demand of 40 GWh/yr.), a 7'500 m3 hot water tank buffer is used to enhance the technical and economic performance of the energy system (gas CHP plants, thermal solar panels, wind turbines and a BTES).

As can be seen in Figure 11, in the Geneva case study, a "one week buffer" would allow to reduce the maximum storage load significantly, with a maximum of 30 MW in the first years, respectively 20 MW in the last years. Such a buffer would typically need a 300 MWh capacity (6'500 m3 water with ΔT of 40 K), with a maximum charging load from the DH designed at 20 MW.

5.1.1.2. Discharging the storage

The evolution of the theoretical DH energy acceptance with the defined merit-order is shown in Figure 13. As can be seen, heat acceptance is mainly present during heating season, apart from August, when the urban waste CHP plant is in maintenance and DHW demand cannot be covered by CHP units and direct geothermal plants. Furthermore, the heat acceptance increases over the years related to DH extension. The evolution of the annual heat acceptance is further shown in Figure 14, in integrated values over the entire year as well as over the 3 winter months (December – February), which confirms that at least 50% of DH acceptance is concentrated on the 3 winter months.

Indeed, with the defined merit-order, there will be no energy restriction to discharge the storage; heat demand seen by the storage is at least twice higher than available "injectable" energy (Figure 12 versus Figure 14). In this case, the DH could accept up to 170 GWh/yr. and 130 MW the first year and almost 600 GWh/yr. (290 MW) by 2035.

The design of the heat transfer capacity between the DH and the storage will depend on the different costs between power and energy facilities. In the case of BTES systems, the number of boreholes have a high impact on the heat transfer capacity, while for PTES systems the volume of the pit conditions the maximum heat content rather than the heat transfer capacity. Concerning ATES, charging / discharging rates depend on hydro-geological conditions, which govern maximum water-flow rate.

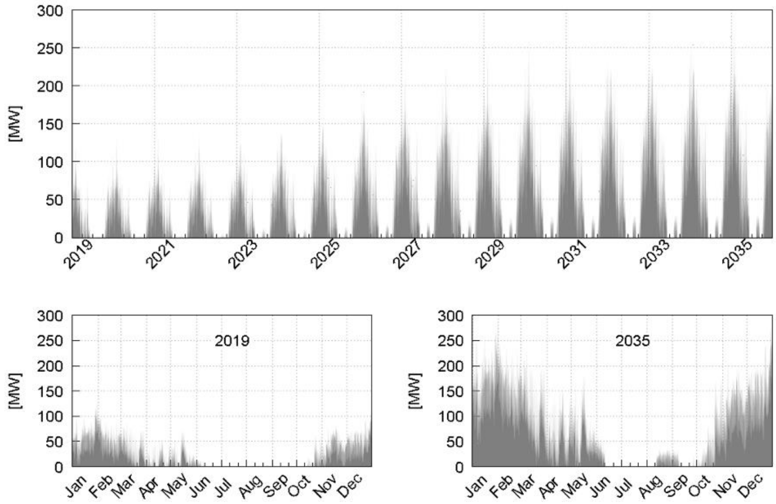

Figure 13 - DH acceptance for charging of a UTES (hourly values): evolution over the entire period (top) and focus on first and last years (bottom). DH energy acceptance defined for the merit-order CHP-Geothermal-Storage-HP-Wood-Gas.

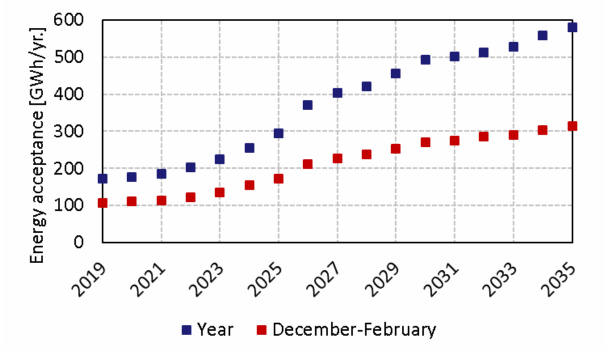

Figure 14 - Evolution of annual DH energy acceptance: integrated values over the entire year and over the 3 winter months (December – February). DH energy acceptance defined for the merit-order CHP-Geothermal-Storage-HP-Wood-Gas.

5.1.1.3. System integration and discharging technics

Underground thermal energy storage (UTES) energy discharge is highly dependent on temperature levels at the DH / storage interface. While the temperature profile of the UTES is a function of injected and extracted energy, it is very difficult to evaluate without specific simulations tools, in particularly for borehole thermal energy storage (BTES) and aquifer thermal energy storage (ATES) systems, where the interaction between the heat-transfer fluid and the underground depends on multiple parameters.

Besides, energy and temperature response of the UTES is also a function of its integration in the DH system. To increase energy recovery (Kallesøe et al, 2019), charging of the UTES is usually done in parallel to DH supply (T_s) and its energy evolution is limited by the temperature differential between the DH supply and the UTES (Figure 15). On the contrary, it is meaningful to discharge the UTES in series with the DH demand, and to inject the recovered heat into the return branch of the DH (T_r). In this way, discharging of the UTES is limited by the temperature differential between the UTES and the DH return, allowing for a larger energy recovery and enhancing storage efficiency. While usually not necessary with BTES, in the case of ATES and PTES, it is further necessary to invert the connection of the hot and cold side of storage to the DH heat exchanger (HEx), so as to properly use the temperature gradient of the storage for discharge.

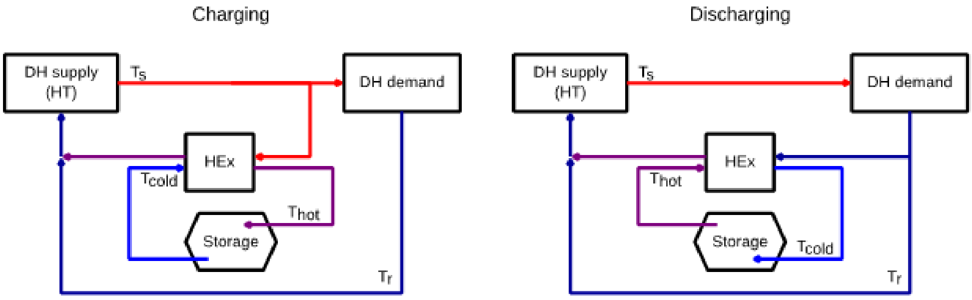

Figure 15 - Integration of a UTES in the DH system, in charging and discharging modes.

Furthermore, depending on the UTES and DH return temperatures, several discharging techniques can be implemented:

- With a UTES temperature higher than the DH return temperature, direct discharge by way of a heat exchanger is possible (Figure 16). As depicted with the 2 cases of Figure 16, the higher the DH return temperature (Tr), the lower the temperature drop in the UTES and, as consequence, the lower the extracted energy. As a matter of fact, once the available UTES temperature reaches the DH return temperature, no additional heat can be directly extracted from the storage, even when its temperature is higher than the natural surrounding environment.
- With a UTES temperature lower than the DH return temperature, assisted discharge can be done by way of a heat pump (Figure 17).
- Finally, direct and assisted heat extraction can be combined to enhance heat extraction and to increase the production temperature on the DH return (Figure 18). In this mode, a first step of heat extraction is done by a heat-exchanger (direct mode), which is followed by a second step of heat extraction by a HP (assisted mode). Notice that more than one HP (connected in series) can be used to realize this temperature increase. Such a hydraulic configuration has been used for several years already in a geothermal DH in Switzerland and has been studied in Finland [Faessler et al. 2018; Todorov et al., 2020).

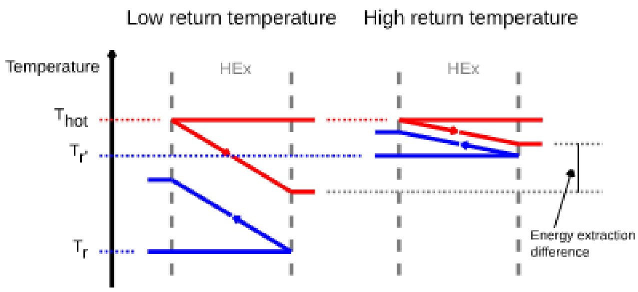

Figure 16 - Direct discharge of a UTES, by way of a heat-exchanger (HEx). Case of a low DH return temperature (left) and of a high DH return temperature (right).

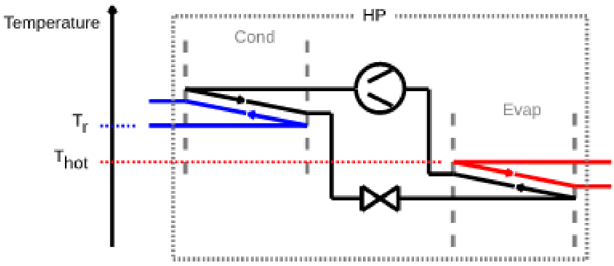

Figure 17 - Assisted discharge of a UTES, by way of a heat pump (HP).

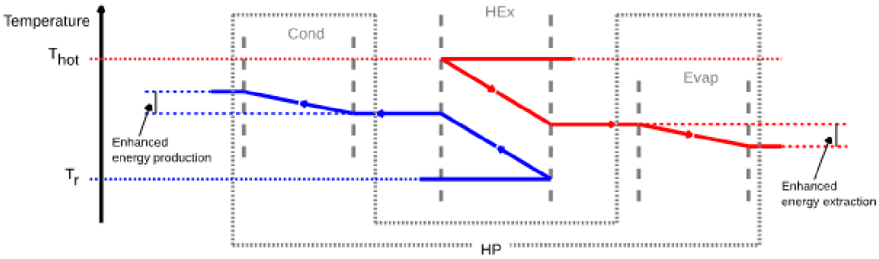

Figure 18 - Direct + assisted discharge of a UTES, by way of a heat-exchanger (HEx) and a heat pump (HP).

5.1.1.4. System design and results

Concerning system integration, it is important to analyze UTES systems with a holistic vision, since their integration within the DH network depends on a vast number of parameters. A long-term market strategy is important to guarantee that enough injectable heat is available throughout the lifespan of the project, and that the DH will be able to accept the extractable heat from the storage. Different merit-order strategies and system integration (hydraulic connections and heat extraction modes) also affect the energy efficiency of the UTES system.

Concerning technical aspects, the hydraulic connections and temperature levels at the UTES / DH interface must be considered very early in the project phase. In this regard, it is meaningful to discharge the UTES in series with the DH demand, and to inject the recovered heat into the return branch of the DH. In this way, discharging of the UTES is limited by the temperature differential between the UTES and the DH return (instead of supply), allowing for a larger energy recovery and enhanced storage efficiency. However, one must pay attention to the effective DH return temperature since a high return temperature will limit the heat extraction and can have an important economic impact. For better exploitation of the UTES, an HP can be used to increase the heat discharge, as well as to increase the amount of heat accepted by the storage.

Finally, a buffer system seems to be a good option for BTES or ATES systems, where infrastructure costs are highly dependent on installed power. For this kind of system, buffer tanks can smooth the loading and unloading profiles and avoid high-frequency power fluctuations. In the case of the of Geneva, integration of a small sized ATES (operative water-flow of 72 m3/h) with a buffer (20 MW and 300 MWh) could bring about an additional 6% fossil fuel saving and help reaching the target of an 80% renewable energy mix on the DH system by 2030.

5.1.2 Drilling results at GEo-01 and GEo-02

The Western Geneva basin is geologically complex and potentially "challenging" for geothermal production including HT-ATES, due to significant topography at the boundaries potentially imposing artesian hydraulic conditions, strike-slip and thrust faults leading to compartmentalization of aquifers and providing potential leak-off structures, inclination of aquifers raising the question of the role of buoyancy in storage, and variable sedimentary facies within the aquifers leading to heterogeneity.

Two geothermal exploration wells, drilled in the framework of the *GEothermies* program to explore the subsurface in a geothermal exploration perspective, have been studied in the HEATSTORE project. The two wells provide excellent subsurface data to assess the potential of HT-ATES installations at the two sites and to enlarge the assessment to a broader scale.

Both wells targeted the Upper Mesozoic carbonates which are considered at present the most favorable geothermal targets for hydrothermal heat production. The interest for these geologic units is related to the potentially favorable hydraulic conditions enhanced by fractures associated with fault corridors and karstification which can locally enhance the permeability of volumes of the reservoir, hence channeling hot geothermal waters. However, being the distribution of such hydraulic properties extremely heterogeneous across the Geneva area, the two wells can also provide solutions for thermal energy storage.

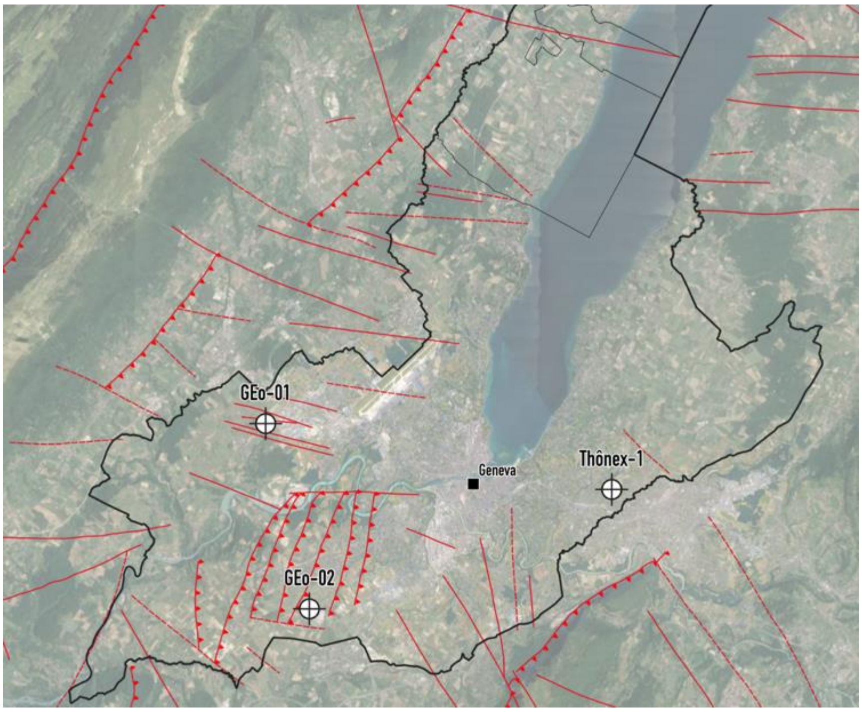

Figure 19 - Location of the GEo-01 and GEo-2 wells (modified from Clerc & Moscariello, 2020). The geothermal well Thonex-01 is reported as reference

The GEo-01 and GEo-02 wells are in the western part of the Geneva Canton and were drilled as exploration wells to characterize the geothermal conditions in the Upper Mesozoic carbonates and assess their geothermal potential for applications as hydrothermal resources or storage (Figure 19).

GEo-01 well is 744 m deep and drilled into the Cenozoic Units down to 407 MD (Measured Depth) to then enter the Mesozoic carbonates of the Lower Cretaceous unit down to 648 m MD and eventually penetrated the Upper Jurassic carbonates until bottom hole. Artesian fluid flow condition characterizes this well, with a flow rate of 55l/s, 32.4 ℃ wellhead temperature and 8bars wellhead pressure, representing a very encouraging geothermal resource suitable for heat production and direct uses. Geothermal fluids rise towards the surface along a strike-slip fault structure cutting through the Lower Cretaceous and Upper Jurassic carbonates, being the former responsible of more than 70% of the total mass discharged (Guglielmetti et al., 2020). The natural recharge of the system here is from the Jura Mountain chains and circulation at depth is related to the hydraulic gradient. The faults encountered in the Lower Cretaceous are most likely open faults, laterally confining and vertically promoting localized fluid circulation.

GEo-02 well is 1456 m deep and drilled the same units as GEo-01 reaching the top of the Lower Cretaceous at 769.9m MD. Artesian fluid flow condition characterizes this well, with low flow rate of 0.3-0.6l/s, 18˚C even if the measured bottomhole temperature observed at the end of the drilling operations was about 55˚C and about 12 bars stabilized wellhead pressure and 8bars. As per GEo-01 the natural recharge of the system is expected to be dominated by meteoric waters infiltrating in the Jura Mountain chains and circulation at depth is related to the hydraulic gradient. The fractures encountered in the Lower Cretaceous and Upper Jurassic are most likely mineralized and tight, preventing large fluid flow in this region.

5.1.3 Mineralogical and petrophysical analysis of the GEo-01 and GEo-02 cuttings

One of the main challenges related to assessing the technical feasibility and sustainability of High Temperature (~25°C to ~90°C) Aquifer Thermal Energy Storage (HTATES) is characterization of the mineralogical composition of the reservoir rocks which control the water rock interactions that can activate in response to the cyclic production/injection of hot water. These reactions have an impact on the potential of dissolution and precipitations of mineralogic phases in the reservoirs and corrosion and scaling potential at borehole and surface equipment scales. In this report we present detailed description of the results from the laboratory analysis carried out on the cuttings material collected from the GEo-01 and GEo-02 geothermal exploration borehole sites situated in the Geneva Basin, Canton of Geneva.

The collection of the cutting samples has been carried out in collaboration with Services Industriels de Geneve and HydroGeo Environnement during drilling operations as part ***of Task 3.1 On site Mineralogical and petrophysical analysis, Interpretation of logs of the proposal*** submitted to BFE and Task 4.1: Case study feasibility assessment and technical design for Demonstration of the European proposal. Analysis and interpretations were carried out in the framework of ***Task 1.1 Specification and characterization for ATES concepts of the proposal*** submitted to BFE in support the geochemical study performed by UniBe in WP2 of the Swiss proposal. The results are reported in Appendix02.

The Automated Quantitative Evaluation of Minerals by SCANning electron microscopy (QEMSCAN) analysis was used to provide a rapid and accurate evaluation of mineral phases in materials. QEMSCAN analysis were performed using a FEI QEMSCAN® Quanta 650F facility installed at the Department of Earth Sciences at University of Geneva. In Addition, Inductively Coupled Plasma Mass Spectrometry or ICP-MS was used for elemental determinations. The whole-rock compositional data for ten major elements and thirty-seven trace elements was acquired by ICP-MS with the same cuttings used for QEMSCAN analysis. The ICP-MS data acquisition was performed at Bureau Veritas laboratory (Vancouver, Canada).

The petrological and geochemical study of the GEo-01 and GEo-02 wells samples revealed important information about the main sedimentary formations of the Upper Jurassic and Lower Cretaceous.

Important lateral variations of facies and reservoir properties have been observed in the Geneva Basin. In the context of the geothermal development of the Canton of Geneva, these variations represent a challenge to better understand, assess, and predict the reservoir properties and locate suitable targets for geothermal production. To assess these variations, a complete petrographic, mineralogical, and geochemical characterization of whole-rock (cuttings) samples issued from these wells was performed. This characterization was performed using QEMSCAN and ICP-MS analysis at high vertical resolution.

By using QEMSCAN and ICP-MS, the present work was able to analyze many thin sections, recognizing and characterizing the main formations crossed by the GEo-01 and GEo-02 exploration wells, defining chemo-zones and chemo-units that can be correlated in the Mesozoic of any future exploration/production wells. Moreover, these zones can be implemented in 3D subsurface models, geological models, and geochemical models to better define the lateral facies variations, chemical changes and predict reservoir volumetrics along the basin (Figure 20).

This study demonstrates the importance of mineral analysis and whole rock geochemistry as effective tools to support subsurface exploration in poorly known sedimentary basins. The use of high-resolution petrographic analyses provided by QEMSCAN allowed the recognition and description of the main stratigraphic units of the Mesozoic sedimentary sequence crossed by the GEo-01 well. The mineralogical and chemical variations observed along the upper Jurassic and lower Cretaceous sedimentary sequences enable the effective application of a chemostratigraphic approach. Usually, time-consuming petrographic and biostratigraphic studies are used to recognize the main sedimentary facies composing this type of deposits. However, by using QEMSCAN and ICP-MS, the present work was able to analyze thin sections, recognizing and characterizing the main formations crossed by the GEo-01 and GEo-02 exploration wells, defining chemo-zones and chemo-units that can be correlated in the Mesozoic of any future exploration/production wells. Moreover, these zones can be implemented in 3D subsurface models, geological models, and geochemical models to better define the lateral facies variations, chemical changes and predict reservoir volumetrics along the basin.

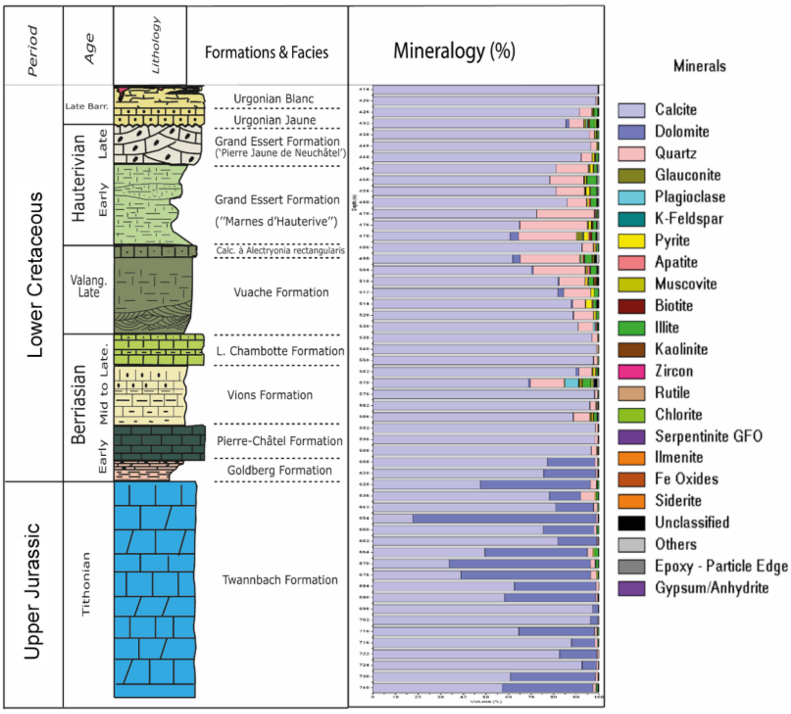

Figure 20 - Litho-stratigraphic column proposed by the interpretation of the QEMSCAN analysis results. In addition, all sedimentary formations identified in the present study are listed and correlated with the results obtained.

Using the chemo-units defined in this work by ICP-MS, the chemostratigraphic correlation between GEo-01 and GEo-02 provided critical information on the lateral variations of thickness (Figure 20). Those variations are especially important in the Lower Cretaceous. Thickness in the Upper Jurassic seems to remain constant. However, as the complete stratigraphy of the Tithonian was not drilled in GEo-01, this assumption remains to be validated. In the Lower Cretaceous, the Goldberg Fm. exhibits the same thickness in the two wells. The Pierre-Châtel Fm. is significantly thicker in GEo-02 while both Vions Fm. And Chambotte Fm. are thinner. The Vuache, Marne d'Hauterive and Pierre-Jaune de Neuchatel Fm. are also thicker in GEo-02 than what observed in GEo-01.

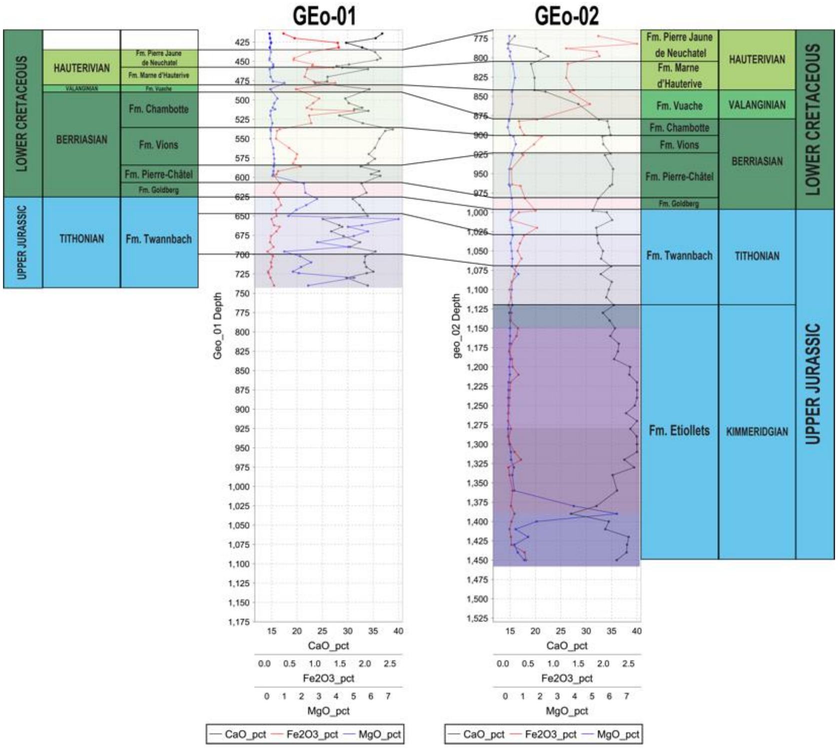

Figure 21 - Chemostratigraphic correlation of GEo-01 and GEo-02

The petrological and geochemical study of the GEo-01 and GEo-02 wells samples revealed important information about the main sedimentary formations of the Upper Jurassic and Lower Cretaceous. The comparison of these data with recent studies allows a better understanding of the Geneva Basin substrate and consequently the location of potential reservoirs. In outcrops, karsts were recognized in the uppermost Cretaceous units affecting principally the massive Urgonian limestones but are observed to extend at least down to the Pierre-Châtel Fm. (Signer and Gorin, 1995, Charollais et al., 2013; Mastrangelo et al., 2013; Godet et al., 2016). The lateral variations of thickness put in evidence by the chemostratigraphic correlations could have an impact on the quality and volumetric of reservoirs that are targeted for geothermal energy production in the Geneva Basin.

5.1.4 Geomechanical characterization of wells GEo-01 and GEo-02

In the context of ***WP3, task 3.1 Drilling, logging, and laboratory tests of the Swiss project,*** which concerns the characterization of the exploration boreholes in Geneva, the University of Neuchâtel has derived geomechanical characterizations from all the relevant data available in the exploration wells GEo-01 and Geo-02. The objective is to quantify geomechanical characteristics of the subsurface including strengths, stresses and fracturing as well as stress/fracture interactions by evaluating the slip tendency. This research should be understood as an initial basis for characterizing the geomechanical conditions in the Geneva basin, which will evolve with the acquisition of new data and the formation of new wells.

This work was mainly carried out within the framework of Morgane Koumrouyan's master's thesis for GEo-01 (Koumrouyan 2019) and Mathieu Andre Ghapgou's master's thesis for GEo-02 (Andre Ghapgou 2021). These results are synthetized in a report for the HeatStore project . These documents are available at the University of Neuchâtel and in the documentation of the Heatstore project (Valley and Sohrabi 2021). We present here a summary of the highlights of these studies.

5.1.4.1. Methodology

The methodology consists first in gathering and pre-processing all the relevant data for the geomechanical characterization of the reservoir from the drilling logs. Imaging data is particularly important as it allows the characterization of fracturing but also the identification of the potential presence of borehole failures which give important indications on the stress conditions. The absence of failure can also be useful information, although of lesser value than the presence of failure. Other types of information can be incorporated such as, if available, the results of mini-fracture tests in wells to estimate stresses. All this information generally gives only a partial estimate of the complete stress tensor. It is then a question of integration, and this is the central part of this work, to propose one or more possible stress scenarios consistent with all the observations. Numerical simulations considering the contrasts in mechanical properties along the well will also allow these models to be validated and completed. We present here a summary of some of the key methodologies that were deployed in these analyses. Refer to the complete reports (Koumrouyan 2019; Andre Ghapgou 2021; Valley and Sohrabi 2021) for complete description of the methodologies.

5.1.4.2. Logging information integration

Wellbore wall images are used to assess natural fracturing. This is a standard technique, and we will not go into detail here. However, it should be noted that images were only available from well GEo-01 (total depth 774 m, see Section 2.1) to a depth of 533 m MD (Measured Depth). Wellbore obstruction related to the presence of karstic features prevented to log the lower part of the well. Thus, the late Mesozoic section of the well was processed in this study. In Geo-02 (drilled to 1456 m depth, see Section 2.1), we could process the entire drilled Mesozoic section from about 800 m MD to total depth. Natural fracturing was determined independently by various analyst in GEo-01. In GEo-02, we used the natural fracture date set provide by the operator.

Wellbore breakouts consist in diametrically opposed failure zone at the wellbore wall. They are forming in response to the stress concentration arising at the borehole wall (see Figure 22a). Theoretical background on borehole breakouts and the way to analyze them as been reviewed by Zoback et al. (2003) and Schmitt et al. (2012). No failure was identified in GEo-01, but some failure was found in GEo-02. An example of the borehole breakouts in GEo-02 is shown in Figure 17b.

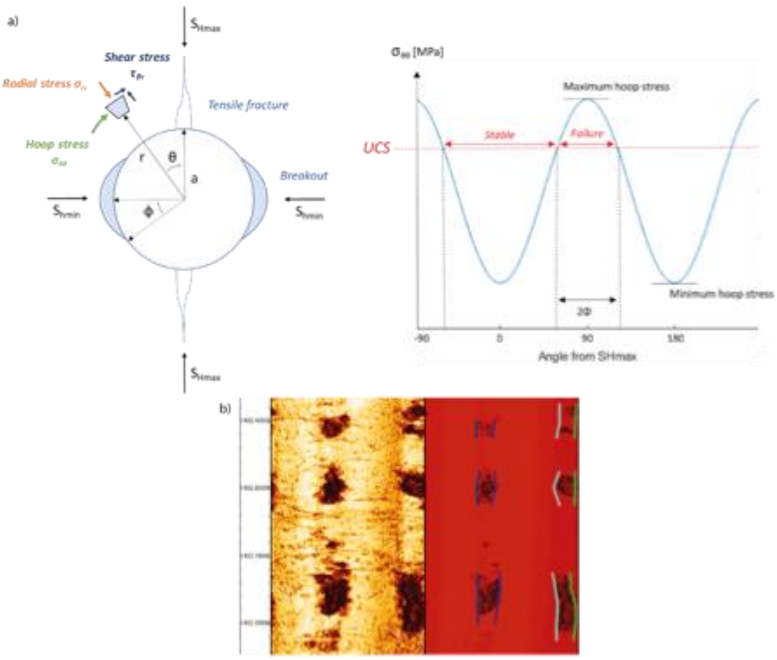

Figure 22 - a) Schematic representation of the stress concentration around a wellbore (Koumrouyan 2019). b) examples of borehole breakouts GEo-02 (Andre Ghapgou 2021).

The analyses of wellbore failure allow to give some constraints on the in-situ stress state but requires an independent estimate of the strength. Since no other information were available elastic and failure parameters for the wells were estimated from the processing of sonic logs. Fullwave form sonic from GEo-01 were reprocessed using semblance analyses (Kimball and Marzetta 1984) to estimate p-wave and s-wave velocities. Dynamic elastic parameters are evaluated based on standard relationships (Schlumberger 2002; Mari and Vergniault 2018). For strength evaluation, relationships between the uniaxial compressive strength and p-wave velocities were evaluated based on a review from Jamshidi et al. (2018). Unfortunately, no testing of local material are available at the time, although geomechanical testing of side cores obtained in GEo-02 could help refining these relationships.

5.1.4.3. Mini-frac data integration

Mini-frac tests (Haimson and Cornet 2003) were performed by Solexpert in the borehole GEo-02 (no similar data have been acquired in GEo-01). The data were analysed by Solexpert using Hubbert and Willis (1957) hypothesis. Large uncertainty are inherent to this approach for the estimation of SH_{Max} magnitude (Evans 1987; Ito et al. 1999). In our analyses, we focused in the in the integration of these data, particularly the estimation of SH_{min} magnitude based on instantaneous shut-in pressures (ISIP).

5.1.4.4. Stress modelling

Simulations of the stress field were performed to complement the data collected in the wells. The basic assumption in these simulations is that the stress field is strongly influenced by the stiffness contrasts between the different sedimentary series encountered by the wells. The stresses are then simulated by the superposition of 1st order gravity effects and tectonic deformation. In this way, the contrasting stiffness of the sedimentary series will induce stress heterogeneities. This is a first-order analysis, neglecting possible second- or higher-order effects arising from disturbances induced by the presence of fractures or faults. Moreover, only a purely elastic behavior of the massif is considered.

The simulations were carried out using analytical solutions from Thiercelin and Plumb (1994) and Blanton and Olson (1999), and numerical simulation in finite elements with the RS3 code from Rockscience. The details on these methods are described in the MSc thesis of Koumrouyan (2019) and Andre Ghapgou (2021).

5.1.4.5. Results

5.1.4.5.1. Natural Fracturing

Natural fracturing was analysed in term of intensity and orientation. The data for GEo-01 are presented in Figure 23 and for GEo-02 in Figure 23. In both cases, shallow dipping fractures are generally dominating and are corresponding to bedding parallel fractures. In GEo-01, there are significant perturbations in orientation, and these seem to be corresponding with well section with water inflows identified with drilling advancement. These are likely representative of local rock mass disturbances associated to fault structures. Fracture intensity is large in GEo-01 with P10 (linear fracture frequency) typically in the range of 2 to 10 fractures per meter. In GEo-02, the fracture intensity is much lower with an average P10 close to 0.5 fractures per meter. There are particularly few mapped fractures between 1150 and 1350 m. However, the fracture determination have not been performed by the same analyst in both well and it is unclear if the large difference in fracture intensity is real, or due to different logging quality or wellbore image analyst. Fracture orientation in GEo-02 is primarily sub horizontal (average dip angle of 10°) while non horizontal fractures are very diffuse. Andre Ghapgou (2021) tentatively identified two additional fracture sets (Figure 24) with orientations of 314/71 and 270/38 (dip direction / dip angle).

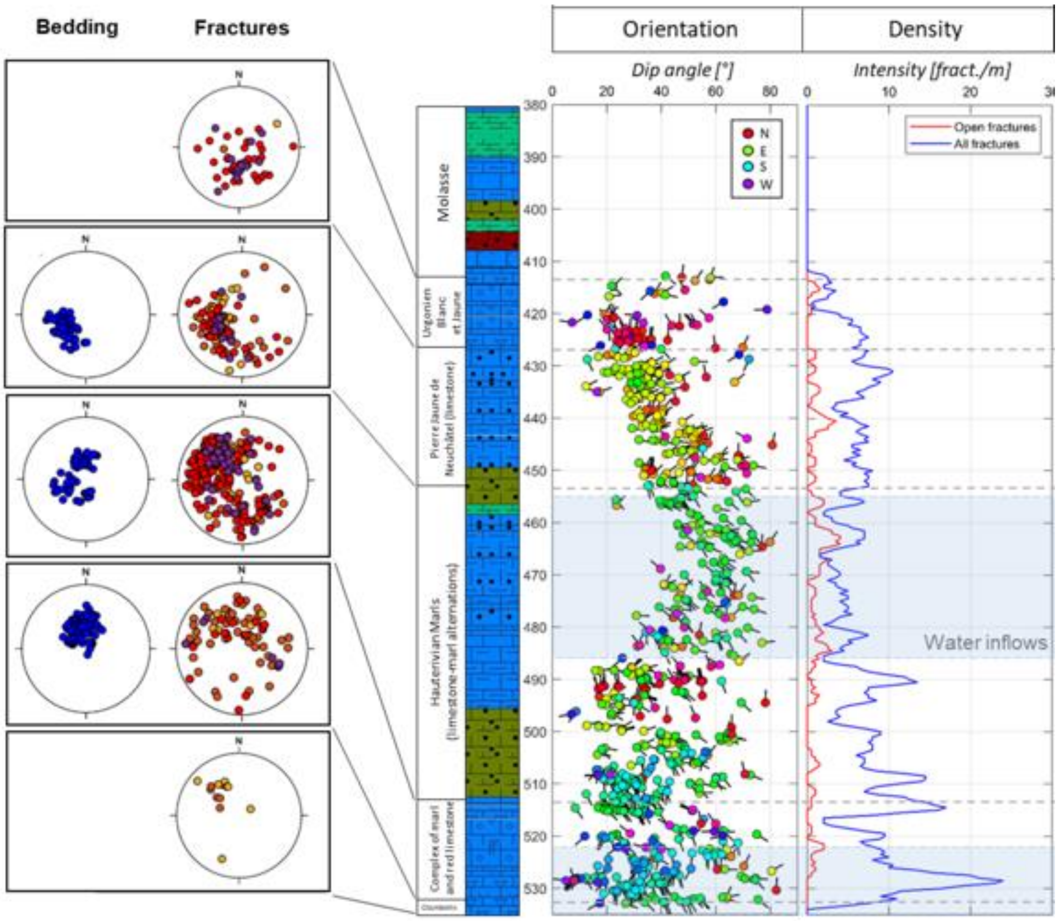

Figure 23 - Natural fracture analyses in the borehole GEo-01 (after (Koumrouyan 2019)

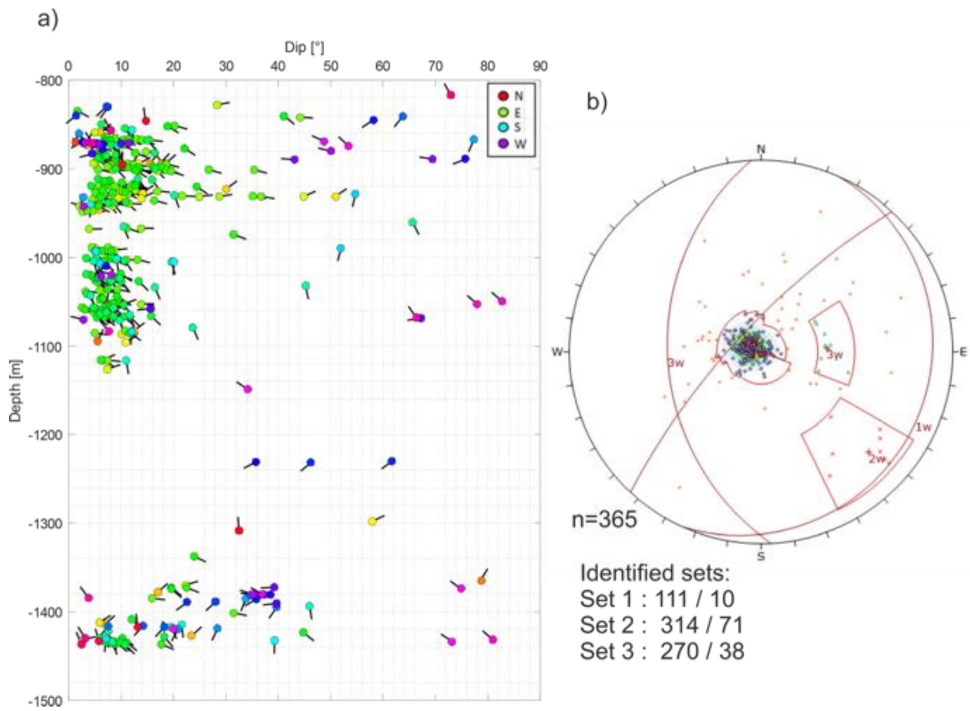

Figure 24 - Fracture analyses in GEo-02. a) tadpoles representation of the fractures. Coloring based on fractures dip direction. b) stereographic projection of the mapped fractures with identification of 3 main fracture sets. (Figures after Andre Ghapgou 2021).

5.1.4.5.2. Rock mechanical characteristics

Rock mechanical characteristics are primarily derived from the analyses of sonic logs as drilling was destructive and full core were not collected. Some side wall cores were collected in GEo-02, but rock mechanical test results are not available at the time of reporting.

Dynamic elastic properties are derived from combination of acoustic velocity and density. Sonic processing has been performed in house for GEo-01 performing semblance analyses, while provided velocities were directly without further processing of the full wave form for GEo-02. The results of these analyses are not reproduced here but can be find in Koumrouyan (2019) and Andre Ghapgou (2021). In GEo-01 the Young's modulus profile in the Cretaceous is characterized by sharp variation with modulus going from about 35 to 60 GPa. These variations are interpreted as reflecting stiffness contrast arising from clay content in the sedimentary series (marls vs. limestones). Variability in Young's modulus is also characteristic of the Cretaceous section of GEo-02. The late Jurassic series is however much more homogeneous with a nearly constant dynamic Young's modulus estimated at about 75 GPa, except for the lower section of the log in the Villingen formation were the dynamic Young's modulus decreases down to about 40 GPa.

Strength parameters have been estimated for both boreholes, although without laboratory mechanical testing available, these results must be considered with caution. For the analyses in GEo-01, strength properties have been estimated from EPFL data base on similar lithologies of the Swiss Cretaceous formations. Assumed averaged uniaxial compressive strength is about 80 MPa for the limestones, 15 to 30 MPa for the marly limestones and down to about 6 MPa for the marls. All these values have large uncertainty ranges.

For GEo-02, uniaxial compressive strength has been evaluated based on published relationship (Jamshidi et al. 2018) with p-wave velocities for similar lithologies. The estimated average strength is about 80 MPa for the Cretaceous limestones and increases to about 120 MPa for the Jurassic limestones. Here again, large uncertainty ranges (about +/- 40 MPa should be considered).

5.1.4.5.3. Principal stresses orientation

In the framework of the limited data available, stress characterization is performed with the basic assumption that one principal stress is vertical. As a first order estimation, this simplification is justified by the fact that large topographical variations are not present in the direct vicinity of the boreholes and the strata in the basin are sub horizontal which suggest that not large oblique anisotropy should be present. In this framework, the stress characterization consists thus in the determination of the profile of maximum horizontal stress orientation and stresses magnitude.

One of the best indicators for stress orientation is the direction of borehole breakouts if present. No breakouts have been identified in GEo-01 and thus with the data set of this borehole, the principal stress orientation remained undetermined. In the absence of breakouts, we performed a shape analysis of the GEo-01 borehole geometry by fitting ellipses on the borehole sections determined from acoustic televiewer data. The data of this analyses are presented in Figure 25a. The ellipses principal axis orientation is generally instable, and it was not possible from these analyses to derive any reliable evidence on the principal stress orientation.

Borehole breakouts are however present in the GEo-02. The breakouts orientations have been mapped and the orientation statistics is presented in the form of a circular histogram in Figure 25b. The breakout orientation is generally consistent and have a mean orientation at N013°, implying a maximum horizontal stress direction of N103°. This a first direct stress orientation information available in the Mesozoic limestones of the Geneva basin obtained in the geothermal exploration of the SIG. Note that the stress orientation has not been validated by hydraulic fracture mapping following mini-frac tests since these fractures couldn't be identified on borehole image logs and impression packer data were not collected.

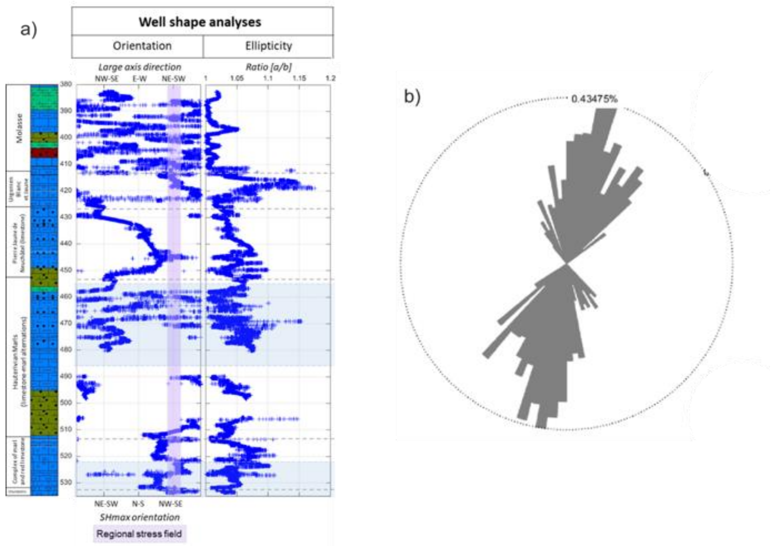

Figure 25 - a) well shape analyses in GEo-01: the ellipticity of the well is determined by using a direct least-square regression on borehole section determined from acoustic televiewer data. The orientation of the ellipse large axis direction and the ellipse axis ration is report.
See Koumrouyan (2019) for details. b) Circular histogram of borehole breakout orientation mapped in GEo-02 (after Andre Ghapgou 2021).

5.1.4.5.4. Principal stresses magnitudes

For the stress magnitudes, we work in the conceptual framework of stress profile dominated by the superposition of gravitational response and tectonic straining on a layered sedimentary series with strong stiffness contrast. We then use all available information pertinent for constraining the stress profiles.

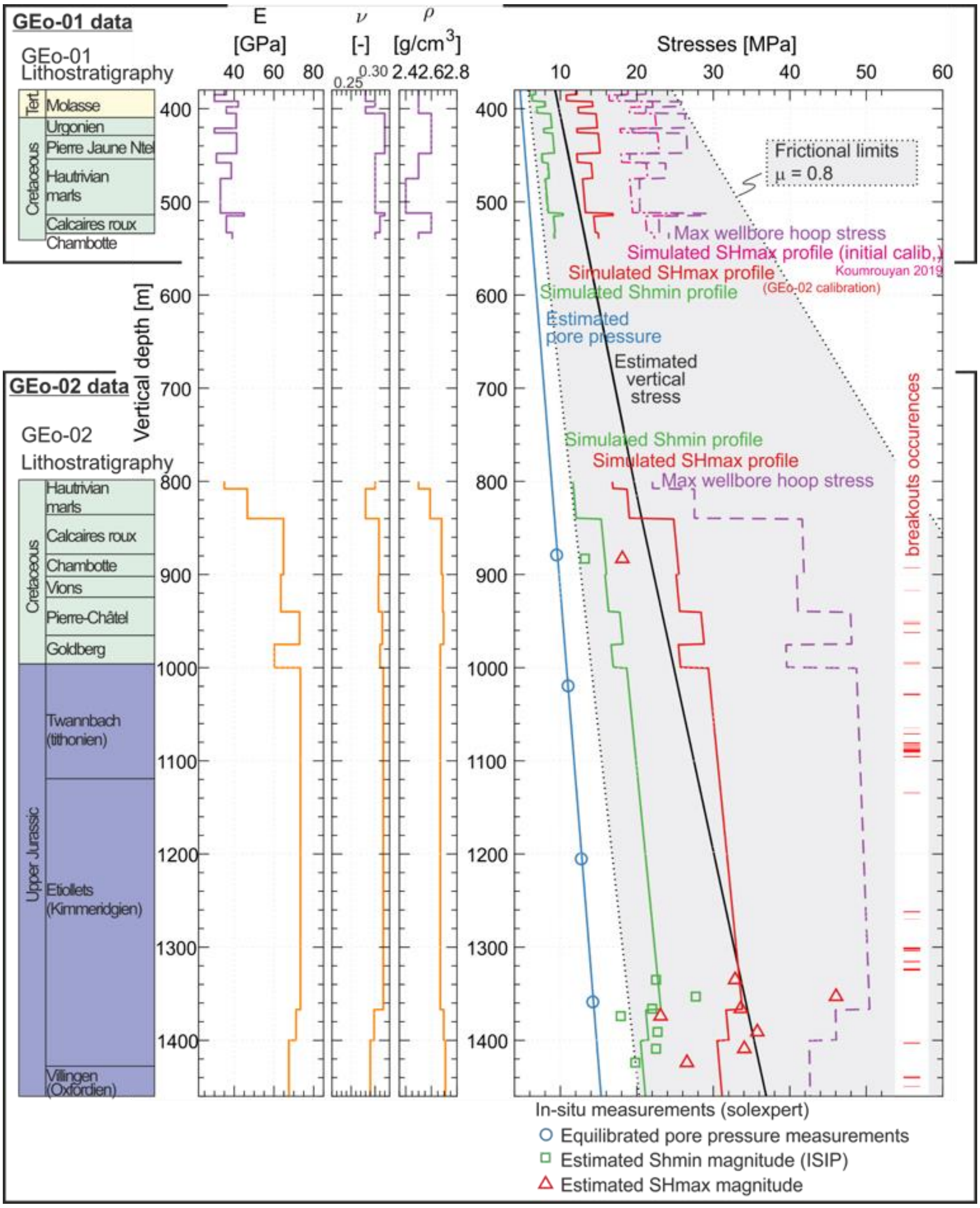

Figure 26 - Summary of stress information for the boreholes GEo-01 and GEo-02. Both boreholes have been represented on the same depth scale, although comparatively equivalent lithostratigraphic units are deeper at GEo-02. Only data from the Mesozoic sections are shown, i.e., data from about 380 to 540 m for GEo-01 and 800 to 1460 for GEo-02. From left to right left: simplified lithostragraphy of the boreholes (SIG personal communication). Middle: Elastic rock properties profile including the Young's modulus (E), the Poisson's ration (n) and the density (r). Right: compilation of stress information. Only limited in-situ measurements are available. This are hydraulic tests and minifrac tests between packers completed in GEo-02. They allow to estimate the pore pressure profile (blue) and give some punctual estimate of the Shmin (green) and SHmax magnitudes (red). The vertical stress magnitude (Sv, black) is estimated from density integration. The Shmin (green) and SHmax (red) profiles are calibrated by using a gravitational and tectonic analytical model from Blanton and Olson (1999) and adjusting tectonic strain for matching stress measurements. The violet dashed line are the computed maximum effective hoop stress at the borehole wall from these stress profiles for comparison with breakout occurrences.

The vertical stress magnitude is not directly measured but estimated from density data integration (see Figure 26 black line). For GEo-01, Koumrouyan (2019) estimated a mean density for the lithological columns of about 2500 kg/m^3, implying a vertical stress magnitude of about 12 MPa at 500 m depth. Slightly larger mean densities are assumed when considering the lower part of GEo-02 well (Andre Ghapgou 2021): with a mean density of 2590 kg/m3, a vertical stress estimation of 35.6 MPa is derived at 1400 m depth.

The in-situ pore pressure is clearly above hydrostatic for both wells. Koumrouyan (2019) considered a 1 MPa (10 bar or 100 m of water head) pressure above hydrostatic conditions at the level of the Mesozoic limestone in GEo-01. Packer test performed in GEo-02 by Solexpert confirm this value of about 1 MPa overpressure (Figure 26 blue line and symbol).

Only limited information exist to constrain horizontal stress magnitudes. Mini-frac test executed in GEo-02 by Solexpert give some indication on the SH_{min} and SH_{Max} magnitude, also some uncertainty remains with these tests since the created or activated fractures were not imaged. Nevertheless, we used this data in GEo-02 for calibrating gravitational and tectonic stress model in layered series with stiffness contrast using the analytical solution from Blanton and Olson (1999) and using finite element simulations. We use an optimization algorithm for iteratively adjusting the tectonic strains so that the sum of the squared differences between models and observations is minimized. More information on these simulations is given on the next sections. This allows us to provide a continuous stress profile along the entire borehole sections considered. Based on the horizontal stress profiles maximum effective hoop stress at the borehole walls were computed (violet dashed lines in Figure 26) for comparison with breakouts. Breakouts occurs only in GEo-02, but are rather limited, with only about 26 m of boreholes affected by breakouts of the about 660 m of investigated borehole wall images. This mean that less than 4% of the borehole is under failure. With the proposed stress profiles, computed maximum effective hoop stress is always below 50 MPa, which is consistent with very limited failure considered the strength estimated presented above.

The proposed stress profile suggests a transitional strike-slip to normal faulting regime for the Geneva basin at the depth of the boreholes. This is consistent with foreland stress regimes derived from focal mechanisms from Kastrup et al. (2004). The proposed stress characterization proposed is also consistent with a frictional strength limit with a friction coefficient of 0.8 (grey area in Figure 26). The current stress characterization should however be considered as preliminary because only limited and uncertain (no imaging of the induced fractures) in-situ stress measurement are available for calibrating and verifying our models.

5.1.4.5.5. Stress simulations

Stress simulations have been performed to complete stress measurements. In GEo-01 where no stress measurements are available and no wellbore failure was observed, this was the only rational for proposing some stress characterization. In GEo-02, the available stress data allowed to calibrate such model. Our models consider the superposition of gravitational and tectonic stresses on a layered series with stiffness contrasts. We solved this problem using numerical tools (final element method using RS3 commercial code) and using an analytical solution (Blanton and Olson 1999). An example of the model used is shown in Figure 27. Numerical solutions and analytical models have been tested satisfyingly for consistency, and thus the analytical solution is preferred for computing efficiency.

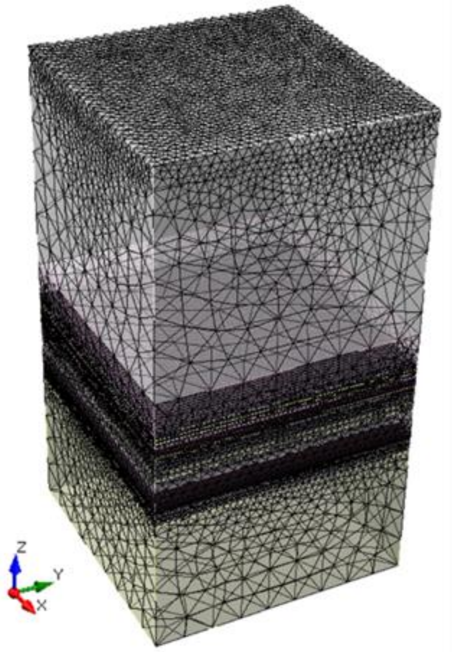

Figure 27 - example of the RS3 mesh and layered model used for stress analyses. The model size is about 400x400x750 m and consists of about 1’000’000 4-noded tetrahedra (Koumrouyan 2019).

The model used are purely elastic and the model inputs are essentially density, elastic modules, and tectonic strains. The density and elastic parameters are derived from the logging data. The tectonic strain is unknow a priori and must be calibrated. Koumrouyan (2019) calibrated strain such that the model reaches frictional limit (no other constraints were available for GEo-01). This led to relatively high maximum horizontal stress magnitudes (see Figure 26, purple curve). The situation in GEo-02 is much more favorable since some data are available for model calibration. In this case, iterative optimization has been used for estimating the tectonic strains that minimize the sum of the squared difference between simulations and measurements. The calibrated strains are ε_{max} = 2.11E^{-04} and ε_{min} = 2.05E^{-05}, for the maximum and minimum principal strain (positive is contraction), respectively.

5.1.4.5.6. Slip tendency

By combining fracturing data and stress characterization, fracture stability has been computed (see Fig. 7). The analyses in GEo-01 (top) is somewhat biased because the stress state was calibrated to obtain critical conditions. In GEo-02, the stress characterization is not constrained by criticality and the obtained fracture stability analyses indicates that fractures are primary not critical. This is also explained by the fact that the identified fractures are primarily horizontal and thus perpendicular to the principal stress direction in our gravity driven stress state. Thus, very little shear stress develops of these fractures.

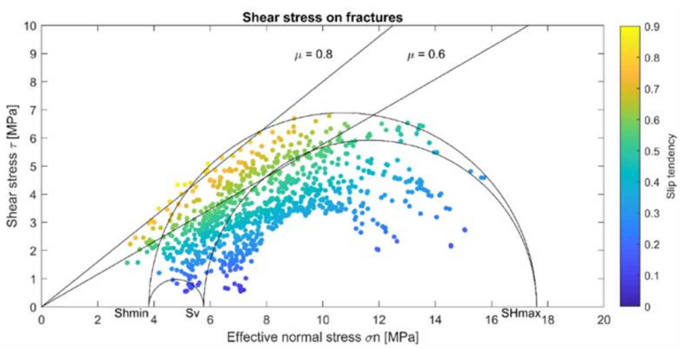

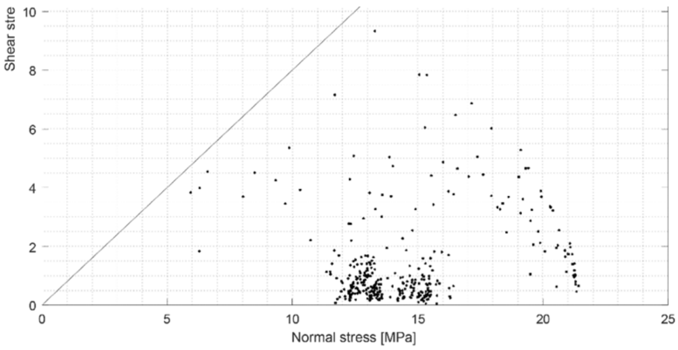

Figure 28 - Fracture stability estimated in GEo-01 (top) by Kourouyan (2019) and for GEo-02 (bottom) by Andre Ghapgou (2021). The analyses used different stress assumption (see original work for details).

5.1.4.6. Outlook

The proposed work is a first geomechanical and stress characterization in the Geneva basin. Starting with GEo-01 data, the stress analyses was very limited because no actual stress measurements were performed. The proposed characterization was thus highly uncertain. With the drilling of GEo-02 and the acquisition of hydraulic fracturing stress measurement data, the constraints for developing a stress characterization are much better, although because the generated hydraulic fractures were not imaged, uncertainties remains on the stress magnitudes. Luckily, some borehole breakouts could be observed in GEo-02 giving a strong base for estimated horizontal stress orientation. The maximum horizontal stress is estimated to be directed toward N103°. The stress regime is a transitional strike-slip to normal regime quite typical for foreland basin situation. Additional data collected in future boreholes of the SIG exploration program in the Geneva basin will be critical for confirming and refining the proposed stress characterization.

5.1.5 Field analogue in fractured and karstified limestones – the Concise test site

In the context of WP1, task 1.1 of the Swiss Project, which concerns the development of techniques to characterize thermo-hydraulic parameters in fractured and karstified aquifers relevant for underground heat storage in aquifers, the University of Neuchâtel has performed a suite of in-situ experiments. To make such experiment possible, an analogue test site has been developed in Concise (VD) in saturated fractured and karstified limestones. Indeed, performing such in the exploration well in Geneva GEo-01 and GEo-02 would have been inefficient or even impossible. The work has been thus focused on the development and the characterization of this analogue test site as well as the execution and analyses of thermo-hydraulic tests. This work was mainly carried out within the framework of three MSc thesis from Andre Ghapgou (2021), Milo (2021) and Jaquet (in prep.). These documents are available at the University of Neuchâtel (Sohrabi and Valley 2021 – Appendix 30). We present here a summary of the highlights of these studies.

5.1.5.1.1. Local geology and hydrogeology

The details of the local geology can be inferred from the data collected in a dozen drill holes drilled in the 1990s as part of the Rail2000 and N5 work. A local geological section was made based on these data and is presented in Figure 29.

The hydrogeological context is dominated by the stratigraphic series with alternating aquifers (fractured and karstic limestones) and aquitards (marly layers). For the study site, the aquifer is the limestones of the upper Hauterivian and Barremian with the aquitard of the Marnes bleu d'Hauterive at the base of the aquifer. The presence of the Lance fault certainly influences the circulations on a larger scale, with an important karstic source (La Raisse) located in the north-east compartment of the fault, at 730 m from our study site. Despite its emergence in the Cretaceous limestones, much of the spring's watershed is in the Jurassic limestones of the Malm. A temporary spring interpreted as an overflow from the karst system (La Dia) is located on the Lance fault, 1.9 km southwest of our study site.

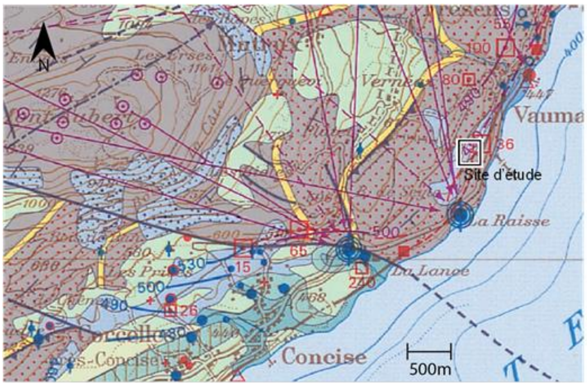

Figure 29 - Extract from the Swiss hydrogeological map

The Raisse spring was historically located at an altitude of 460 m (about 30 m above lake level) but is now tapped in the SBB tunnel and discharged downstream in the hamlet of La Raisse. This main perennial spring at the regional level should represent the low point of the water table in regional approximation. The Dia spring is temporary and is at an altitude of 470 m. We found several boreholes equipped with piezometric tubes. The elevations of the water table measured between December 2018 and April 2019 are shown on the map in Figure 30. This information gives us the necessary background combined with logistic rational for selecting an appropriate location for implementing our test site.

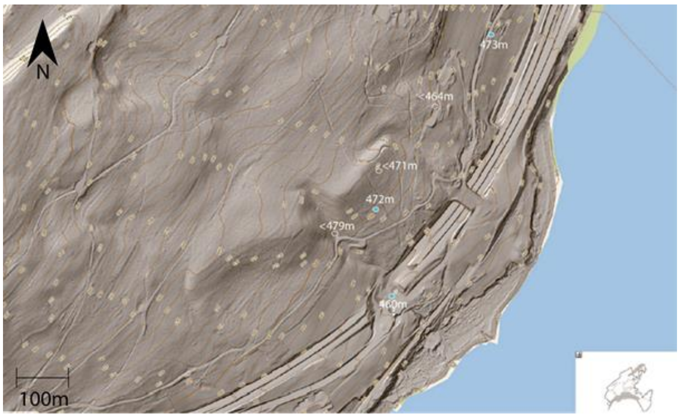

Figure 30 - Digital elevation model (DEM) with observations of the water table. Blue symbols: Source or water table observed in existing piezometers. Open symbols: existing dry piezometers where the water table is lower than the bottom of the is lower than the bottom of the piezometer.

5.1.5.1.2. Drilling implementation

The choice of the location of these boreholes was studied beforehand with the information available, the geological section (presented in chapter 1) and the two nearest boreholes CN116 and CN117 (drilled in 1996). The criteria for site selection were as follows:

- The longest possible length of the boreholes must be in a fractured and saturated limestone aquifer.
- The boreholes are vertical and do not exceed approximately 50 m.
- The site is also positioned at a distance from the lake and the road and rail tunnel infrastructures present in the region to avoid their influence zone on the hydraulics and the thermic of the water table.

- The drillings remain in a single aquifer to respect the environmental constraints which impose not to put in contact distinct aquifers.
- The distance between the boreholes has been determined to allow heat transfer experiments and must therefore be short (5-10 m maximum)
- The site must be easily accessible and can be secured to work without risk (traffic, etc.)

The chosen drilling site finally corresponds to the connection between the road between Concise and Vaumarcus and an agricultural road. The coordinates of the boreholes are presented in

Table 1.

Table 1 - Coordinates of the boreholes at the Concise test site.

Borehole	Coordinate E	Coordinate N	Altitude [m]
RSBV1	547683.47	191276.69	475.60
RSBV2	547685.97	191280.6	475.50
RSBV3	547681.22	191280.49	475.48

5.1.5.1.3. Borehole Trajectometry

Borehole deviation and tilt measurements were collected in all three-borehole part of wellbore imaging logging. The measurements are based on magnetometer for the azimuth and such data cannot be used in the first 10 m of the borehole because the acquisition is perturbed by the steel casings. The azimuth and deviation data were resurveyed using standard techniques (Walstrom et al. 1972) to compute boreholes trajectories. (Figure 31). Since the target depth is 50 [m], the deviation is small as there is not enough distance to be deviated. The map view shows that the boreholes are mainly vertical. According to the results obtained, in the next analyses, truly vertical boreholes will be considered for almost all processes.

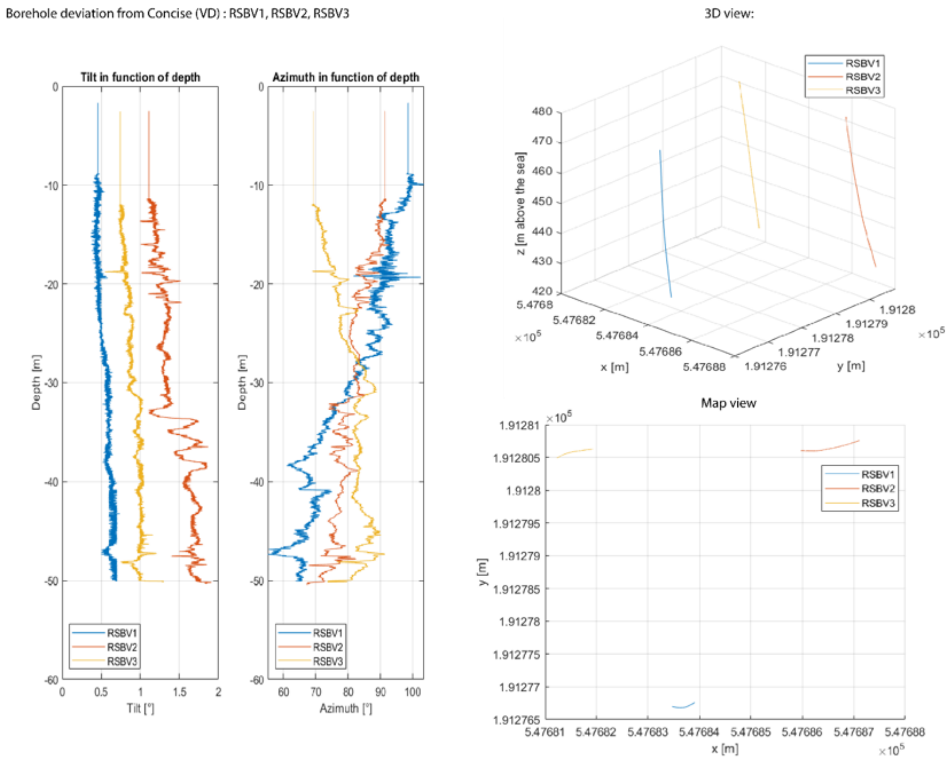

Figure 31 - Deviation calculation of the RSBV boreholes.

5.1.5.1.4. Hydrogeological monitoring during drilling campaign

The follow-up of the drillings at the geological and hydrogeological level was carried out by the CHYN. It included the following aspects:

- Follow-up of the site
- Collection and documentation of cores (see geological profile)
- Hydrogeological monitoring of the Raisse springs
- Basic hydrochemistry of the water collected from the boreholes

5.1.5.1.4.1. Hydrochemistry of the local waters

Waters flowing in carbonate aquifers, such as those in the Cretaceous units of the study area, generally have geochemical facies dominated by calcium Ca and bicarbonate HCO3. Here, the composition is normal for shallow waters. If these had been deep with long residence times, these fluids would have exhibited more complex geochemical compositions. Furthermore, if deeper fluids were present, they would flow to the surface through fault corridors, where secondary minerals dominate the water-rock interactions during the final stages of circulation. When waters can reach several km in depth and temperature above 100˚C, the main geochemical signature is dominated by sodium Na and chloride Cl. This is not the case here.

The boreholes show a predominant Ca-HCO_3 signature (Figure 32and Figure 33). This is normal for shallow waters in limestone

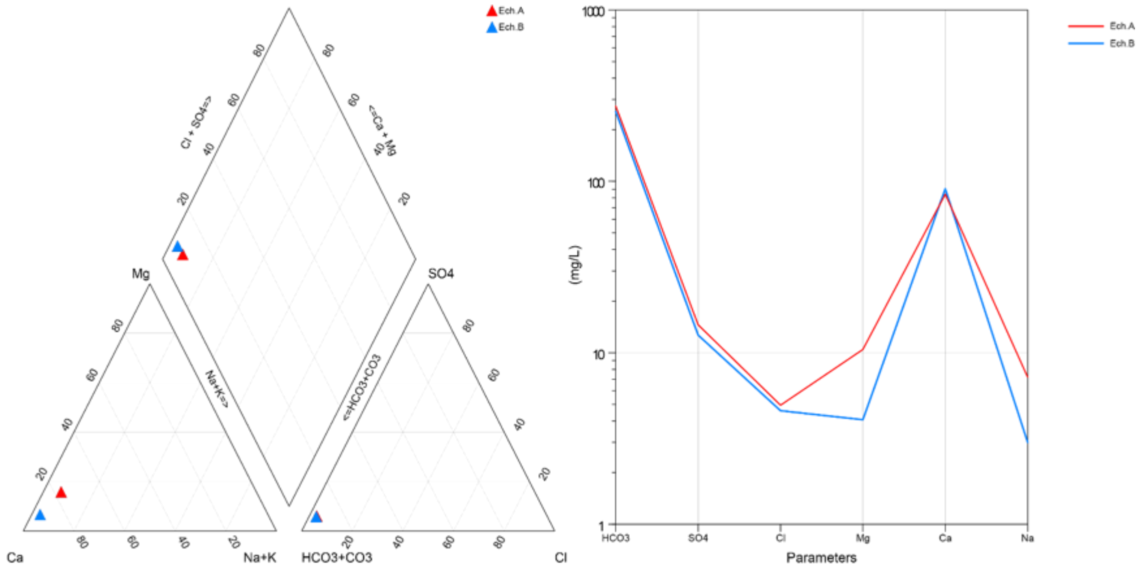

Figure 32 - Piper diagram (left) and Shoeller diagram (right) of major ions in RSBV1, December 2019

Table 2 - Hydrochemical analysis of RSBV1 drilling water, December 2019.

Date	Sample	Ca [mg/l]	HCO3 [mg/l]	Na [mg/l]	Cl [mg/l]	Mg [mg/l]	SO4 [mg/l]	K [mg/l]	NO3 [mg/l]	pH
20.12.2019	Sample A	84.1	274.87	7.2	4.94	10.64	14.57	2.72	23.26	8.015
20.12.2019	Sample B	90.41	255.1	3	4.59	4.07	12.68	1.33	27.17	7.808

5.1.5.1.4.2. Monitoring of the Raisse spring

Data from the spring are presented in Figure 33. The turbidity and electric conductivity are influenced by natural discharge variations of the spring and not by our drilling campaign. It was concluded that the drilling had no impact at the Raisse spring.

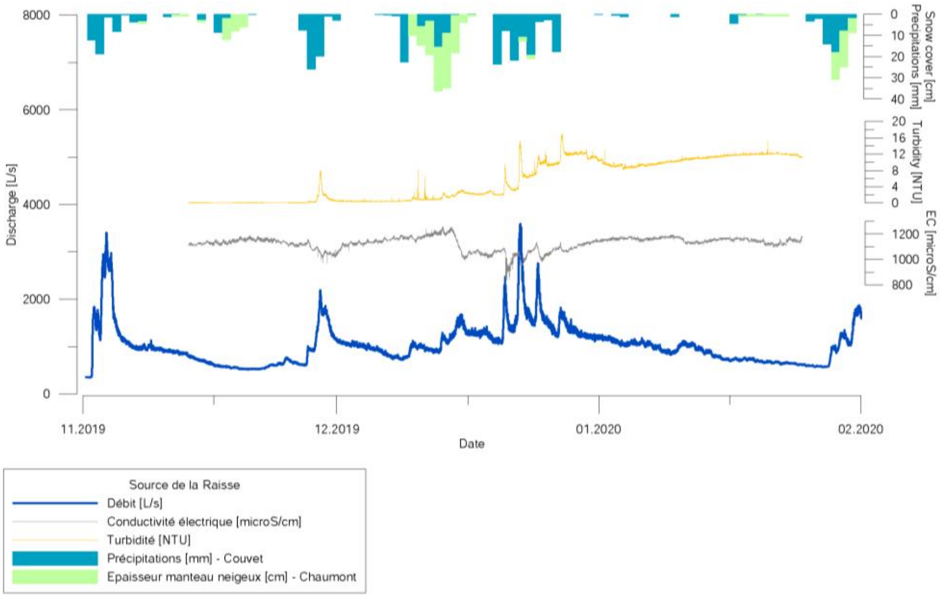

Figure 33 - Hydrological and hydrogeological evolution at the Raisse spring during the drilling campaign

5.1.5.1.5. Geological and petrophysical characterization

5.1.5.1.5.1. Core logging, borehole logging and geological well profile

Cores taken during the drilling campaign were stored in the basement of the University of Neuchâtel for a description of the lithologies encountered up to 50 [m]. The lithological logs presented in this section show an analysis of the lithologies, the number of fractures per meter, the Rock Quality Designation (RQD), the Total Core Recovery (TCR) and the equipment inside the boreholes. Images are also incorporated to the logs to visualize the fractures and main lithologies changes. The formation crossed on the site are the Vallorbe, Gorges de l'Orbe and Grand Essert formation. As mentioned previously, the period crossed is the early Cretaceous from the Barremian to the lower and upper Hauterivian stage. The boreholes are differentiated in 4 main lithologies: the oolitic limestones, the coarsely oolitic limestones, the yellow limestones, and the blue marls.

5.1.5.1.5.2. Fracturing analyses in RSBV boreholes

5.1.5.1.5.2.1. Equipment for data acquisition

An optical image log and an acoustic image log were used in the three boreholes to provide high resolution images. The device used ISA QL40-OBI-2G and QL40-ABI-2G provided by Advanced Logic Technology (ALT). A sensor on the device records the reflection of the light source (10 high efficiency LEDs) sent on the borehole wall through a fisheye lens and the images are recorded in 360°.

To highlight productive fractures, flow logs and conductivities measurement along the boreholes were performed to understand the flow system. The device used consists in a propeller that rotates when flow is present at a certain depth. Coupled with gamma-ray and conductivity measurements, we highlighted lithologies and detected water arrivals at different depth.

5.1.5.1.5.2.2. Fracture density processing

The analysis of the fracture's density is important to see if there is a correlation between the lithology and the number of fractures. It also indicates the productive intervals to perform hydraulic tests.

Two methods were used to obtain the fractures number per meter:

- The first one consists in the observation of the fractures on cores that were taken during the drilling. This approach is useful because we quickly get an idea of the fractures density before performing hydraulic tests.

- The second one is linked to the picking of fractures. Images that were taken in the three boreholes with an optical televiewer allow us to easily identify fractures. Then, analyses are performed to obtain the number of fractures per meter.

The images recorded with the mentioned device are also used for the fractures picking.

The picking is done as illustrated on Figure 34 and give information about the number of fractures families. Images obtained with the optical televiewer are used to analyse the fractures. On optical images, fractures are darker than the matrix and veins are lighter. As the optical televiewer is georeferenced, these analyses give us directly information about the orientation and the dip of the fractures. Adding a vertical line corresponding to the borehole orientation, we also obtain the spacing between the fractures for each family. All the fractures picked numerically are treated to determine the number of fractures families and mean orientations for each family represented on Figure 35.

Mapped fractures are also analysed to understand the connection between boreholes. The projection of a fracture mapped in a borehole to another one allows to estimate the entry point of water injected in the first one. This analysis is important for the creation of the future models and compare with stochastic fracture implementation.

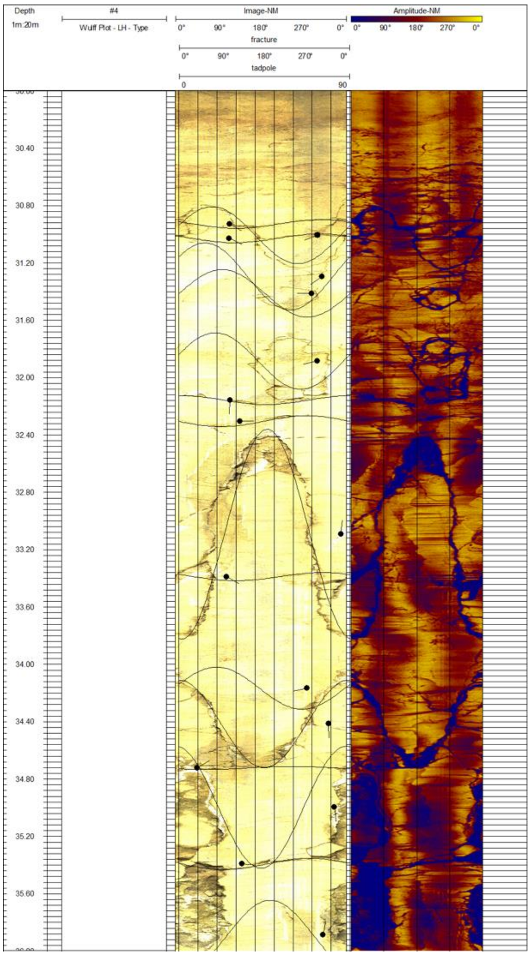

Figure 34 - Fractures mapping for orientation and intersection analyses in borehole RSBV2. The middle image is an optical televiewer inmage and the right image is an amplitude image form an acoustic imaging log. Determined fractured are overlayed on the optical image as sinusoidal traces and tadpoles.

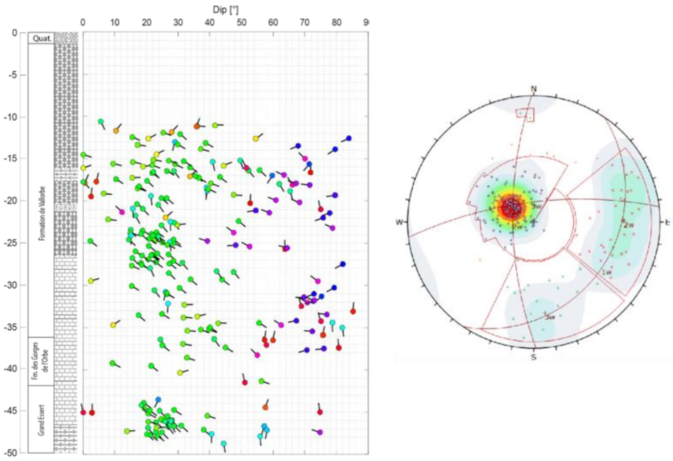

Figure 35 - Example of presentation of the fracturing data for one of the boreholes left: simplified lithological column and fracture orientation presented as tadpole. Tadpoles are color based on their azimuth to help identifying families. Right: stereographic projection of the fracture data with 3 main fracture families identified.

5.1.5.1.6. Hydraulic tests

Extensive characterization of the boreholes was carried out by conducting packer tests in July 2019. An overview of the data collected is presented in figures Figure 36, Figure 37 and Figure 38. The tests performed consisted of pulse tests, slug tests, pumping tests and injection tests. The possibility to perform tests between packers proved to be crucial for the good understanding of the system hydraulics. Indeed, in the lower parts of the boreholes we have formations with low transmissivity but high hydraulic heads. These conditions cannot be identified without performing packer tests. For the hydraulic characterization of complex systems such as fractured and karst aquifers it is necessary to acquire this type of data, and we can only recommend the application of tracker testing for the hydraulic characterization of reservoirs intended for heat storage.

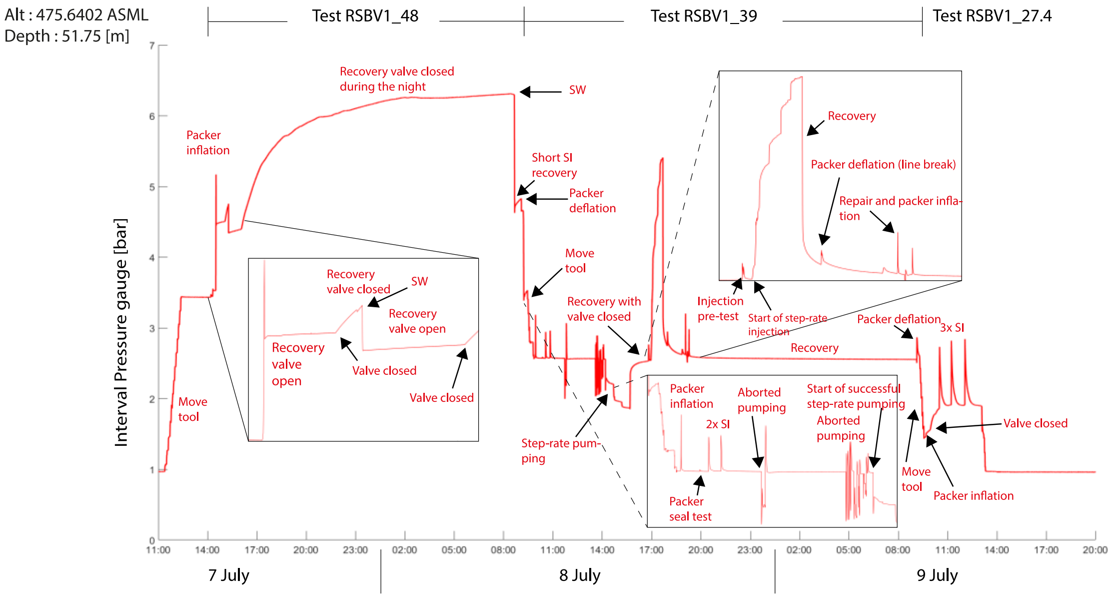

Figure 36 - Test overview in RSBV1 during the hydraulic campaign test in July 2020

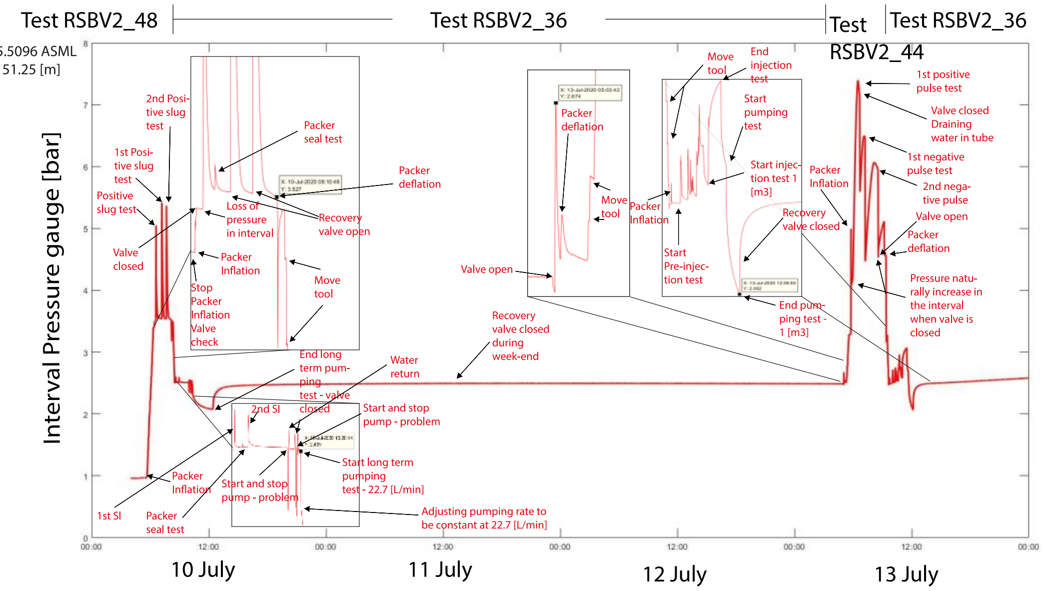

Figure 37 - Test overview in RSBV2 during the hydraulic campaign test in July 2020

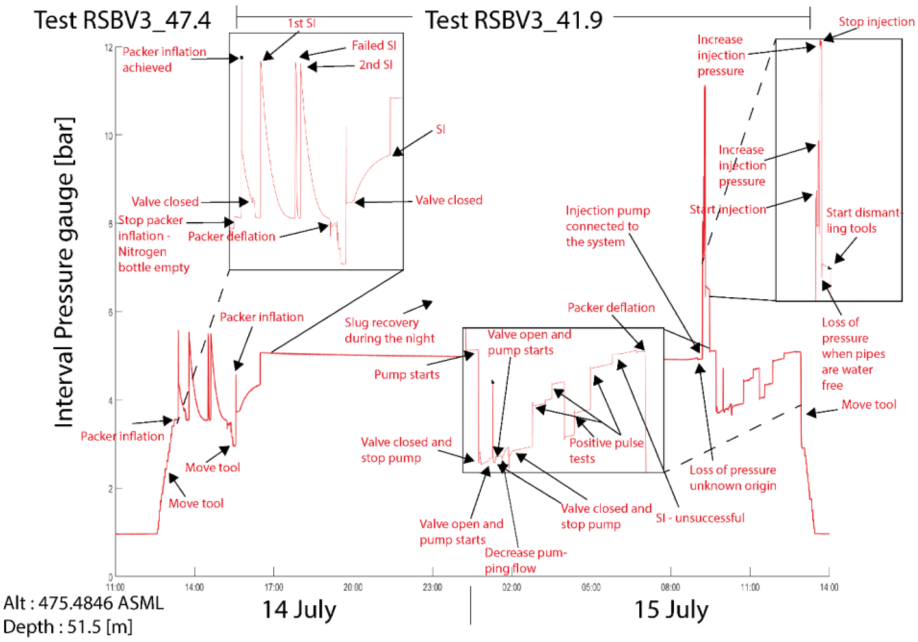

Figure 38 - Test overview in RSBV3 during the hydraulic campaign test in July 2020

5.1.5.1.6.1. Hydraulic conductivity Results

A summary of the results of the hydraulic tests is presented in Figure 39. The results are obtained by interpreting the different types of tests with analytical models. They allow deriving a picture of the transmissibility distribution along the well. We observe variations in transmissivities over several orders of magnitude along our wells. We find that higher transmissivities are present in the RSBV1 and RSBV2 wells at depths ranging from 30 to 35 m. These depths correspond to the presence of major fractures intersecting the wells. RSBV3, on the other hand, seems less well connected hydraulically with the other two wells, although the distance between the wells is similar, i.e., 4.5 m.

The characterization of the transmissivities and its distribution along the wells is essential for the hydraulic understanding of the studied system. These data were also important for the planning and execution of thermal-hydraulic tests. They allowed the dimensioning of the flow rates and thus the quantities of injectable energy available in the system.

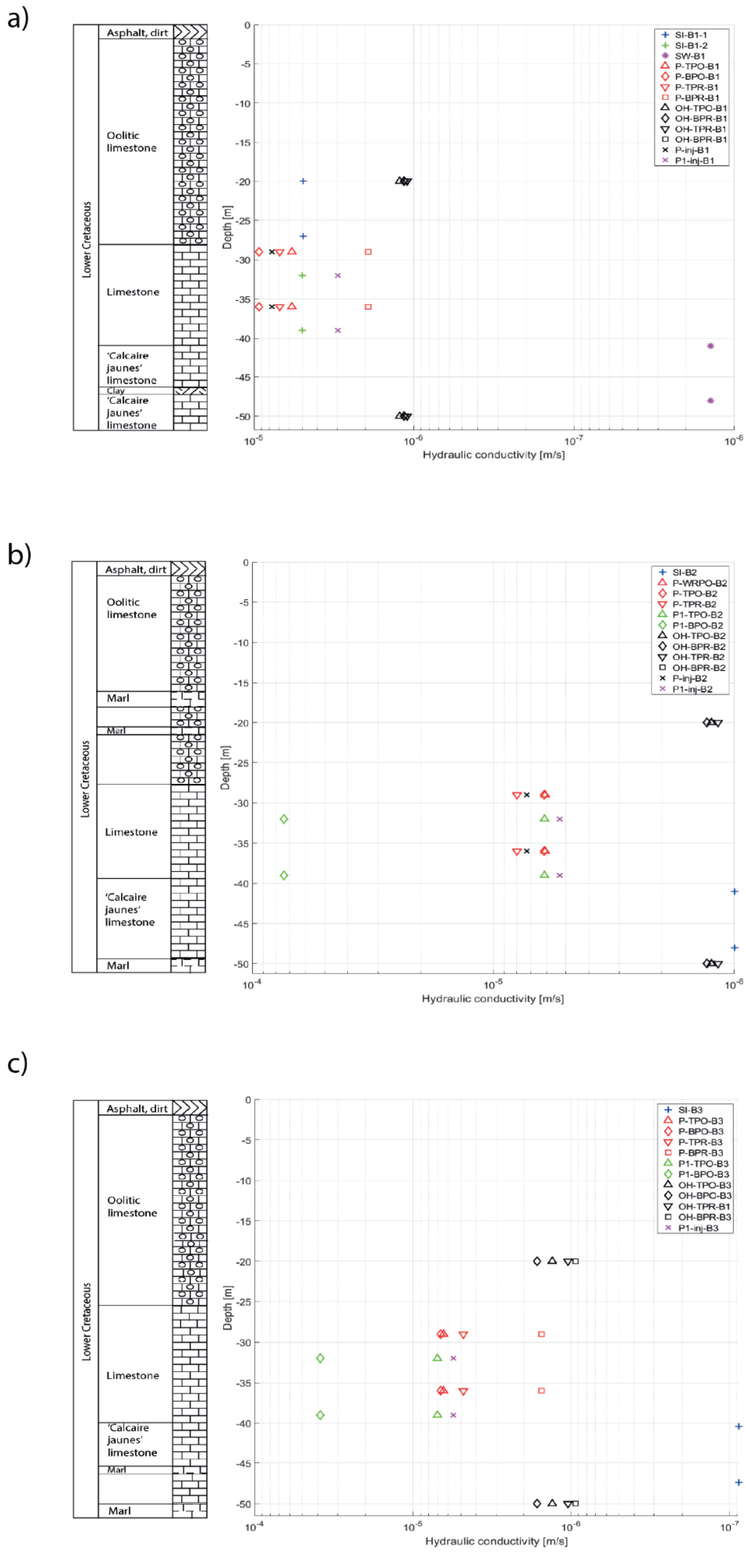

Figure 39 - Hydraulic conductivity calculated with different hydraulic tests in the a) RSBV1, b) RSBV2 an c) RSBV3. Description of the nomenclature used: Slug Injection (SI), Slug Withdrawal (SW), Packer test in RSBV2 interval 29-36m (P), Packer test in RSBV1 interval 32-39m (P1), Open Hole test (OH).

5.1.5.1.7. Thermo-hydraulic testing

Thermal-hydraulic and fluorescent tracer tests were carried out at various times during the project. These tests were used to characterize the exchange surfaces in the fractured system and to characterize the heat storage capacities of the system. An extensive measurement infrastructure was deployed during these tests, including not only the heating systems and an injection logistics, but also a monitoring infrastructure including temperature distributed by optical fiber. We present here some examples of the tests performed to illustrate the work done.

5.1.5.1.7.1. Test setup

As an illustration of the infrastructure deployed during the thermal-hydraulic tests, Figure 40 shows the distributed fiber-optic temperature measurement system deployed during the tests in August and September 2021. This system provided continuous and distributed temperature measurements with a spatial resolution of one meter along the entire length of the wells tested. A heat injection followed by a shut-in and then a recovery was carried out in these wells with this measurement system deployed. The results of these tests are presented below.

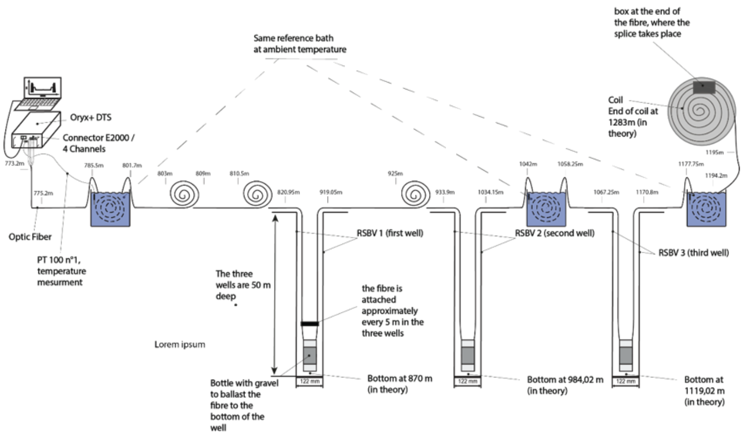

Figure 40 - FO-DTS set up during the thermo-hydraulic experiment (August-September 2021).

5.1.5.1.7.2. Results

An example of the data collected during these thermal-hydraulic tests is shown in Figure 41, where we see the flow rates and temperatures injected and recovered in addition to the temperatures measured along the wells and the hydraulic head variation in the wells. This type of data when finely analysed allows for a detailed characterization of the heat exchange in the reservoir. For example, it is possible to identify and quantify the amount of heat flowing into the different hydrogeological components of the system. They also form the basis for the development of conceptual models of the system under test and the calibration of coupled numerical thermal-hydraulic simulations to anticipate the response of this type of heat storage system.

In the example presented here, we can clearly see the heat injected into the RSBV2 well (Figure 41 b). If the temperature in the injection well is relatively homogeneous during injection, the temperature becomes heterogeneous during recovery because the amounts of energy injected in the different components and fractures of the system are unequal. The regions that have assimilated more energy will rebalance more slowly during recovery and this can be seen in the image in Figure 41 b by the horizontal bands in the heatmap showing the temperatures. We also note that the observation wells (Figure 41 a and c) show very little thermal response to injection despite being located less than 5m from the injection well. A detailed analysis of the temperatures, not presented here, shows an initial decrease in temperatures in the observation wells due to a hydraulic piston effect which pushes the formation water towards the wells during injection. The duration of our test, in this case a 6-hour injection, was not sufficient to transport heat to the observation wells. This is an important limitation of our tests and thus of tests that can be planned to characterize deep heat storage systems. As the time realistically and logistically available to characterize and determine the important parameters of the system is limited, it is necessary to scale up the results obtained in a short time. This scaling up of this type of test over a long period of time remains difficult but can be approached through properly calibrated numerical simulation and verification on the type of experimental results presented here.

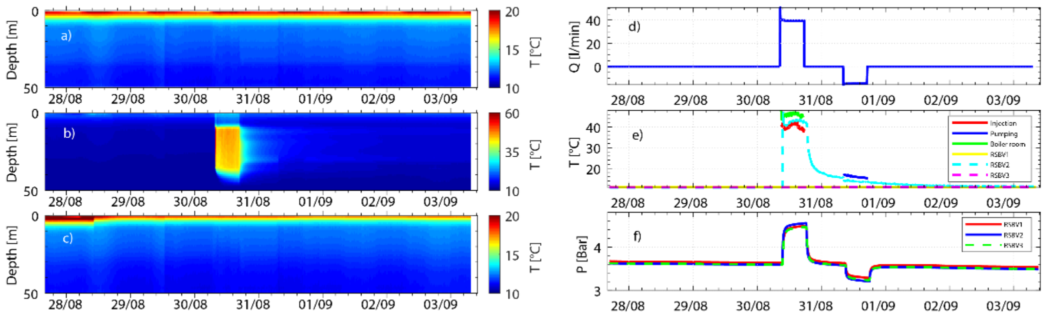

Figure 41 - Temperature variations from the fiber optic measurements (FO-DTS) with flow rates, injection temperature, pumping temperature and pressure in the three wells. a) FO DTS values for RSBV1, b) FO-DTS values for RSBV2, c) FO-DTS values for RSBV3, d) Flow rate during the injection and pumping, e) Temperature measurements according to different locations, f) Pressure variations during the injection and the pumping.

5.1.5.1.8. Modelling

The characterization data of the Concise test site was integrated to form the basis for numerical simulations. Four scenarios were chosen to conduct these simulations and they are presented in Figure 42. The results of these simulations are shown in Figure 43. There is a large difference between the temperature distributions obtained for the different models. The continuous and homogeneous models' scenario does not represent well the conditions observed in our reservoir while the discontinuous models present better results. The quantification of heat recovery after an injection period with these models is shown in Figure 44 against experimental data obtained at the Concise site. Again, the models including the main discontinuities in a deterministic manner allow for a better representation of the thermal-hydraulic response, thus suggesting that it is important to decipher the reservoir structure in detail to make predictions and design a robust heat storage system.

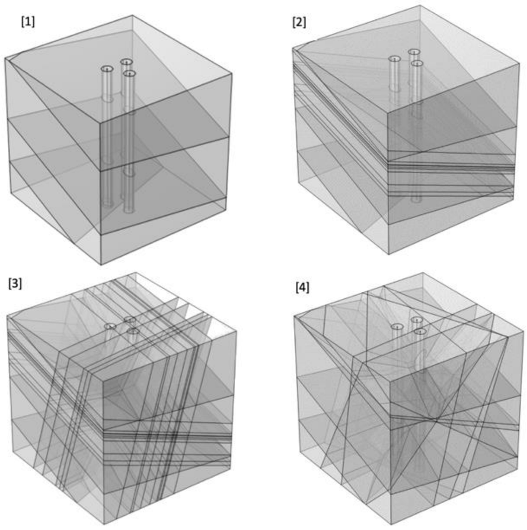

Figure 42 - 1) Model with the main geological units, 2) model with the bedding, 3) model with the deterministic approach, 4) model with a stochastic approach DFN.

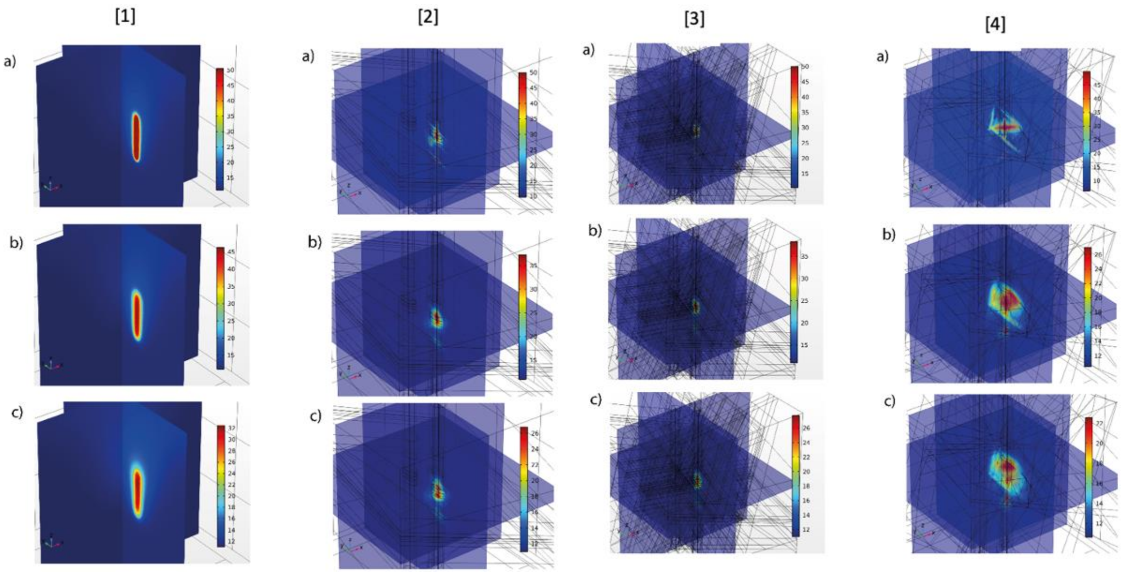

Figure 43 - 1) Model with the main geological units, 2) model with the bedding, 3) model with a stochastic approach DFN, 4) model with the deterministic approach. The temperature displayed is at the end of the injection (t = 6h), b) at the end of the thermal recovery (t = 22.6h) and c) at the end of the pumping (t = 28.6h)

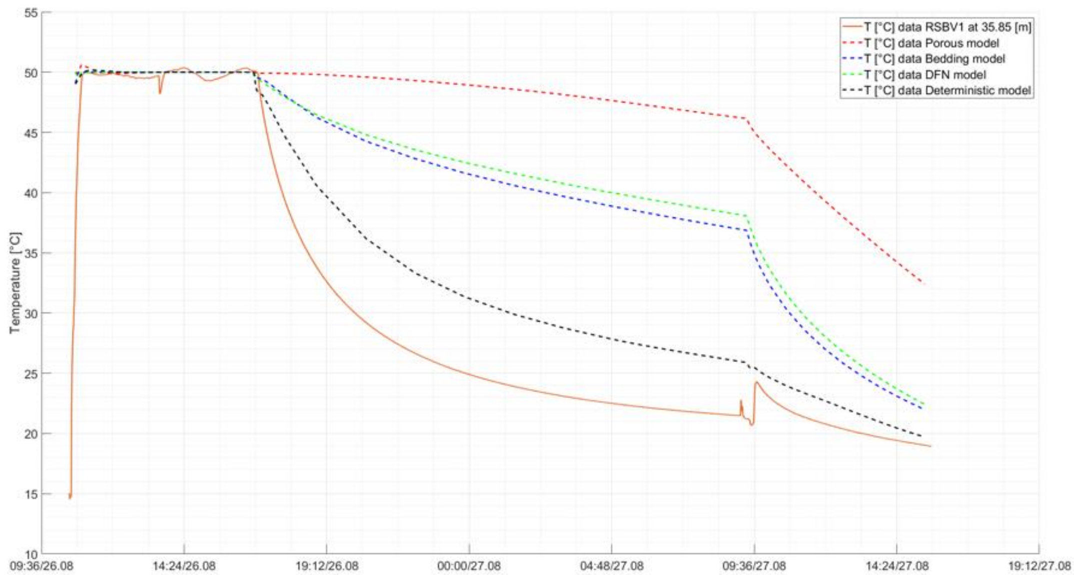

Figure 44 - Benchmark with simulated temperatures and data measured into RSBV1 where the thermo-hydraulic test, at 35.85m, was performed.

5.1.5.1.9. Synthesis and outlook

The development of the Concise test site has enabled the application of methods for hydraulic and thermohydraulic characterization of karst fractured reservoirs. Unique data sets are generated to verify and calibrate numerical simulation models. These results also highlight the importance of explicit consideration of reservoir structures to obtain robust thermal-hydraulic responses and provide the basis for recommendations for the development and characterization of deep heat storage systems.

5.1.6 Subsurface 3D static models at GEo-01 and GEo-02

One of the main challenges related to assessing the technical feasibility and sustainability of High Temperature (~25°C to ~90°C) Aquifer Thermal Energy Storage (HT-ATES) is to properly depict the subsurface conditions via the generation of multiple scenarios to identify the most favorable conditions to operate an HT-ATES system.

In this final report we present subsurface characterization of the GEo-01 and GEo-02 geothermal exploration borehole sites, investigated in HEATSTORE.

These activities have been carried out in the framework of ***Task 1.1 Specification and characterization for ATES concepts*** of the proposal submitted to BFE and ***Task 5.3: Model validation for Subsurface dynamics*** of the European proposal.

The full report about 3D static model is available in Appendix03.

The workflow that was implemented was based on the integration of geophysical and petrophysical data initially available at the beginning of the project and subsequent update of the models as new data become available. The overall approach was based on the baseline that 3D static models serve as inputs in integration with energy system information, to produce dynamic models (thermo-hydraulic TH, Thermo-hydraulic-mechanic THM or HM, thermo-hydraulic-chemical THC and Thermo-hydraulic-economic THE) to predict the performance of HT-ATES systems in Geneva (Figure 45).

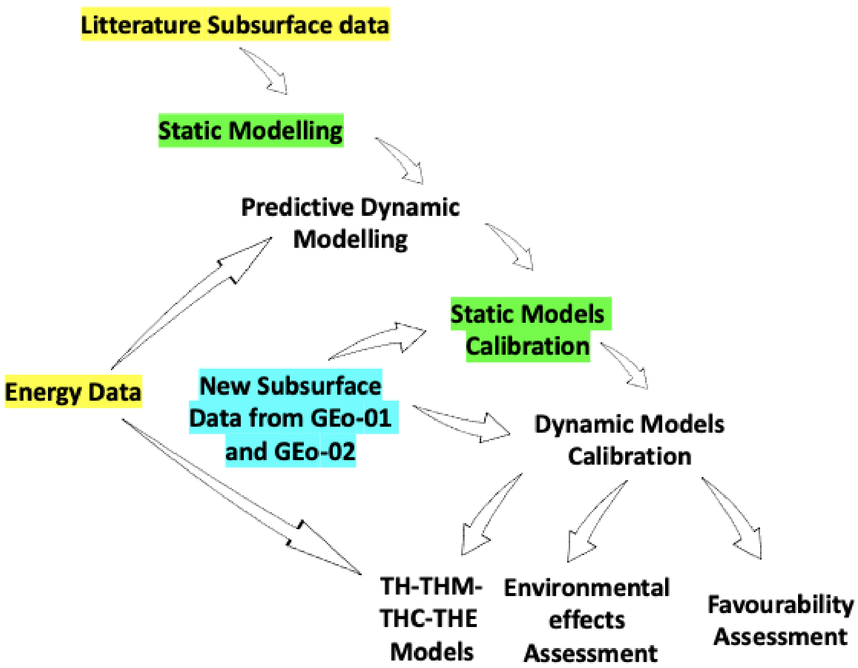

Figure 45 - General workflow implemented in HEATSTORE for HT-ATES potential assessment. Highlighted are the different phases involved in the static modelling activities

The results have been achieved from the interpretation of several vintages of 2D seismic reflection dataset, well logs from GEo-01 and GEo-02, well reports and outcrop analogues. Because of the different interpretations and their evolution as new data become available, 3 scenarios have been identified for GEo-01 and 2 scenarios for GEo-02.

Seismic interpretation reveals a well-developed flower structure deforming the Mesozoic and parts of the Cenozoic sediments in the GEo-01 area across all the models developed for this area (Figure 46).

On the contrary, the subsurface structural situation around GEo-02 site is different comprising of thrust faults system and other normal faults deforming the Cenozoic and Mesozoic sediments.

Petrophysical analysis suggests the Lower Cretaceous Formation in the GEo-01 area is tight, generally characterized by low porosity and permeability values. However, the presence of fracture networks and faults deforming a substantial part of this unit may promote localized fluid circulation. Three candidate horizons have been identified as potential Lower Cretaceous targets (CT) suitable for HT-ATES in fractured intervals characterized by tested water outflows and devoid of hydrocarbon impregnation.

In the GEo-02, well test results suggest that the formations within the Mesozoic succession have low fluid flow and weak hydraulic properties despite targeting fault structures which in this area act rather as a seal then a fluid channels.

The multi-scenario modelling (Figure 47) adopted in this study provided data (horizons thickness, depth, petrophysics and hydraulic properties) that were used as input for numerical heat flow and predictive TH, HM, and THE models for the Geneva Basin.

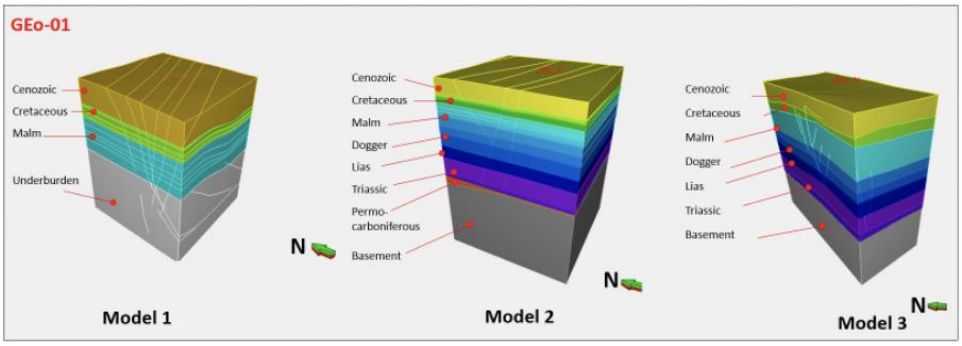

Figure 46 - Geological model for the three different structural and stratigraphic frameworks modelled or GEo-01.

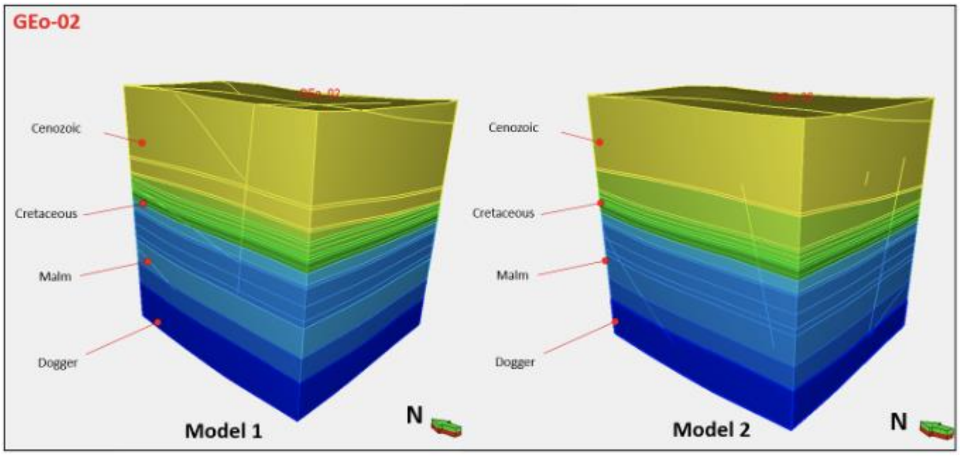

Figure 47 - Two different geological model (Model-1 and Model-2) developed for GEo 2 arising from the two different structural model used as input.

The results of these project also provided a detailed evolution of the knowledge of the subsurface geology in this segment of the Swiss Molasse basin is well captured by comparing geological models developed using the pre-drill database developed and post-drill database. Importantly, the discovery of more than 150m of meter thick Siderolithic sediments in GEo-02, not encountered by the GEo-01 suggests the geology of the Geneva Basin, changes dramatically within a short spatial extent impacting the potential of identifying suitable storage reservoirs. In all, our findings highlight the need for subsurface data augmentation in the Geneva Basin. It also shed light on the implication of the subsurface manifestation of hydrocarbons as geohazard to heat storage and other geo-energy related projects at large across the Swiss Molasse Basin.

5.1.7 Dynamic reservoir modelling for the Geneva sites

This chapter aims at resuming the results of the subsurface dynamic modelling activities carried out for the Geneva case study and implemented in the framework presented in Figure 01. In particular, the focus is directed to the evolution of TH and HM models produced before and after site-specific data from Geo-01 and GEo-2 data become available.

These activities are part of WP2 Models and tools for subsurface dynamics for optimal/efficient heat storage of the Swiss project and of ***WP2 Tools and workflows for modelling the subsurface dynamics*** and ***Task 5.3: Model validation for Subsurface dynamic*** of the European project and the results are part of a set of full reports where ETHZ, UniBe and UniGe worked in collaboration with the other international partners involved. All the reports are available in the Appendix04 and Appendix05.

The overall approach has always been to combine subsurface and energy system data to produce static 3D models and then 3D dynamic models to predict the performance of the HT-ATES system object of the study.

In a first phase, subsurface literature data were used to provide constraints with respect to petrophysical and hydraulic properties of the potential reservoirs. A set of simplified geological models were created to run dynamic TH and HM models and understand the overall physical processes controlling HT-ATES operations. In a second phase, once new data were available from the GEo-01 and GEo-2 wells, site-specific modelling, were performed resulting in improved and calibrated version (Figure 48). The results also were used for ***T6.6 Environmental impacts*** and for ***T1.3 Screening of national potential for UTES*** (both led by UniGe) of the European project corresponding to the task ***Mapping technical potential and expansion in Switzerland*** of WP 6 of the Swiss proposal.

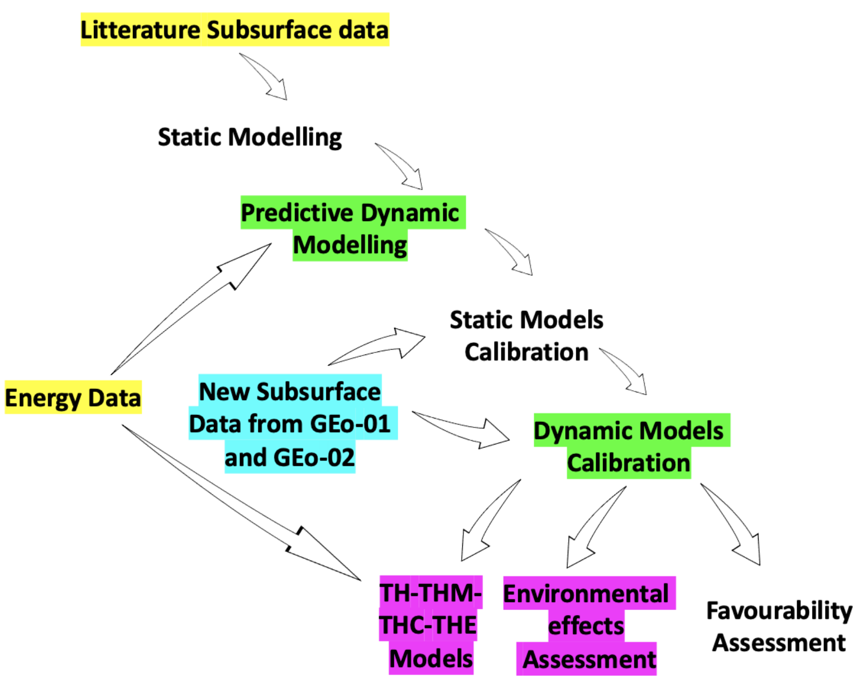

Figure 48 - Modelling framework implemented for the Geneva case study

Several targets have been identified in the Upper Mesozoic Carbonates at different depths and have been modelled on a fluid and soil mechanics perspectives for screening of the favorable conditions and potential effects which can support the selection of an HT-ATES site in such complex geologic context.

Modelling therefore starts with addressing the question of how these complexities can that potentially affect possible storage by simulating generic scenarios of geologic situations to be encountered in the Geneva underground. Results provided a foundation for identifying the "best" underground parameters such as reservoir transmissivity within the target units. Such characterization will allow the industrial partner to plan future activities such as drilling additional wells, design the development of the district heating network and integrate storage solutions in the energy system, define business models, and evaluate the overall sustainability of the HT-ATES system in Geneva.

Since the availability of suitable drilling sites is relatively low on the Geneva territory, the choice of geological sites is strongly influenced by surface boundary conditions such as proximity to the wastewater plants, suitability of nearby crops, and SIG's future to increase the district heating network coverage. Drilling targets have nevertheless been defined according the available geological and geophysical data, which consists mainly of 2D reflection seismic data. This allowed the identification of the Mesozoic units as the most favorable targets for geothermal development. With these targets in mind, it is important to have a broader view of the surrounding geology to be able to construct geometrically relevant simulation models.

5.1.7.1. TH models simulation scenarios

Within the HEATSTORE project objectives, a set of TH reservoir simulations were initially performed (see D2.1 and D2.2 of the European project in the Appendix06 and Appendix07) to produce predictive general sub-scenarios of the performances of HT-ATES systems using the available data from literature end in a second phase using the site-specific geologic, hydraulic and petrophysical data from GEo-01 and GEo-02.

The work carried out by ETHZ focused on GEo-01 well and the aim was to simulate underground fluid flow and heat transport to estimate the efficiency, feasibility, and safety of using the Geneva subsurface as an HT-ATES site. The methodological approach is full reported in ***D2.1 Initial report on tools and workflows for simulating subsurface dynamics of different types of High Temperature Underground Thermal Energy Storage***.

TH simulations focused on (a) assessing thermo-hydrological challenges to heat storage in the complex subsurface of the Geneva Basin and (b) on quantifying overall thermal efficiency plausible-yet-simplified realizations of the underground heterogeneity (i.e., formation layers, faults and fractures) as well as pre-existing hydrological conditions (e.g., ground water flow). The computational approach used for TH modelling is based on a combined Finite Element (FE) and Finite Volume (FV) numerical discretization methodologies of the following governing equations that represent the assumptions of conservation laws of mass (1), momentum (2) (a.k.a. Darcy's Law), and energy (3) + (4)

$$\frac{\partial(\rho_f \phi)}{\partial t} + \nabla \cdot (\rho_f \mathbf{v}) + q_{\rho,f} = 0 \tag{1}$$

$$\mathbf{v} = -\frac{k}{\mu}(\nabla p - \rho_f \mathbf{g}) \tag{2}$$

$$\frac{\partial(\phi \rho_f h_f)}{\partial t} + \nabla \cdot (\rho_f h_f \mathbf{v}) = 0 \tag{3}$$

$$C_{p,t}\frac{\partial T}{\partial t} - \nabla \cdot (\lambda_t \nabla T) + q_H = 0 \tag{4}$$

Where:

ρ_f is the fluid density,

ϕ is the porosity,

$\mathbf{v}$ is the Darcy velocity vector,

$q_{p,f}$ represents fluid mass sources and sinks,

p is the fluid pressure,

$\boldsymbol{g}$ is gravitational acceleration,

$\boldsymbol{k}$ is the permeability, and

μ is the fluid viscosity.

$\mathbf{h}_f$ is the specific enthalpy of the fluid,

$C_{p,t}$ is the non-specific bulk heat capacity,

T is the bulk temperature, λ_t is the bulk thermal conductivity,

q_H represents heat sources and sinks.

The result from such a simulation algorithm is a sequence of fluid pressure, fluid velocity, temperature, and any other dependent variable values at the end of each time-iteration.

Each sub-scenario inputs are summarized in Table 3. The meaning and values associated to each code is explained throughout this section (Mindel et al, 2020).

Table 3 - Parameters and values used in TH simulations. A factorial design for all parameters is used resulting in 1152 3D reservoir simulations. All simulations use a temperature of 90 °C for HT-ATES charging and a well spacing of 141m.

Aquifer Permeability	Aquifer Thickness	Well Strategy	Groundwater	Fracture Configuration	Aquifer Dip
K13	L200	single	YGW	F0	FLAT
5K13	L300	doublet	NGW	FU	INCL
K12	L400	5spot		FD	

5.1.7.2. Geometrical-geological model

Based on the detailed geological study carried out by the University of Geneva (UniGe) and Services Industriels de Genève (SIG) (see Figure 3), a cube-shaped 1 $km3$ geological model was constructed by UniGe using the original analysis of a collection of subsurface datasets available that time this phase of modelling was performed, therefore mimicking the stratigraphy of GEo-01 also based on the data available from the GEOMOL 3D Project (Bayerisches Landesamt für Umwelt, n.d.) (Swiss Federal Office of Topography, n.d.) , where a 3D geological model of the Geneva area was extracted. Additionally, the model was populated with petrophysical and hydraulic properties from literature.

All horizons were initially considered as horizontal surfaces, simplifying structures in preparation for simulation work, however a dip angle of 15º was introduced in the simulation scenarios to include its possible effects on the thermal efficiency.

While keeping the supplied material properties in mind, we have further simplified the model geometry to the basic necessary elements for an ATES, consisting of a single permeable aquifer rock layer confined between two layers with lower permeability and porosity (see Figure 49). This simplification was assumed sufficient for a first design iteration given the relatively large number of simulations needed. .

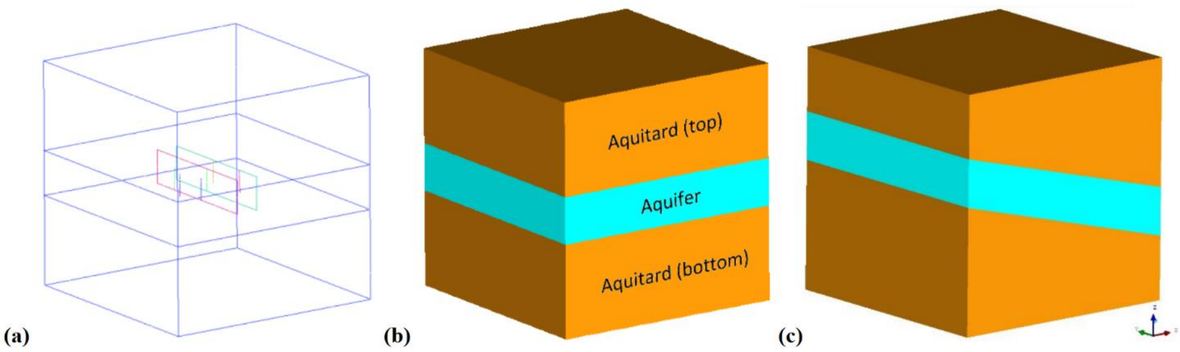

Figure 49 - Geometrical/Geological model representing the basic elements of an ATES, depicting (a) possible well and fracture locations, (b) a flat version of the model, and (c) a version of the model possessing an aquifer with a 15º angle of dip.

A summary of the values used, including permeability (assumed to be fully controlled by fractures for the aquifer layer) and thickness values is presented in Table 4 (Mindel et al, 2020).

Table 4 - Summary rock material parameters

Parameter	Units	Aquitard (top)	Aquifer	Aquitard (bottom)
Density (ρ_r)	[kg/m³]	2450	2450	2680
Permeability (k) (original matrix)	[m²]	10^{-17}	10^{-15}	10^{-17}
Permeability K13 (k) (fractured, effective)	[m²]	10^{-17}	10^{-13}	10^{-17}
Permeability 5K13 (k) (fractured, effective)	[m²]	10^{-17}	$5 \cdot 10^{-13}$	10^{-17}
Permeability K12 (k) (fractured, effective)	[m²]	10^{-17}	10^{-12}	10^{-17}
Porosity (ϕ) (matrix, effective)	[-]	0.01	0.2	0.01
Permeability (k) (fracture, effective)	[m²]	N/A	10^{-11}	N/A
Porosity (ϕ) (fracture, effective)	[-]	N/A	0.5	N/A
Fracture thickness	[m]	N/A	0.1	N/A
Specific Heat Capacity ($c_{p,r}$)	[J/(Kg·K)]	860.2	832.9	849.9
Thermal Conductivity λ_r (λ_r)	[W/(m·K)]	2.275	2.806	2.692
Thickness L200 (L)	[m]	400	200	400
Thickness L300 (L)	[m]	350	300	350
Thickness L400 (L)	[m]	200	400	400
Groundwater velocity (v_{gw}) (assumed)	[m/yr]	N/A	2	N/A

5.1.7.3. Operational design

Thermal power output from the waste incineration plant Les Cheneviers in Geneva, heat demand, and temporal load/unload cycles over a one-year time frame were provided by UniGe and SIG based on SIG's district heating systems development plan. With this information we obtained the necessary parameters for all the simulation configurations needed (Table 5). The basic operational yearly cycle strategy consists of a period of continuous charge for 120 [days], followed by storage for 60 [days], discharge for 120 [days], and further storage for 65.25 [days]. Well patterns considered both a mono-well and 5-wells configuration.

Table 5 - Summary of basic input parameters

Total Energy to Inject (E_{GWh}) (per year cycle)	50 [GWh]
Temperature of injection (T_i)	90 [℃]
Period of injection/charge (t_c)	120 [days]
Period of production/discharge (t_d)	120 [days]
Period of storage (2) ($t_{s,1}$, $t_{s,2}$)	60 [days], 65.25 [days]
Volume injected (V_i)	622080 [m³]
HT-ATES life time	15 [yr]

5.1.7.4. Results and discussion

We obtained results for 324 simulations produced by the combinations of simulation variant codes provided in Table 1. To assess the effects of the varying parameters on the cyclic efficiency using this relatively large volume of data, we applied an exergetic analysis for the HT-ATES expected lifetime, since it accounts for the temperature at which water is produced from the aquifer (Dincer and Rosen, 2011).

Exergy efficiency tends to be lower than energy efficiency in ATES systems, given that as T approaches T_{ref} the exergy contribution approaches zero. If T < T_{ref} at any point in time, the amount of exergy for that period is negative. As a result, the amount of energy input, stored, and discharged from the ATES will only be useful, or of good enough quality, if the temperature of the flow can be maintained above T_{ref}. Over subsequent cycles and theoretically depending on the discharge time and overall length of each cycle, the exergy lost to the aquifer surroundings results in an increase of the temperature near the well at the end of each cycle, thus increasing η_{ex} and η_{ex} over time as shown in Figure 50Figure 50.

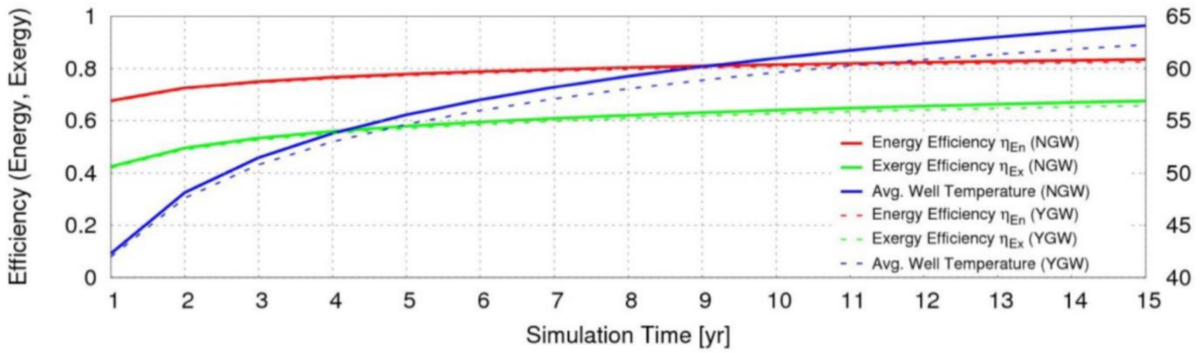

Figure 50 - Energy and Exergy efficiency variation with time for the expected ATES lifetime comparing a case with and without groundwater flow

5.1.7.5. Conclusions

We have carried out a numerical study of various HT-ATES system realizations based on parameters of aquifer permeability, aquifer thickness, well pattern, groundwater conditions, dip angle, and fracture configurations. By simplifying an originally complex geological situation, we obtained a series of scenarios aimed at a fundamental understanding of how ATES systems respond to their settings and surroundings, and how to best design them. Considering the geology, material properties, fluid properties, and industry-based operational conditions we have also investigated the plausibility storing hot water and recovering it at the maximum temperature possible via an exergetic analysis of many simulations.

Our study further confirms some observations that have already been made in the literature, particularly with respect to groundwater drift and buoyancy effects present in high permeability aquifers. We have also observed that when active, auxiliary wells help mitigate pressure-peak related effects, improve the thermal front sweep, and provide some measure of shielding against the drift due to the flow of groundwater.

We observed that although a permeability design sweet-spot could be numerically found for a particular geologic/geometric configuration, the design process is rather driven by the geo-availability in the prospective site, thus highlighting the importance of a thorough and continued (hydro-)geological study. In a similar light, lower aquifer thicknesses seem to be a favorable configuration, although to inject an equal amount of energy through a water volume rate at the same temperature, higher injection pressures are required which may impose mechanical limitations. Furthermore, particularly in terms of simulations when flow-rate values are equivalent, permeabilities do impose a numerical limitation since resulting injection and production pressure values can be unrealistically high and low, respectively. Further work should be carried out in expanding this study, particularly to better contextualize the geological configurations with particular emphasis on fractures and faults, analyse the effects of aquifer depth, and assess the influence of surface temperature conditions.

5.1.7.6. TH models site-specific

5.1.7.6.1. Thermal effects on the reservoir natural state temperature

Thermo-Hydraulic (TH) models have been performed to optimize the design of a preliminary HT-ATES system based on a under different configurations of subsurface conditions (Mindel & Driesner, 2020). The goal for the Thermal-Hydraulic (TH) modelling of GEo-01 and GEo-02 wells is to understand the performance of the considered aquifers for heat storage and to assess the extent of the thermal radius after 15 years of operation. This assessment makes us of simple layer-cake models following the insights and overall design as presented by (Mindel and Driesner, 2020).

5.1.7.6.2. Methodology

The Delft Advanced Research Terra Simulator (DARTS) (DARTS, 2021) is used to perform the different simulation scenarios, using the Operator Based Linearization approach (Khait and Voskov, 2018) that has been shown to be accurate and fast against other simulators (Wang et al., 2020). Water properties are based on IAPWS97 (Huber et al., 2009) as implemented in the python package IAPWS (Romera, 2020).

The scenarios considered in the models are listed in Table 6.

Table 6 - Modelling scenarios (LC: Lower Cretaceous; UJ: Upper Jurassic)

Well and Scenario	Targeted Reservoir	Reservoir Permeability (m^2)	Reservoir Thickness (m)	Injection Rate (kg/s)
GEO-01	LC + Siderolithic	$3 \cdot 10^{-13}$	350	60
GEO-02 SC1	LC-UJ	$7 \cdot 10^{-16}$	700	3.9
GEO-02 SC2	Siderolithic	$7 \cdot 10^{-16}$	150	0.7
GEO-02 SC3	Siderolithic	$3 \cdot 10^{-13}$	150	60

5.1.7.6.3. Results

5.1.7.6.3.1. Geo-01

Figure 51 and Figure 52 show the temperature distribution in the production interval after 15 years of production, using the inputs from Table 7 Input parameters Geo-01 model. The large reservoir thickness combined with a relatively high permeability results in the hot plume being more prominent in the upper part of the aquifer. Additionally, due to the interaction between the hot and the cold well, the hot plume is asymmetrical, having a reduced extent between the wells and a larger extent away from the wells. The thermal radius is therefore slightly larger at shallower depths and exceeds the 3˚C at 100m radius distance from the well as defined by the Swiss water protection law (OEaux, annexe 2 chapitre 21 alinéa 3) at the end of the 15 years operation period simulated.

Table 7 - Input parameters Geo-01 model

Parameter	Value
Domain x, y, z	500 m, 500 m, 454 m
Discretization dx, dy, dz	10 m, 10 m, 2 m

Cell count	567,500
Well rates	60 l/s - 5184 m^3/day
Permeability	$3 \cdot 10^{-13}$ m^2 - 304 mD

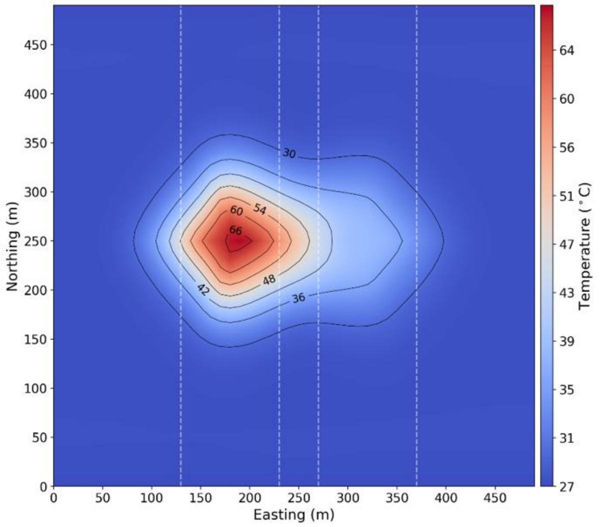

Figure 51 - Geo-01 map view at a depth of 575 m after 15 years of operation. The vertical dashed white lines represent 100m on each side of the hot and cold well respectively.

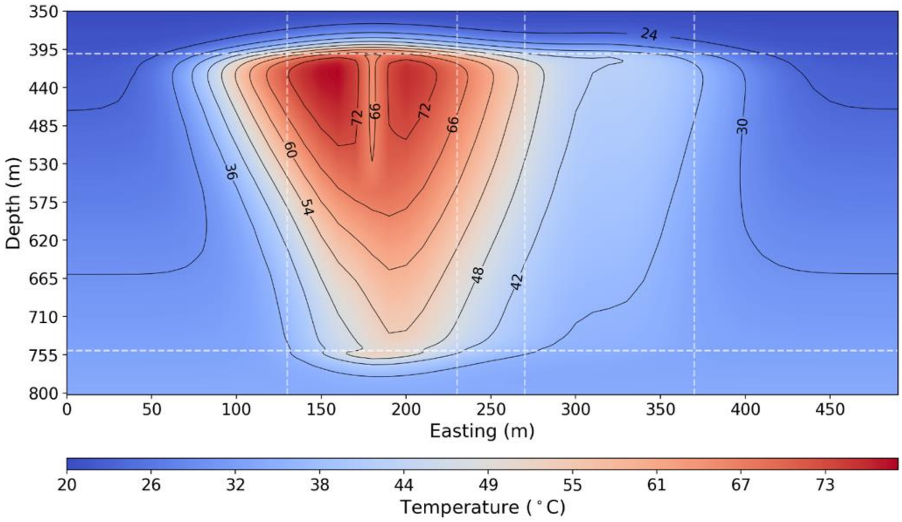

Figure 52 - Geo-01 vertical section across the wells (northing = 500 m) after 15 years of operation. The horizontal dashed white lines mark the production interval, while the vertical dashed white lines represent 100m on each side of the hot and cold well respectively.

5.1.7.6.3.2. Geo-02 SC1

Figure 53 and Figure 54 show the temperature distribution in the production interval after 15 years of production, using the inputs from Table 8. The low permeability and low rates result in a very small thermal radius. Differences between the bottom and the top of the hot plume are attributed mostly to conduction, which is laterally favorable at shallower depths due to the increased temperature gradient with the undisturbed temperature field. Reservoir temperature does not exceed the 3˚C at 100m radius distance from the well as defined by the Swiss water protection law (OEaux, annexe 2 chapitre 21 alinéa 3) at the end of the 15 years operation period simulated.

Table 8 - Input parameters Geo-02 SC1 model

Parameter	Value
Domain x, y, z	500 m, 500 m, 704 m
Discretization dx, dy, dz	10 m, 10 m, 2 m
Cell count	1,005,000
Well rates	0.7 l/s – 60.5 m^3/day
Permeability	$7{\cdot}10^{-16}$ m^2 – 0.7 mD

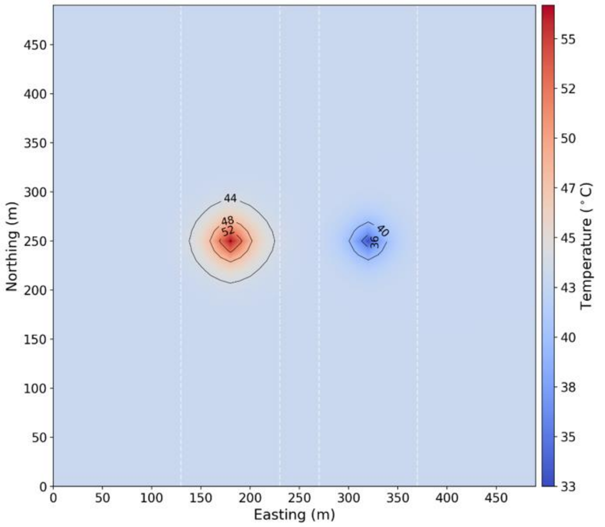

Figure 53 - Geo-02 SC1 map view at a depth of 1100 m after 15 years of operation. The vertical dashed white lines represent 100m on each side of the hot and cold well respectively.

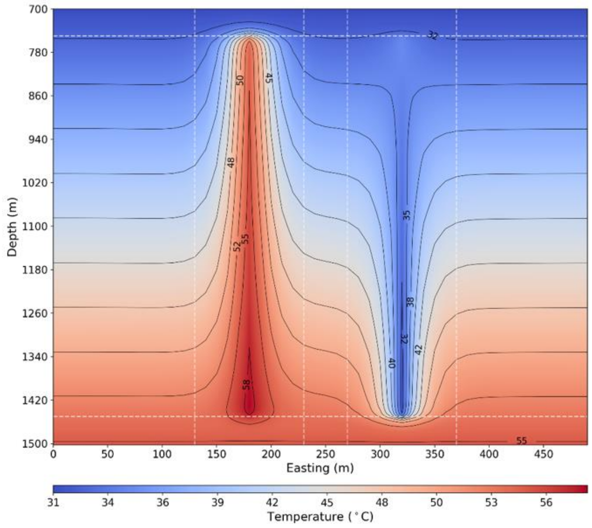

Figure 54 - Geo-02 SC1 vertical section across the wells (northing = 500 m) after 15 years of operation. The horizontal dashed white lines mark the production interval, while the vertical dashed white lines represent 100m on each side of the hot and cold well respectively.

5.1.7.6.3.3. Geo-02 SC2

Figure 55 and Figure 56 show the temperature distribution in the production interval after 15 years of production, using the inputs from Table 9. Compared to SC1 using the same rates with a significantly reduced reservoir thickness results in a slightly larger extent of the hot plume. Additionally, the smaller temperature difference at the top and bottom of the domain (due to the lower thickness) results in a more homogeneous lateral extent of the cold plume. The shallower parts of the domain remain slightly less extensive compared to the deeper ones, but differences are minor. Reservoir temperature does not exceed the 3˚C at 100m radius distance from the well as defined by the Swiss water protection law (OEaux, annexe 2 chapitre 21 alinéa 3) at the end of the 15 years operation period simulated.

Table 9 - Input parameters Geo-02 SC2 model

Parameter	Value
Domain x, y, z	500 m, 500 m, 154 m
Discretization dx, dy, dz	10 m, 10 m, 2 m
Cell count	317,500
Well rates	0.7 l/s – 60.5 m^3/day
Permeability	$7 \cdot 10^{-16}$ m^2 – 0.7 mD

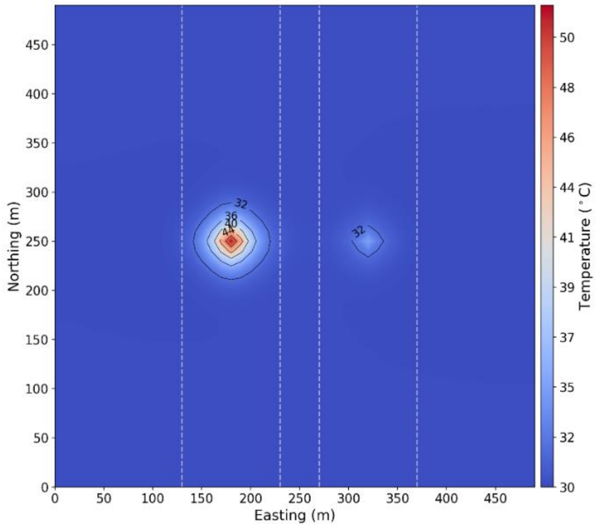

Figure 55 - Geo-02 SC2 map view at a depth of 675 m after 15 years of operation. The vertical dashed white lines represent 100m on each side of the hot and cold well respectively.

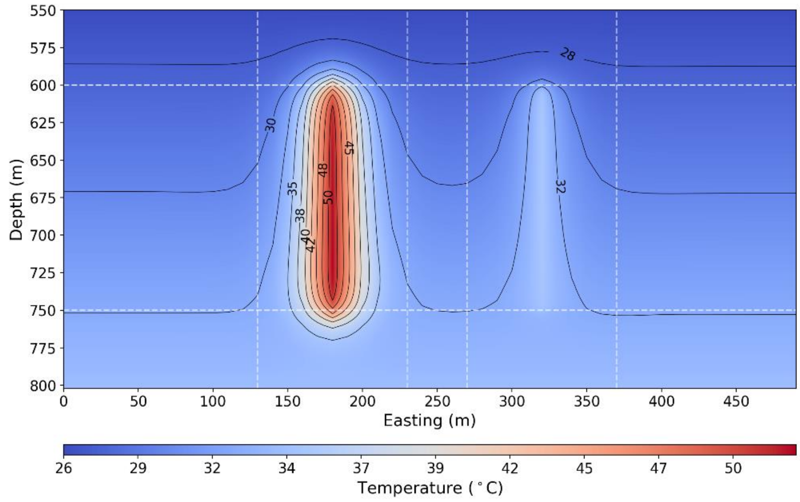

Figure 56 - Geo-02 SC2 vertical section across the wells (northing = 500 m) after 15 years of operation. The horizontal dashed white lines mark the production interval, while the vertical dashed white lines represent 100m on each side of the hot and cold well respectively.

5.1.7.6.3.4. Geo-02 SC3

Figure 57 Figure 58 show the temperature distribution in the production interval after 15 years of production, using the inputs from Table 10 Input parameters Geo-02 SC3 model. Increasing both the rate and permeability with the same reservoir thickness as SC2 results in a noticeably larger hot plume laterally and a larger thermal radius. Moreover, the vertical shape of the hot plum is now more pronounced in the shallower part. This is attributed to the large contribution of convection in the temperature field and resembles qualitatively the Geo-01 model. Similarly, to the Geo01 model, the hot plume is asymmetric and extends farther away from the wells compared to the space between the two wells. Reservoir temperature exceeds the 3˚C at 100m radius distance from the well as defined by the Swiss water protection law (OEaux, annexe 2 chapitre 21 alinéa 3) at the end of the 15 years operation period simulated.

Table 10 - Input parameters Geo-02 SC3 model

Parameter	Value
Domain x, y, z	1000 m, 1000 m, 154 m
Discretization dx, dy, dz	10 m, 10 m, 2 m
Cell count	317,500
Well rates	60 l/s – 5184 m^3/day
Permeability	$3{\cdot}10^{-16}$ m^2 – 304 mD

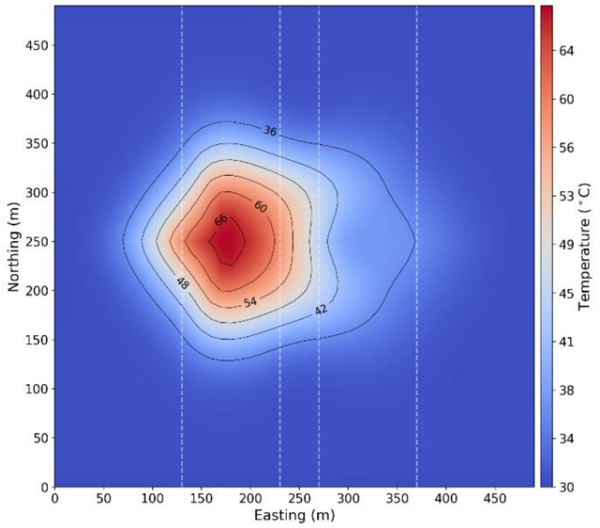

Figure 57 - Geo-02 SC3 map view at a depth of 675 m after 15 years of operation. The vertical dashed white lines represent 100m on each side of the hot and cold well respectively.

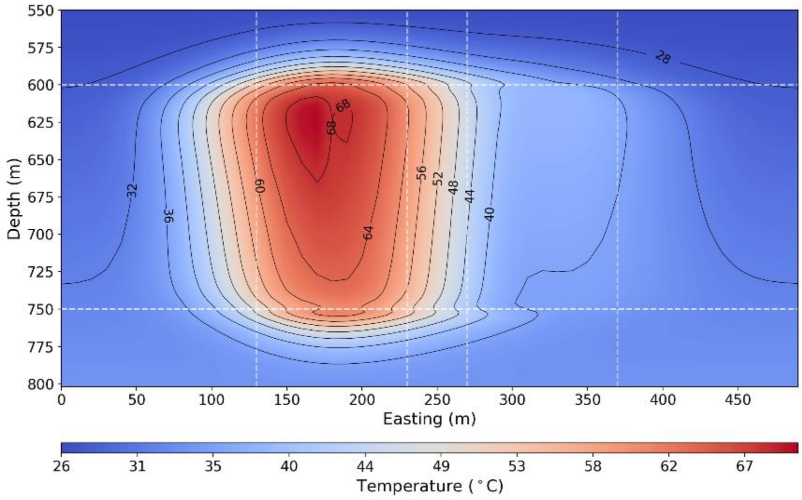

Figure 58 - Geo-02 SC3 vertical section across the wells (northing = 500 m) after 15 years of operation. The horizontal dashed white lines mark the production interval, while the vertical dashed white lines represent 100m on each side of the hot and cold well respectively.

5.1.7.7. Thermo-Hydro-Mechanical models

THM and HM modelling were carried out by ETHZ with the goal to predict the potential ground deformation effects associated with repeated seasonal cycles on injection and extraction. The methodological approach is full reported in ***Deliverable 2.1*** of the European project Initial report on tools and workflows for simulating subsurface dynamics of different types of High Temperature Underground Thermal Energy Storage and the results in D6.6 Environmental effects of UTES technologies in Europe and D2.1 Final Report on tools and workflows for simulating subsurface dynamics of different types of High Temperature Underground Thermal Energy Storage of the European project available in Appendix04.

A porous media is expected to expand when hot fluid is injected into it. There are two mechanisms that cause this expansion: (1) thermal expansion, and (2) gradients in pore pressure, which act like a body force. These deformations can affect fluid flow by altering the porosity and permeability of the porous media as it deforms. Furthermore, the motion of the solid matrix means that fluid velocity must be considered as a velocity relative to the solid rock. The deformations can also alter the heat transfer by "advecting" the heat with solid grain motion. Finally, the thermal and hydrological systems are also coupled through the equation of state and the fluid motion, which advects heat. The most notable aspect of the mechanical expansion in the context of HT-ATES may be the potential for the ground surface to deform. While ground surface deformation has been studied in other contexts, it has received very little attention in the context of HT- ATES, and it could lead to regulatory and/or geotechnical challenges.

In early work (e.g., Birdsell and Saar 2020), we established that an auxiliary well is important to balance pore pressure within the reservoir, which reduces HM deformation and allows for higher flow rates. This is consistent with the design of many LT-ATES systems and with results from the hydro-thermal modelling within HEATSTORE. Therefore, all our predictive models used an injection-extraction doublet pair.

5.1.7.7.1. Thermo-Hydro-Mechanical and Hydro-Mechanical results

We explore two aspects of ground deformation at the Geneva wells using HM and THM models. First, we model ground deformation during the pumping test at GEO-01 and compare to measurements from Work Package 5. Secondly, we perform predictive simulations of the potential ground deformation resulting from HT-ATES to explore the question: what ground deformation could we expect if GEO-01 or GEO-02 were used as one well in an HT-ATES doublet? During the pumping test, our simulations are HM because changes in temperature are not expected to be significant. During the predictive modelling of deformation during HT-ATES operations, we perform both HM and THM simulations. In all cases, we add as much realism from the Geneva-area geology and energy systems as possible, while balancing complexity with enough simplicity to efficiently run and interpret the models.

5.1.7.7.1.1. Subsidence during the GEo-01 pumping test

There are two goals for the hydro-mechanical (HM) modelling of the GEO-01 pumping test. Firstly, the HM modelling is used to understand potential for ground subsidence during the pumping test. This includes investigating the sensitivity of hydrologic and mechanical parameters on ground subsidence. Secondly, by comparing modelled deformation to GPS deformation data, we are able to infer a lower bound on the static, field-scale Young's modulus of the GEo-01 site.

Figure 59 shows the predicted ground subsidence versus time for several permeability scenarios. For all permeabilities, the magnitude of the subsidence increases as the pumping test progresses. Smaller permeabilities result in a greater predicted subsidence. For example, after 60 days, the predicted subsidence is <0.1 cm for a permeability of $6x10^{-13}$ m^2, whereas subsidence is >1.3 cm for permeability of 10^{-13} m^2. For the range of permeability observed at GEo-01 (i.e., 10^{-14}-10^{-13} m^2), the subsidence is relatively insensitive to the permeability.

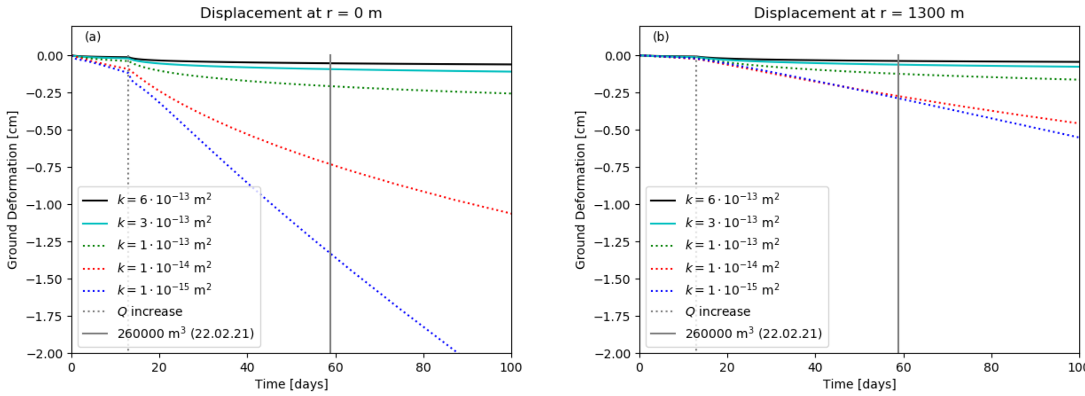

Figure 59 - The effect of permeability on subsidence at the locations of GPS monitoring stations: (a) at the well and (b) 1300 m away from the well. Black and teal solid curves represent the range of permeability from the GEO-01 pumping test, while dotted lines represent hypothetical, lower-permeability scenarios.

Figure 60 shows subsidence from two sources: (a) GPS monitoring near GEO-01 from Nicolas Houlié Geologie GmbH and SIG and (b) the HM numerical model. There is not a clear trend of subsidence (or uplift) in the GPS data. The ground deformation was both positive (upwards) and negative (downwards), depending on the time and the GPS station. For the most part, the magnitude of deformation was less than the size of the error bars, so we cannot interpret any significant deformation from the GPS data. In contrast, the numerical model shows a clear trend of subsidence that increases with increasing time. A sensitivity analysis was performed on the Young's modulus, and smaller Young's modulus corresponds to a larger magnitude of subsidence. This makes intuitive sense because Young's modulus is a measure of the strength of the rock, and a weaker rock will deform more under the same pressure change.

Since the modelled ground deformation is sensitive to the employed Young's modulus, it is important to have a good estimate of the Young's modulus. There are two aspects of estimating Young's modulus that need to be considered. First, the Young's modulus needs to represent the quasi-static physics of poroelasticity, rather than the dynamic physics of seismic waves. Second, the Young's modulus needs to reflect the field-scale rock deformation. At this scale, it is computationally difficult to account for mechanical heterogeneity, and it is useful to upscale mechanical properties that account for the stronger (in-tact rock) and weaker (fractures, faults, and joints) portions of the subsurface. While some effort has been made to upscale mechanical properties (Khajeh, Chalaturnyk, & Bosivert, 2012), there are still not well-established ways of upscaling to our knowledge.

We use two ways to estimate the field-scale Young's modulus for the predictive simulations in Sec. 2. The first estimate comes from seismic data, which gives the dynamic Young's modulus (Koumrouyan, 2019). However, the dynamic modulus must be converted to a static Young's modulus according to a heuristic correlation, which introduces some uncertainty (Eissa & Kazi, 1988). This seismic-based approach gives a static modulus ~35 GPa.

In the second approach, we propose to put a lower bound on the static, field-scale Young's modulus through comparison to GPS deformation data at GEO-01. The GPS data in Figure 60 shows that no ground deformation has occurred, within the confidence of the error bars. In the numerical model, the Young's modulus must be less than ~35 GPa to result in deformation that is larger than the error bars on the GPS data. Therefore, we infer that the Young's modulus could possibly be one to two orders of magnitude larger than the estimate from seismic data and must be ≥35 GPa. Smaller error bars from the experimental GPS data and/or a longer duration of the pumping test could facilitate a tighter estimate on the Young's modulus.

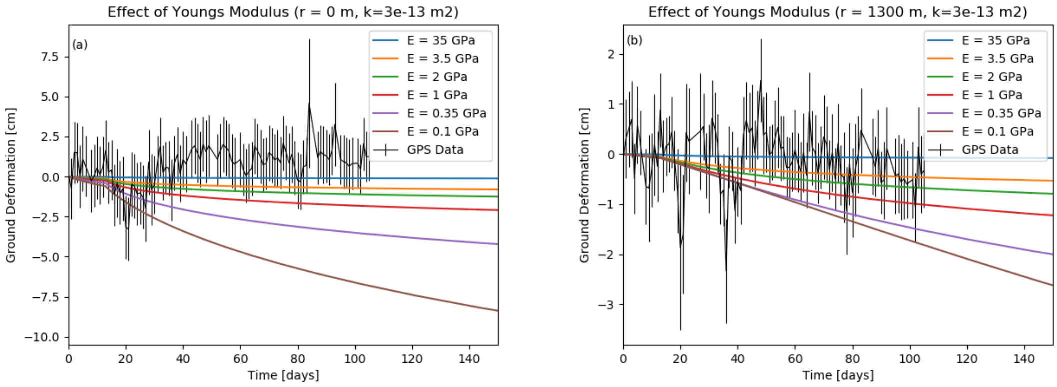

Figure 60 - Ground deformation versus time (a) at the well, representing the first GPS station, and (b) 1300 m from the well, representing the second GPS station. Black lines represent GPS data with error bars, and colorful lines represent HM model results for a sensitivity analysis on Young's modulus.

5.1.7.7.1.2. HM predictive simulations

In this section, we set up predictive HM models to answer the question: what poroelastic ground deformation could we expect if GEO-01 or GEO-02 were used as one well in an HT-ATES doublet? We consider several scenarios that vary parameters such as: targeted reservoir, reservoir permeability, and Young's modulus.

Four scenarios are simulated, which are summarized in Table 11. The GEo-01 scenario uses the permeability from the GEo-01 pumping test. GEo-02 Scenario 1 investigates targeting the LC-UJ and uses a permeability that agrees with values observed from a pumping test at GEo-02 and within the range observed at the Thônex well. GEo-02 Scenarios 2 and 3 target the Siderolithic. Due to the uncertainty in the permeability of the Siderolithic at GEo-02, the GEo-02 Scenarios 2 and 3 use reservoir permeabilities that match GEO-02 Scenario 1 and the GEo-01 scenario, respectively. To investigate the uncertainty of the Young's modulus, each scenario is run with three values to cover the full range of uncertainty identified: 35 GPa, 2 GPa, and 0.35 GPa. The non-reservoir formations are assigned permeability of m^2 for all simulations.

Table 11 - Predictive Simulation Scenarios and Results

Well and Scenario	Targeted Reservoir and Depth [m]	Reservoir Permeability [m^2]	Reservoir Thickness [m]	Flow Rate [kg/s]	Young modulus [GPa]	Years simulated	Maximum ground deformation [cm]
GEO-01	LC-UJ (400 – 750)	$3*10^{-13}$	350	60	35	15	<0.01
					2	1	0.10
					0.35	15	0.49
GEO-02 Scen. 1	LC-UJ (750-1450)	$7*10^{-16}$	700	3.9	35	15	0.015
					2	1	0.053
					0.35	1	0.055
GEO-02 Scen. 2	Siderolitic (600-750)	$7*10^{-16}$	150	0.7	35	1	<0.01
					2	1	0.015
					0.35	1	0.016
GEO-02 Scen. 3	Siderolitic (600-750)	$3*10^{-13}$	150	60	35	1	<0.01
					2	1	0.097
					0.35	1	0.40

Figure 61 shows change in pressure and ground surface deformation for GE0-02 Scenario 1 with GPa. The pressure in the aquifer is shown at the end of each operational stage in Year 1. While the changes in pressure are large at the end of the Injection and Drawdown stages, the pressure dissipates to near the baseline in the resting stages (i.e., Falloff and Buildup). The pressure in later years do not change substantially from the first cycle and are therefore not plotted.

The ground surface rises near the well that injects and falls near the well that produces fluid. Furthermore, the ground surface deformation reaches its largest magnitude at the end of the first year Injection stage.

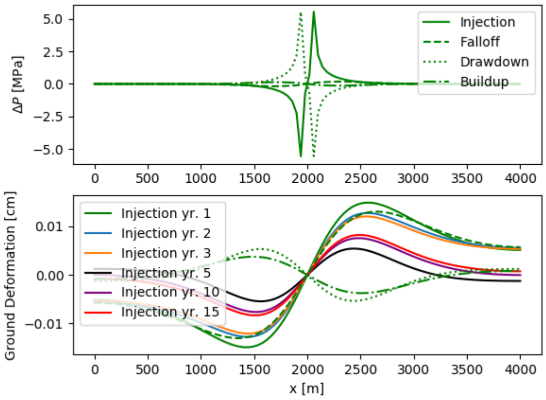

Figure 61 - Results for GEO-02 Scenario 1 with GPa. (Top) Difference in aquifer pressure from the initial condition versus x along the line seen in Figure 1.1 .4(c) at the end of each stage in Year 1. (Bottom) Ground deformation versus x along the line seen in Figure 1.1 .4(b) at the end of each stage in Year 1 (green) and at the end of the Injection stage in later years.

In Figure 62 we present the pressure and ground deformation at the end of the first year of injection for each scenario. Analysing only the first year is justified because the pressure does not change substantially from year to year, and the magnitude of ground surface deformation tends to be largest in the first year. Additionally, this approach saves computational cost so that the full 15-year lifetime is only run for GEO-01 and GEO-02 Scenario 1 (see Table 11)

The largest change in pressure is reached in GEO-02 Scenario 1, followed by GEO-02 Scenario 2. This makes sense because these are the scenarios where the flow rate is limited by the hydraulic fracturing constraint. The GEO-01 scenario and GEO-02 Scenario 3 both employ a large permeability, and therefore pore pressure gradients are not large. Additionally, the pressure profile does not change substantially between the scenarios with Young's modulus equal to 35 and 2 GPa. This suggests that the pressure profile may approach a steady state by the end of each injection stage, because the Young's modulus affects the storage of fluid.

The ground surface deformation is sensitive to the Young's modulus but is relatively small even when the lower-bound Young's modulus is used. For the large Young's modulus (35 GPa), the maximum magnitude of ground surface deformation is <0.02 cm (for GEo-02 Scen. 1, Table 11). For the smallest Young's modulus (0.35 GPa), the maximum magnitude of ground surface deformation is <0.5 cm (for GEO-01, see Table 11)

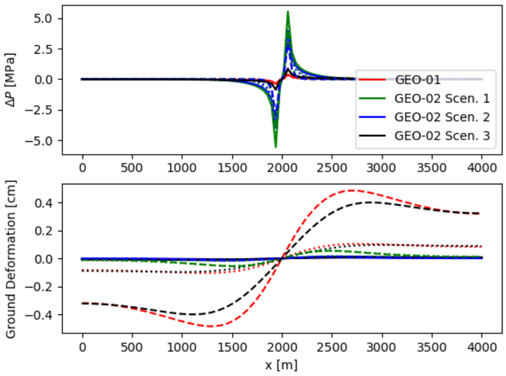

Figure 62 - Top) Difference in aquifer pressure from the initial condition versus spatial coordinate x along a line that intersects the two wells and (Bottom) ground surface deformation versus x at the end of Year 1 injection for each scenario. Solid lines use Young's modulus equals 35 GPa, dotted lines use 2 GPa, and dashed lines use 0.35 GPa. The cold/production well and hot/injection well are located at x = 1925 m, and x = 2075 m, respectively.

5.1.7.7.1.3. HM predictive simulations

In this section we present 3D THM simulations with the goals of understanding (a) if poroelastic or thermoelastic deformation will be larger and (b) if reservoir geometry will play a significant role in the amount of deformation.

Figure 63 shows the base-case pore pressure, temperature, and displacement response on the vertical, center plane that intersects the two wells. The pore pressure is elevated at the injection well and decreased at the production well and has reaches a steady state before the end of the simulation. The thermal plume extends away from the injection well and is pulled preferentially towards the production well. The horizontal displacement in the x direction is laterally away from the injection well and towards the production well. The vertical displacement is upward above the reservoir and downward below the reservoir.

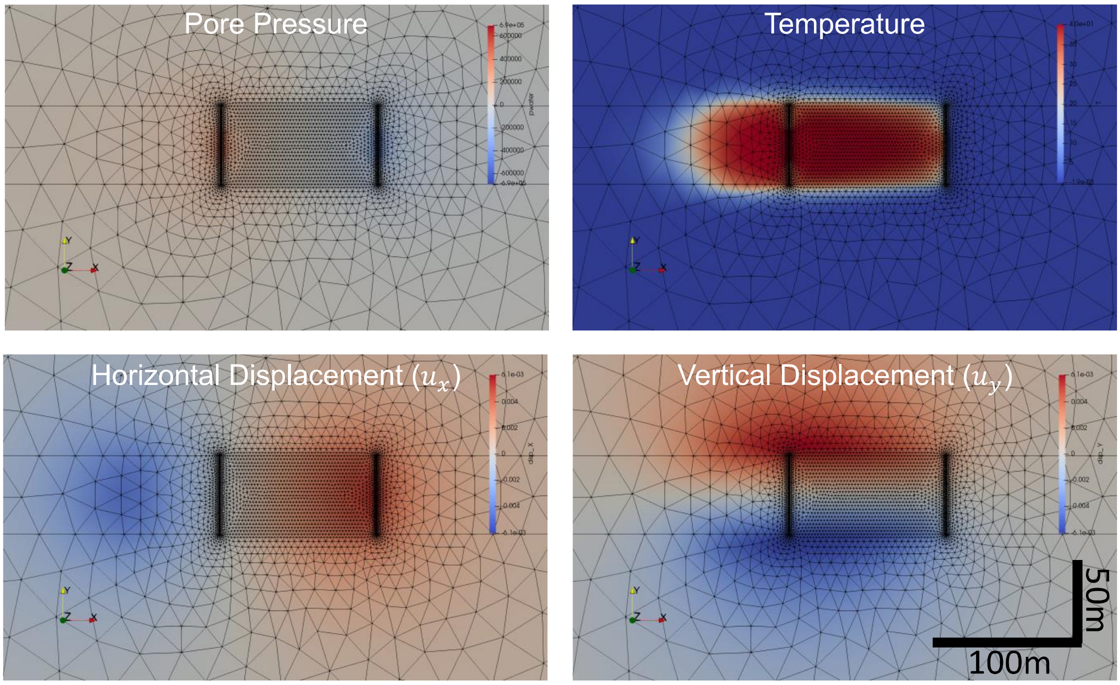

Figure 63 - Horizontal displacement, temperature, and pressure in the middle of the aquifer for three scenarios. The injection and production wells are in the highly discretized regions on the left and right, respectively

The horizontal displacement within the reservoir is analysed in Figure 64 for all three scenarios. In the first and second scenarios (the base case and the reef scenarios, respectively), the horizontal displacement reaches a maximum magnitude of approximately 0.5 cm, while in the third scenario (i.e., the one with no) the maximum magnitude of displacement is <0.01 cm. In the first and second scenarios, the region between the wells and somewhat past the injection well are heated to 35°C. The end of this elevated-temperature region corresponds closely with the location of the maximum magnitude of deformation. The pore pressure response is almost identical for the first and third scenarios, while the second scenario has more gradual pressure falloff due to the lower permeability outside of the reef. It appears that the thermoelastic deformation is more influential than the poroelastic deformation, for the scenarios considered.

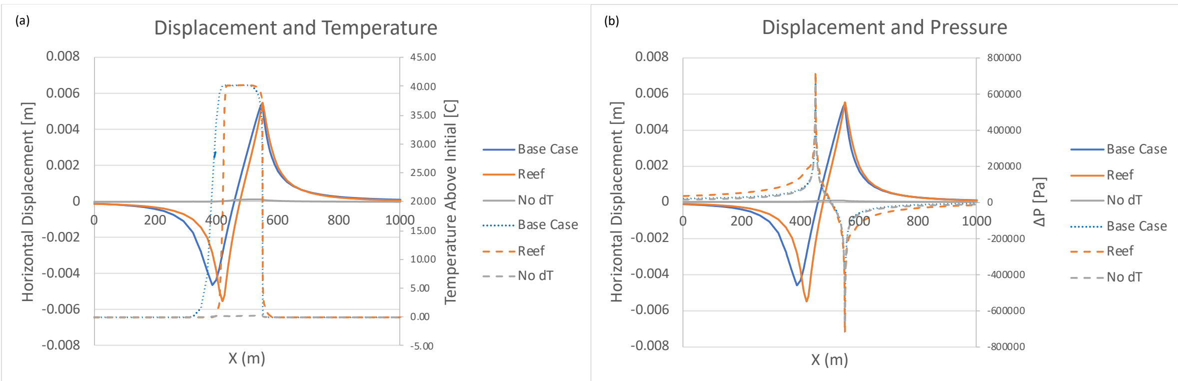

Figure 64 - Horizontal displacement, temperature, and pressure in the middle of the aquifer for three scenarios. The solid lines show the displacement response, and the dashed lines show the (a) temperature and (b) pressure response

The vertical displacement at the top of the reservoir (not the ground surface) is shown in Figure 65. The first scenario has the largest amount of uplift (0.60 cm), followed closely by the second scenario (0.57 cm), with scenario three displaying much less vertical deformation (<0.01 cm). In fact, the third scenario shows a small degree of downward deformation near the production well, which is not observed in the first and second scenarios. This suggests that the thermoelastic effect is causing upward deformation at the top of the reservoir, while the poroelastic effect is causing upward deformation at the injection well and downward deformation at the production well.

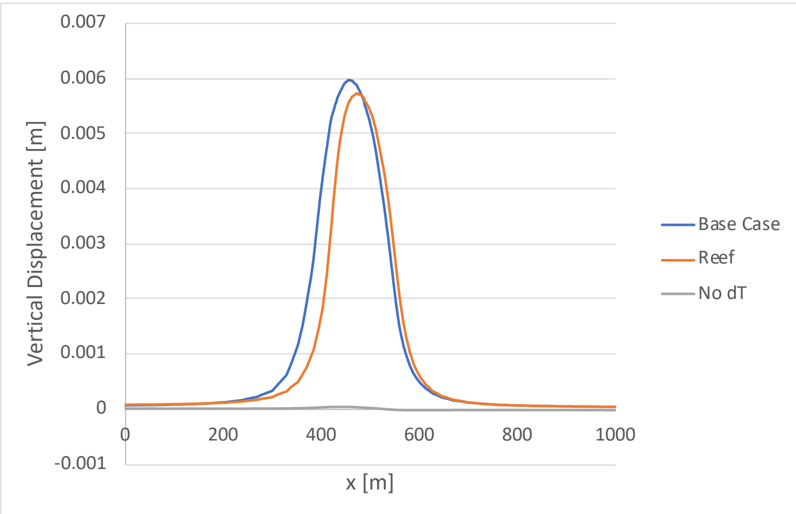

Figure 65 - Vertical displacement versus x along the top of the reservoir

5.1.7.7.2. Thermo-Hydraulic-Mechanical and Hydro-Mechanical conclusions

THM and HM simulations were performed to explore potential for ground surface deformation: (a) during the pumping test at GEo-01 and (b) in a predictive mode for HT-ATES operations at GEo-01 and GEo-02.

The THM results indicate that both pore pressure and temperature changes can lead to deformation. However, it is too early to draw definitive conclusions from the THM work because only a small parameter space was explored. It was not possible to explore a large parameter space due to numerical convergence problems. Therefore, future work could focus on improving 3D THM numerical simulators and applying them to understand HT-ATES.

In most HM simulations, the deformation remains small, suggesting that poroelastic deformation is manageable. For the GEo-01 pumping test, the GPS data shows no significant deformation. Modelling suggests that, given no deformation has occurred thus far, it is unlikely that large deformation will occur for the full duration of the pumping test. In the predictive HT-ATES simulations, the two scenarios with largest deformation both utilize the lower-bound value for the field-scale Young's modulus. One scenario targets a relatively shallow reservoir (GEo-01) and the other targets a relatively shallow and relatively thin reservoir (GEo-02 Scenario 3). All other scenarios resulted in ≤0.10 cm of ground surface deformation. It seems that poroelastic deformation can be managed by choosing operating pressures and flow rates based on the target reservoir in conjunction with monitoring. For example, flow rate may need to be curtailed if: (a) reservoir permeability, thickness, or depth are not sufficient, especially if the pressures would approach the hydraulic fracturing threshold or (b) observed deformation becomes large.

5.1.8 Geochemical models for seasonal storage/injection phases

Two reports have been delivered by University of Bern dealing on the prediction of the water-rock interactions occurring during storage/production cycles for the Geneva and Bern study sites. The full reports are available in Appendix07 and Appendix08.

5.1.8.1. The Geneva study case

5.1.8.1.1. Fluid geochemistry in the Geneva area

This chapter presents the results of the fluid geochemistry analysis carried out in the Geneva area in the framework of the ***Task 3.1 Drilling, logging, and laboratory tests*** of the Swiss project. Water samples were collected by UniGe over the entire Geneva basin from cold springs and deep geothermal wells (GEo-01, GEo-02 and Thonex-01) to reconstruct the geochemical evolution of the deep thermal groundwaters and contain the water-rock interaction processes. Additionally, modelling was performed by UniBe to predict the potential of activation of chemical reactions in the reservoir during production/injection operations and assess their potential effects for scaling/corrosion at the borehole and surface equipment scales associated with dissolution/precipitation of minerals composing reservoir rocks.

5.1.8.1.1.1. GEo-01 hydro-chemical features

In the framework of HEATSTORE a series of groundwater sampling surveys were carried out at the GEo-01 with the initial goal to characterize and better constrain the fluid circulation paths, time and water-rock interaction of geothermal waters across the entire Geneva Basin and eventually monitor the production tests still ongoing at present at GEo-01 (Figure 66). Data were collected by University and Geneva and HydroGeo Environnement under a contract with SIG. Analysis were carried out at the laboratories of Hydroistop GmbH. The results have been presented at the World Geothermal Congress 2020 and available as paper in Appendix09.

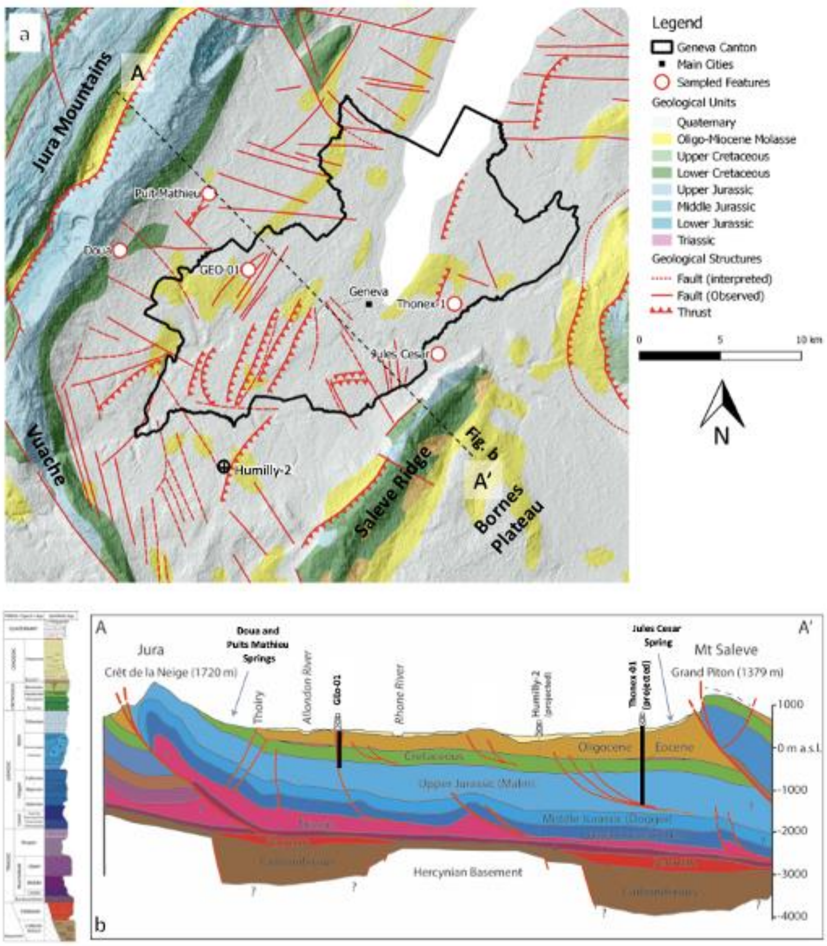

Figure 66 - a) Geological map over the Geneva Basin with indication of the main deep wells and sampled features (modified. from Brentini, 2018); B) Cross section cutting though the GB (modified from Clerc & Moscariello et al., 2020)

The sampled waters in this study show geochemical composition that reflects circulations within the Upper Mesozoic units which origin can be located between 800 and 1200m the Jura Mountains. The infiltration for the three springs occurred in recent times as confirmed by Tritium data, which also reveal a longer residence time for GEo-01 and Thonex-01 wells. If for the former well the residence is not now fully constrained, previous studies on the Thonex-01 well estimated a residence time of 10’000-15’000 years.

The geochemical composition of the sampled features reveals that three main geochemical facies can be identified:

- Puits Mathieu, and Doua springs show a classical Ca-HCO_3 composition dominated by water-rock interactions that occur during rapid circulation in the Mesozoic units as also confirmed by the equilibria with respect to the carbonate mineralogical phases.
- Jules Cesar spring shows a dominant Ca-HCO_3 with higher temperature and concentrations in Na-Cl-SO_4-SiO_2 compared to the two other springs. This can be interpreted as partially related to anthropic pollution due road salt contamination but also to the result of mixing processes between two endmembers which recharge zone from the Saleve ridge cannot be excluded: a recent (according to Tritium values) and shallow Ca-HCO_3 endmember and a deeper and slightly warmer Na-Cl>SO_4 endmember probably originating by leaching of deeper Mesozoic Units.
- At GEo-01 the observed composition in Na>Ca-HCO_3 reflects a circulation within the Jurassic units, recharged in the Jura Mountains before the atmospheric nuclear tests (1953-1964). The waters discharged are in equilibrium with the carbonate mineralogical phases. The reservoir temperature estimated by the Na-K-Ca geothermometer is consistent with the one measured at the wellhead during the sampling campaign thanks to the large artesian flow observed. The discharged waters result from a mixing of relatively different water between different productive fractures in the Lower Cretaceous giving a pure Ca-HCO_3 composition and in the Upper Jurassic which can contribute to the Na, Mg concentrations. The presence of Mg rich endmember can be representative of the Oxfordian dolomite-rich lithologies which were not drilled by the GEo-01 well but that are most probably cut by fault structures that act as a preferential up-flow pathways towards the surface.
- At the Thonex-01 well the Na-Cl geochemical imprint is correlated to long circulation both in terms of distance from the recharge zone and residence time. In fact, the waters discharging from the well are recharged by meteoric waters which infiltrated in the Jura Mountains in climatic conditions colder than at present and the residence time has been estimated to be between 10’000 and 15’000 years. During this time the infiltrated waters cover the distance of about 20km from the Jura Mountains to the well and have the time to get into full thermal equilibrium with the reservoir host-rock in the Jurassic formations. The Na-Cl composition results from Ca-Na ion exchange reaction that might occur at the Oxfordian formations which have been drilled in the last 400m of the well. This is also supported by the Magnesium concentration (higher than in the other sampled features, which can result from the water-rock interactions with dolomite-rich lithologies such as those in the Oxfordian.

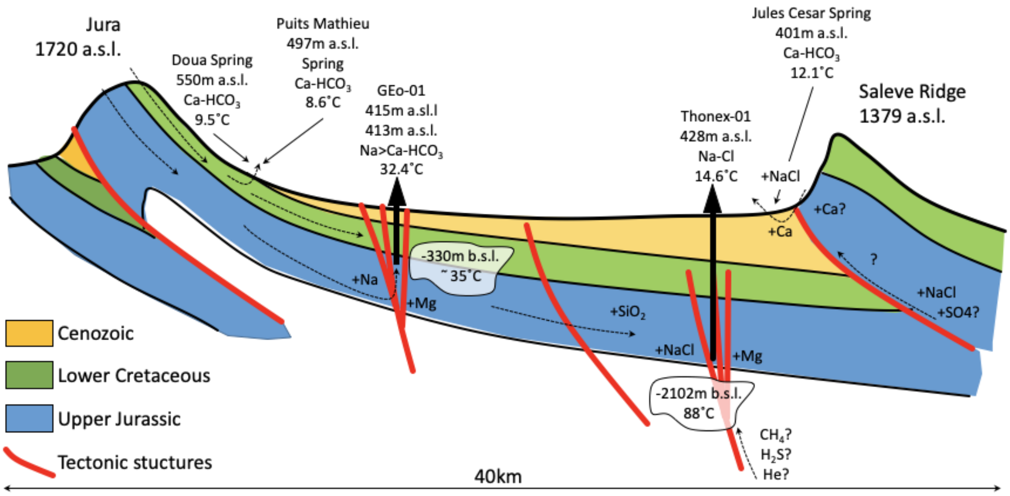

Figure 67 - Conceptual model of groundwater circulation in the Geneva Basin (vertical and horizontal scales are not proportional).

In this first step of screening, the results of the geochemical investigation on the liquid phase discharged from springs and two geothermal exploration wells are presented. The study focusses on the understanding the geochemical evolution of groundwater across a NW-SE oriented cross-section passing though the main infiltration zone of meteoric waters in the Jura Mountains towards NW, the Puits Mathieu and Doua springs located at the Jura foothills, the geothermal exploration wells GEo-01 drilled in 2018, and Thonex-01 drilled in 1993 and the Jules Cesar spring located at the SE of the section. All the analysed samples show a meteoric origin, and the main recharge zone is in the Jura Mountains. Only the Jules Cesar spring shows geochemical composition that can be most probably associated to an infiltration of meteoric waters at the Saleve Ridge and in part to anthropic contamination. The Puits Mathieu and Doua cold spring show the typical Ca-HCO_3 composition due to circulation in Lower Cretaceous, most probably controlled by karstic pathways allowing very rapid circulation as shown on Tritium data. The GEo-01 is 744m deep and discharges thermal waters at 32.4˚C with an artesian flow of 55.6 l/s and a wellhead pressure of 10bars. The geochemical composition of the discharged waters is most probably associated to a mix of pure Ca-HCO_3 groundwater from the Lower Cretaceous with a second endmember representative of water interacting with dolomite-rich lithologies such as those located at the base of the Upper Jurassic. The residence time of the water discharged by the GEo-01 well are not associated to recent and rapid circulations as shown by Tritium data, but Carbon isotopes reveal a residence time of probably some thousands of years. The Thonex-01 has been drilled to reach the Upper Jurassic reservoir at more than 2500m in depth. The bottomhole temperature recorded after drilling was 88˚C and residence times of more that 10’000 years have been estimated confirming previous analyses. The well discharge water at 14.6˚C having a Na-Cl geochemical composition due to the water-rock interactions that occur within the Upper Jurassic lithologies that compose the main reservoir. The Jules Cesar cold spring discharges a complex mix of waters most probably due to mixing processes between a cold, shallow and recent Ca-HCO_3 endmember and a deeper and warmer Na-Cl>SO_4 endmember (Figure 67).

The results of this study highlight how deep circulation in the Geneva Basin have a common meteoric origin but complex circulations due to the heterogeneities i.e., in the reservoir rock in terms of mineralogical composition, tectonic setting and lithology. To further constrain the understanding of deep circulations in the Geneva Basin the study of the Carbon and Sulphur isotopes as well as the noble gases, hydrocarbon content will contribute reducing the uncertainty of the interpretation and providing new insights for future geothermal developments in the area.

5.1.8.1.1.2. Hydro-chemistry monitoring at GEo-01

Since the execution of drilling operation, the hydro-chemical composition of the fluid discharged by GEo-01 has been monitored to assess its possible evolution. As the production tests are still running, final data and results will be available only after the end of the project and will be published in peer-review scientific journals.

If looking at the main major elements defining the geochemical facies of the GEo-01 groundwater, only minor fluctuations can be observed indicating stable hydrogeological conditions controlling the water-rock interactions. This is also supported by the high flowrate and stable pressure conditions observed at the wellhead (Figure 68).

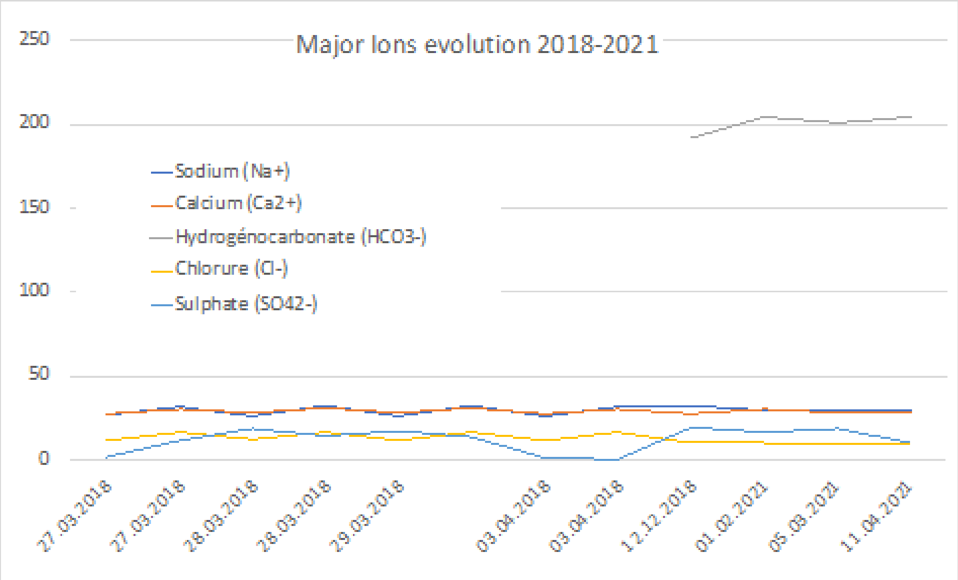

Figure 68 – Major ions evolution at Geo-01

5.1.8.1.1.3. GEo-02 hydro-chemical features

In July 2020, after drilling operation were completed, water samples were collected from the GEo-02 wells at two levels:

- 880-945 at the base of the Lower Cretaceous carbonate
- 1360-1425 in the Upper Jurassic carbonates

All groundwater samples refer to the general Na-HCO3 water type. At the wellhead, they are strongly supersaturated with respect to calcite and dolomite. The strong supersaturation is likely inherited from the degassing of CO2 during sampling. At reservoir conditions, all samples must be at saturation with respect to both dolomite and calcite based on the rather fast reaction kinetics of these carbonate minerals (Table 12).

Table 12 – Water composition at GEo-01 and GEo-02

Well	Unit	GEO-02	GEO-02
Sampling date		14.07.20	14.07.20
Sampling depth	m	880-945	1360-1425
Sampling temperature	°C	21	20
In-situ reservoir temperature	°C	38.4	53.4
pH		8.41	8.22
Oxygen concentration	mg/l	5.7	1.7
Redox potential	mV	384	395
Sodium (Na+)	mg/l	152	52.5
Potassium (K+)	mg/l	6.92	5.35
Calcium (Ca2+)	mg/l	16.0	35
Magnesium (Mg2+)	mg/l	8.0	14.2

Ammonium (NH4+)	mg/l	0.6	0.2
Bicarbonate (HCO3-)	mg/l	325	179
Chloride (Cl-)	mg/l	31.2	15
Sulfate (SO42-)	mg/l	5.1	32.8
Nitrate (NO3-)	mg/l	< 0.1	< 0.1
Sulfide total (HS-, S2-)	mg/l	not measured	not measured
Iron (Fe2+)	mg/l	< 0.01	< 0.01
Water type (simplified)		Na-HCO3	Na-HCO3
Saturation index calcite		0.57	0.45
Saturation index dolomite		1.14	1.85
Log(PCO2) at reservoir T		-2.00	-1.85

In October 2020, SIG collaborated with IFP Energies Nouvelles and SEMM Logging to carry out a water sampling survey at depth at GEo-02 well. As no final report is available from IFP now, this chapter reports only the results of the analysis with very little interpretation.

The schematic structure of the GEo-02 well is shown in Figure 69 .

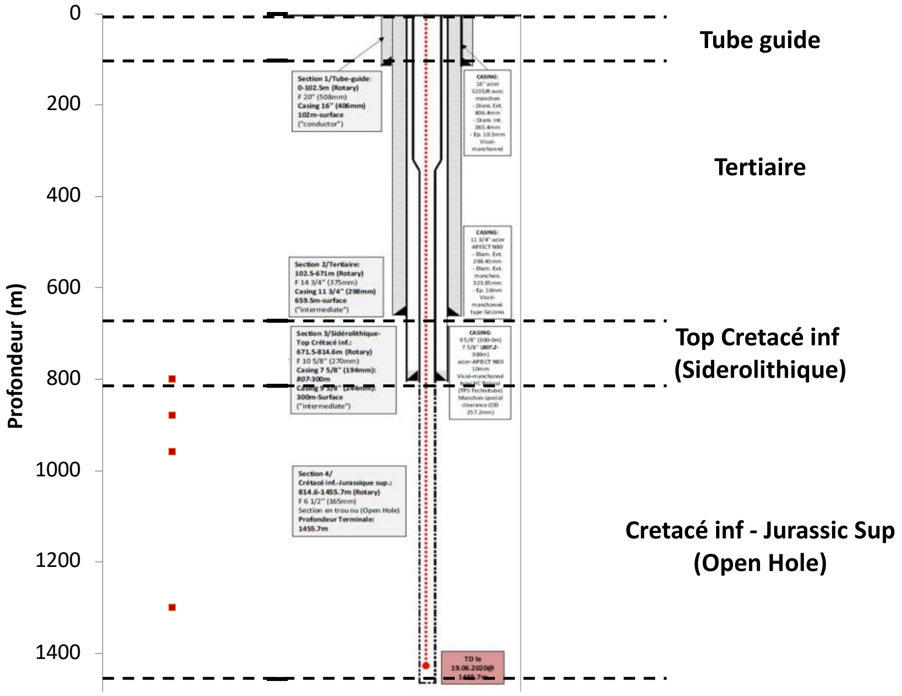

Figure 69 – Structure of the GEo-02 well. The red dots indicated the sampling depths

In total 2 surface (Table 13) samples and 5 sampling levels were collected in the Lower Cretaceous between 800 and 1361m in depth, focusing specifically on gas composition at the conditions resumed in Table 14.

Table 15 reveals a very low contamination from atmospheric air, less than about 3.5%

Table 13 – Surface water sampling and dissolved gas analysis for the samples collected at GEo-02

	pH	Temperature (˚C)	Average CH4 (mmol/l)	Average $\partial^{13}C$ CH4 (‰)	Average DIC (mmol/l)	Average $\partial^{13}C$ DIC (‰)
Sample 13/10	8.14	16.4	0.43	-62.24	5.8	-1.5
Sample 15/10	8.31	11.2				

Table 14 – Groundwater samples collected at GEo-02

	Depth (m b.g.l.)	Fluid Volume (cc)	Temperature (˚C)	Pressure (bars)
Level 1 13/10	1360	570	51.0	133

Level 2 14/10	880	570	39	90
Level 3 14/10	996	570	42	101.5
Level 4 15/10	880	570	39.1	89.7
Level 5 15/10	800	570	37.5	82.3

Table 15 – Results of the gas field analyses at GEo-02

Sample	2 analyses	He	H2	O_2	N_2	Ar	CH_4	CO_2	C_2H_6	C_3H_8	H_2S	Total	% air
1360 m* 13/10	GWR=0.0003	0.02	0	0	99.2	0.14	0.27	0.36	0	0	n.a.	100	0.65
880 m 14/10	Average	0,08	0,0015	0	38,7	0,92	59,7	0,62	0,016	0,001	0,024	100,000	3,50
880 m 15/10	Average	0,07	0,0040	0	39,3	0,87	59,1	0,60	0,016	0,002	0,006	100,000	3,37
800 m 15/10	Average	0,06	0,0103	0	39,1	0,92	59,3	0,55	0,016	0,001	0,005	100,000	1,47

The dissolved gas compositions dominated by CO2, N2 and Ar as atmospheric gases plus CH4 generated in the subsurface (Table 16). Preliminary interpretation about the origin of CH4 indicate that it derived from biogenic processes, mainly related to carbonate reduction and methyl fermentation (Table 17 and Figure 70)

Table 16 – Dissolved gas composition at well sampling conditions calculated with the SØreide Witson Thermodynamic Model at GEo-02

Depth (m b.g.l.)	T (˚C)	P (bars)	CO_2 (mmol/l)	H_2S (mmol/l)	CH_4 (mmol/l)	C_2H_6 (mmol/l)	C_3H_8 (mmol/l)	N_2 (mmol/l)	H_2 (mmol/l)	He (mmol/l)	Ar (mmol/l)
880 13/10	39	90	0,29	1,32E-02	3,1	6,88E-04	2,87E-06	0,33	3,90E-05	0,007	0,11
880 15/10	39,1	89,7	0,29	3,40E-03	3,1	7,10E-04	8,34E-06	0,34	1,05E-04	0,006	0,10
800 15/10	37,5	81,5	0,36	3,62E-03	35,8	9,57E-03	5,22E-04	21,92	6,04E-03	0,034	0,56

Table 17 – Results of the methane gas field analyses at GEo-02

Depth (m b.g.l.)	$\delta^{13}C$ CH_4 (‰)	δD CH_4 (‰)
880 m	-62,93	-242,0
800 m	-62,04	-249,1

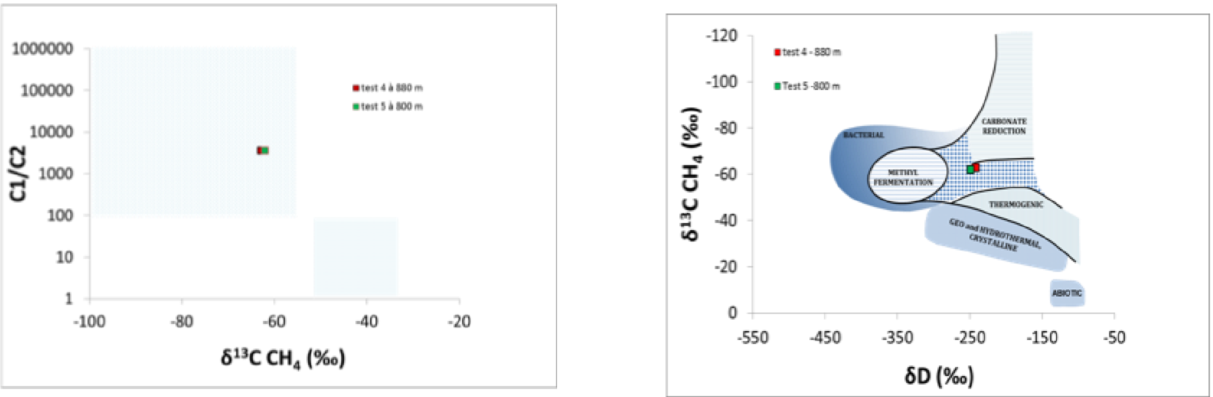

Figure 70 – Origin of Methane in the GEo-02 gas (Source: SIG/IFPN; plots modified after Whiticar et al., 1999)

5.1.8.1.2. Groundwater flow observations while drilling at GEo-01

Drilling was performed using mud in the upper 407.5 m where the Cenozoic Molasse sediments were drilled, which did not reveal any evidence of occurrence, loss, or other fluid flow evidence of interest.

However, during drilling in the Cretaceous and Upper Jurassic formations, various increases in flow were already observed at the surface thanks to their artesian character (Figure 71 and Table 18).

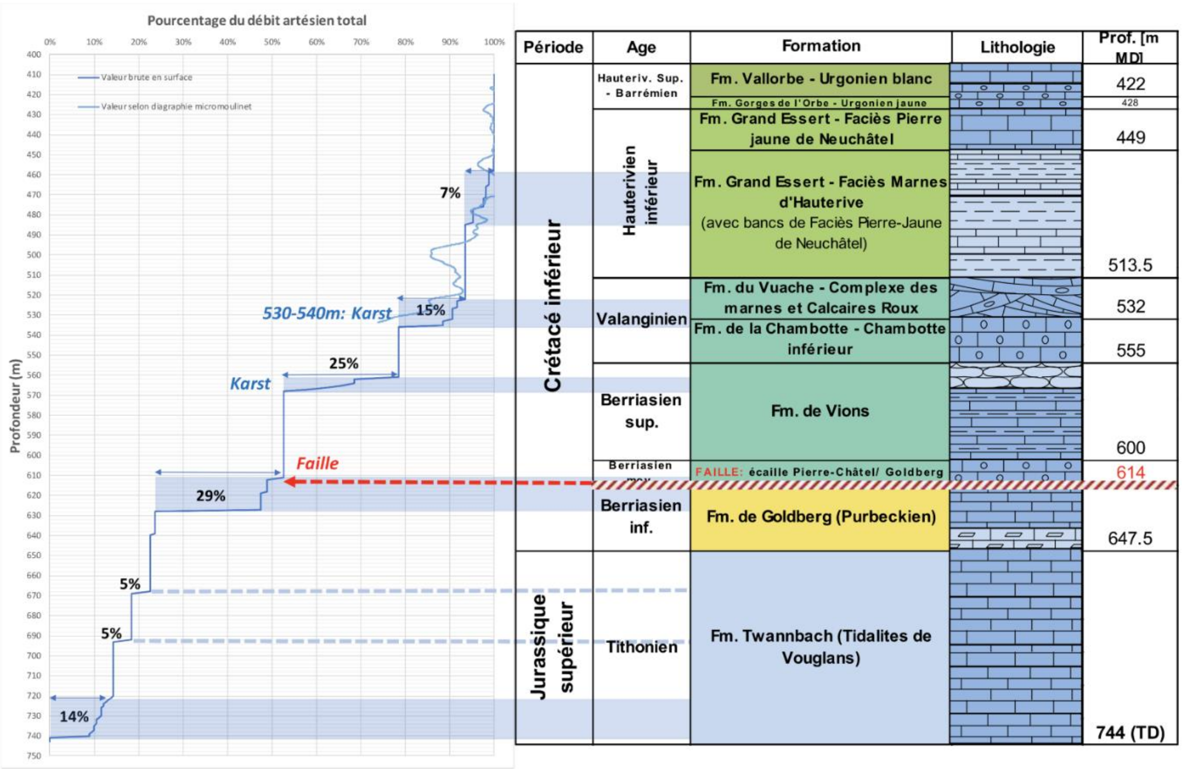

Figure 71 – Localization of water flow level at GEo-01 well (source: SIG)

Table 18 – Summary of the water flow levels and reservoir pressure conditions at GEo-01 well (source: SIG)

Water Flow Level	Top	Botto m	Flow rate (m³/h)	Flo w %	Geologic Unit	Type of Permeability	Reservoir Pressure (bar)	Time for pressure to stabilize (seconds)
1	455	486	14	7	Lower Cretaceous	Fractures	9.38	543
2	522	537	30	15	Lower Cretaceous	Karst	9.22	520
3	561	569	50	25	Lower Cretaceous	Karst	10.24	360
4	611	628	58	29	Lower Cretaceous	Fractures	11.75	205
5	662	668	10	5	Upper Jurassic	Fractures		
6	692		10	5	Upper Jurassic	Fractures	11.45	235
7	720	740	28	14	Upper Jurassic	Fractures		

From the first water inflow, the wellhead pressure was around 10 bar (Figure 72), which corresponds to an average hydrostatic level of about 515 a.s.l. (with variations of +/- 20m). This level corresponds approximately to the altitudes of the main springs at the foot of the Jura. Increase in wellhead pressure was observed as new productive fractures were encountered indicating that:

- The upflow is achieved more and more rapidly with increasing arterial flow,
- The higher the artesian pressure, the faster the upflow.

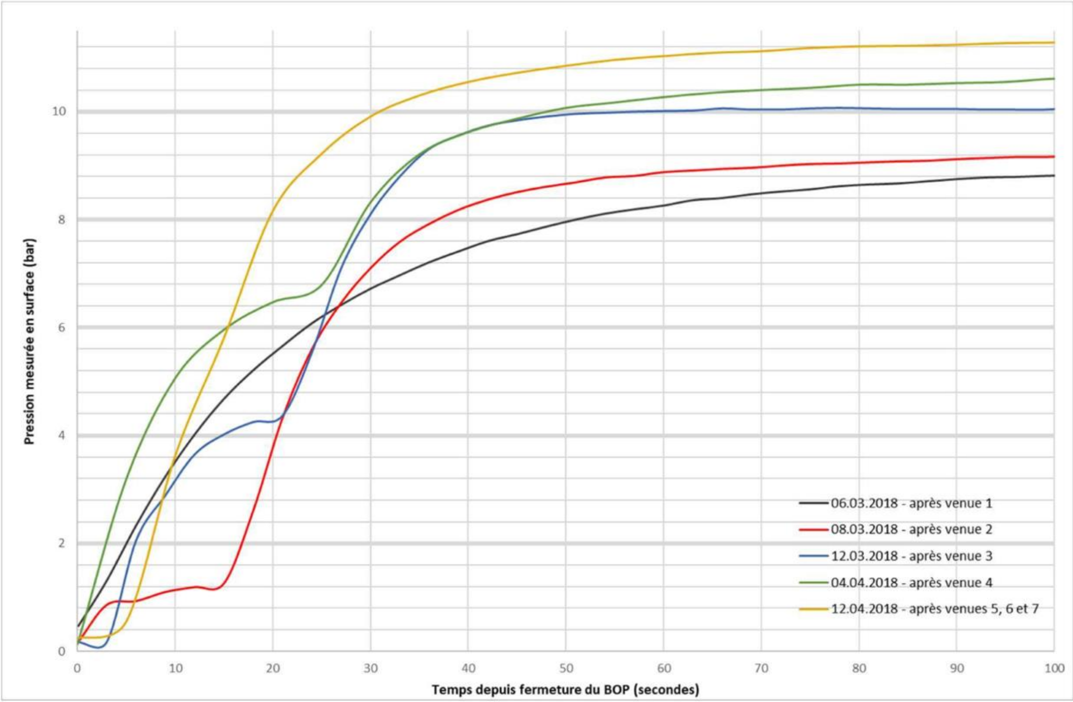

Figure 72 – Observed wellhead pressure during drilling (source: SIG)

5.1.8.1.3. Hydraulic tests during drilling

In this chapter we resume the results of the available hydraulic tests performed while drilling GEo-01 and presented as internal report by SIG. The results are part of ***Task 3.1 Drilling, logging, and laboratory tests*** of the Swiss proposal and integrated to ***Task 5.2 Monitoring results and Deliverable 5.2 Report on analyses of gathered data of demonstration sites and show cases*** of the European proposal.

The artesian conditions made it easy to carry out hydraulic tests as drilling operations advanced. These tests made it possible to accurately monitor the evolution of the well flow as it deepened.

These tests were carried out in two formats:

- Pressure and artesian flow measurements before and/or after the drilling days
- Step drawdown tests with increasing artesian flow until stabilization carried out after each observation of water flow more than 10m^3/h, after each major lithological change, or after a drastic change in the drilling parameters (e.g., significant increase in rate of penetration)

Pumping tests were also carried out at the end of the Cretaceous drilling at 637m depth.

Table 19 shows the results of all these measurements and tests.

Table 19 – Synthesis of the results of hydraulic testing during drilling (source: SIG)

Depth 455m (MD)				
Step	Flow rate (m3/h)	Pressure (bar)	Duration (h)	Productivity index (m3/h/bar)
0	0	9.03		
1	0.2	0.1	0.25	0.025
Depth 472m (MD)				
0	0	8.03		
1	2	4.92	0.5	0.643
2	4	0.27	0.5	0.515
Depth 487m (MD)				
0	0	9.43		
1	3	8.07	0.5	2.206
2	6	5.91	0.5	1.705
3	9	1.41	0.5	1.122

4	11.4	0.13	0.5	1.226
Depth 502m (MD)				
0	0	9.2		
1	11	0.13	0.25	1.213
Depth 537m (MD) - Test 1				
0	0	9.34		
1	19	0.13	0.25	2.063
Depth 537m (MD) - Test 2				
0	0	9.32		
1	4	9.09	0.75	17.391
2	8	8.55	0.75	10.39
3	15	6.98	0.75	6.41
4	26	1.9	0.75	3.504
5	27.7	0.1	0.75	3.004
Depth 552m (MD)				
0	0	9.32		
1	41	0.13	0.25	4.461
Depth 562m (MD)				
0	0	10.31		
1	92	0.13	0.25	9.037
Depth 594m (MD)				
0	0	11		
1	16.7	10.54	0.75	36.304
2	31.8	9.51	0.75	21.342
3	48.5	7.86	0.75	15.446
4	56.6	6.79	0.75	13.444
5	92	0.13	0.75	8.464
Depth 627m (MD)				
0	0	10.86		
1	102	0.13	0.25	9.506
Depth 637m (MD) - Test 1				
1	115	0.13	0.75	10.658
2	48.8	7.33	0.75	16.379
3	38.7	9.03	0.75	20.476
4	0	10.92	0.75	
Depth 637m (MD) - Test 2				
0	0	10.65		
1	132	0.13	0.25	12.548
Depth 637m (MD) - Test 3				
0	0	8.79		
1	5.8	9.73	0.5	96.667
2	9.9	9.66	0.5	76.154
3	15	9.55	0.5	62.5
4	23	9.32	0.5	48.936
5	39.5	8.65	0.5	34.649
6	59.5	7.5	0.5	25.983
Depth 637m (MD) - Test 4				
0		9.78		
1	131	-0.182	0.75	13.149
2	135	-0.478	0.75	13.161
3	140	-1.49	0.75	12.422
4	145	-2.197	0.75	12.106
5	148	-2.781	0.75	
Depth 637m (MD) - Test 5				
0		9.78		
1	127	-0.11	0.75	12.841
2	145	-2.088	0.75	12.218
Depth 637m (MD) - Test 6				
0	0	10.62		
1	15.2	10.36	0.75	58.462
2	30.5	9.86	0.75	40.132
3	45.7	9.1	0.75	30.066
4	62	8.1	0.75	24.603
5	140	0.13	0.75	13.346
Depth 690m (MD)				
0	0	10		
1	165	0.13	0.25	16.717
Depth 712m (MD)				
0	0	11.14		
1	175	0.13	0.25	15.895
Depth 744m (MD) - Test 1				
0	0	11.66		
1	188	0.13	0.25	16.305
Depth 744m (MD) - Test 2				
0	0	11.66		
1	205	0.13	0.25	17.78

The graph below (Figure 73) shows the results of these different tests in the form of an overlay of characteristic curves. It should be noted that the y-axis shows the measured pressure / observed dynamic level, not the obtained drawdown. The differences in natural pressure, measured between 9.32 and 11.66 bar, are therefore not erased.
Furthermore, the results presented are raw surface results, not corrected for the various induced pressure losses (presence of the tool, presence of the drill string, choke line, weight of the water column, etc.). The long-term production tests will make it possible to refine all the results obtained during drilling and during the short-term tests.

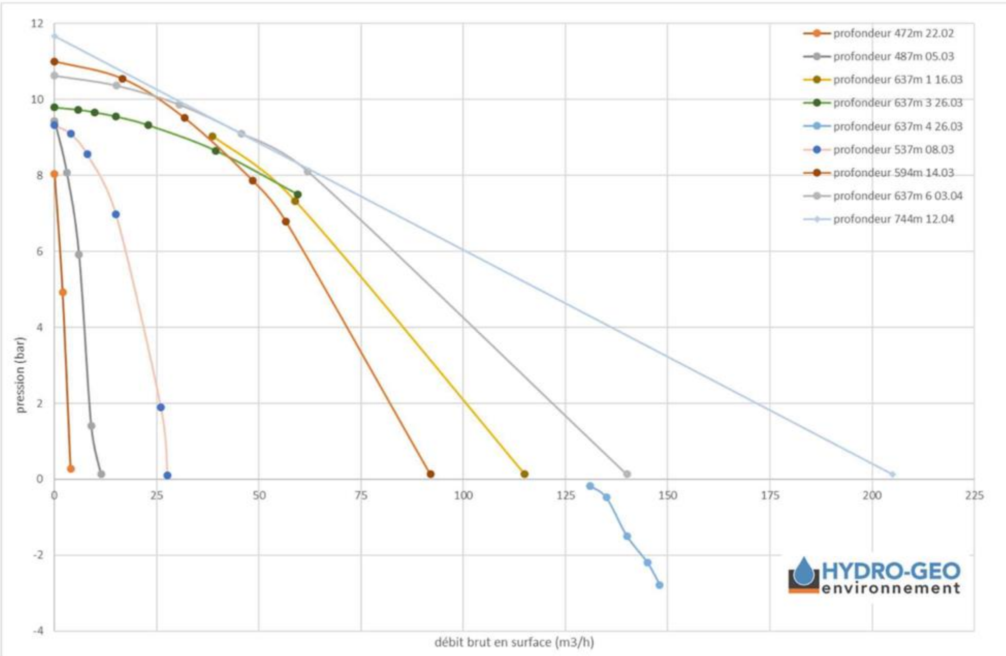

Figure 73 – Results of hydraulic testing during drilling (source: SIG)

The plot in Figure 4 Figure 7shows the evolution of the productivity of the GEo-01 well as drilling operations advanced. It also shows that for the first tests carried out, the 'critical' flow rate appears very quickly because of the pressure losses induced by the drill string and other technical equipment (including the Choke Line) and induced by the critical circulation speeds within the producing fractures. Thus, the gross productivity index reaches:

- at the end of drilling in the Cretaceous, about 1.20 m^3/h/m of drawdown,
- at the end of drilling (Cretaceous + Upper Jurassic), about 1.82 m^3/h/m of drawdown

5.1.8.1.4. Short-term production tests at GEo-01

At the end of the drilling operation on the lower Cretaceous formations (at 637.4m), hydraulic pumping test tests were carried out with an average flow of 148 m^3/h. This average flow rate of 148 m^3/h was only 15-25 m^3/h higher than the natural artesian flow rate.

The graph in Figure 74shows the evolution of pumped flow and drawdown level during this short 48-hour test.

This plot shows that the water level in GEo-01 does not show any stabilization of the drawdown level: after a drawdown of 23.4m at the start of the pump, the level evolves slowly to reach a rise of 1.7m. This rise:

- Is due to the increase of the reservoir load at this period, visible on the Mathieu well,
- It has a slight influence on the pump's flow rate, by regulating the flow rate/HMT couple: when the level rises naturally, the pump operates more easily, and its flow rate increases slightly (from 147 to 149 m^3/h)
- Does not allow the interpretation of the test from a hydrodynamic point of view, nor the calculation of transmissivity/permeability parameters.

During this test, the in-situ physio-chemical parameters evolved as follows:

- pH and conductivity remained very stable at 7.4 and 360 us/cm respectively.
- Turbidity evolved between 5 and 25 NTU.
- The dissolved oxygen concentration evolved between 0.1 and 0.3 mg/l.

- Redox stabilized very quickly in the range -340/-350 mV.

The extraction of a volume of 7,100 m^3 (of which 1,300 m^3 is more than the natural artesian flow) does not therefore generate any notable impact on the Cretaceous reservoir, which therefore appears to be very important.

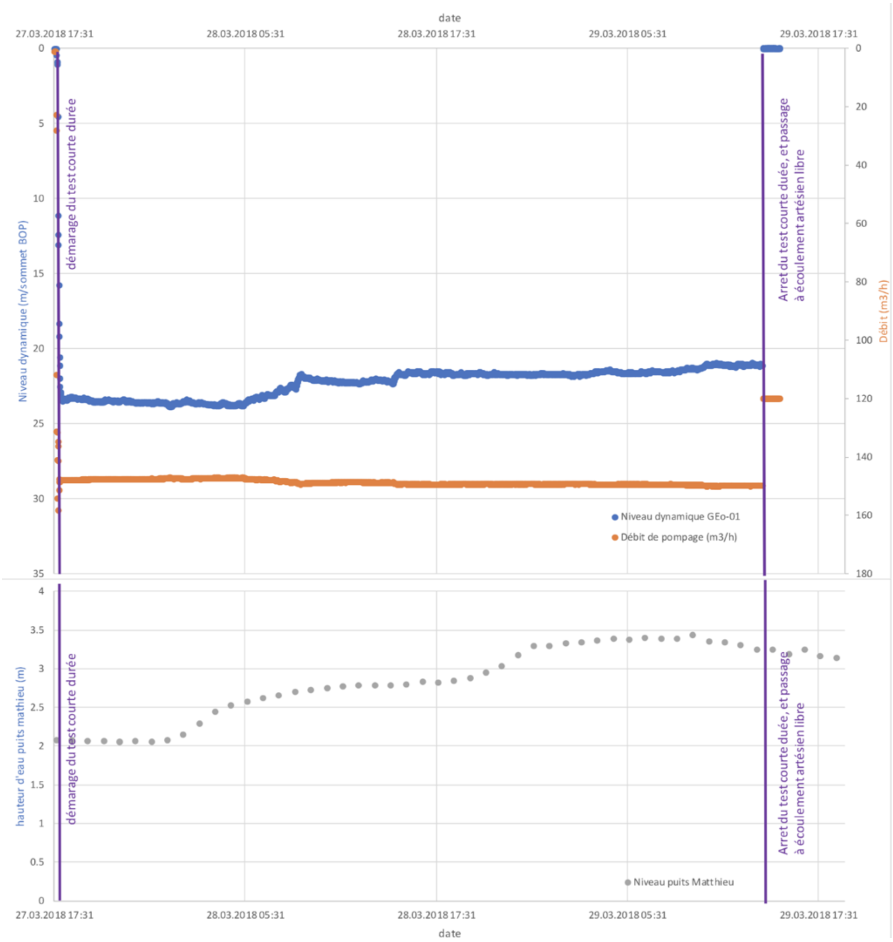

Figure 74 – Results of the short-term production tests in the Lower Cretaceous section (source: SIG)

The outcomes of the tests allowed calibrating the hydraulic properties of the Mesozoic carbonates at GEo-01. Long-term production tests started in early 2021 and will are still ongoing at present.

From a hydrogeological point of view, the objectives of GEo-01 were to:

- Recognize the hydrogeology of the Cretaceous and Upper Jurassic units in the Geneva basin
- Clarify and/or confirm the hypotheses concerning the hydrogeology of these units, and the local hydrogeological concept, including in particular
    - Reservoir pressure,
    - Flow / productivity,
    - Type of porosity, permeability, degree of fracturing and karstification (and recrystallisation and infilling of these systems),
    - Location and vertical compartmentalization of reservoir levels,
    - Physico-chemical properties of the fluids,

to allow a better understanding of the hydrodynamics of the Geneva basin, in parallel with other studies in progress or to come:

  - Relation with the recharge, and the Jura massif, including possible compartmentalization between the different sub-basins
  - Sustainability of the resource in case of exploitation,

- The hydrogeological monitoring of the GE0-01 borehole aimed to
  - To collect information related to the hydrogeological reconnaissance of the formations crossed, by placing them in the local context,
  - To be able to set up an adapted reaction in case of events during the operations.

5.1.8.1.5. Hydraulic mini-frac tests at GEo-02

As part of the geological and hydrological characterization of the fractured carbonate reservoir targeted by the Geo-02 well, Services Industriels de Geneve (SIG) awarded Solexperts AG to carry out hydraulic fracturing stress measurements in the vertical borehole GEo-2 of 1455 m depth, besides comprehensive hydraulic tests. The full report from Solexperts AG is available in Appendix10.
The main objective of the hydraulic fracturing tests was to determine the magnitude and the orientation of the in-situ stress. In summary, a total of 8 hydraulic-fracturing tests was conducted during 15.-20.07.2020. For fracture orientation determination, BHTV-logging was conducted prior and after hydraulic fracturing. The present chapter resumes the results of the test which are described in detail in the final report provided by Solxeperts available in the Annexes.
The borehole penetrates the following geologic units:

- Sedimentary rocks of the Quaternary (0-38 m, average density 2.4 g/cm3),
- Molasse (38-630 m, 2.55 g/cm3),
- Siderolithic (630-769.9 m, 2.5 g/cm3)
- Lower Cretaceous (769.9- 996 m, 2.66 g/cm3)
- Upper Jurassic (996-1455 m, 2.66 g/cm3).

Thus, the vertical stress Sv due to the weight of the overburden rock can be estimated to 37 MPa at the bottom of the borehole at 1455 m.
Seven test sections between 1335 m and 1424 m depth were selected for the tests, and one test section within the Cretaceous rocks at 883 m was selected although the borehole diameter of about 7-3⁄4 inch only allows packer pressurization up to 20 MPa (Figure 75).

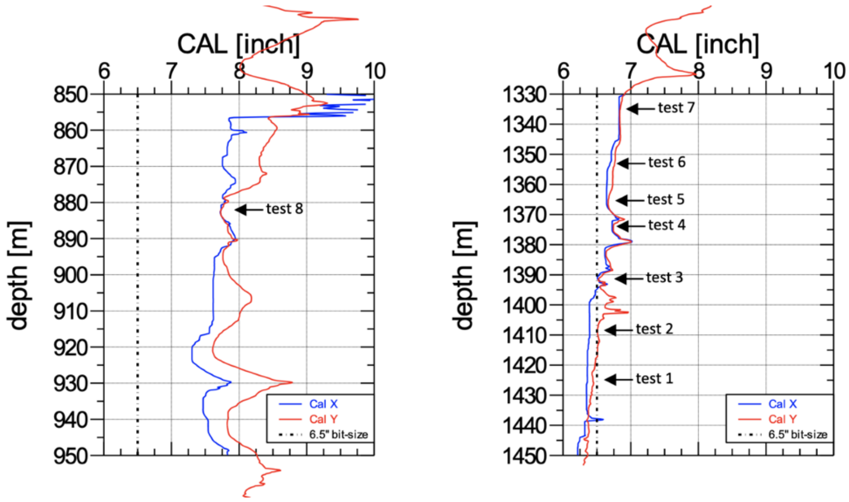

Figure 75 – Caliper-log borehole GEo-2 (source: Solexpert, 2020)

The derived characteristic hydrofrac pressure data (breakdown pressure Pc at fracture initiation, fracture re-opening pressure P_r, shut-in pressure Psi, and the resulting in-situ tensile strength T = P_c - P_r) are shown graphically in Figure 76.

Of the 8 tests, the 5 tests at 1335.0 m, 1366.0 m, 1374.0 m, 1409.0 and 1424.0 m are characterized by (weak) fracture initiation events with low breakdown pressure values ranging from 21.0 MPa to 24.9 MPa. In the remaining 3 test sections at 883.0 m, 1353.0 m and 1391.0 m pre-existing fractures without distinct pressure peaks were stimulated (Figure 77). The refrac-pressure values vary between 12.8 MPa at 883.0 m and 23.5-24.0 MPa at 1353.0 m, the corresponding in-situ hydraulic tensile strength T between 2.8-3.1 MPa and 4.6-4.9 MPa with a mean value of T = 3.8 ± 0.7 MPa. The tests yield rather distinct and reliable shut-in pressure values which scatter significantly between 1335.0 m and 1424.0 m depth between 17.9 MPa to 27.7 MPa, besides the value of 13.2 MPa at 883.0 m depth. As shown in Figure 78, the characteristic hydrofrac pressure values are considerably lower than the calculated vertical stress S_v due to the weight of the overburden rock mass. The low shut-in pressure indicates the initiation or stimulation of non-horizontal fractures.

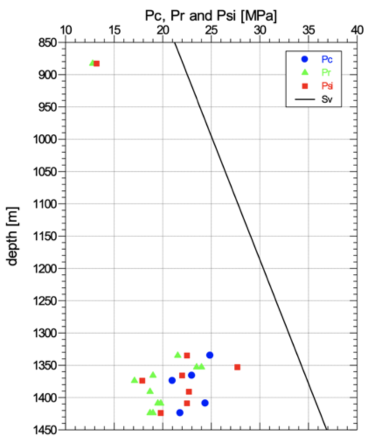

Figure 76 – Breakdown - pressure Pc, refrac-pressure Pr, and shut-in pressure Psi in bore-hole GEo-2 in relation to the vertical stress Sv

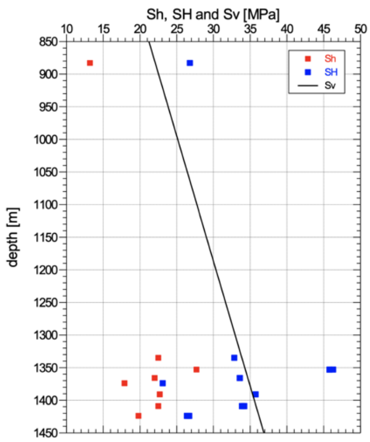

Figure 77 – Principal stresses for borehole GEo-2.

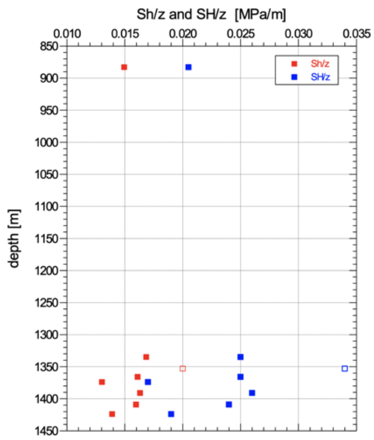

Figure 78 – Horizontal stress gradients Sh/z and SH/z for borehole GEo-2.

5.1.9 Environmental effects evaluation and prediction of HT-ATES operations in Geneva

As part ***of D6.6 Environmental effects of UTES technologies in Europe*** of the European project, a multi-disciplinary analysis has been carried out to identify and assess potential positive and negative effects associated with the operations of an HT-ATES in Geneva. The full report is available in APPENDIX 11.

The analysis focused on the analysis of the effects observed during drilling operations at GEo-01 and GEo-02 and on the prediction of the effects on soil mechanics, ground water and CO_2 intensity reductions

5.1.9.1. Observations associated with drilling operations at GEo-01 and GEo-02

The environmental layers identified to perform the assessment are:

- Air quality
- Noise and Vibrations
- Groundwater quality
- Surface clear water

- Soil occupation
- Wastes and dangerous substances
- Environment
- Nature

All precautions have been taken to mitigate the impacts of the drilling operations and are listed in D6.6. The selection of the drilling techniques employed for both wells was also driven to ensure the mitigation and management the environmental effects and the main elements are:

- Mud drilling: The choice of mud drilling was driven by the desire to reduce as far as possible the geological and technical risks incurred during such medium-depth drilling. Compared to conventional drilling with clear water and/or air, drilling with mud ensured higher borehole stability in the upper section (Molasse) and prevention of potential undesired flow of fluids such as hydrocarbons known to be often present in the Molasse sediments.
- Installation of a Blow-Out Preventer (BOP): The two wells are in sectors of the Geneva Basin where the risk of liquid and gaseous hydrocarbon occurrences within the fractured units and Molasse reservoirs is highly probable. To technically control these potential hydrocarbon occurrences without creating safety and environmental problems on the surface (uncontrolled eruptions), a BOP system was installed.
- Borehole casing: A drilling protocol with continuous casing and cementing was implemented to ensure the safety of the hole and the surrounding environment including protection against the connection of deep aquifers. The installation of a casing is a response to the need to securely form the drilled hole to 1) isolate the borehole from the natural environment; 2) withstand the pressures likely to be encountered during the drilling of the next phase; 3) provide mechanical support for the wellhead components. Cementing allows to 1) anchor the column to the ground; 2) channel the fluids towards the surface; 3) avoid pollution of the shallow groundwater; 4) separate the different producing layers that may contain different fluids at different pressures.

5.1.9.2. Geophysical monitoring results at GEo-01 well

This chapter deals with the activities carried out in the framework of ***Task 5.1: Monitoring plan demonstrations and case studies*** of the European proposal and which results are presented in ***Deliverable 5.2 Report on analyses of gathered data of demonstration sites and show cases.***

This study was carried out to assess the potential of combine application of GPS, InSAR and inclinometers to:

- Monitor the baseline deformation near and at the Geo-01 Satigny borehole before the production tests and its evolution during and after the tests
- Measure the troposphere state in the area using GPS
- Constrain surface deformation parameters and compare them to Thermo-Mechanic reservoir response stimulation as performed in Task 6.6

The Satigny site is one of the best-equipped in the world. Because of the colocation (<1km) of one broadband seismometer, 2 permanent GPS and 2 inclinometers, plus the monitoring of the water parameters coming out of the borehole it allows innovative investigation impossible elsewhere.

The monitoring strategy is composed of three layers: GPS/InSAR, seismometer/inclinometers and water quality. These three layers allows to monitor vibrations (seismometer and inclinometers), long-term motions and tilts (GPS, InSAR and inclinometers) and at last atmospheric contributions (InSAR and GPS). Available space allowed temporary deployment of additional instruments (gravimeter of U of Neuchatel) for short periods.

5.1.9.2.1. Results

5.1.9.2.1.1. GPS time-series

All data were collected at 15s and then subsampled for processing at 30 seconds. The GPS data processing was defined following guidelines as defined in (Houlié and Romanowicz 2011; Houlié et al. 2018). The solutions obtained during previous research projects were compared to current solutions to assess the quality of the data. The processing was including existing positions in the ITRF 2008 (International Terrestrial Reference Frame; Altamimi et al. (2012)). We show Figure 79 the permanent GPS sites which were available for processing in the area. Some of them are part of the ITRF2008 such as ZIMM, ZIM2 and BSCN (Besancon, France).

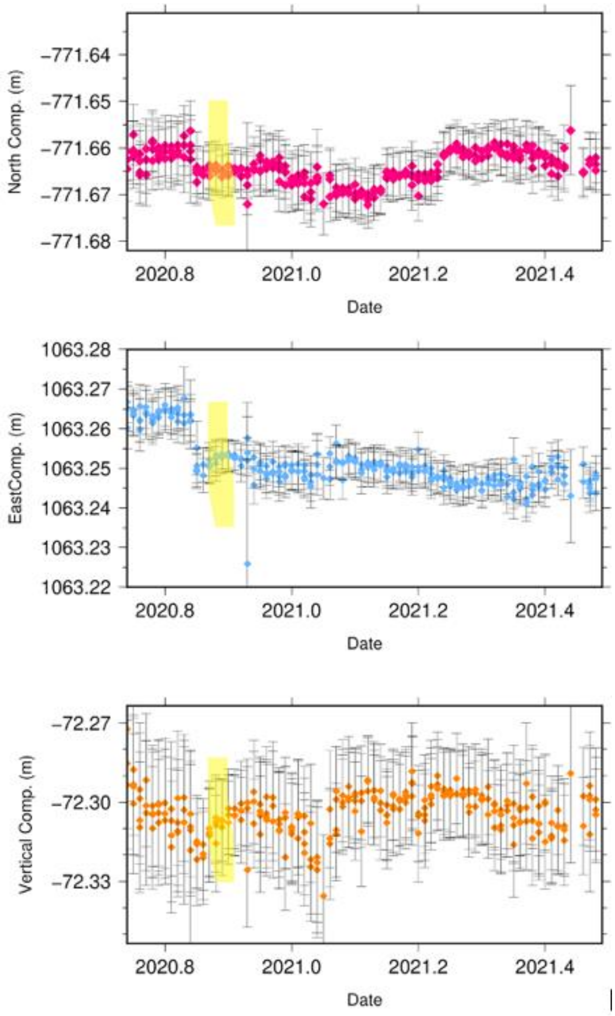

Figure 79 - SAT1-SAT2 baseline components from mid-2020 to mid-2021. Components are computed using the formula SAT2-SAT1. We show the start of the productions tests by using a yellow rectangle. The time-series presented here are used to constrain the Young modulus of the reservoir

We show in Figure 3 the baseline parameters between the sites SAT2 (Geo-01), and the site located at the SAT1 (located in the wine country close to the locality of Choully. Those show that since December 2020 no motion could be detected using data collected GPS located at SAT1 and SAT1 over the production testing period. It suggests no deformation has been occurring during the production phase.

5.1.9.2.1.2. Sentinel1 (InSAR)

Nicolas Houlie Geology GmbH processed > 360 interferograms covering the period May 2020 to May 2021. All data used are Copernicus Sentinel data [2020, 2021]. Retrieved from ESA [06 06 2021], processed by ESA. All data were processed using GMT/GMTSAR tool Suite. Data are visualized using the software QGIS (QGIS Development Team 2009). The coverage obtained from the processing is good with a very good coverage of the Satigny.

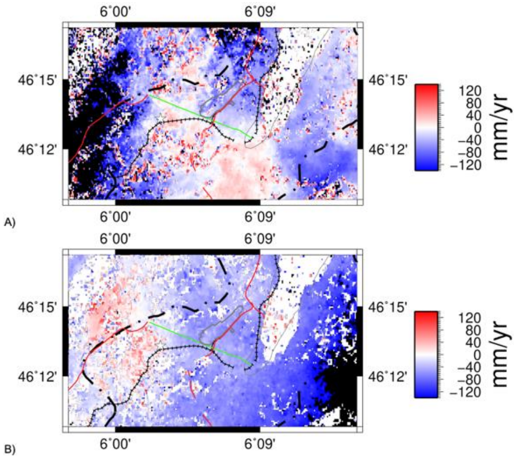

Figure 80 - Average surface motion (mm/yr) between A) December 2020 and Jan 2021 and B) October 2020 in the surrounding of the GEO-1 site (white star). For the purpose of location , we locate main train lines with faulted black lines, highways using red lines. The Route de Meyrin is shown as a green line, the footprint of the airport in grey.

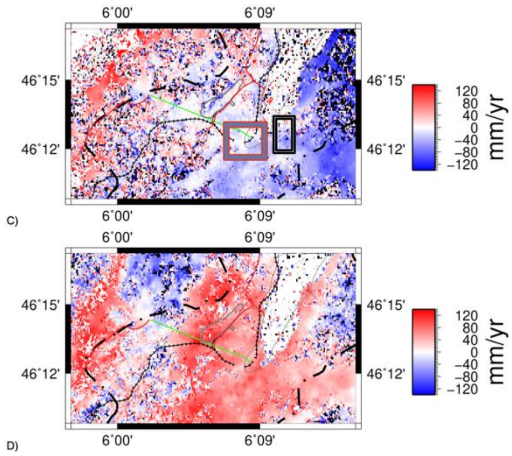

Figure 81 - continued, C) April 2021 and D) March 2021 in the surrounding of the GEO-1 site (white star). For the purpose of location , we locate main train lines with faulted black lines, highways using red lines. The Route de Meyrin is shown as a green line, the footprint of the airport in grey.

As expected, atmospheric noise is contributing to most of the signal for interferometers made in for Geneva area. This is not problematic as local features can still be constrained through the analysis of the motion horizontal gradient (Figure 7). Some geological features are visible on some images (Figure 8), mostly for images covering wet-dry transition periods. For instance, the motion along the shoreline of the Geneva Lake (blue square) and near the Golf (white square). In 2021, we can note for the future that the period was quite humid in Switzerland; drought effects may appear in the coming months. Troposphere corrections may be necessary to improve the image quality.

5.1.9.2.2. Natural Micro-seismicity in the Geneva Basin

The Geneva area is located in a rather seismically quiet region, despite the proximity to the tectonically active western Alpine front. However, the knowledge of the occurrence and distribution of micro-seismic event is poorly constrained.

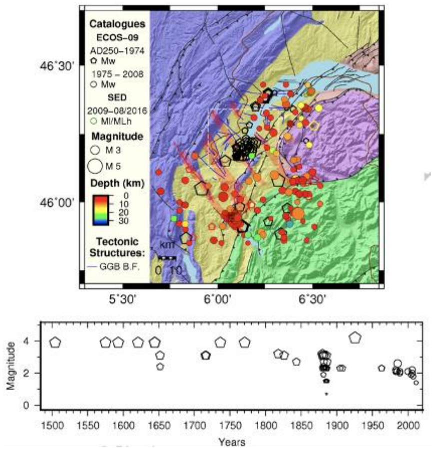

Figure 82 - Seismicity map for the GGB area with information about the background seismicity according to literature data (Antunes et al. 2020)

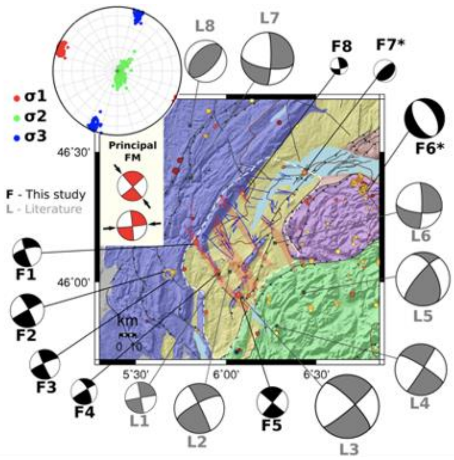

Figure 83 - Geological and tectonic map with the relocated events, their magnitudes ML, and retrieved focal mechanisms (Antunes et al. 2020)

The University of Geneva has implemented (from September 216 to January 2018) a temporary seismic network to densify the existing seismic monitoring network and to improve the identification on micro-events (Antunes et al. 2020). The 17 months of seismic data show a low seismic rate for the GGB, with 17 detected events counting a total of 12 earthquakes per year. No events were identified in the canton of Geneva, where the geothermal activities will take place (Figure 82 and Figure 83).

As part of the GEOBEST-CH research project, the Swiss Seismological Service (SED) at ETH Zurich is using seven additional measuring stations to monitor the Geneva Basin, the area on which the GEothermie 2020 project is focusing. One aim of this monitoring is to improve knowledge about natural, local seismicity. But it should also help to detect earthquakes quickly and accurately, and to clarify whether they are associated with the geothermal project or are instead of natural origin (Figure 84).

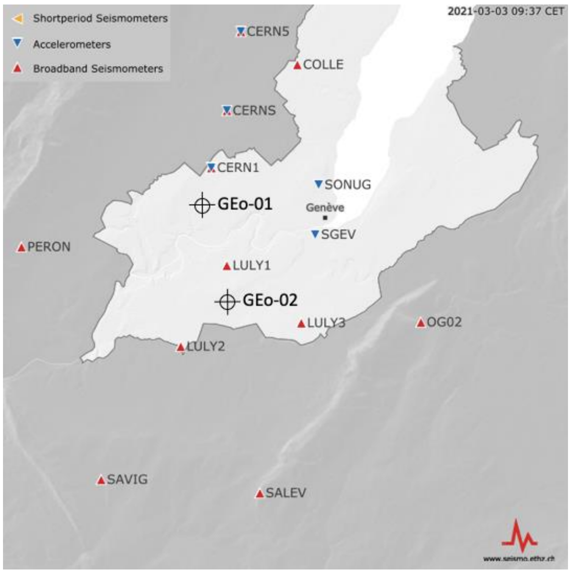

Figure 84 - Seismicity monitoring network in the Geneva basin (mod from http://www.seismo.ethz.ch/)

5.1.9.3. Assessing geochemical issues expected during High Temperature Aquifer Thermal Energy Storage (HT-ATES) in the Mesozoic limestones of the Geneva Basin

As part of D6.6 of the European project available fluid-mineral simulations and laboratory experiments have been performed by UniBe with the goal to predict potential effects associated with HT-ATES operations in Mesozoic carbonates.

This chapter briefly describes the main outcomes of the study which are available in Appendix07

The composition of the major ions of groundwater produced or pumped from GEo-1 and GE0-2 is listed in Table 20.

Table 20 - Chemical composition of groundwater samples produced or pumped from GEO-1 and GEO-2

Well	Unit	GEO-01	GEO-02	GEO-02
Sampling date		12.12.18	14.07.20	08.07.20
Sampling depth	m	>400 m	880-945	1360-1425
Sampling temperature	°C	32.2	21	20
In-situ reservoir temperature	°C	32.2	38.4	53.4
pH		7.7	8.41	8.22
Oxygen concentration	mg/l	0.1	5.7	1.7
Redox potential	mV	-103	384	395
Sodium (Na^+)	mg/l	32	152	52.5
Potassium (K^+)	mg/l	2.2	6.92	5.35
Calcium (Ca^{2+})	mg/l	27	16.0	35
Magnesium (Mg^{2+})	mg/l	14.0	8.0	14.2
Ammonium (NH_4^+)	mg/l	0.18	0.6	0.2
Bicarbonate (HCO_3^-)	mg/l	192	325	179
Chloride (Cl^-)	mg/l	10	31.2	15
Sulfate (SO_4^{2-})	mg/l	19	5.1	32.8
Nitrate (NO_3^-)	mg/l	< 0.2	< 0.1	< 0.1
Sulfide total (HS^-, S^{2-})	mg/l	21.7	not measured	not measured
Iron (Fe^{2+})	mg/l	< 0.02	< 0.01	< 0.01
Water type (simplified)		Na>Ca-HCO_3	Na>Ca-HCO_3	Na>Ca-HCO_3
Saturation index calcite		0.34	0.57	0.45
Saturation index dolomite		0.81	1.14	1.85
Log(P_{CO2}) at reservoir *T*		-2.25	-2.00	-1.85

When hot water is injected into an aquifer, it will interact with the minerals present. The most important reactions in an HT-ATES reservoir are mineral dissolution and precipitation as they change the fluid composition and can lead to an (undesired) redistribution of porosity and fluid flow pathways inside the reservoir. In the carbonate reservoirs of the Geneva basin, the following reactions are most likely to occur:

- Dissolution/precipitation of carbonates
- Dissolution of silicate minerals

Generally, formation water is used as the working fluid in the operation of a HT-ATES site. The water is therefore saturated with respect to the minerals present in the reservoir under in-situ physico-chemical conditions. Upon extraction from the formation and heating in the heat exchanger, the water becomes undersaturated with respect to minerals with a normal (prograde) solubility, such as most silicates. Thus, upon reinjection, the hot water can dissolve any silicate minerals in the reservoir until saturation with respect to that mineral is reached. Mineral such as carbonates, on the other hand, become supersaturated during heating due to their retrograde solubility. Depending on the precipitation rates of the carbonate minerals and on the injection rates, the fluid can either be injected in a supersaturated or saturated state. If precipitation rates are low and no/little precipitation takes place in the surface installations, the fluid is still supersaturated upon entering the reservoir, and carbonates might precipitate close to the wells until the fluid is saturated with respect to these minerals. If precipitation in the surface installations is rapid (= mineral scaling), the fluid is already saturated when injected. In either case, carbonates may dissolve at some distance away from the borehole as the water cools when moving further into the reservoir, becoming undersaturated again.

To evaluate which of these possible mineral reactions are likely to occur in the target reservoir of the Geneva heat storage system, we conducted so called “batch experiments”. In these experiments, we mix rock fragments with an artificial pore water (APW) and heat them to different temperatures. Fluid samples are taken at different time intervals to evaluate the changing fluid composition as a function of time. By attempting to replicate the observed trends using different mineral reactions in a kinetic model, reactions (un)likely to occur can subsequently be identified.

5.1.9.3.1. Batch Experiments

The batch experiments were designed to replicate the rock-water interaction occurring in the target reservoir during heat storage (Figure 85). This replication was done by mixing rock fragments representative of the potential reservoir with an artificial porewater based on groundwater in the region. The two components were allowed to react over 13 days at three different temperatures. The vessels were sampled at specific time intervals throughout the experiment allowing changes in fluid composition to be monitored as a function of time. The mineral reactions taking place were identified by comparing the composition of the solution before and after the experiments.

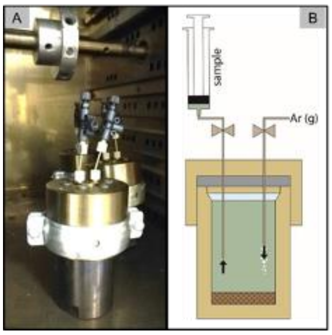

Figure 85 - Experimental set-up of batch experiments: Ti-vessel with holder inside rotisserie oven (A). One of the disks to which the samples are attached can be seen in the background above the vessels. The inside of the vessels and the sampling set-up (Ar on one side and syringe on the other) is shown schematically (B). The same conditions are established in all vessels, and they are opened at different times to establish a time series.

After 13 days, we see significant increases of silicon, potassium, aluminum, and magnesium (Si, K, Al, and Mg) ions in solution along with a decrease in Calcium (Ca) (Figure 86) at all temperatures. Changes in sodium, chloride, and sulphate (Na, Cl and SO4) concentrations all occur within the analytical errors, meaning no significant change in concentration of these ions occurred.

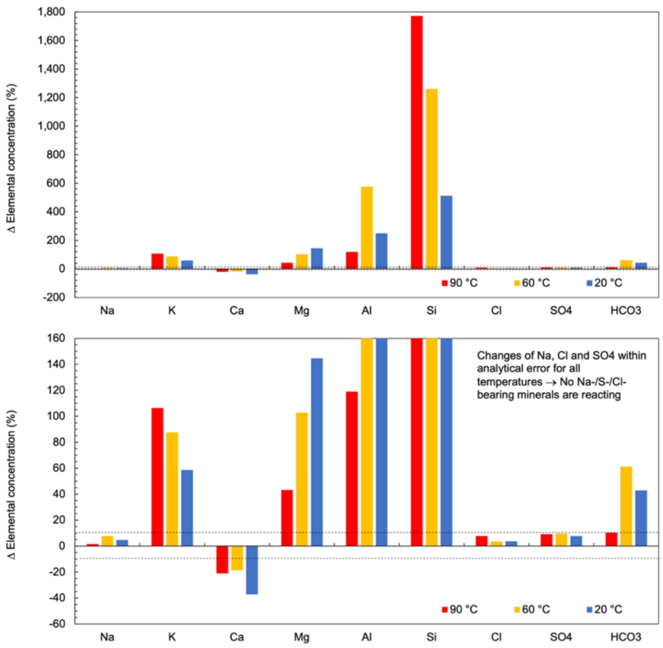

Figure 86 - Net loss/gain of major solutes (in mol%) in the pore water after the duration of the batch experiments (13 days) at 20, 60 and 90 °C. A decrease is indicative of precipitation of a phase containing that solute; an increase is indicative of dissolution. The dotted horizontal lines show the uncertainties in the original solute concentrations. Both panels show the same data but different x-axes.

5.1.9.3.2. Kinetic modelling

Based on the solution compositions and considerations of saturation states, several mineral reactions have been identified so far. In order to check these interpretations (carbonate minerals) and narrow down potential mineral reaction further (silicates), kinetic models were run to replicate the concentration trends observed in the 20 and 90°C experiments.

5.1.9.3.3. Corrosion and scaling in the GEo-01 well during shut-in

Indications from previous sampling campaigns at the GEo-01 well suggest similar processes. In 2019, it was observed that the water produced from the geothermal GEo-01 well contained a black-colored suspended particle load after the well had been shut in for several weeks prior to production (Figure 87). A preliminary study suggested that the color is due to pyrite that precipitated during the corrosion of the steel casing (Güntert, 2020). To test this hypothesis and to elucidate the governing processes driving corrosion, we have carried out a time dependent sampling of both the produced water and the suspended load in June 2020 after the well had been closed for more than 3 months due to Covid-19 restrictions

Figure 87 - Wellhead of GEo-1 producing thermal water containing a black-colored suspended load.

The chemical and Sulphur isotope composition of the thermal water sampled from GEo-1 as a function of time is shown in Figure 88

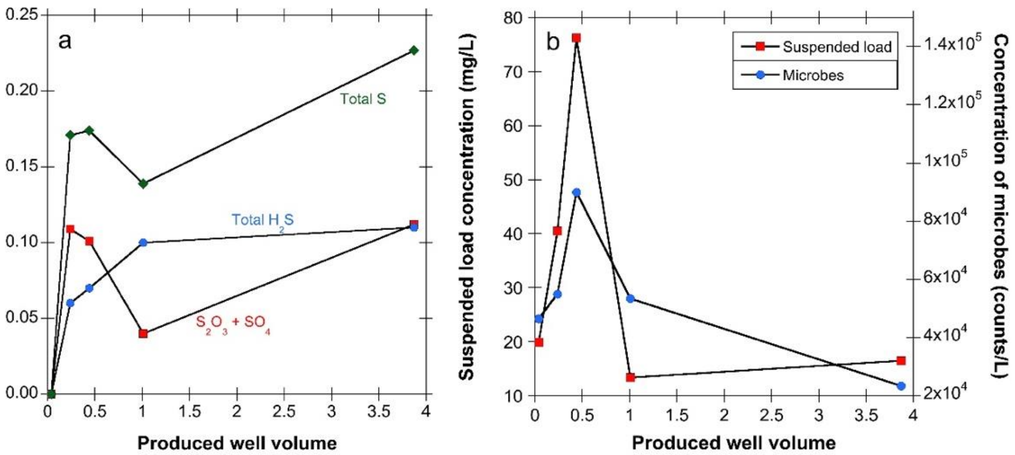

Figure 88 - Concentrations of (a) dissolved Sulphur species and (b) the suspended particle load as well as microbes as a function of the produced well volume (1 volume = 73500 L). Note that the produced well volume is a proxy of the location of the corresponding water samples along the depth of the GEo-01 well and in the nearby reservoir. In other words, produced well volumes smaller than one refer to water samples taken within the well, whereas produced well volumes greater than one refer to samples originating from the adjacent aquifer.

5.1.9.3.4. Microbial analyses

The concentration of microbes in the thermal water was greatest for the sample taken after producing for 0.44 well volumes (Figure 88b), which was also the sample showing the highest suspended load concentration. The sequencing data further demonstrates that the microbial community changed with production time. For the four samples taken during the production of the first well volume (Geo-01-1, Geo-01-2, Geo-01-3, Geo-01-4), Methanobacteria formed an important microbial class while it only appeared in trace amounts in the sample collected after 3.9 well volumes.

5.1.9.3.5. Discussions

The strong variations of the concentration and isotopic composition of oxidized and reduced Sulphur species demonstrate that the Sulphur system is highly reactive in the GEo-1 well. Based on the identification of pyrite in the suspended load samples, the generally increasing total Sulphur concentration with increasing production time, the short-term maximum of oxidized Sulphur species, and the minimum Ca and HCO_3 concentrations observed in the water samples taken after producing for 2 minutes only, the following processes are interpreted to have taken place in the well:

- Corrosion of the steel casing and precipitation of pyrite
- Reduction of sulphate to sulphide
- Oxidation of sulphide to sulphate
- Precipitation of calcite

The identification of both Sulphur and iron metabolizing microbes in the produced thermal water confirms the strong reactivity of the Sulphur system and demonstrates that it was mediated by microbial activity.

Based on the results of this study, the following effects have been identified for the use of these waters for HT-ATES:

- Owing to their retrograde solubility (i.e., decreasing solubility with increasing temperature), carbonates such as calcite will likely precipitate when the waters are heated to 90°C during storage cycles. This could impede flow and heat exchange in the surface installations.
- In case of the water produced from GEo-01, corrosion of technical installations such as pumps, casings, and heat exchangers may occur due to the high sulphide concentration. This could lead to material failure and operational problems.

In addition to minerals precipitating from the reservoir water, mineral reactions will also take place in the reservoir formation during HT-ATES. These reactions were investigated in batch experiments, where fragments of dolomite (81 wt.% dol, 18 wt.% cc, 1 wt.% qtz) from the Calcaire de Tabalcon were reacted with an artificial porewater modelled after the composition of the reservoir water sampled from GEo-02. The experiments were conducted at 20 degrees and 90 °C over two weeks, taking solution samples as a function of time.

The following mineral reaction have been identified:

- The increase in Mg is the result of dolomite dissolution.
- The dissolution of dolomite also releases Ca.
- The Ca concentration decreases, suggesting that additional calcite must form. Calcite is more soluble at lower temperatures, explaining the smaller decrease at 90 °C compared to 20 °C.
- Increase in Si and K suggest that one or several minerals not identified by XRD are present and dissolving. Likely candidates are illites, smectites or mixed-layer I/S.

5.1.9.4. CO_2 intensity for the Geneva case study

The CO2 intensity has been assessed based on HT-ATES performance by combining dynamic reservoir simulations on synthetic models' representative of the average Geneva subsurface conditions, and energy system inputs (Daniillidis et al. 2021 submitted) for a 15-year operation.

The operational CO2 emissions balance is analysed based on current electricity CO2 intensity data. The avoided CO2 emissions include the operation of the system and do not consider the installation of the wells and other equipment required for the functioning of the ATES system. The operational CO2 intensity of the HT-ATES system is given by:

$$HTATES_{CO_2} = \sum_{t=0}^{n} HTATES_{E_{el}} C_{el} - \sum_{t=0}^{n} HTATES_{E_{th}} C_{gas}$$

Where:

- $HTATES_{Eel}$ is the energy (MWh) required by the HT-ATES system for operation of both pumps and heat pumps,
- C_{el} is the CO_2 intensity of the electricity mix,
- $HTATES_{Eth}$ is the heating energy (MWh) provided by the HT-ATES system and
- C_{gas} is the CO_2 intensity of gas heat provided to the DH network that the HT-ATES system is replacing. The latest national Swiss database for CO_2 intensity per source is used as a reference according to (KBOB, 2016)

Table 21 - CO2 intensity values used

Electricity intensity scenario	CO_2 intensity
Electricity High (CHP biogas)	0.177 kg CO_2 eq/kWh
Electricity Mean (CH mix)	0.102 kg CO_2 eq/kWh
Electricity Low (geothermal CHP)	0.031 kg CO_2 eq/kWh
Gas heat (provided by DH)	0.3140 kg CO_2 eq/kWh

The HT-ATES systems that were simulated include a set of 1152 scenarios that were computed combining a complex combination of subsurface and surface constraints ()Table 22.

Table 22 – Constraints for CO2 intensity simulations

Parameter	Value	Units
Aquifer thickness	50, 100, 150	m
Aquifer permeability	1×10^{-14}, 5×10^{-14}, 1×10^{-13}	m^2
Aquifer porosity	10, 20	%
Well pattern	Doublet, 5-spot	-
Cut-off temperature	20, 50	℃
Aquifer depth	500, 1000	m
Aquifer dip	0, 15	°
Aq. groundwater velocity	0, 2	m/y
Artesian conditions	0, 1	MPa

Results show that with a cut-off temperature of 50 ℃ the HT-ATES is strongly affected by the depth, with values staying below 3% for a 500 m depth aquifer and at least 4% for an aquifer depth of 1000 m (Figure 49). For a cut-off temperature of 20 ℃ the depth difference does not affect the ATES share as drastically, but the amount of avoided CO2 emissions increases strongly with deeper systems and almost doubles for the systems with a transmissivity of 1.5 ×10-11 m3 and artesian conditions (Figure 49). In this case the avoided emissions are more than 1 billion kg of CO2 equivalent when the high profile is used for the electricity grid CO2 intensity.

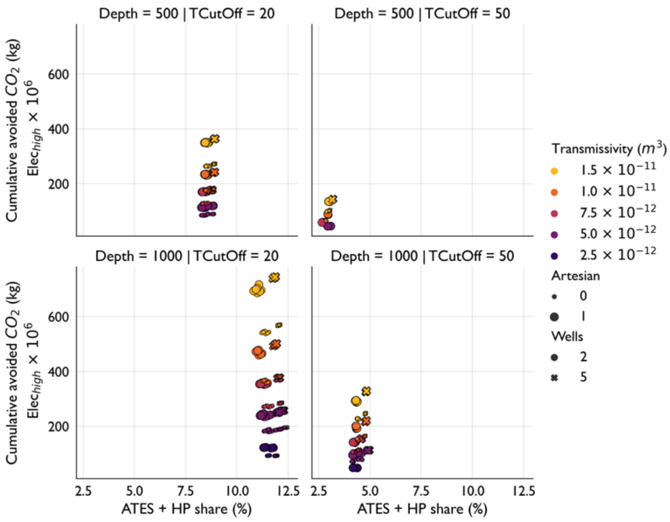

Figure 89 - ATES share and cumulative avoided CO_2 emissions for the simulations with an LCOH below 200 CHF/MWh.

An increase of the avoided CO2 emissions with higher efficiency is evident (Figure 90a). With increasing efficiency, the range of the avoided CO2 emissions increases. Above an efficiency of circa 50% the range of avoided CO2 emissions expands substantially. The aquifer depth, the presence of artesian conditions and the CO2 intensity of the electricity grid define the final level of avoided CO2 kg. The cumulative histogram shows an increasing separation between the avoided CO2 emissions as more CO2 is avoided that depend on the CO2 intensity of the electricity grid increases (Figure 90b).

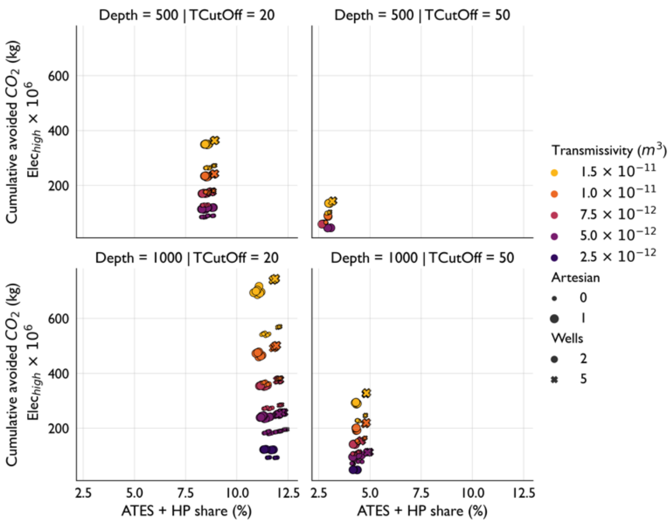

Figure 90 - Cumulative avoided CO2 emissions over 15 years of operation as a function of energy efficiency (a) and cumulative histogram of the avoided CO2 emissions over 15 years of operation (b).

5.1.9.5. Fast-Track Risk assessment

According to the results of the evaluation of the different effects associated with the drilling activities and production operations a fast-track assessment of the risk linked to the different components in presented in Table 23 (full report available in Appendix11).

Table 23 - Fast-track risk assessment for the Geneva case studies

GEo-01												
Phase / Effect	Drilling						Operations (predicted)					
	P	A	M	Probability	Consequences	Risk	P	A	M	Probability	Consequences	Risk
Air quality				H	L	M				L	L	L
Noise and vibration				H	L	M				M	L	L
Formation water quality				L	L	L				H	M	H
Formation water temperature										H	L	M
Surface clear water				H	L	M				L	L	L
Soil occupation				H	L	M				H	L	M
Wastes and dangerous substances				H	L	M				M	L	L
Environment				M	L	L				L	L	L
Nature				M	L	L				L	L	L
Soil mechanics										L	L	L
Seismicity				L	H	M				L	H	M
CO2 intensity redyction										H	M	H

GEo-02												
Phase / Effect	Drilling						Operations (predicted)					
	P	A	M	Probability	Consequences	Risk	P	A	M	Probability	Consequences	Risk
Air quality				H	L	M				L	L	L
Noise and vibration				H	L	M				M	L	L
Formation water quality				L	L	L				H	M	H
Formation water temperature										H	L	M
Surface clear water				H	L	M				L	L	L
Soil occupation				H	L	M				H	L	M
Wastes and dangerous substances				H	L	M				M	L	L
Environment				M	L	L				L	L	L
Nature				M	L	L				L	L	L
Soil mechanics										L	L	M
Seismicity				L	H	M				L	H	M
CO2 intensity redyction										H	M	H

5.1.10 Thermo-hydro-mechanical-economic (THM$) analytical framework

In order to assess the impact of the subsurface parameters to the economics of an HT-ATES operating systems ETHZ developed a novel general thermo-hydro-mechanical-economic (THM$) analytical framework to balance three reservoir-engineering and economic constraints for an HT-ATES doublet connected to a district heating network. The results have been published in Birdsell, et al. 2021.

They find the optimal well spacing and flow rate are defined by the ''reservoir constraints'' at shallow depth and low permeability and are defined by the ''economic constraints'' at great depth and high permeability. The optimal well spacing is 1.8 times the thermal radius and eventually the results showed that the levelized cost of heat is minimized at an intermediate depth. The minimum economically viable transmissivity (MEVT) is the transmissivity below which HT-ATES is sure to be economically unattractive. The MEVT is relatively insensitive to depth, reservoir thickness, and faulting regime. Therefore, it can be approximated as $5 \cdot 10^{-13}$ m^3. The MEVT is useful for HT-ATES pre-assessment and can facilitate global estimates of HT-ATES potential.

The methodology considers a generic HT-ATES doublet (Figure 91). The conceptual model includes four stages: (a) heat injection, (b) storing, (c) heat extraction, and (d) resting, which each last one quarter of a year and correspond roughly to summer, fall, winter, and spring, respectively. No water is injected or extracted through the wells in the storing or resting stages.

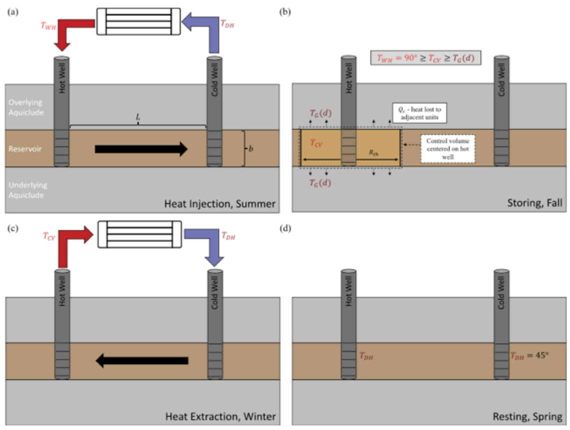

Figure 91 - Conceptual model of a HT-ATES doublet for (a) heat injection, (b) storing, (c) heat extraction, and (d) resting stages. Bold arrows indicate the direction of flow, when

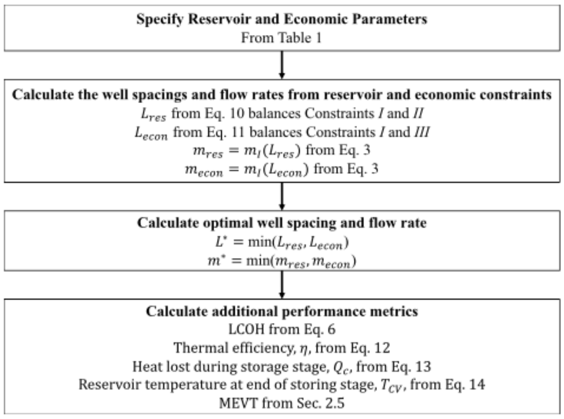

Figure 92 - Block diagram for the THM$ calculations.

Figure 92 shows a block-diagram overview of the THM$ calculations. First, all the reservoir and economic parameters must be specified. Second, the well spacing and flow rate are calculated in two ways: (a) from the reservoir constraints and (b) from the economic constraints. Third, the optimal well spacing and flow rate are calculated as the minimum of the two well spacing and flow rate values, respectively. Finally, additional performance metrics such as the LCOH, thermal efficiency, heat loss, reservoir temperature, and MEVT are calculated.

The study analyses and balance three constraints that apply to HT-ATES systems:

- Constraint I define a maximum flow rate so that the reservoir's thermal capacity is not over-utilized.
- Constraint II defines a maximum flow rate so that the reservoir pressure does not lead to hydraulic fracturing (HF).

- Constraint III defines the flow rate that minimizes the levelized cost of heat (LCOH). It does not make sense to pump at flow rates above the flow rate that minimizes LCOH, so Constraint III defines a ‘‘maximum’’ flow rate in the same way as Constraints I and II.

Using this approach, several practical conclusions can be derived, that are useful for the design and pre-assessment of HT-ATES systems:

- By balancing the three constraints, we find an optimal well spacing and flow rate. The well spacing and flow rate are linked, and they are chosen so that the flow rate is maximized without violating any of the three constraints. The reservoir-constrained regime applies to shallow or low-permeability reservoirs (i.e., Constraints I and II). In contrast, deep or high-permeability reservoirs are dictated by the economic-constrained regime (Constraints I and III). In the reservoir-constrained regime, increased flow rate would HF the reservoir, whereas in the economic-constrained regime, increased flow rate would lead to higher LCOH.
- The optimal well spacing is $1.8R_{th}$, which is at the lower end of the range suggested for LT-ATES. This tight spacing makes intuitive sense because thermal breakthrough at the cold well is probably not as bad for the thermal efficiency of HT-ATES as it is for LT-ATES, since HT-ATES is only used for heating whereas LT-ATES is also used for cooling. Nevertheless, there is room to further explore optimal well spacing with hydro-thermal numerical models.
- The LCOH is minimized at an intermediate depth. This minimum occurs because of trade-offs between the amount of heat recovered and the costs, which increase at different rates with respect to depth (see Figure 93). At shallow depths, the LCOH is large because the capital costs are high with respect to the low amount of heat recovery. At intermediate depths, the LCOH is low because the heat recovery is large, while the capital costs are moderate, and the operating costs are low. At great depths, the LCOH is large despite a high amount of heat recovery, because the combined capital and operating costs increase at an increasing rate with depth.

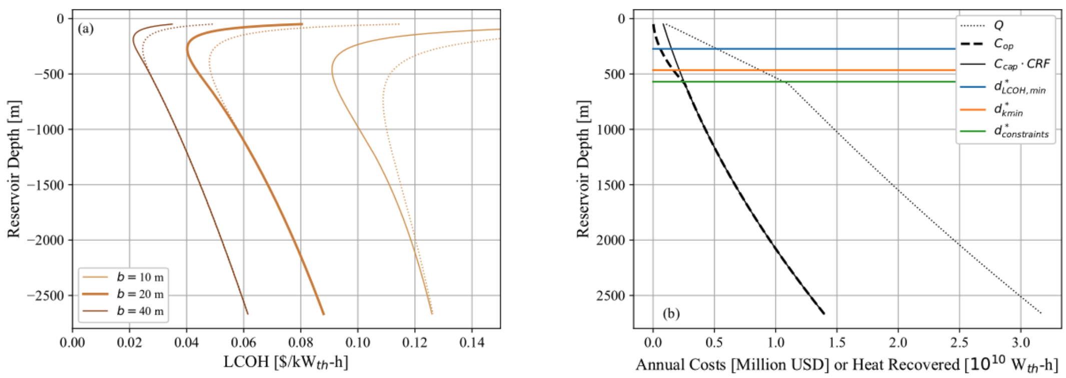

Figure 93 - (a) Depth versus LCOH and (b) depth versus annual operating costs (Cop), equivalent annualized capital costs ($Ccap \cdot CRF$) and annual heat recovery per doublet (Q), for base-case permeability and reservoir thickness. In (a), the base-case scenario is plotted with a bold line, solid lines use $\alpha II = 1$, dotted lines use $\alpha II = 0.8$ to represent an alternative faulting regime, and color shade corresponds to the reservoir thickness. In (b), various measures of optimal depth are also plotted for reference

The LCOH of a system is more sensitive to reservoir transmissivity than depth or faulting regime. We found that the LCOH can vary by orders of magnitude within the range of transmissivities tested (see Figure 94), whereas it varies by a factor of < 2.5 due to depth and ≈1.2 due to the faulting regime (see Figure 93a). The sensitivity of LCOH to transmissivity is considerable because of the wide range (i.e., many orders of magnitude) over which transmissivity varies in nature. Therefore, transmissivity is a key property in determining the economic success of HT-ATES.

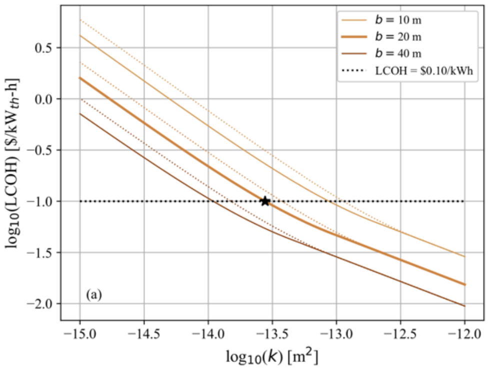

Figure 94 - The logarithm of LCOH as a function of the logarithm of permeability

Some reservoir transmissivities are so small that it becomes impossible to pump meaningful flow rates without HF. For the base-case depth and stress state, the flow rate is limited to ≤ 3.3 kg/s if the transmissivity is ≤ $2 \cdot 10^{-13}$ m^3.

The minimum economically viable transmissivity (MEVT) can be approximated as a single value of $5{\cdot}10^{-13}$ m^3. This approximation is possible because the MEVT is relatively insensitive to depth, reservoir thickness, and faulting regime. The MEVT is perhaps the most useful result of our analysis because it can be used in a pre-assessment at a specific site, or to assess national or global potential for HT-ATES.

5.1.10.1. Techno-economic performance assessment of HT-ATES in Geneva

The demonstrator in Geneva is focused on developing an integrated model that is able to quantify the implementation cost of geothermal heat storage in the existing district heating network and planned projected extension by 2035. This will allow the evaluation of alternatives with regards to the business model.

In this study, we combined assessment of subsurface performance and surface District Heating Networks (DHN) configuration to evaluate the scenarios prone to the success of storage solution implementations in a techno-economic performance perspective of the joint system.

Our results show that, subject to subsurface constraints, the nominal capacity ranges from 0.4 MW to 81 MW, with aquifer permeability and thickness being the major control variables. A minimum transmissivity of 2.5 ×10-12 m3 is required to keep the Levelized Cost Of Heat (LCOH) below 200 CHF/MWh and a capacity of 25 MW or higher is needed for the HT-ATES system to become competitive with other large-scale DHN heat sources. The capacity increase from the addition of Heat Pumps (HP) incurs non-recoverable costs and in turn increases the LCOH. Nonetheless, the addition of HP increases the nominal capacity of the system and results in higher cumulative avoided CO2 emissions.

5.1.10.1.1.1. Methods

Based on hourly measurements at Geneva of an existing district-heating network (430 GWh on 2014 - Quiquerez et al., (2017)), dimensionless dynamics of a typical DHN heating demand have been created. We assume that renewable energy capacities cover 20% of maximum hourly heat load, which corresponds to cover about 50% of DHN energy demand. The daily averaged heat load average is depicted in Figure 2a; availability of heat for charging the HT-ATES system covers the period between May and September (Figure 95a). HT-ATES capacity was determined based on results from the simulations and constraints therein, while the DHN capacity was scaled accordingly, ensuring a match of available energy for storage. During HT-ATES simulation available heat for charging was not restricted, therefore charge capacity was only limited by subsurface characteristics. HT-ATES operation cycle was 120 days charging, 60 days rest and 120 days discharging followed by 65.25

days rest (Figure 95b), repeated yearly for 15 years of total simulated time. Representative yearly charging and discharging cycles are shown in normalized values in (Figure 95b).

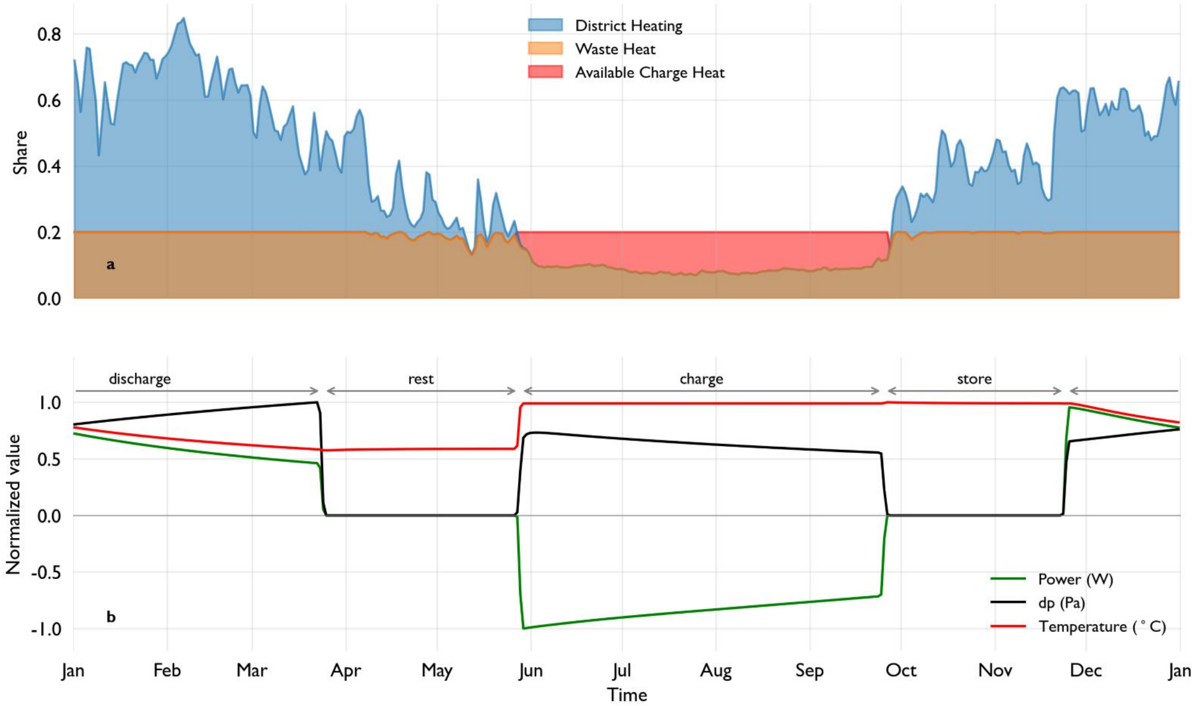

Figure 95 - Daily averages for district heating demand, waste heat and available heat for charging (top) HT-ATES indicative yearly production scheme normalized to unit value (bottom).

Negative power corresponds to charging and positive power to HT-ATES discharging. During discharge, production temperature gradually drops until either the discharge period ends, or the cut-off temperature is reached. Due to this temperature reduction produced fluid density decreases resulting in increasing pressure difference. During charging, if the warm fluid from the hot well affects the cold well, a slight drop in system power can be observed. Data shown for the simulation with aquifer thickness 50 m, aquifer permeability 1×10^{-13}, aquifer porosity of 10%, two wells (doublet), no groundwater velocity, a 15° aquifer dip, a temperature cut-off of 20 ℃ and an aquifer depth of 1000 m. The DHN heat share is lower than 1 due to daily averaging of underlying hourly heat demand data.

5.1.10.1.1.2. Energy demand models

Energy studies were based on Geneva's values for future DHN evolution. Geo-referred final energy consumption for heating is available at building level in a public database. Based on this geospatial information, the public-owned energy provider (SIG) planned future facilities and associated production to answer increasing grid heat demand and ensure a minimum share of renewables (~ 80%). An hourly input-output model inspired from EnergyPLAN was used to design heat power capacity of different plants and evaluate annual heating network production mix. A production merit-order has been chosen based on direct CO2 emissions and energy consumption, waste heat recovery is used to cover the base load while wood and gas boilers are activated to ensure peak production. High temperature HPs have also been used to increase local renewable resources temperature (geothermal, lake and sewage water). Higher source temperatures received a higher priority since HP's electric consumption is proportional to the difference between source and sink temperatures. HT-ATES was activated after waste heat recovery, before large-scale HP, with HT-ATES energy being directly injected into the DHN while its temperature is higher than the DHN return temperature.

5.1.10.1.1.3. Thermo-Hydrologic Simulations for the Geneva case study

Thermo-hydrologic simulations were carried out using state of the art 3D porous media flow reservoir simulator Nexus-CSMP++. Data used consist of a set of simulation scenarios generated as described in 5.1.7.1 to perform a sensitivity study of a simplified HT-ATES system to a set of pre-established key characteristics (see Table 24). The 1152 scenarios simulated were designed to answer first stage feasibility and design questions related to geology, hydrology, and system operation. Parameters varied include hydro-geologic aquifer properties of thickness, permeability, porosity, depth, dip, artesian conditions, and groundwater hydraulic gradient, as well as the operational ones of well pattern and cut-off temperature. Simulation results are used here as input to a combined economic and CO2 emissions analysis.

Table 24 - Parameters and values used for the reservoir simulations. A factorial design for all parameters is used resulting in 1152 3D reservoir simulations. All simulations use a temperature of 90 ℃ for charging the HT-ATES system and a well spacing of 141m.

Parameter	Value	Units
Aquifer thickness	50, 100, 150	m
Aquifer permeability	$1{\times}10^{-14}$, $5{\times}10^{-14}$, $1{\times}10^{-13}$	m^2
Aquifer porosity	10, 20	%
Well pattern	Doublet, 5-spot	-
Cut-off temperature	20, 50	℃
Aquifer depth	500, 1000	m
Aquifer dip	0, 15	°
Groundwater hydraulic gradient	0, 51.7	%
Artesian conditions	0, 1	MPa

HT-ATES charging was carried out with a temperature of 90 ℃ for all simulations. A value of cut-off temperature was used for two main purposes: a) to calculate exergy values and thus measure the usefulness of energy charged and discharged, b) to trigger an operational mode change when the ATES was in discharge mode. In the latter situation, the system went into rest mode if the output temperature from the main/hot well dropped below the cut-off temperature. Cut-off temperature values were selected to be aligned with DHN required temperature without (50°C) and with the use of a HP (20°C).

During discharge, two different cold temperatures were simulated, 50°C or 20°C. The 50°C temperature on the cold well represents the direct use of heat. In this case, heat was transferred from the HT-ATES hot well to the DHN by a heat exchanger. For the 20°C temperature simulated heat-pumps were used to increase the energy extracted from the storage. After a direct use of heat, the geothermal water temperature was cooled down by a series of HPs before been re-injected into the aquifer (Figure 96). A similar system is in place since 1994 in Riehen, Switzerland. This assisted heat extraction enabled production of heat at a higher temperature and the extraction of more energy from the aquifer since the temperate difference between the cold and the hot well was increased when compared to a direct use of heat.

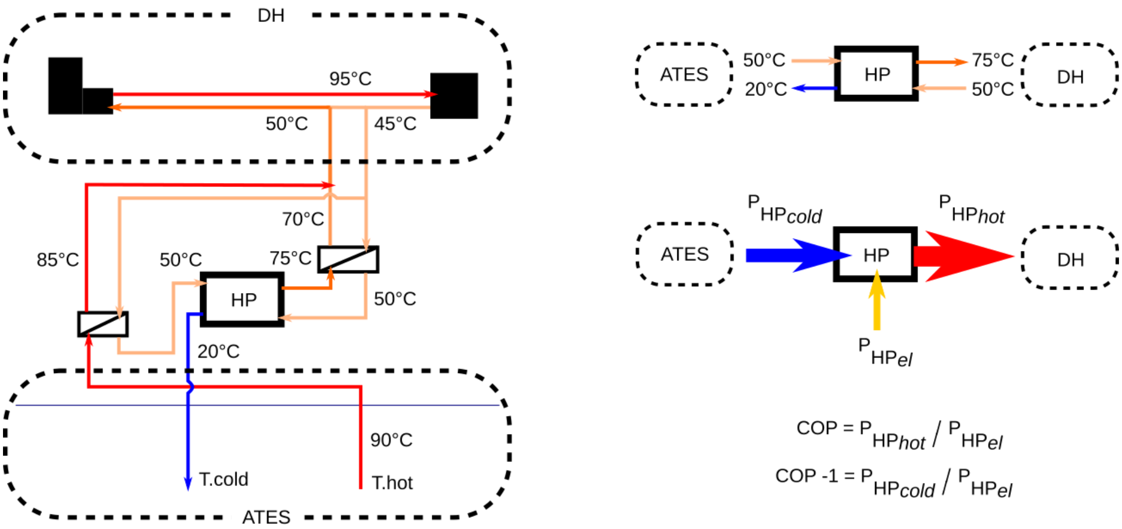

Figure 96 - Schematic representation of the HT-ATES system and the HP integration for the case of 20°C re-injection temperature and the respective energy conversions related to the HP. Notice that to enhance the system efficiency, the HT-ATES and the HP production are injected in the return branches of the DHN.

The HPs were assumed to have a constant COP of 3, even though it is widely known that the COP is dependent on the cold source temperature. This simplification was done because i) after the direct use of the heat, the inlet temperature in the heat pump is limited to the range 50°C to 20°C; ii) the amount of energy extract by the HP from the ATES is independent from COP assumptions (see below); and because iii) this relatively low COP can be seen as a worst-case scenario for electric consumption., a COP of 6 would reduce the HP electricity consumption of HPs by 60%.

Drilling costs were computed with the use of an analytical formula based on the drilling cost per depth provided of the Netherlands, adjusted to fit the few data points for drilling costs available for Switzerland. Operation Expenditures and Levelized cost of Heat (LCOH) were eventually also considered in the full analysis. Inputs used for the economic assessment are summarized in

Table 25.

Table 25 - Inputs used for the economic analysis

Parameter	Value	Unit	Reference
Facilities costs	10	% of drilling costs	
Electricity price	120	CHF/MWh	[50]
Waste heat price	35	CHF/MWh	[51]
Discount rate	5	%	
OpEx % CapEx	3	%/y	[50]
Drilling costs	Eq. 7	CHF	Modified after TNO ThermoGIS (2019)
Pump cost	500	kCHF	
Pump replacement	5	years	
Discharge cycle pump efficiency	40	%	
Charge cycle pump efficiency	50	%	
HP cost	800	kCHF/MW	[52]
HP COP	3	-	

5.1.10.1.1.4. DHN integration for the Geneva case study

The HT-ATES system was modelled without any limitation to the available energy used for charging. Therefore, the DHN that it could contribute to should have at least that amount of energy available for storage. This was introduced via a scaling factor, that scales the DHN network capacity based on the required energy for charging each HT-ATES simulation. For simplicity, we ignored minor, short-term differences (7 days window) at the beginning of the charging cycle between the available heat for charging and the ATES stored energy, that amounted to less than 1.3% of charged energy per cycle. The scaling factor was calculated during the charge period where the DHN power demand is lower than the available waste heat and therefore there is enough energy for charging the storage.

5.1.10.1.1.5. Results

Nominal HT-ATES discharge capacity together with HP spans a range between 0.4 MW to 81 MW and is mostly controlled by aquifer permeability, with higher permeability resulting in significantly higher nominal capacity (Figure 97b). Notably, a low permeability of 1×10^{-14} m^2 results in nominal discharge capacity below 8 MW under all other parameters tested. Higher nominal discharge capacity is reached with thicker aquifers and higher permeability (Figure 97a). Cut-off temperature reduction results in nominal capacity increase since the extractable amount of heat is higher due to the increased temperature difference and HP contribution (Figure 97e). A deeper aquifer increases nominal capacity by raising the pressure threshold for injection, due to the higher lithostatic pressure, and also aquifer temperature (Figure 97f). Artesian conditions of 1 MPa slightly improve on the nominal capacity compared to no artesian conditions by increasing the pressure headroom available for storage (Figure 97iArtesian condition increases for systems with higher nominal capacity. Aquifer porosity, number of wells, aquifer dip and presence of a hydraulic gradient do not impact HT-ATES nominal discharge capacity (Figure 97c, d,g&h respectively).

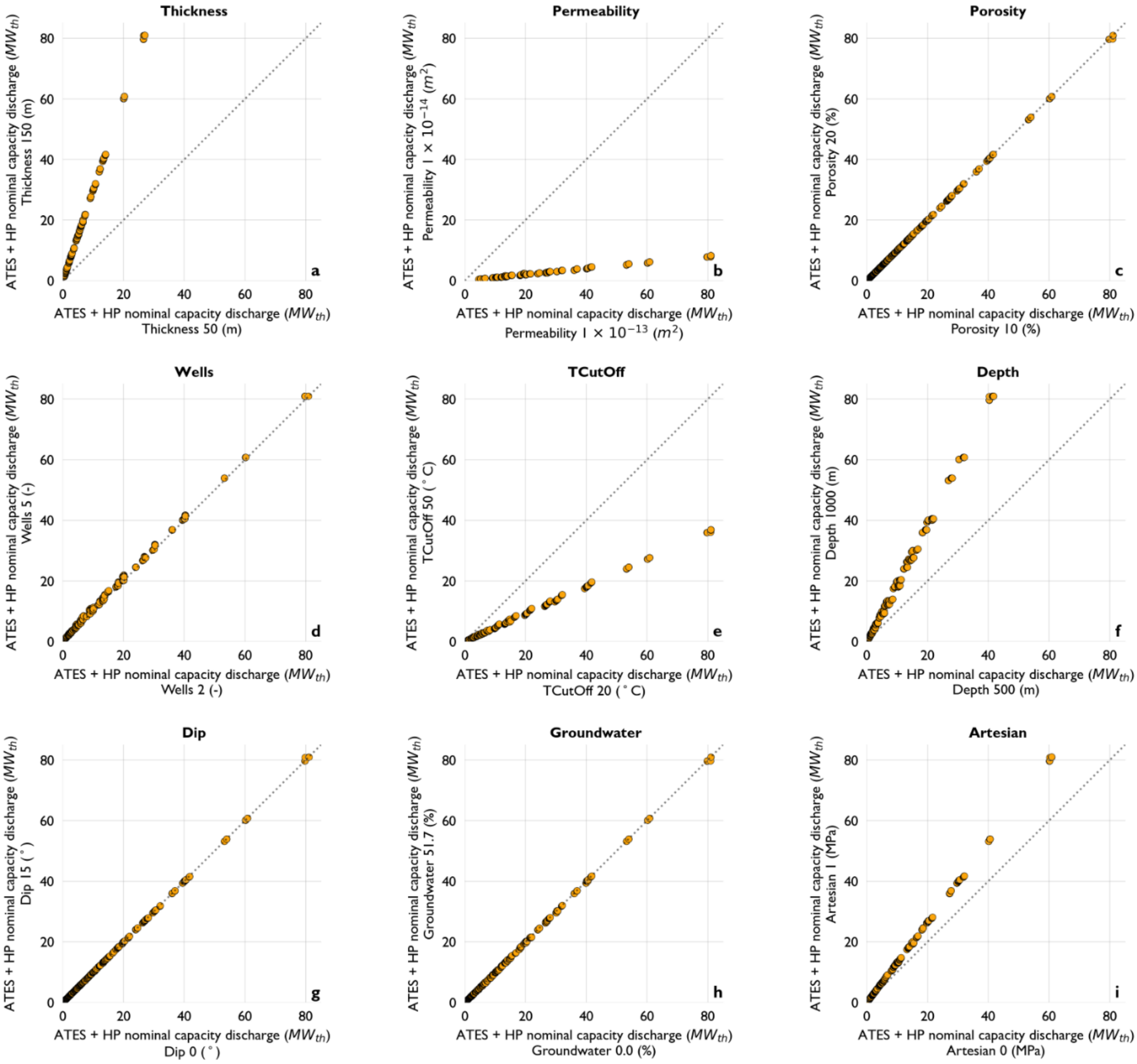

Figure 97 - Parameters affecting nominal discharge capacity of the HT-ATES system. The subplots show the change in nominal discharge capacity for each highest and lowest value of the respective input parameter in the title, with all other parameters being identical for each point plotted. The dashed line represents an ideal one-to-one ratio between the two values; therefore, points plotted along the dashed line imply that no change is introduced in the metric by altering the parameter value. All inputs show a linear relation in terms of nominal capacity.

5.1.10.1.1.6. Levelized Cost Of Heat assessment

LCOH is primarily affected by aquifer permeability. For a high permeability of 1×10^{-13} m^2 LCOH always remains below circa 600 CHF/MWh, while for low permeability of 1×10^{-14} m^2 LCOH increases beyond 5000 CHF/MWh (Figure 98b). A less thick aquifer results in a significant increase in LCOH, while for an aquifer thickness of 150 m LCOH remains below 2000 CHF/MWh (Figure 98a) regardless of other parameter values. A cut-off temperature of 20 ℃ yields an LCOH that is lower than that of the 50 ℃ (Figure 98e, see also Figure 99) for most simulations. However, this trend is reversed for systems that achieve an LCOH below circa 150 CHF/MWh (Figure 98e inset axes). When conditions are favorable, a cut-off temperature of 50 ℃ result in lower LCOH due to avoiding HP related costs. A deeper aquifer decreases the LCOH but the relation here is not completely linear and two separate trendlines appear (Figure 98f). Additional well costs required in the 5-spot configuration does not offset pumping costs (pumps and operational costs for pumping) and therefore increases the HT-ATES LCOH (Figure 98d).

Artesian conditions reduce the LCOH by increasing the nominal capacity slightly due to higher-pressure threshold as previously discussed (Figure 98i). Groundwater flow due to a hydraulic gradient slightly increases LCOH, by reducing aquifer efficiency in storing and recovering heat (Figure 98h). Aquifer porosity and dip do not affect LCOH (Figure 98c&g respectively).

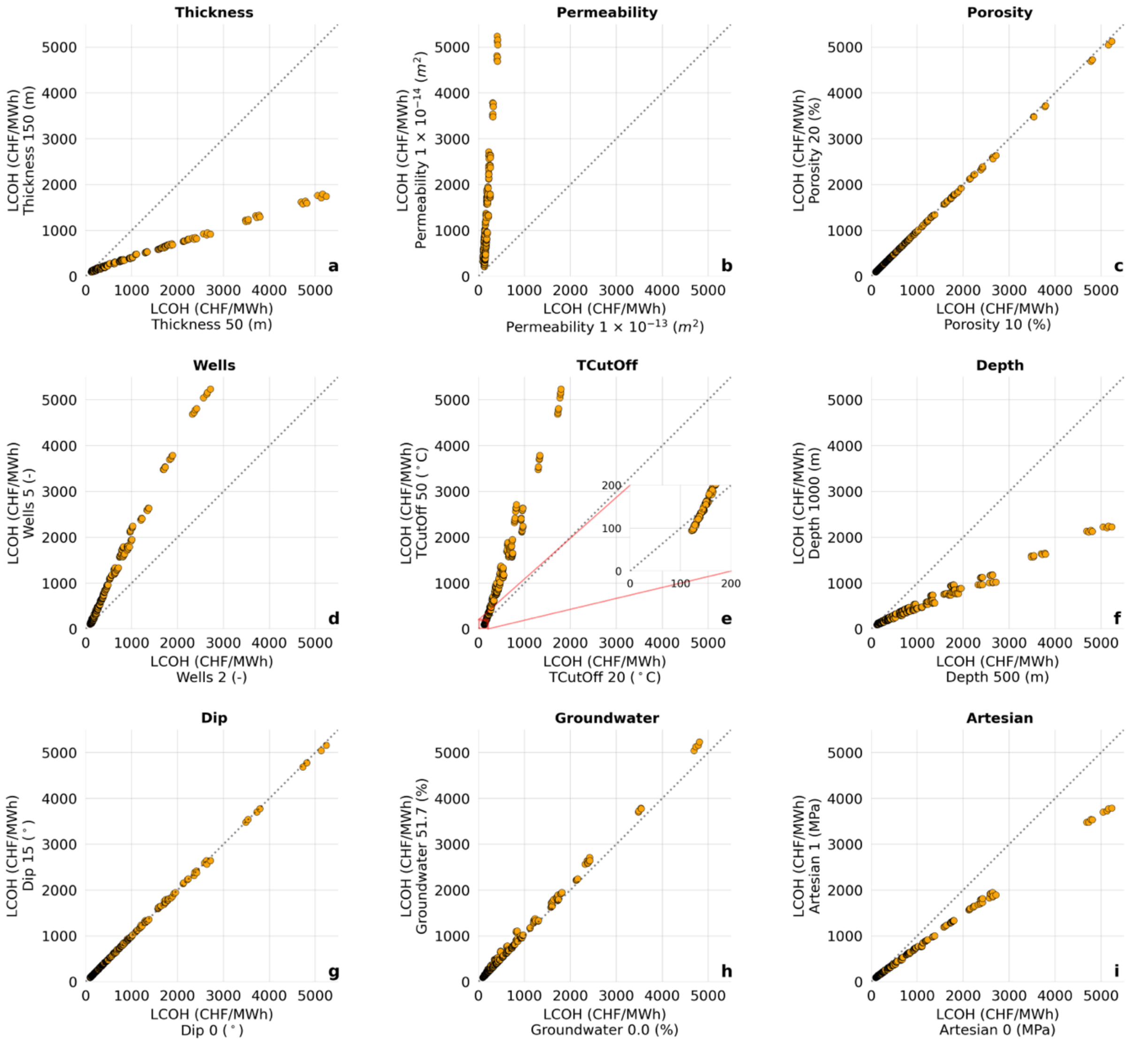

Figure 98 - Parameters affecting the LCOH. The subplots show the change in the LCOH for each highest and lowest value of respective input parameter in the title, with all other parameters being identical for each point plotted. The dashed line represents an ideal one-to-one ratio between the two values; therefore, points plotted along the dashed line imply that no change is introduced in the metric by altering the parameter value.

LCOH as a function of nominal discharge capacity shows an inverse relationship, with higher nominal capacity resulting in lower LCOH (Figure 99a). Notably, many simulations achieve a similar nominal capacity but span a very large range of LCOH for capacities up to circa 5 MW (Figure 99a). LCOH spread is reducing as the nominal capacity increases further and reduces to circa 130 CHF/MWh above a capacity of 40 MW. For simulations that resulted in an LCOH lower than 200 CHF/MWh (Figure 99b), a minimum transmissivity is of 2.5 ×10^{-12} m^3 is required. Additionally, we observe that a cut-off temperature of 20 ℃ reached a lowest LCOH value of circa 120 CHF/MWh for the most favorably transmissivity of 1.5 ×10^{-11} m^3 and a nominal discharge capacity of circa 80 MW (Figure 6b). Comparably, simulations with a cut-off temperature of 50 ℃ and a transmissivity of 1.5 ×10^{-11} m^3

achieve LCOH values as low as circa 90 CHF/MWh, at nominal discharge capacity > 35 MW (Figure 99b).

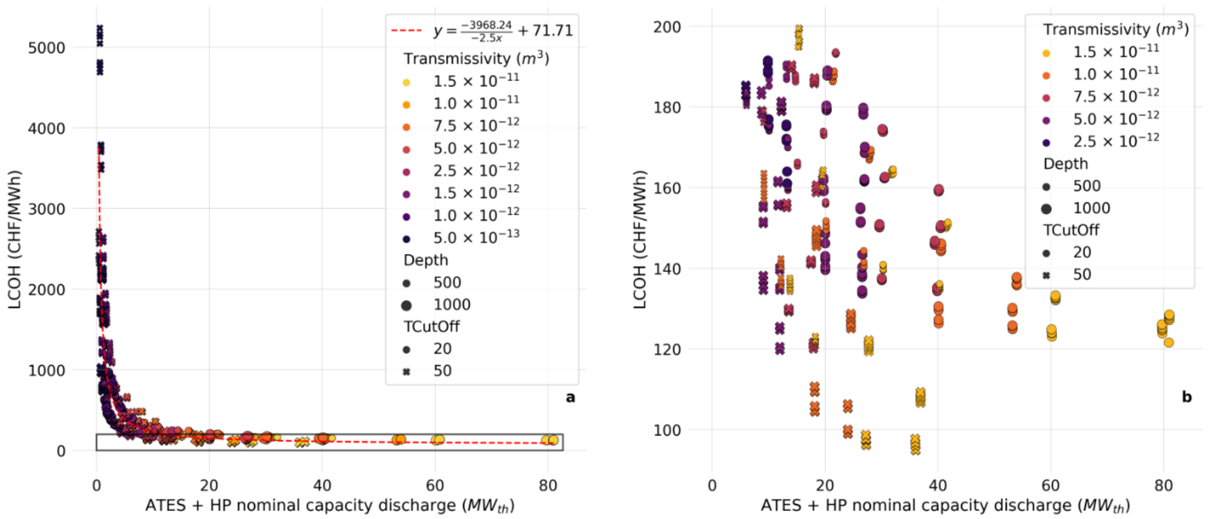

Figure 99 - LCOH against nominal production capacity colored by reservoir transmissivity, sized by depth and marked by temperature cut-off (a). The dashed line in the left-hand figure (a) outlines right-hand side figure extent (b).

With respect to other energy sources for heating, the studied HT-ATES system starts to be comparable when nominal capacity is above circa 10 MW. To become competitive, HT-ATES systems require capacities ≥ 25 MW to achieve a median LCOH below 165 CHF/MWh and requires a transmissivity of at least 7.5 ×10^{-12} m^3 (Figure 99b).

5.1.10.1.1.7. LCOH and HT-ATES efficiency

Energy against exergy efficiency after 15 years of HT-ATES operation shows a linear relationship for the cut-off temperature of 50 ℃ (Figure 100a). A slight deviation from this linear behavior is observed towards better energy efficiencies as the energy efficiency increases and deeper systems are used (Figure 100a). For a cut-off temperature of 20 ℃ higher energy efficiency is achieved compared to exergy efficiency, with deeper systems exhibiting further energy efficiency improvement and values reaching close to 100% (Figure 100a). A large spread in LCOH for similar energy efficiency values is evident for low permeability aquifers (Figure 100b). This spread decreases with increasing permeability. A similar trend is observed with deeper systems that further improve efficiency and reduce LCOH. Therefore, with favorable conditions a correlation is observed between higher efficiency and lower LCOH (Figure 100b).

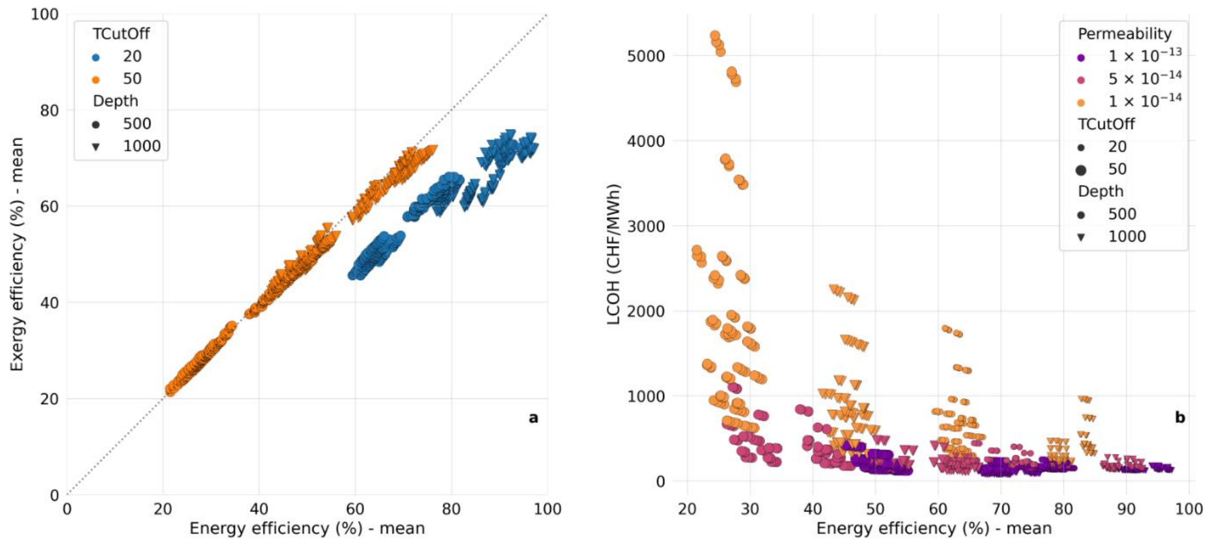

Figure 100 - Mean HT-ATES energy vs exergy efficiency after a 15-year cycle, color coded based on cut-off temperature and marked according to depth (a) and energy efficiency vs LCOH color coded based on permeability, sized according to cut-off temperature, and marked according to depth(b)

5.2 Bern study site

5.2.1 The Energy Hub

“The replacement as an opportunity” - that is what Energie Wasser Bern (EWB) proclaimed when the planning of the Forsthaus location began in 2005.

With the creation of the Energy Hub “Energiezentrale Forsthaus” (EZF), previously separate energy and heat providers were connected. In addition to a waste incineration plant (KVA), a wood-fired thermal power station (HHKW) and a gas and steam combined cycle power station (GuD) were built (Figure 101).

Figure 101 - Energy Hub at Forsthaus Bern

The KVA takes on the task of a reliable permanent supplier, which however, cannot be heavily regulated because it was not built primarily for energy generation.

In order to be able to cover the seasonally changing demand, the HHKW is operated. Since the HHKW also shows a certain inertia and cannot react immediately, the GuD is used for rapid changes in demand and peak loads.

Since March 2019, the EZF has an electrode boiler for even faster response. A concerted operation of these four pillars, grants the continuous and efficient coverage of all energy demands today and in the future.

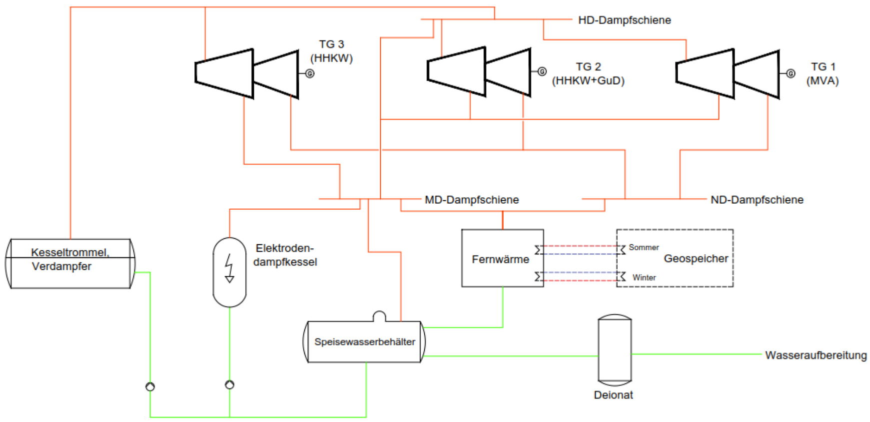

Figure 102 - Simplified process flow diagram for the Forsthaus energy hub

The formation of the Energy Hub with the connected systems also contributes to more redundancy, making EWB even more attractive as a safe and stable supplier of energy and heat. Figure 102 shows a simplified process flow diagram with the most important components of the plant in Bern.

5.2.2 The Challenge

As previously described, it becomes clear that brief fluctuations in energy demand can be easily managed by the Forsthaus energy hub. Due to the continental climate in Switzerland, which is characterized by strong seasonal differences, the demand for (district) heating varies seasonally.

While a significant part of the remaining energy can be used as district and process heat in the cold winter months, only a fraction of the external heat consumers is available in summer. This seasonal problem means that existing systems for heat recovery from residual energy are only economical for half of the year.

This unused energy contradicts the goal of increased efficiency as per the Swiss energy strategy. The lack of demand for heat in summer could be compensated for by storing it in a heat storage. In winter, when the demand for heat exceeds the production of the waste incinerator, the heat from the storage facility could be fed back into the system. This would increase the profitability and thanks to the heat release from the storage, the use of fossil fuels for heat generation would decrease. Heat storage therefore has great potential both ecologically and economically.

5.2.3 Investigating a High Temperature - Aquifer Thermal Energy Storage (HT-ATES)

A possible solution to this problem is the operation of a seasonal Energy Storage facility. Individual layers of rock take on the function of heat storage. In contrast to geothermal probe fields or surface aquifer storage, the HT-ATES as an open system is highly efficient and does not affect ground water layers.

With this project, EWB decided to seize the opportunity of heat storage. Therefore, the Energy Hub Forsthaus was planned to be supplemented with the pilot project “Geospeicher”. The position of the potential Heatstorage “Geospeicher” was planned adjacent to the Energy Hub.

Geo-storage systems are already in operation in Europe and around the world. These usually store heat in the low temperature range between 20°C and 30°C. HT-ATES are less common.

A corresponding practical example can be found in the center of Berlin under the Parliament buildings in the Berlin Spreebogen ("Heating and cooling network of the German Bundestag").

The system there consists of two storage layers. A near-surface cold storage (quaternary loose rock at a depth of approx. 50 m) and an approx. 300 m deep heat storage with storage temperatures of around 70°C. The plant has been operating successfully since 1999.

The now planned geo-storage facility in Bern would be the first storage facility in Switzerland to be operated on this scale.

5.2.4 Geology of the exploration area

5.2.4.1. Regional geology and tectonics

The state of geological knowledge is described in detail in Ladner 2018 and only a summarizing outline is given here. The Bern region is in the Swiss Molasse Basin, which sank in connection with the formation of the Alps and was largely filled with debris from the mountains that formed (the so-called Molasse sediments). The base of the Molasse Basin is formed by the crystalline basement with local, relatively narrow troughs with Permo-Carboniferous sediments (Figure 103). In the Bern region, the basement is covered by around 2,000 m thick sediments from the Mesozoic Era (Triassic and Jurassic) and around 1,550 m in Molasse sediments (Lower Freshwater Molasse (USM)), above which are Quaternary loose rock deposits of fluvial and glacial origin.

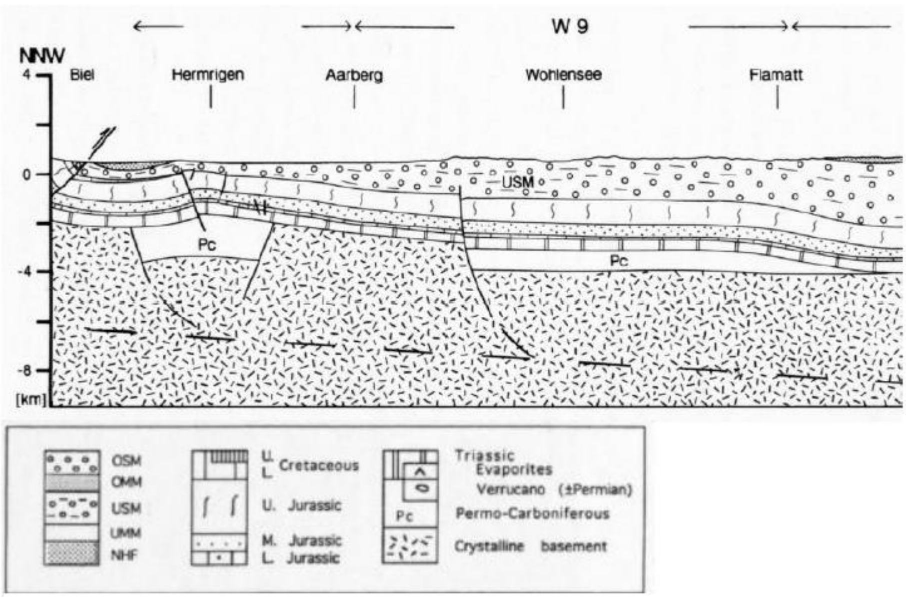

Figure 103 - Geological NW-SE section west of Bern (Pfiffner et al., 1997).

The evaluation of seismic data from the oil industry over the past ten years (Allenbach et al.2017, Figure 104) indicate that there are no significant Faults present. Only at distances greater than approx. 15 km were N-S oriented Fracture structures observed, for example in the Laupen-Friborg area, under the Gürbe and Aare valleys, or south of Solothurn.

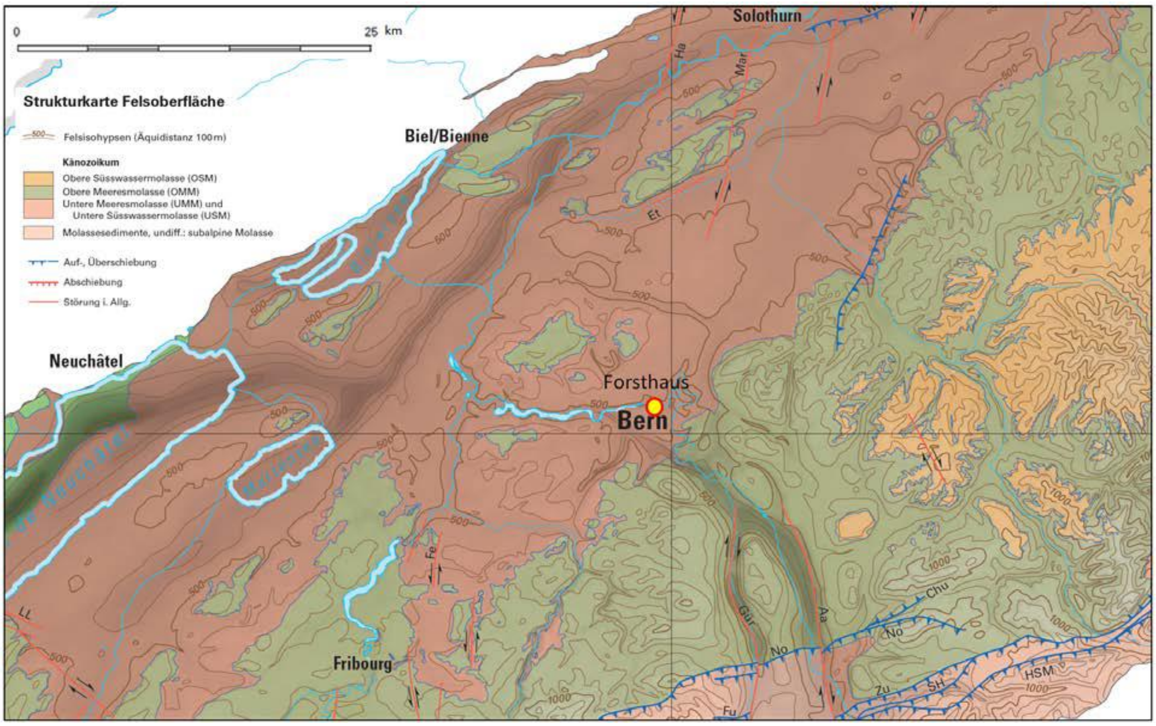

Figure 104 - Geology of the rock surface under the Quaternary cover (Allenbach et al. 2017).

5.2.4.2. Reference wells

In addition to a large number of shallow exploratory wells, which generally provided date only to the type and thickness of the unconsolidated Quaternary, all of the reference wells that drilled the USM are more than 10 km from the project site (Figure 105). The most important reference wells within a 15-20 km radius of the project location are:

- Ruppoldsried-1: 230 m Aquitainian USM (lower part)
- Hermigen-1: 390 m Aquitainian USM (lower part)
- Tschugg-1: 60 m Aquitainian USM (only the lowest part)
- Fendringen-1: 900 m Aquitainian USM
- Courtion-1: 770 m Aquitainian USM
- Burgdorf-EWS: 200 m Aquitainian USM

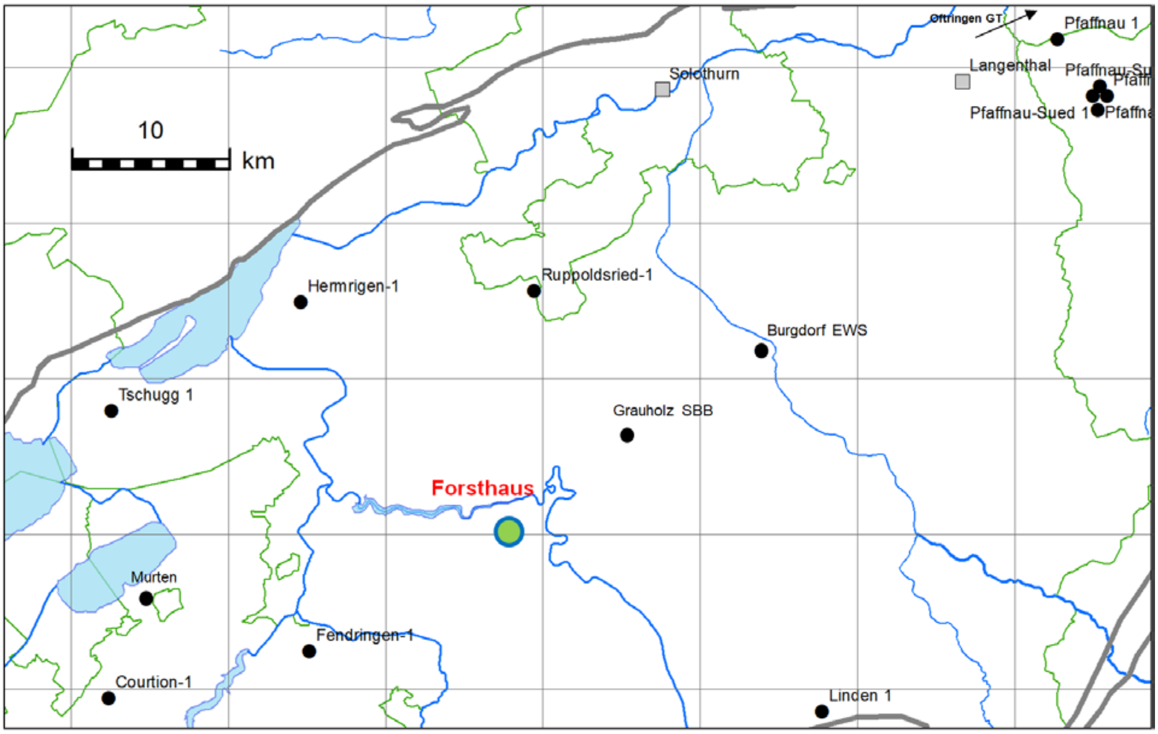

Figure 105 - Location of the most important reference wells and outcrops.

The Oftringen (NOK) wells and 4 natural gas exploration wells Pfaffnau-Süd-1-4 have been completed in more than 45 km in NE direction. These bores are also already in another sedimentation area (distal USM).

An important reference point is a short sandstone core from an exploratory borehole near the Bern train station, around 2 km SE of the project site, that was available for reservoir geological Laboratory testing (Figure 106).

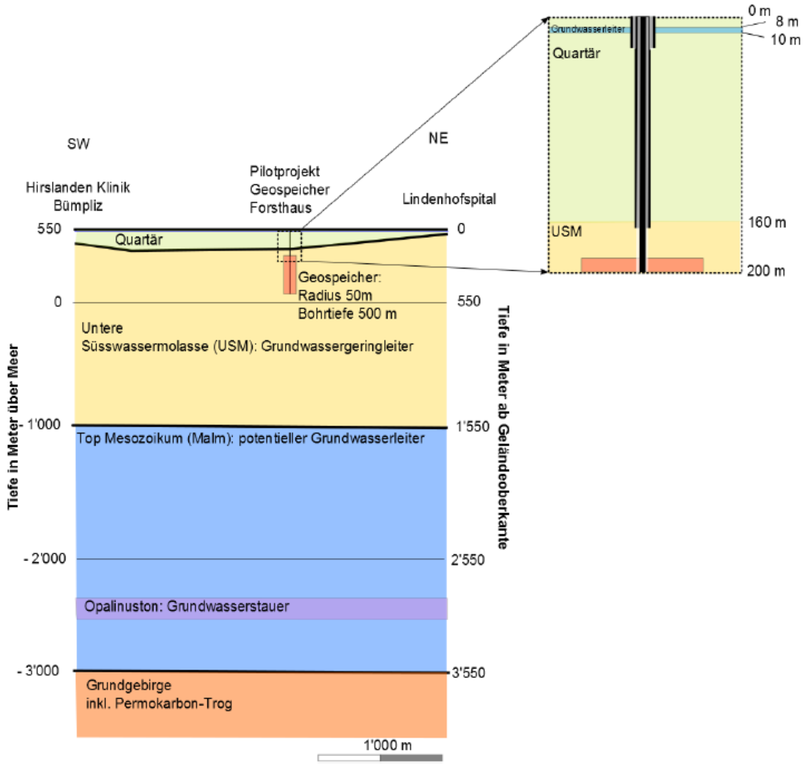

Figure 106 - Geological cross-section down to the deeper subsurface of the planned geothermal storage facility (Ladner 2018).

The 500 m deep boreholes (TVD) of the Forsthaus project penetrated only the Aquitainian part of the Lower Freshwater Molasse (Nagra NTB 94-10). This interval is an equivalent of the Aquitainian Gümmenen formation.

The Lower Freshwater Molasse consists of fluvial deposits. Keller et al. (1990) and Keller (1992), based on detailed sedimentological studies on natural outcrops, clay pits, tunnel and boreholes developed a facies model showing and describing the internal structure of the Lower Freshwater Molasse by five different architectural elements. These elements differ through their genesis and their characteristic facial structure, their geometry, and dimensions as well as their petrophysical properties (Figure 107 and Figure 108).

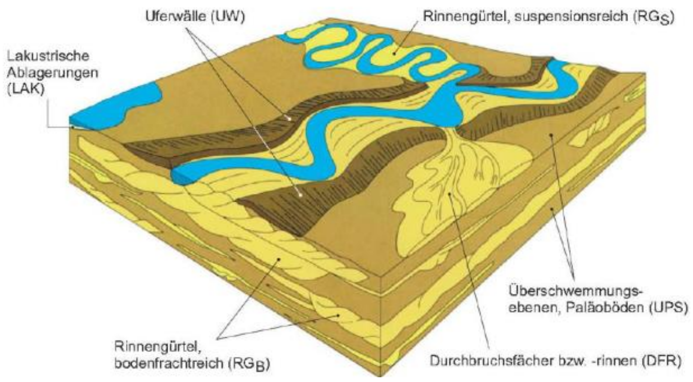

Figure 107 - Facies model according to Keller et al. (1990) for the distal area of the USM.

The target horizons for the geothermal storage facility are mainly the medium to coarse grained sandstones of the channel belts (“Rinnengürtel” in Figure 108).

These are the deposits in the central channels of rivers (high flow energy of the water > good sorting of the sandstones), the often coherent, homogeneous sandstone bodies several kilometers in length, 150-1'500 m wide and 2-15 m thick. These, in the best case, very permeable sandstone bodies are often isolated within poorly permeable, fine-grained sediments . They have a meandering geometry with a longitudinal alignment parallel to the general drainage system in the Alpine foreland. In the clay pit Schüpfen (NW of Bern) they show a general orientation from SW to NE (direction of flow of the rivers against NE, oral communication Prof. F. Schlunegger). One of the main targets of the first three holes of the HEATSTORE was to determine this geometrical orientation and the vertical frequency.

Due to the expected and confirmed geometric arrangement of the sandstone bodies (target horizons, see above) it was important to drill the first three holes in different directions.

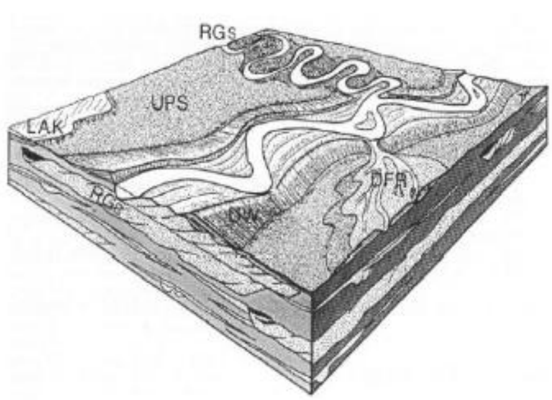

ARCHITEKTUR ELEMENT		VEREINFACHTE GEOMETRIE	DURCHLÄSSIGKEIT K (m/sec)
RG	RINNENGÜRTEL	H=2-15m B=150-1500m L=n·10 m	1E-04 bis 1E-07
DFR	DURCHBRUCHSRINNE	H≤4m B<10m L=n·10 m	1E-06 bis 1E-08
	DURCHBRUCHSFÄCHER	H=1-2m B=n·10 m L=n·10 m	
UW	UFERWÄLLE UND DISTALE ÜBER-SCHWEMMUNGSSANDE	H<3m B=10-30m L=n·10 m	1E-07 bis 1E-10
UPS	ÜBERSCHWEMMUNGS-EBENE MIT PALÄO-BÖDEN UND SÜMPFEN	H<6m B=n·10 m L=n·10 m	1E-08 bis 1E-11
LAK	LAKUSTRISCHE SEDIMENTE		KEINE DATEN

Figure 108 - Dimensions and permeability properties of the architectural elements in the distal USM according to Keller (1992)

The results of the comprehensive investigations in the three boreholes are documented in the final and partial reports of the Geospeicher Forsthaus project.

5.2.4.3. Stability and gas flow in the Aquitaine

5.2.4.3.1. Stability of the Aquitaine Sediment Sequence

To estimate the stability (borehole stability or breakouts) for the drilling planning the existing data from the reference boreholes was evaluated.

Direct information on the drilling results is only sparse in all reference wells available. The caliper log data of the Courtion-1, Ruppoldsried-1, Tschugg-1 and Burgdorf wells M-1400 over the Aquitaine interval, however, indicate that generally in marl-rich lithologies (fine-grained sediments of the fluvial flood plain) washouts and breakouts are more likely.

Ruppoldsried-1 is an exception, where washouts and breakouts tended to occur in (unconsolidated?) Sandstone layers.

However, there were no indications of any major problems relating to the borehole stability. No indications of swellable clays layers could be found.

5.2.4.3.2. Possible Hydrocarbon gas in the Aquitaine

Near Forsthaus, there are weak signs of methane in the sandy facies of Aquitaine (USM). This is proven by observations and measurements in the SBB-Grauholz tunnel and the Les Vignes motorway tunnel near Murten. Stronger and constant methane indications were predominantly observed in the sandy lower part of the Chattien (USM) in the reference boreholes Hermigene-1, Ruppoldsried-1, and Tschugg-1, that is below the Aquitaine strata penetrated by the geo-storage wells at the Forsthaus site in Bern. More methane deposits were also found in the observed lower intervals of the USM in the Langenthal-Pfaffnau-Suhr area.

5.2.4.4. Geological measurement program

The geological measurement program had the following objectives:

- Recording of the geological structure of the Lower Freshwater Molasse USM. Distribution and geometry (dimensions and connectivity) of the facial architectural element of the channel belt sandstones ("Rinnengürtel").
- Measurement of the hydraulic parameters of the channel belt sandstones (permeability, transmissivity, Hydrochemistry etc.).
- Characterization of the formation pressures and hydraulic flow gradients between the wells.
- Determination of the geothermal parameters (temperature, thermal conductivity, and heat capacity) for the purpose of estimating the heat flow.

The entirety of this data was used to calibrate the coupled geothermal / hydrochemical model calculations of the long-term behavior of the planned ATES.

The geological measurement program consisted of the following (Figure 109):

- Mud logging (drilling parameters, cuttings, gas, etc.)
- Core evaluation
- Laboratory analyses
- Wireline logging
- Hydraulic testing

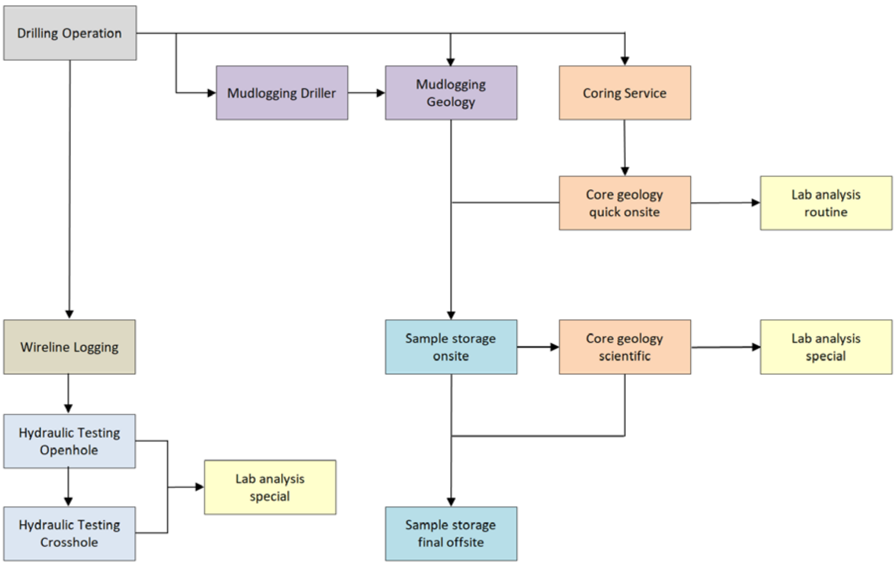

Figure 109 - General workflow of the geological measurement program

5.2.5 Geochemical pre-study (University of Bern)

In preparation for the start of drilling operations, a geological and geochemical pre-study (including water–rock experiments, scaling experiments and numerical simulations) was commissioned by EWB. The entire report can be found as Appendix08.

The following aims were defined:

- Understand which challenges might be encountered during operation of the Geospeicher Forsthaus based on problems encountered in previous projects. This knowledge also informs the conditions for the experiments presented here and planned in the future.
- Acquire as much knowledge as possible about the geology and hydrogeology of the target formation (Lower Freshwater Molasse, USM) and the heterogeneity of the properties before drilling starts to judge if (a) the drill cores and groundwater compositions used during the experiments are representative for the USM and (b) find reasonable input values for different parameters to be included in the numerical simulations.
- Assess potential mineral reactions at the site through experimental work by (a) investigating mineral reactions in the reservoir through core and batch experiments and (b) assessing the potential for carbonate scaling during heating of the formation fluid.
- Conduct numerical modelling simulations of the thermal-hydraulic-chemical (THC) processes expected to occur during operation of the system, to identify potential red flags before drilling starts.

5.2.5.1. Information sources - project planning phase

In the absence of subsurface data from the Bern site itself, the planning of the project at Forsthaus was based on five sources of information: (1) scientific literature documenting experience in similar projects; (2) scientific literature on the regional geology, which provides a basis to estimate reservoir properties at the Forsthaus site; (3) analyses of drill core and formation waters from shallow wells 2 km from the site, which provide material for experiments; (4) laboratory experiments involving heating of the sandstones and formation water to identify the governing water–mineral reactions and to calibrate their rates; (5) 3D numerical simulations of the coupled thermal–hydraulic–chemical processes during the heat loading and unloading cycles at the reservoir scale, to assess the influence of water–mineral reactions on pore clogging and rock-cement dissolution, and on the thermal evolution and feasibility of the storage concept.

5.2.5.2. Information gaps – project planning phase

The geological literature already showed that the reservoir properties of the target sandstones are site-specific. Without drillhole data it was not possible to accurately predict the response of the Forsthaus reservoir to fluid injection/extraction. Key missing information on the sandstones includes whether they are even present under Forsthaus, their geometries and dimensions, their porosity, permeability, mineralogy and degree of cementation, and the extent to which they are hydraulically connected. Likewise, the characteristics of the in-situ groundwaters are site-specific. Missing information included their salinity, flow rates, microbial activity, and solute composition including corrosive components. These properties were determined during drilling and testing. For the project planning, properties extrapolated from other sites had been used to assess potential issues with the Geospeicher system.

5.2.5.3. Critical issues – project planning phase

Within this context of incomplete information during the project planning phase, the evaluation revealed no critical issues suggesting that the project might fail or that a completely different storage strategy would be required.

5.2.5.4. Cautionary issues – project planning phase

In the project planning phase, the following risks and complications were viewed as non-critical, but required consideration:

- Preferential flow paths may develop between the main and supporting wells due to heterogeneous permeability of the sandstones. This could reduce the volume of rock swept by the injected hot water, lowering the efficiency of heat storage below previous expectations.
- Calcite is predicted to precipitate in some regions of the reservoir and to dissolve in others during the water injection/extraction cycles. Regions clogged by calcite may become barriers to the injection/extraction flow regimes. Regions of moderate calcite depletion may focus flow and thereby leave other regions of the reservoir unswept by the injected hot water. Thus, both calcite clogging and dissolution may contribute to lowering the heat-storage efficiency of the reservoir.
- Extreme dissolution of calcite cement may induce local mechanical disintegration and compaction of the sandstones, and mobilize fines that clog pore throats, reducing permeability and hence further lowering the efficiency of the water injection/extraction cycles.
- Microbes may form biofilms and clog the casings of the supporting wells, where temperatures are < 50 °C. Microbial activity is expected to diminish as the reservoir heats up to 90 °C.
- The evolving thermal plume and the water–rock reaction zone around the main well are predicted to remain within a 50 m radius from the well. However, the influence of the entire heat storage reservoir, if defined by the distance to which non-reactive solutes injected or released from the rock can travel in the USM reservoir water system, is much larger. There is therefore a possibility that unwanted chemical compounds are transported over large distances.
- Significant carbonate scaling is expected in the surface installations during the heat-loading cycle. This could impede flow and exchange of heat in the surface installations.

5.2.6 HEATSTORE Forsthaus

5.2.6.1. Concept and characteristics

The geo-storage concept is divided into an upper and an underground part (Figure 110). Essential components of the underground heat storage system are the horizontal elements of the reservoir and the wells that lead through and open up the individual reservoir elements.

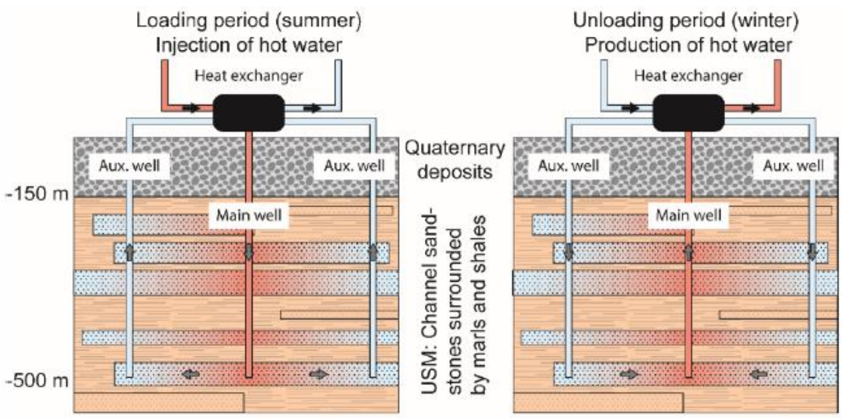

Figure 110 - Schematic representation of the geothermal storage facility (above and below ground). The system consists of several horizontal reservoir elements that are accessed through two or more boreholes. Depending on whether loading or unloading, these serve alternately as injection or production wells

The following Table 26 shows the characteristic values that were used during the project planning phase for the geo-storage at the Forsthaus site in Bern:

Table 26 - Main Characteristics of the planned heat storage

Amount of wells	maximum 6
Drilling depth	500 m (TVD)
Storage rock	Sandstone layers of the Lower Freshwater Molasse (USM)
Depth	approx. 200 to 500 m
Radius	approx. 50 - 100 m
Circulation rates	25 - max. 60 l/s
Temperatures	Charging cycle max. 90 ° C - 120 ° C Discharge cycle 60 ° C - 90 ° C

5.2.6.2. Basic drilling data

The drilling site for the project was on the northwest corner of the Forsthaus energy hub. The wells were drilled from one location (pad drilling) at angles between 4 to 20 degrees from the vertical in a south-west direction under the Bremgartenwald so that each reached the landing point as shown in Figure 111 at a depth of 500 m below the terrain.

The HEATSTORE itself was foreseen in the area of the boreholes at a depth of approx. 200 to 500 m below the terrain with a radius of approx. 50 - 100 m (Figure 111).

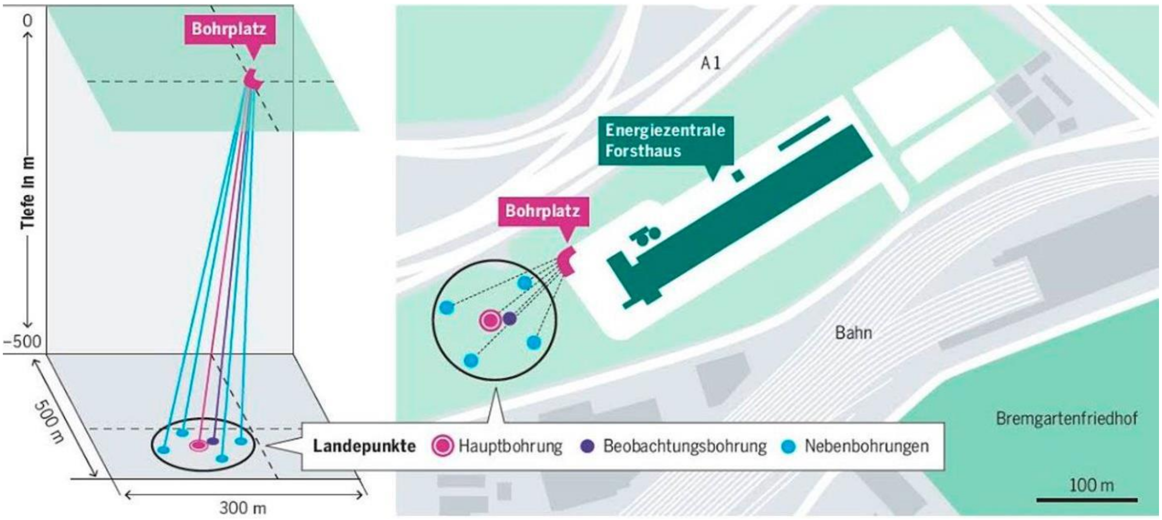

Figure 111 - Situation plan for the pilot project Geospeicher Forsthaus

Figure 112 illustrates the trajectory of the wells, starting from the drilling site at the northwest corner of the Forsthaus energy hub.

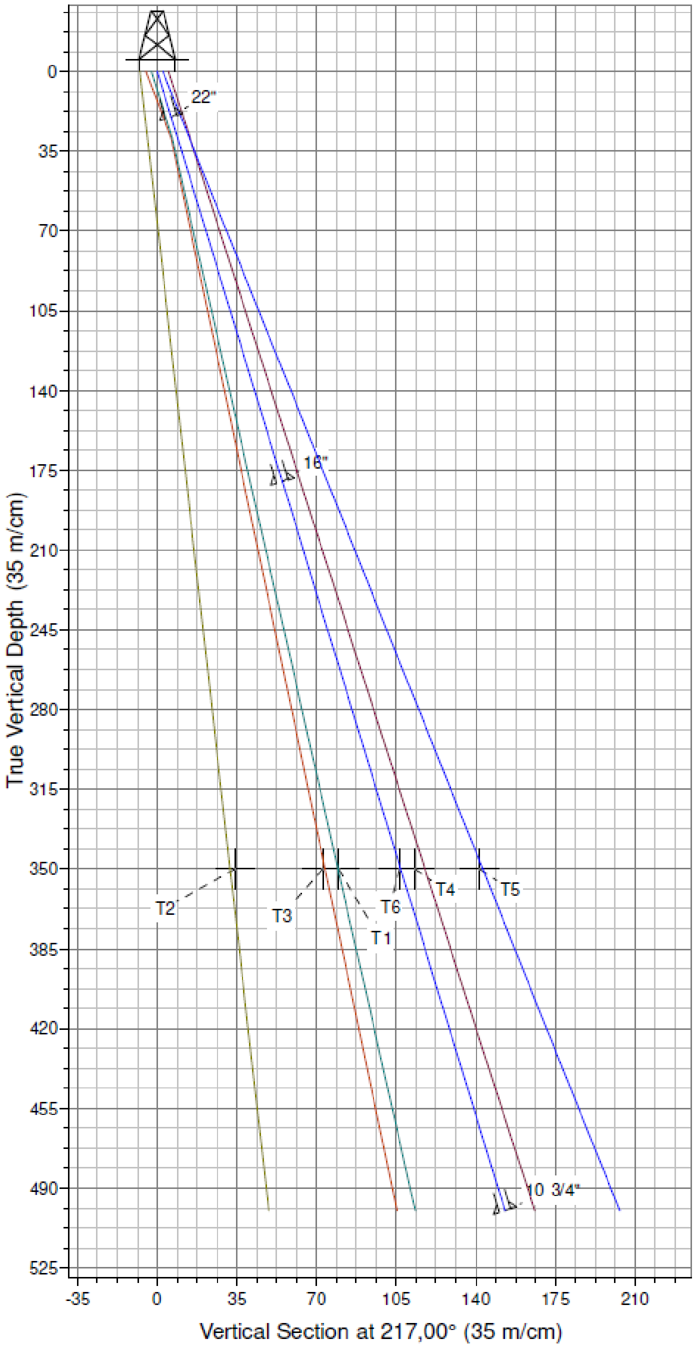

Figure 112 - Illustration of a possible trajectory for the wells starting from the drilling site at the northwest corner of the Forsthaus energy hub. Main well (T1), secondary/support wells (T2-T6). The geothermal storage is located in a depth range of approx. 200 - 500 m below the terrain.

Three of the maximum six boreholes were drilled from a central cellar (Figure 113). This cellar houses the entire wellheads and Christmas tree stack (Figure 114) and can be covered with concrete elements for protection. The wellheads and Christmas trees were installed on the surface casing to prevent uncontrolled release of gases and liquids.

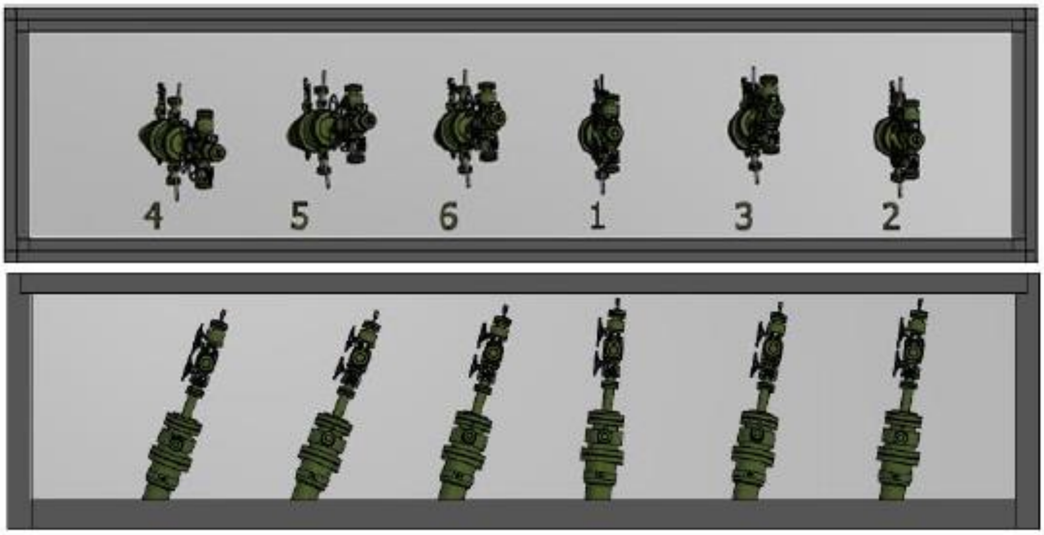

Figure 113 - Representation of the position of the wellheads and Christmas trees in the drilling cellar.

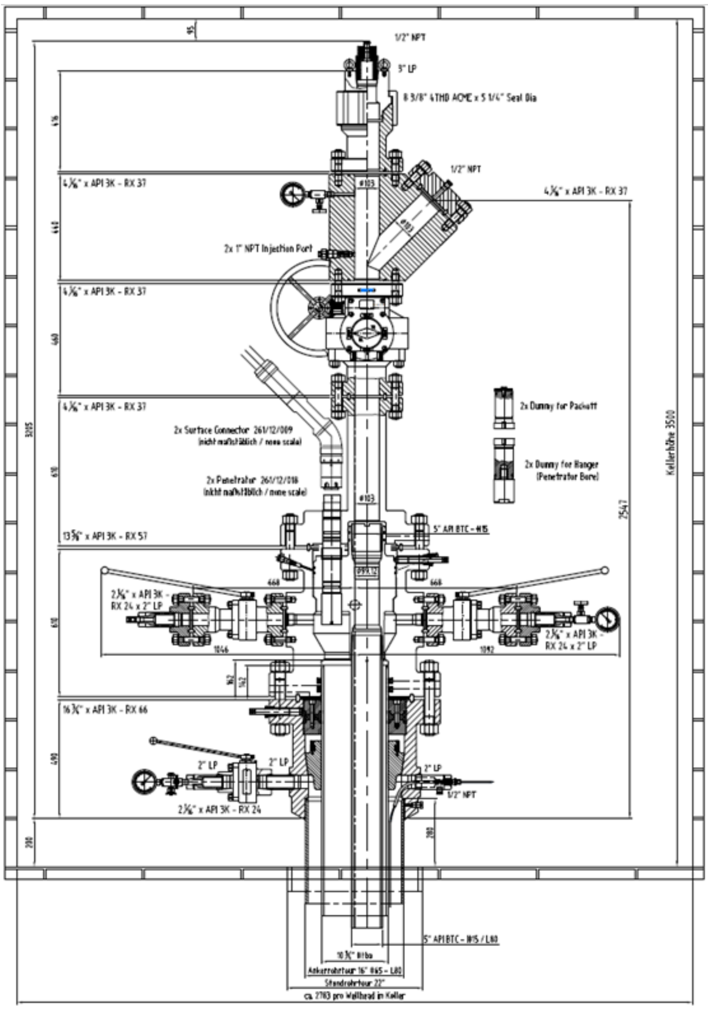

Figure 114 - Technical Drawing of the wellhead and Christmas trees in the drilling cellar.

In order not to endanger the stability of the borehole, a continuous 24hour drilling operation took place. The wells are all cased (steal casing) and cemented. The latter serves in particular to protect the groundwater layer and to avoid flow paths behind the casing strings.

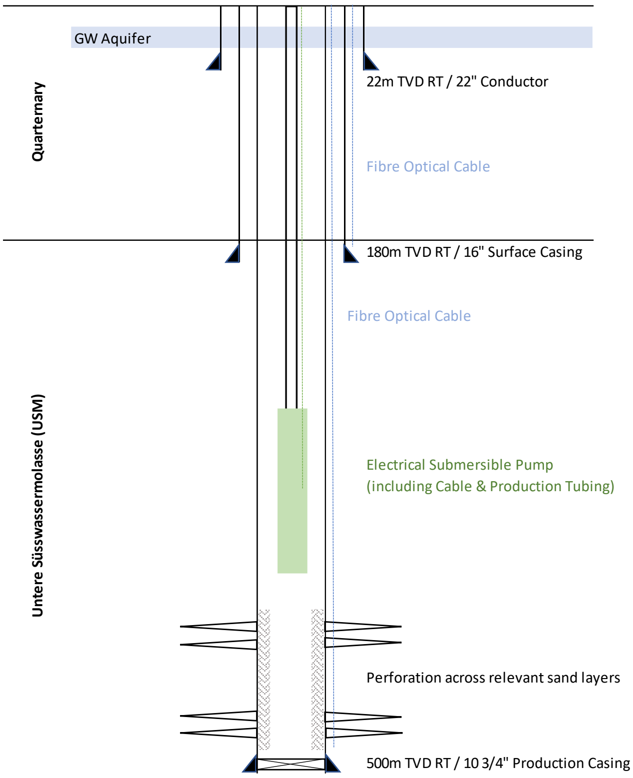

Figure 115 - Final planned well schematic

The utilized casing strings have a telescopic structure. As can be seen in Figure 115, the first casing, the conductor, has the largest diameter (22 in / 558.8 mm). It was planned to be installed to a depth of around 20 m. This pipe protects the groundwater aquifer, which is located at 8-10 m, from any impact. In addition, it enabled the installation of a diverter and annulus preventer, which if unexpectedly encountered, would have been used to safely divert all over pressured gases and liquids and then to enclose the borehole.

The drilling was then planned to continue to a depth of 180 m with a drilling diameter of 20 in (508 mm) to then install the surface casing (pipe diameter 16 in / 406.4 mm). Due to the greater thickness of the Quaternary units, drilling was carried out to a greater depth (TVD of the three wells between approximately 200 and 265 m).

Surface casing extends into the Molasse rock and secures the borehole from the Quaternary unconsolidated formations above.

The first section of the wellhead (borehole enclosure) was installed on the surface and on the production casing after that. Due to the inclination of the wells from the surface, increased wear of the pressure-resistant sealing surface on the inside of the wellhead sections was to be expected. In addition to a wear bushing, which already provides temporary protection for this sealing surface, a drilling spool was used while coring (Figure 116).

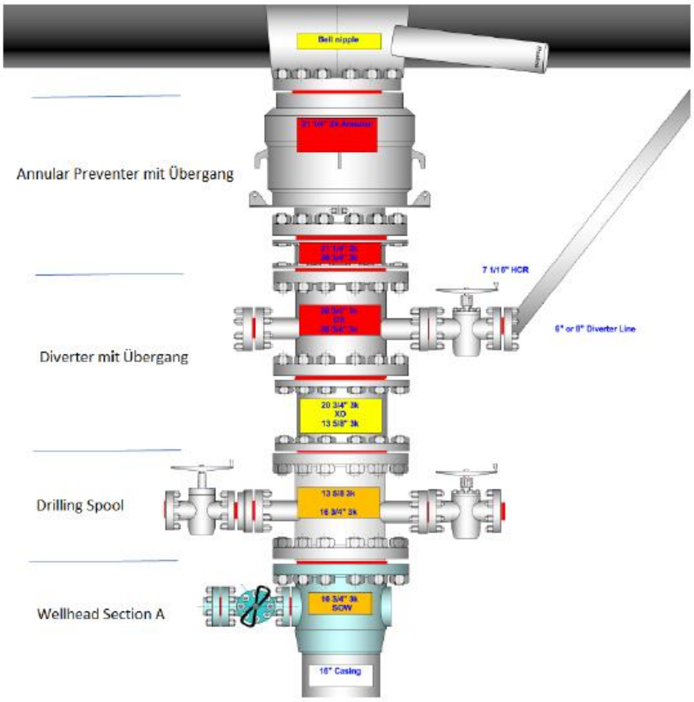

Figure 116 - Structure of wellhead section A, drilling spool and diverter with annulus preventer in the drilling cellar

The third well section was then carried out to the desired target depth of 500 m TVD (550 m MD) and opened the lower freshwater molasse as a potential geothermal storage facility.

To ensure that the meander belt sandstone (Rinnengürtel-Sandsteine) and the clay layers in between are evaluated as precisely as possible, the entire section was drilled through using the oriented wireline coring method (Figure 117). This means that a ring-shaped drill bit was used to drill, so that the core of the rock remained intact, and the type, position and inclination of the various rock layers could have been examined. The core in the inner tube was pulled up by means of a wireline so that the drill string did not have to be removed and reinstalled.

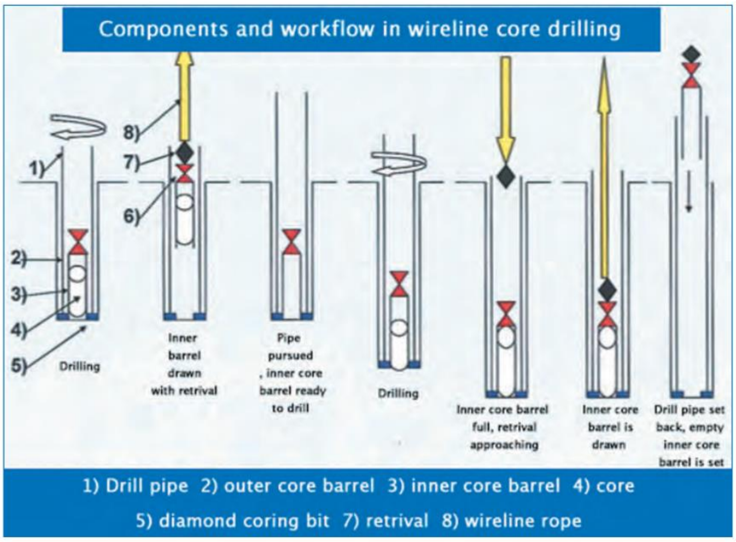

Figure 117 - Schematic representation of the wireline coring process

After the core had been brought to the surface, the inner core barrel was brought back down to core the next 6m long section.

As soon as a channel sandstone had been drilled, it was tested hydraulically. To do this, the coring work was interrupted, and a packer was installed to isolate the sandstone area from the rest of the well. Then this area was tested by reducing the mud column in the Drill pipe prior opening the isolated below the packer to this now reduced hydrostatic overhead. This forced an influx of reservoir water from the sandstone layer into the drill string (Figure 118). The recorded volumes, pressures, flowrates and final height of the column in the drill string gave information to the permeability of this individual sand layer.

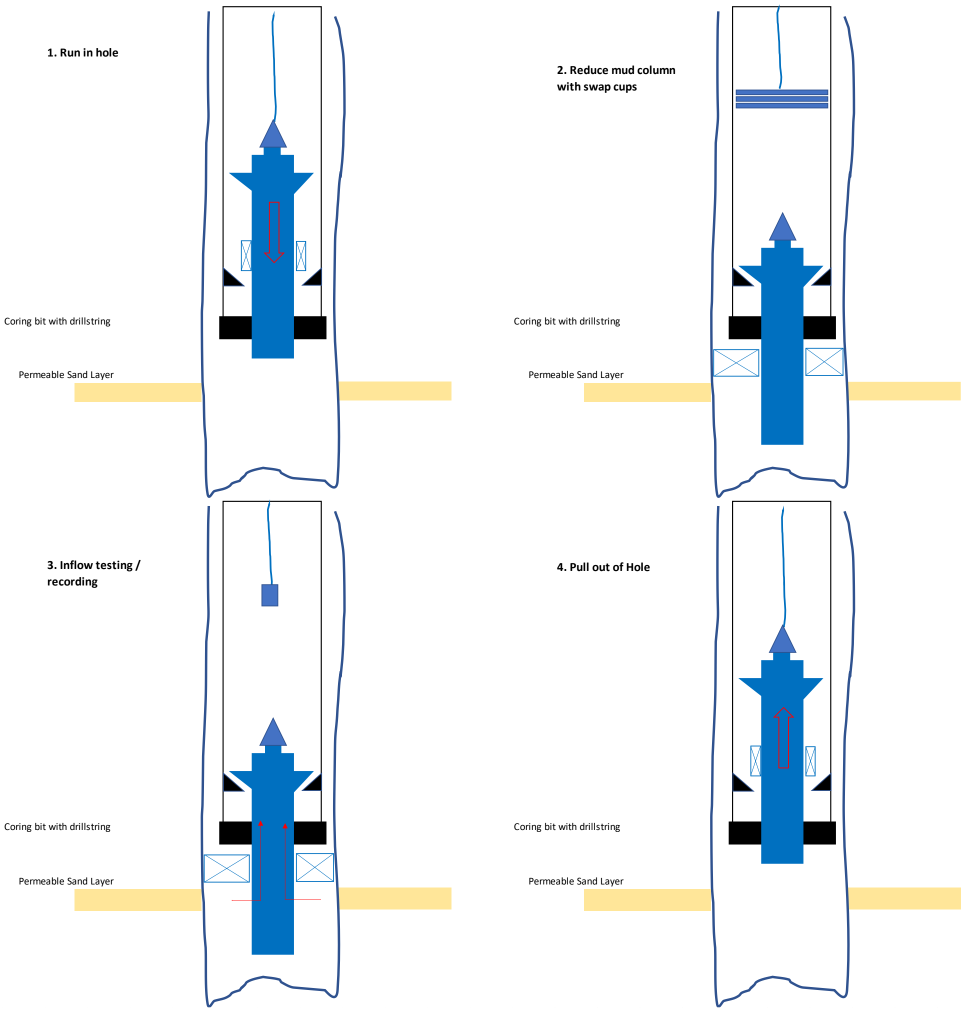

Figure 118 - Hydraulic test borehole set-up

The hydrogeological data obtained enabled a better understanding of the storage area and would have been an important input parameter for the detailed planning of the final number of required wells and the operation of this area as a HEATSTORE.

After reaching the final depth with the coring system, the borehole was enlarged to 14¾ in (374.65 mm) and the production casing (10¾ in / 273.05 mm) was installed and cemented.

To regain access to the identified sandstones, the production casing was perforated at the required depth.

5.2.6.3. Environmental impacts

As described in the previous chapter, to protect the groundwater, the standpipe was cemented in at the beginning of each well, separating the borehole from the groundwater aquifer.

To prevent uncontrolled leakage of mud or hydraulic equipment, the borehole had a diverter system installed throughout. Furthermore, the drilling site was divided into an inner (red) and an outer (yellow) area.

System components that contain potentially environmentally hazardous substances were only positioned in the inner area. All liquids from the inner area were collected separately and could be disposed of separately if necessary (Figure 119).

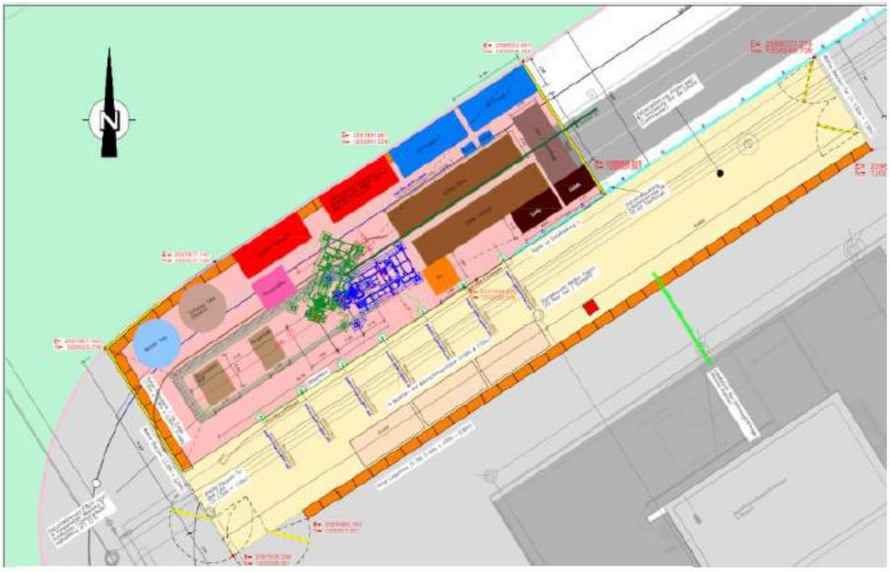

Figure 119 - Drilling site with inner (red) and outer (yellow) area

During drilling, the borehole stability was guaranteed by using a mud density that was adapted to the well conditions and was continuously slightly over balanced with reference to the pore pressures. This formed a filter cake around the borehole, which prevented drilling mud from penetrating into the formations.

After reaching the final depth of a drilling section, a hydraulic connection was eliminated by installing cemented casing strings. This was done according to the current state of drilling technology.

5.2.6.4. Surface Temperature Simulation

A conservative approach was chosen to assess the warming of the near-surface groundwater in the shallow ground water horizon. The heat input into the groundwater from a non-insulated borehole was calculated; with this heat input, the further heat transport in the ground water horizon was simulated under the assumption of a pressure gradient of 0.0075 m/m (value from a comparable regional study). The modelling covers a period of 20 years, with permanent water at 120 ° C (in the sense of a conservative assumption). The natural groundwater temperature was set at 13 ° C. The result of the modelling is shown in Figure 120.

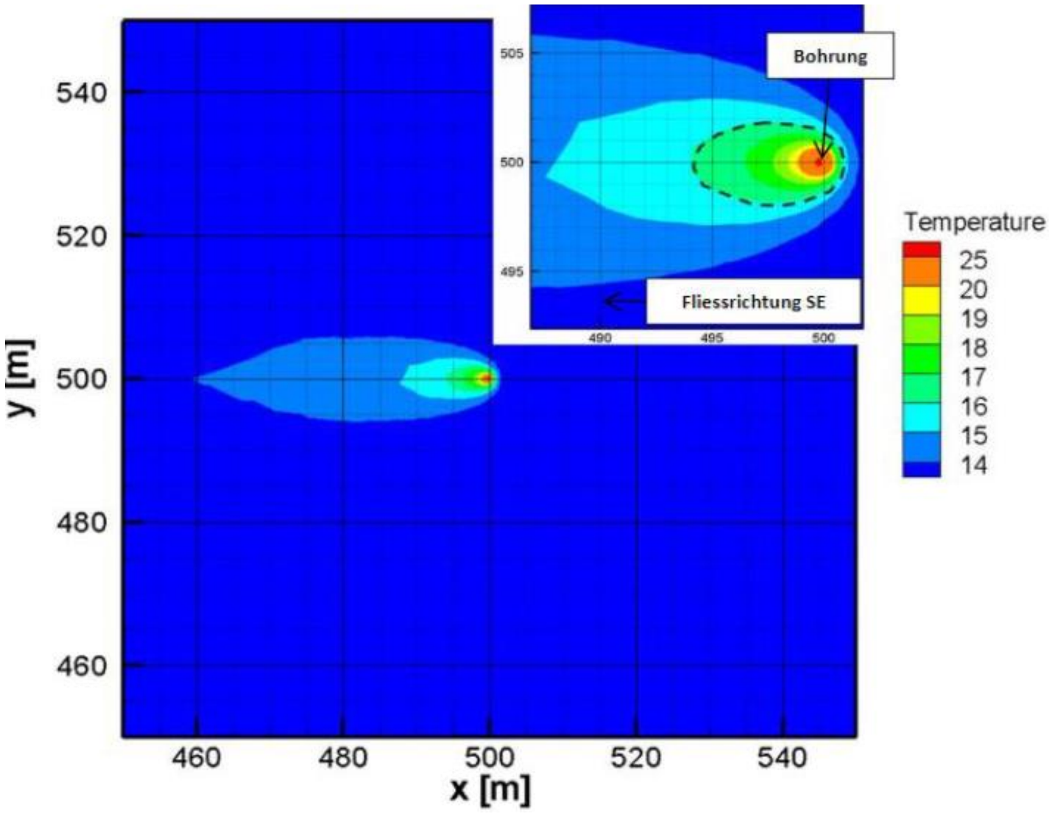

Figure 120 - Top view of the expansion of the heat plume in the Quaternary aquifer under the assumption of permanent 20-year operation of the geothermal reservoir with pumping of water at 120°C from a non-insulated borehole. The boundary at which the temperature change is 3°C (ΔT = 3°C isoline) is shown in black.

After 20 years of permanent operation of the geothermal reservoir with 120°C hot water, a heat plume appears along the direction of flow. It has a maximum extension of about 40 m in the direction of flow and about 10 m perpendicular to it. The maximum extension of the heat front with a temperature change of 3°C and more is about 6 m in the direction of flow and about 2 m perpendicular to it. The operation of a geothermal reservoir with a non-insulated borehole heats the near-surface aquifer in the Quaternary only locally and is far below the acceptance limit of 3°C at 100 m.

The completion of wells could also be equipped with double-walled insulating production tubing, which would further greatly reduce the temperature influence.

5.2.7 Reservoir Temperature Simulation

Figure 20 shows the vertical section of a second simulation, namely that of the lower freshwater molasse with the assumption of 20 years of operation with 2,000 hours of charging per year and 90°C hot water for the storage of 10 MW_{th}. 50 m from main to secondary boreholes was assumed. Otherwise, typical thermal and hydraulic parameters for the rock layer were used (Figure 121).

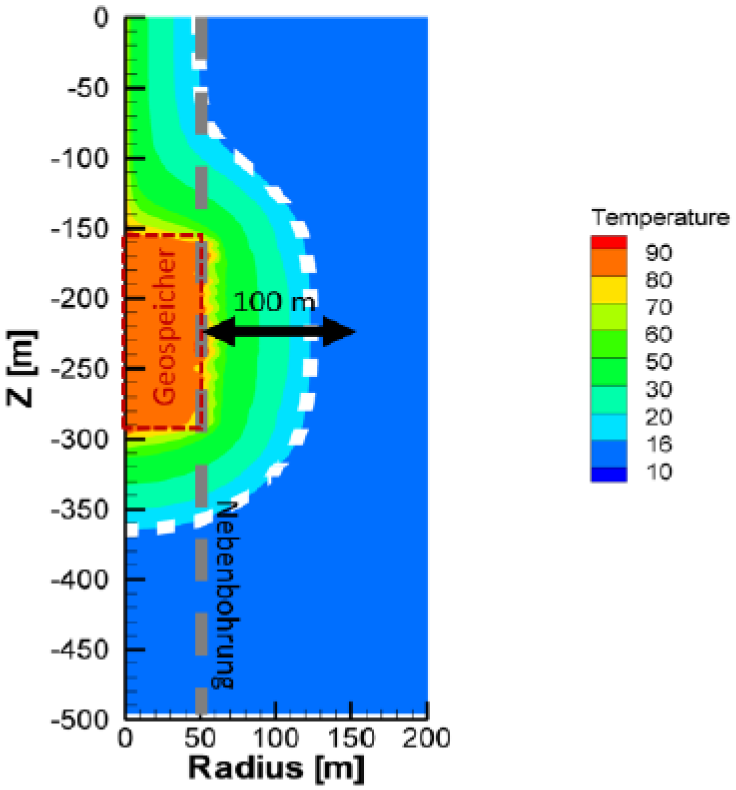

Figure 121 - Vertical section of the extent of the heat front in the geostorage with 12 sandstone layers in the Lower Freshwater Molasse in the last loading cycle of the 20th operating year. The ΔT = 3°C isoline is shown dashed white

From this, it can be determined that the storage area of the model is concentrated in the used sandstone layers. The horizontal thermal expansion reaches 130 m after 20 years. The vertical extension of the heat front from the geothermal reservoir itself does not reach far beyond the target sandstone layers even after 20 years of operation and is clearly below the surface, so that no heating of the ground takes place.

5.2.8 Ground deformations

There can be two causes for possible heave or settlement. On the one hand, changes in the original pore water pressure caused by injection or production of water, and on the other hand thermal expansion or regression of the reservoir rock during the charging and discharging cycles. When assessing the effects of uplift and subsidence, it is important to consider that the geostorage facility is in a forested area and therefore the hazard potential is low.

During geostorage operation, no terrain deformations due to a change in pore water pressure are expected because the operational concept provides for at least one production well and one injection well. This ensures an even volume balance.

Deformations in the reservoir rock due to thermal expansion and regression during the charging and discharging cycles must be considered. At a depth of 200 - 500 m, the overlying rocks will absorb most of the possible deformations, so that no or only minor deformations are to be expected at the surface itself.

To monitor heave and settlement, a reference levelling was carried out and repeated regularly during the drilling and testing work, and was also foreseen for a later operational phase. In addition, potential deformations in the subsoil were monitored with the help of installed fiber optic cables.

5.2.8.1. Monitoring Concept

Such monitoring was part of a comprehensive monitoring concept that had been drawn up, based on which irregularities could have been detected at an early stage.

Specifically, the following measures for monitoring the area around the geo-storage construction site were defined (Figure 122):

- Settlement measurements: Network of 22 measuring points on surrounding buildings, in the ground and on wooden stakes in the forest. Carrying out zero measurements before the start of drilling, weekly follow-up measurements of 11 measuring points during the drilling and testing activity.
- Vibration measurements: Installation of three vibration measuring devices on surrounding buildings. Continuous measurement and mapping via a web portal in real time including an alarm system.
- Crack logs: Photo documentation of the buildings around the drilling site including exterior shots of the facades and compilation of building profiles.
- Inclination and azimuth measurements: The alignment of the drilling rig (conductor and derrick) is checked for inclination and azimuth before spudding each well.
- Monitoring of the spring Glasbrunnen: The water quality of the nearby spring Glasbrunnen is monitored weekly by taking samples. Measurement of temperature and flow rate are taken on site as well as bacteriological and chemical analyses in the laboratory. Weekly report compiled in the form of a log.

Figure 122 - Overview of the monitoring measures in the geothermal storage project. Settlement measurements (blue), vibration measurements (green), crack logs (yellow areas), monitoring of the spring Glasbrunnen (orange). The drilling site including the alignment of the first holes are shown in red.

5.2.9 Conducted work and Methodology

Between 2019 and 2025, the Geospeicher Forsthaus pilot project investigated the suitability of the USM channel-belt sandstones for geothermal heat uses and HT-ATES. The work was carried out in three phases.

In Phase 1 (2019–2023), planning, risk assessment and drilling of three deviated boreholes (F-1, F-2A, F-3A) were completed (Figure 123). More than 450 m of drill core were recovered and digitally photographed using 360° scans. Following a detailed sedimentological description, selected samples were analysed in the laboratory of Wintershall Dea for porosity, permeability, grain density/size, and geomechanical parameters. Additional samples were examined to determine their mineralogical and chemical composition as well as thermal properties. During drilling operations, 20 hydraulic tests were conducted using a single-packer cable system. All boreholes were subjected to an extensive geophysical logging program, including borehole geometry and orientation, gamma radiation, temperature, acoustic imaging of the borehole wall, and cement quality. In borehole F-3A, additional wireline logging tools were tested that may in the future replace complex and costly core drilling operations. These investigations enable a detailed characterization of the USM regarding all key parameters for geothermal use and heat storage.

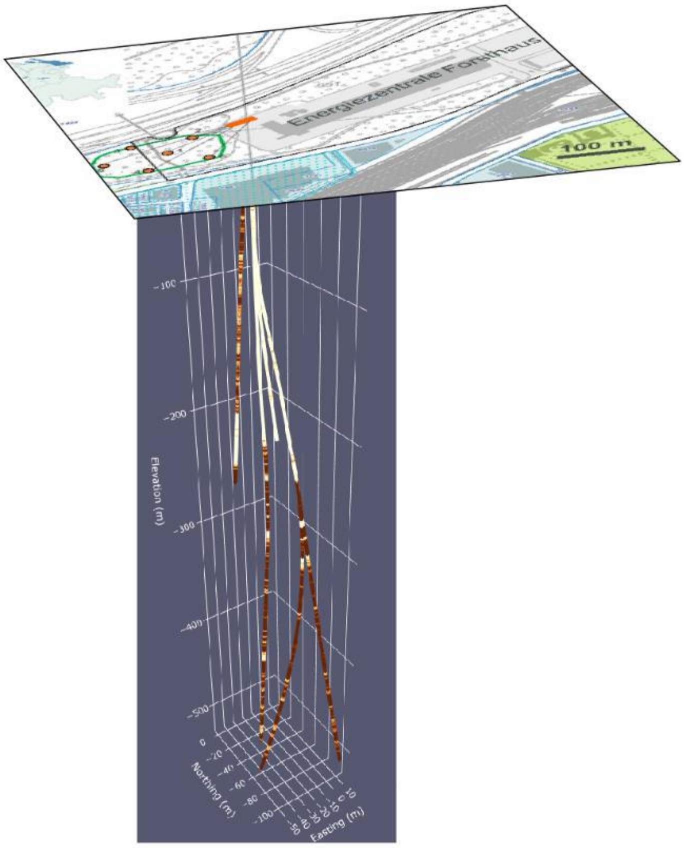

Figure 123 - Layout of the borehole trajectories beneath the project perimeter at the Forsthaus energy hub (EFZ).

In Phase 2 (January–December 2024), the reservoir was hydraulically connected through micro sidetracks, and a series of hydraulic tests were performed, including cross-hole tests, step-pressure tests (hydraulic jacking), a long-term circulation experiment, and chemical stimulation by CO_2 acidization followed by backflushing. Fiber-optic cables and double-packer systems enabled precise monitoring of pressure, temperature, and strain.

For these tests, the channel-belt sandstone Layer 6c at ~490 m depth was selected, and both wells were perforated along this unit by drilling up to 5 m long micro sidetracks (diameter 4 cm). Injection and step-pressure tests were first conducted to characterize stress conditions and hydraulic properties. Subsequently, a hydrochemical circulation experiment assessed connectivity and storage volume: a total of 622 m³ of freshwater from the fire hydrant was injected into F-3A and 168 m³ of water produced from F-2A, with systematic sampling and analysis of major ions, trace elements, and stable water isotopes. This enabled characterization of the in-situ groundwater composition and assessment of scaling, corrosion, and environmental risks.

A CO_2 acidization experiment was then carried out in Layer 6c. Over 17 days, CO_2-enriched water (5.6 t CO_2 mixed with 214 t freshwater) was injected into F-3A to dissolve calcite cement and enhance permeability. This was followed by a 90-day backflushing program with simultaneous injection at F-2A and production at F-3A, enabling removal of dissolved minerals and avoiding backreaction and re-clogging. Produced water quality monitoring confirmed compliance with regulatory limits for industrial wastewater and safe discharge into the on-site sewage system.

Finally, initial numerical modelling was initiated to couple chemical and hydraulic effects of acidization, constrained by datasets from both the circulation test and backflushing operations. These preparatory steps laid the foundation for the comprehensive modelling campaign in Phase 3.

In Phase 3 (2024–2025), reactive transport modelling with PFLOTRAN was used to calibrate the field data and to analyse flow and transport processes under different scenarios of heterogeneity and stimulation.

5.2.10 Results

5.2.10.1. Phase 1

The boreholes of the Geospeicher Forsthaus project show that the site is covered down to a depth of ~240 m (~312 m a.s.l.) by Quaternary unconsolidated sediments. Prior to drilling, the transition from the Quaternary to the USM was expected at around 180 m. The Forsthaus project is situated within a narrow, incised and overdeepened valley of the former Aare glacier. Hence, the shallower and younger USM section, as exposed at surface at other sites in the town of Bern, has been eroded.

Below the Quaternary, approximately 280 m of USM sediments were explored by drilling. These comprise a heterogeneous succession of coarse- to fine-grained sandstones (channel-belt fills), clay-rich siltstones (floodplain deposits), and weathered paleosols, documenting - as anticipated - a paleo-fluvial, meandering drainage system in the Alpine foreland. Within these channel-belt sandstone layers, there is a large heterogeneity of permeability and porosity in the vertical direction and a moderate heterogeneity in the horizontal direction. Individual layers range in thickness from 0.5 to 15 m, with a cumulative thickness exceeding 50 m (see Figure 124).

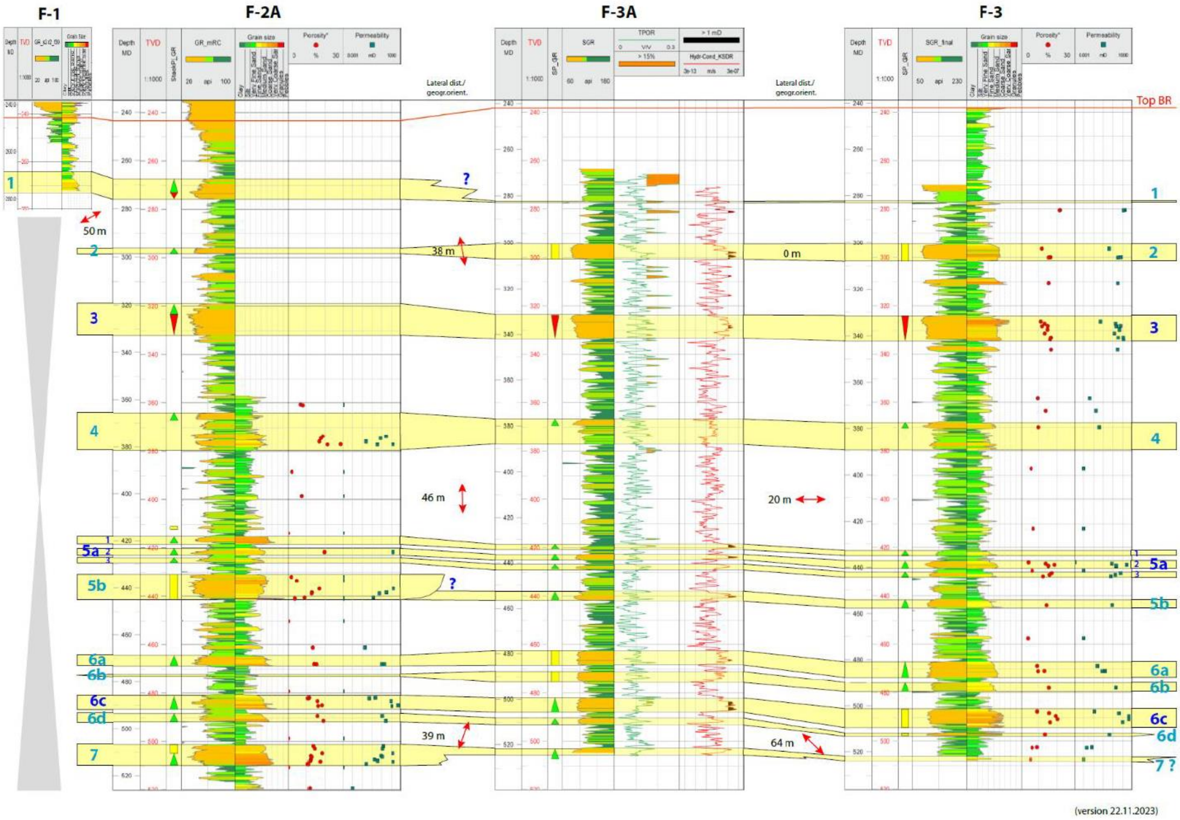

Figure 124 - Correlation of the main reservoir units in the investigated USM, based on gamma-ray logs and grain-size profiles.

Gamma-ray logs and grain-size observations in the cores allow a detailed correlation of the sedimentary succession between the three boreholes. In total, seven medium- to coarse-grained sandstone intervals (RG1–7) were identified. Mineralogical parameters of the channel-belt sandstones show little variation and compare well with those reported for other USM samples in the Swiss Molasse Basin. At Forsthaus, the channel-belt sandstones are dominated by quartz (~50 wt.%) followed by similar amounts of K-feldspar, plagioclase and calcite (10-20 wt.%). The clay content is between 4-13 wt.%. Analysis of sedimentary structures enabled the determination of the approximate spatial orientation of the channel-belt sandstones, forming the basis for a numerical 3D model of sandstone horizon distribution (channel-belts) beneath the EFZ (Figure 125).

Measured porosities range from 1.8% to 21.7%, and permeabilities from 1.5 µD to 587 mD (1.4E-18 to 5.8E-13 m²). The potential storage sandstones show permeabilities in the range of 20 to 50 mD. The mean uniaxial compressive strength (UCS) is 31.9 MPa with a standard deviation of 16.3 MPa. Hydraulic tests indicate a hydrostatic pressure in the USM at ~515 m a.s.l., corresponding to 39 m below surface, and a hydraulic conductivity between 1E-8 and 5E-6 m/s.

The hydraulic conductivity of the Quaternary sands at depths between ~200 and 240 m is at least one order of magnitude higher (≥7E-5 m/s) than in the USM.

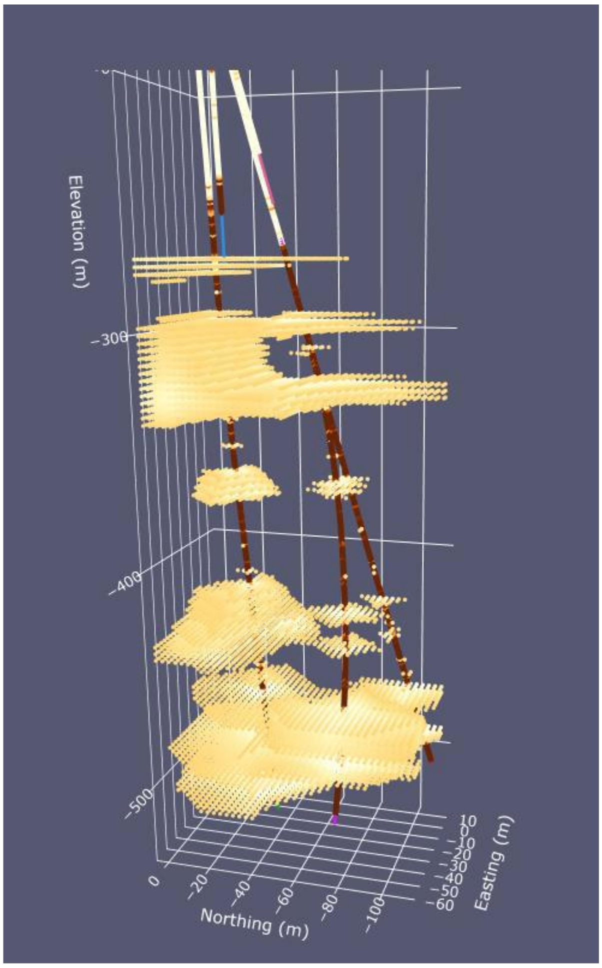

Figure 125 - 3D model of the channel-belt sandstone horizons in the USM, based on gamma-ray measurements and grain-size profiles.

5.2.10.2. Outcomes and Recommendations for Phase 2

Phase 1 provided the key results required to justify the continuation into Phase 2 and to define recommendations for the subsequent work. In particular:

This first drilling campaign confirms the existence of laterally continuous and homogeneous channel-belt sandstone layers in the depth interval of ~240–520 m (= USM), each up to 15 m thick, representing potential storage units for the heat storage project. The cumulative thickness of the channel-belt sandstones exceeds 50 m, meaning that the targeted sandstone volume was achieved.

These reservoir units are characterized by porosity and permeability values that justify further hydraulic testing. They show the same correlation trends as values known from other projects in the greater Bern area. However, the highest values of porosity and permeability in the channel-belt sandstone units in Burgdorf and Bern Train Station are absent in Forsthaus or Bassersdorf (see discussion below).

A robust porosity/permeability prediction based only on the lithotypes (grain size) is not possible.

The mineralogical composition and the geomechanical parameters measured in the sandstone units allows further stimulation measures, such as acidization or radial drilling, to enhance porosity and permeability.

The Base Quaternary provides a potential alternative storage horizon in case the permeabilities in the USM prove insufficient.

5.2.10.3. Phase 2

The cross-hole circulation test between wells F-3A (injection) and F-2A (production) demonstrated hydraulic connectivity across approximately 40 m in Layer 6c (Figure 126 a). After ~55 days of continuous injection, chemical and isotopic analyses revealed that 1.8–3.5% of the water produced at F-2A consisted of the injected freshwater, with the remainder being pristine, highly saline formation water (Figure 126 b). This delayed but measurable breakthrough provides direct evidence of hydraulic connection and water mixing processes within the reservoir. It also confirms that transport occurs preferentially along thin, high-permeability pathways. Taken together with the observed pressure and flow conditions, these results quantify the effective pore volume and highlight the strong heterogeneity of the flow system. A generalized porosity–permeability correlation could not be established due to heterogeneity between wells. This was later confirmed by modelling in Phase 3.

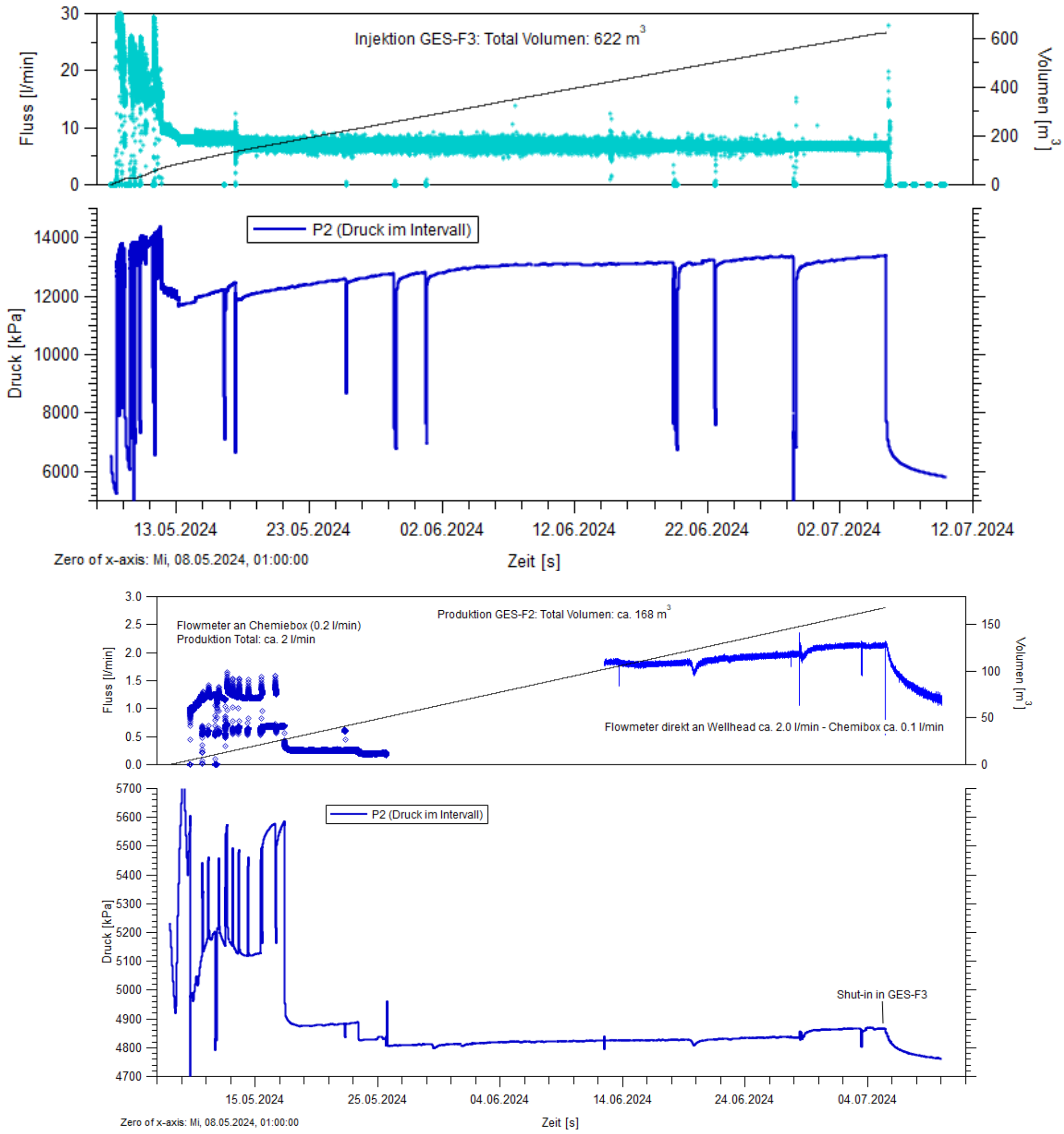

Figure 126 - a) (upper figure) Volume of fire hydrant water injected into well F-3A, the corresponding injection rate and water pressure along the packed-off interval of sandstone Layer 6c, all as a function of time. b) (lower figure) Volume of water produced from well F-2A, the corresponding production rate and the water pressure along the packed-off interval of sandstone Layer 6c, all as a function of time.

5.2.10.3.1. Circulation test and hydrochemical characterisation

The key results are:

- The 5 m thick channel-belt sandstone Layer 6c behaves as a fully connected aquifer over a distance of ~40 m.
- The accessible storage volume for hot water injection in this thin layer amounts to at least 600 m³.
- The in-situ groundwater is of Na-Cl type with high salinity (12.4 g/L), inherited from marine conditions of the Upper Marine Molasse. It represents an almost stagnant aquifer with a mean residence time of several million years (see below).
- The pristine, in-situ groundwater is saturated with respect to calcite and is fully anoxic, with elevated aqueous iron concentration (~2 mg/L).
- Strain measurements with fiber-optic cables along the F-2 well show that the USM behaves largely deformable during high-pressure step-tests.
- No micro-seismicity was detected during the injection test.
- The observed deformation behaviour implies that any induced fractures will quickly close again.

5.2.10.3.2. Hydrochemical effects of acid stimulation

Injecting CO_2-enriched water into Forsthaus well F-3A to enhance permeability of sandstone Layer 6c had some effects:

Injection of CO_2-enriched water into Layer 6c dissolved at least 900 kg of calcite cement. Dissolution of calcium was coupled with cation exchange - sodium cations sorbed onto clay minerals were displaced by calcium cations - thus enhancing the amount of calcite removed.

Produced water quality consistently met regulatory requirements and was safely discharged.

A 90-day backflushing program removed dissolved minerals and prevented any backreaction and re-clogging of the reservoir.

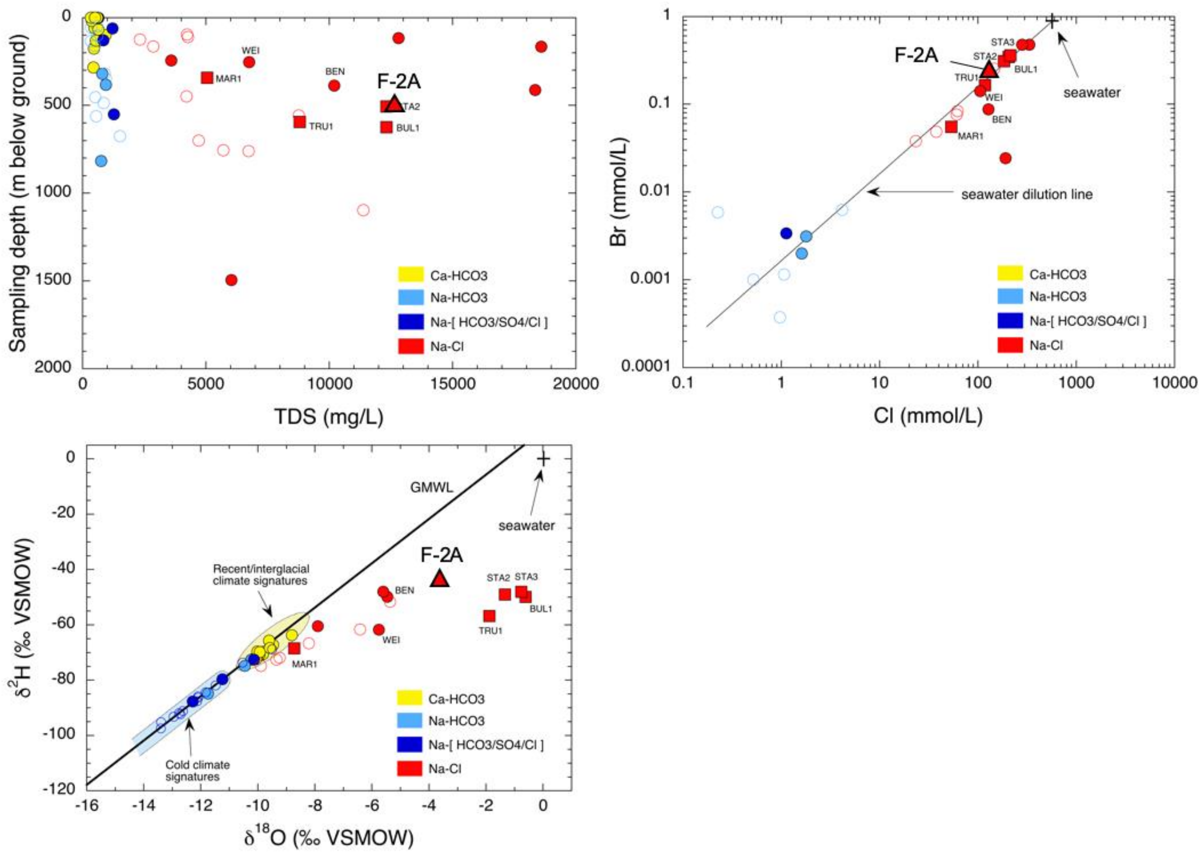

Figure 127 - Cross-plots illustrating the behaviour of selected hydrochemical parameters in groundwaters collected from the Malm (closed symbols) and Tertiary aquifers (open symbols) in the Swiss Molasse Basin. All plots are taken from Nagra (2024) and supplemented with data for the pristine, in-situ groundwater naturally occurring in Layer 6c at Forsthaus (red triangles). Filled circle and square symbols represent samples reported in Waber & Traber (2022) and collected during the recent Nagra deep drilling campaign (Nagra, 2024). The pristine, in-situ groundwater naturally occurring in Layer 6c at Forsthaus is plotted as a red triangle.

5.2.10.3.3. Model age determination of USM formation water

The in-situ groundwater produced from Layer 6c was further analysed for ^{81}Kr to estimate its residence time. This yielded a low ^{81}Kr abundance (18.5 ± 0.6 pm^{81}Kr) corresponding to a high ^{81}Kr model age of about 560’000 years. As the groundwater sample is most likely a mixture between very old marine / brackish and meteoric waters that have only minor differences in their total Kr contents, the ^{81}Kr model age is interpreted to reflect the mixing proportions and respective residence times of the two components. Based on stable water isotopes (Figure 127), the younger meteoric component must have infiltrated in a previous interglacial period and hence at least 115’000 years ago (Schlüchter et al., 2021). In contrast, the residence time of the marine / brackish component is on the order of at least several millions of years and likely ^{81}Kr free. The very high residence times of both groundwater components demonstrate the excellent hydraulic isolation of Layer 6c.

5.2.10.3.4. Monitoring

Fiber optic cables and double packer systems enabled high-resolution monitoring of pressure, temperature and strain during the tests.

5.2.10.4. Phase 3

Numerical modelling with PFLOTRAN was carried out to reproduce the hydraulic and hydrochemical processes observed between wells F-2A and F-3A. The modelling aimed to test different conceptual scenarios of sandstone heterogeneity and stimulation in order to achieve optimal agreement with all observational constraints.

Numerical reactive transport modelling revealed thin preferential flow paths (~10 cm combined thickness), with only ~50 % of the layer hydraulically active.

According to the simulation results, the permeability increase of Layer 6c by CO_2-injection was almost negligible and restricted to the thin (~10 cm) but highly permeable preferential flow channels. Since the numerical model is underconstrained with respect to input data, the magnitude of the permeability enhancement and its spatial distribution cannot be fully quantified.

Moreover, the simulations clearly show that perforation of the well casing by micro-turbine sidetrack drilling created a zone of < 1 m radius and 0.6 m thickness around the wellbore of F-3A where the permeability increased by a factor of about 6. The extent of this zone is sufficient to hydraulically connect well F-3A with the thin but highly preferential flow channels present in Layer 6c.

Although more than 900 kg of calcite was dissolved by CO_2-injection, the overall porosity increase was minor (< 1 vol.%).

The simulations revealed that the chemical and hydraulic effects of CO_2-enriched water injection depend strongly on the hydraulic architecture between the wells, particularly the distribution of preferential flow paths and inactive layers. As Layer 6C shows different sand- and clay-rich sequences in each well, the inter-well architecture cannot be defined precisely. With the current dataset, a generalized quantitative porosity–permeability relationship cannot be derived.

A comprehensive hydro-geochemical characterization of sandstone Layer 6C is derived which can also be applied to other sandstone layers within the USM.

Overall, the modelling confirmed that only macro-dispersion through discrete high-permeability layers, combined with a stimulated zone around F-3A, could consistently reproduce both, the measured pressure conditions and the breakthrough curves.

The numerical simulations also showed that a generalized porosity–permeability relationship cannot be derived for USM sandstones, due to strong heterogeneity and preferential flow paths.

5.2.10.5. Summary Main Results

In line with the project application, the project explicitly addressed two key questions: the suitability of the USM as a geothermal play and/or for geothermal heat storage.

The investigations confirmed that the USM contains several channel-belt sandstone layers ("Rinnengürtel") of sufficient thickness and lateral continuity, and that hydraulic connection between wells was established over more than 40 m. The targeted sandstone volume was therefore achieved.

The geothermal gradient of 31–35 °C/km supports suitability for geothermal use. Although no pronounced positive temperature anomaly is present within the upper 500 m, this alone does not allow the exclusion of a hydrothermal system at greater depth, particularly within the potential Muschelkalk aquifer.

Transmissivity of the channel-belt sandstones below the Forsthaus is significantly lower than at comparison sites such as Burgdorf or Bern Train Station. This is directly related to the lower porosity and permeability values that remain always below 22% and 600 mD compared to the other sites. This illustrates the spatial variability within the USM. Hydraulic stimulation increased transmissivity along thin (~10 cm) preferential flow channels. On the scale of the tested sandstone layer, however, it remained unaffected at ca. 2 x 10-7 m2/s and hence below thresholds for economic operation.

The USM channel-belt sandstones are hydraulically very well insulated from the overlying Quaternary aquifers. Despite a vertical separation of only about 250 m, the measured data confirms long residence times of the formation water and excellent hydraulic and chemical isolation. Such properties are key attributes for long-term underground storage performance.

Hydrochemical analyses revealed highly saline, anoxic groundwater saturated with calcite. Risks of calcite and iron hydroxide scaling, as well as corrosion, are expected in surface installations but can be controlled with inhibitors and appropriate materials.

Modelling showed that only macro dispersion through discrete high permeability layers can reproduce observed breakthrough curves, highlighting strong lateral heterogeneity between wells.

Phase 1 results showed that porosity and permeability values vary strongly between lithotypes. No robust correlation between porosity and permeability could be established, indicating that lithotype (grain size)-based predictions of reservoir quality are unreliable. Phase 2 and 3 results confirmed that even with acidization and modelling, no generalized quantitative porosity–permeability correlation could be derived, due to heterogeneity between wells and preferential flow paths.

In the lowermost section of the Quaternary an adequately thick interval was encountered, whose natural hydraulic conductivity is significantly higher than in the USM.

All publicly accessible reports can be found under the keyword “Forsthaus Geospeicher” at assets.swissgeol.ch

Direct link: assets.swissgeol.ch – Forsthaus Geospeicher

The original borehole data are available via the following links:

Borehole Geospeicher Forsthaus 1 (GES-F1): https://boreholes.swissgeol.ch/49502/location
Borehole Geospeicher Forsthaus 2:

- GES-F2: https://boreholes.swissgeol.ch/49537/location
- GES-F2A: https://boreholes.swissgeol.ch/49503/location

Borehole Geospeicher Forsthaus 3:

- GES-F3: https://boreholes.swissgeol.ch/49504/location
- GES-F3A: https://boreholes.swissgeol.ch/49505/location

5.3 Spatial Multi-criteria analysis for favorability assessment of HT-ATES systems in the Swiss Molasse Plateau

This chapter resumes the results of the study carried out to map technical potential and expansion in Switzerland as part of WP6 of the Swiss proposal and Task 1.3 Screening of national potential for UTES coordinate by UniGe of the European project and associated Deliverable 1.3 which is available in Appendix12.

The work carried out in this task comprise a screening of the national potential for UTES in the Netherlands, Switzerland, Germany, Denmark, and France. Geological, hydrogeological, geochemical, etc. (sedimentary basins, mining basins, host rock formations) have been analysed to identify and characterize locations with more favorable conditions for different types of UTES systems.

In Switzerland a spatial multi-criteria play-fairway framework was implemented focusing on the potential of implementation of HT-ATES systems in two main geologic units: the Cenozoic sediments (i.e., target of the Bern project) and the fractured Upper Mesozoic carbonates (i.e., target of the Geneva project), the latter being of interest considering the heterogeneous permeability distribution in such fault-controlled reservoir across the Molasse Plateau. Despite the two sites in Geneva revealed to be challenging for HT-ATES, they can be considered as “extremes” for HT-ATES in terms of hydraulic performances, but an entire range of intermediate conditions can be identified across the entire Swiss Molasse Plateau. Subsurface data down to 2000m in depth as well as surface constraints have been combined to produce a set of favorability maps representing different potential scenarios.

This study focusses on the development of a framework for the assessment of the favorability for HT-ATES development in the Swiss Molasse Plateau (SMP) centered on multi-criteria spatial analysis based on the combination the geologic plays controlling the geologic features suitable of interest for HT-ATES

implementations and the energy system components of excess heat and heat demand as well as proximity to thermal networks and waste incineration plants. The choice of focusing on the SWM was driven by the availability of subsurface data as the 3D geologic model available from Swisstopo only covers this region.

- Two main reservoirs have been identified in the Cenozoic Molasse (e.g., target of the Bern pilot site) and the Upper Mesozoic carbonates (e.g., target of the Geneva pilot site). Additionally, a minimal underground temperature threshold is set to 25˚C which is the temperature commonly considered as separating low temperature ATES from HT-ATES systems. These two units show different lithological, petrophysical and hydraulic conditions, locally enhanced by lithological heterogeneities in the Cenozoic Molasse and by enhanced fracture conditions thanks to the presence of fault corridors in the Mesozoic. A maximal depth of 2000m was set as boundary as it was arbitrarily considered as a reasonable depth for the techno-economic favorable implementation of HT-ATES systems (Figure 128).

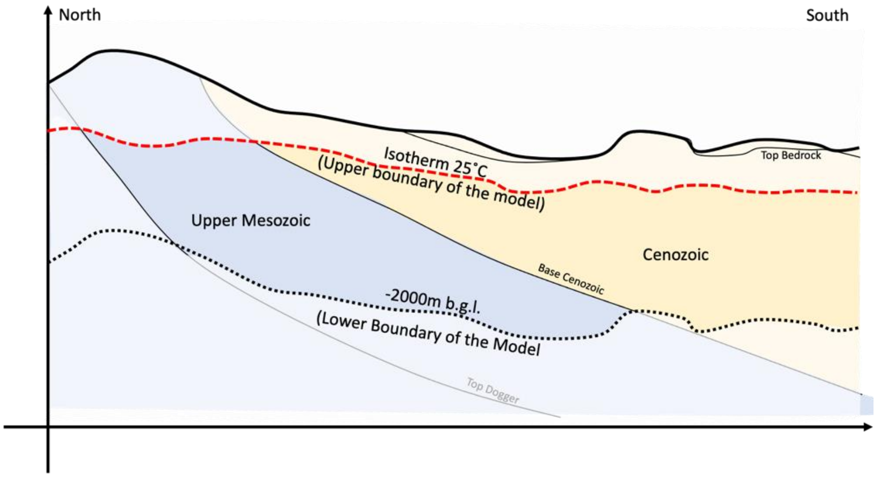

Figure 128 - Sketch of the subsurface of interest along a hypothetical N-S oriented cross-section across the

The framework can be broken down as follows:

- First, a geothermal play analysis approach was applied to identify and weight the subsurface elements controlling the circulation of fluids in the area.
- Secondly a data reliability assessment was carried out based on the proximity from the main source of subsurface data (i.e., exploration wells and 2D-3D seismic surveys). Weighting was given to each dataset according to Table 27, to consider, the proximity and the quality of the information that each dataset can provide to assess the favorability.

Table 27 – Criteria for data reliability assessment

Data Type	Proximity	Score
Exploration wells	0-200 200-1000	10 Linear interpolation 1-10

	>1000	0
2D seismic	0-200 200-15000 >15000	7 Linear interpolation 1-7 0
3D seismic	-	9

The third step was to compute the storage capacity according to the 3D geometries and temperature distribution from the GeoMol model and petrophysics properties from literature (Guglielmetti and Moscariello, 2021 and references therein) as shown in

Table 28

Table 28 – Parameters used for storage capacity calculations

Stratigraphic units	Min	Mean	Max	Faulted
Cenozoic permeability (mD/m^2)	0.1 / 9.869×10^{-17}	13.1 / 1.293×10^{-14}	50.75 / 5.009×10^{-14}	-
Cenozoic density (kg/m^3)	2100	2300	2650	-
Mesozoic permeability (mD/m^2)	0.01 / 9.869×10^{-18}	3.5 / 3.454×10^{-15}	350 / 3.454×10^{-13}	300 / 2.961×10^{-13}
Mesozoic density (kg/m^3)	2500	2600	2700	2600

- The fourth step was to extract the excess heat data (Zuberi et al., 2018) with heat temperature< 120˚C a and carry our proximity analysis with respect to the thermal networks and waste incineration plants (Table 29).

Table 29 – Input criteria for proximity from thermal networks and waste incineration plants

Data Type	Proximity	Score
Thermal Networks	0-1000 1000-2500 2500-5000 5000-10000	Linear interpolation 1-10
Waste Incineration Plants	0-1000 1000-2500 2500-5000 5000-10000	Linear interpolation 1-10

- The final step was then to integrate the different favorability into a combine favorability index, calculated, multiplying the proximity score by the weight

$$I(x_{ij}) = x'_{ij} \cdot w$$

The final favorability index that combines all the individual favorability indexes is given by the weighted average scheme:

$$I_{comb} = \frac{\sum_{i=1}^{n} I(x_{ij})}{\sum_{i=1}^{n} w}$$

The results of the favorability assessment are presented in Figure 129

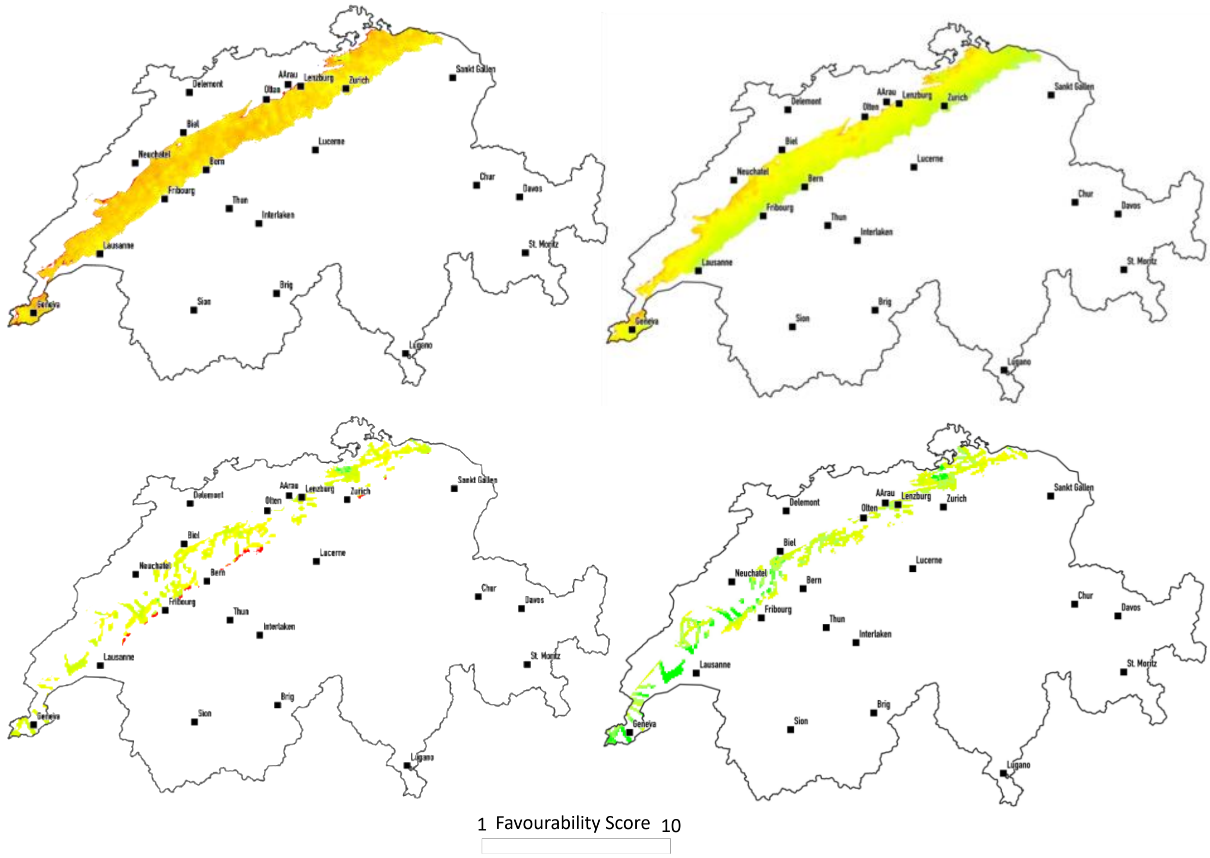

Figure 129 - Favorability assessment for the Cenozoic and faulted Mesozoic reservoirs

The results of the scenario modelling show how the Cenozoic has some theoretical potential storage in the southern part the study area, where also some major cities are located (Zurich, Bern, Lausanne) for the scenario that account for the maximum value of permeability (300mD) also because of the large thickness of the Cenozoic sediments whereas in case of permeability values below. It must be pointed out that in this study we considered as potential reservoir the entire thickness of the Cenozoic sediments, however we know large vertical and lateral lithological heterogenies locally characterize this Unit, and only part of the entire unit is suitable for storage. Therefore, a more detailed characterization of the *net-to-gross* assessment will need to be performed for an accurate assessment at a more site-specific scale. For the average permeability value of 3.5 some regions the same region also shows some storage potential. However, the low permeability scenario (0.1 mD) can be excluded, as also confirmed supported by the transmissivity analysis, not reaching the threshold of $5\cdot10^{-13}m^3$. This same result applies to the faulted Mesozoic, where the worst-case scenario in terms of permeability values (0.01 mD) represents a tight reservoir not suitable for any fluid circulation. According to the results for the two other scenarios (permeabilities of 3.5 and 350 mD), faults can be promising targets as shown in Figure 3-19. According to the data available, fault structures can be suitable as targets in Aarau, Biel and Geneva. However, as demonstrated by the GEo-01 well in Geneva, high permeabilities characterizing fault corridors lead to high wellhead pressure and natural artesian flow being, therefore, a limiting factor for storage. A more detailed characterization of the hydraulic properties of the fault structures will be necessary in the future to improve such type of assessment.

5.4 Regulatory Framework for HT-ATES in Switzerland

In Switzerland there is not a specific regulatory framework for HT-ATES systems and the Swiss legislation applied to geothermal project is based on the Federal Ordinance on Water Protection (OEaux, appendix 2, chapter 21, paragraph 3): "*The injection or withdraw of heat must not alter the natural temperature of the groundwater by more than 3°C; very limited local temperature fluctuations are considered under reserve"*. In its 2009 implementation aid, the Federal Office for the Environment (FOEN) sets out standard obligations regarding the exploitation of groundwater heat indicating that *"The variation may be greater than 3°C in the immediate vicinity, i.e., within a radius of up to 100 m*".

These requirements are listed and detailed in the standard SIA 384/ 2015 (Utilisation de la chaleur de l'eau souterraine) where it is stated that "The temperature differential between the ground water in the aquifer and the natural seasonal temperature over a wide area must not exceed 3K. Within the immediate perimeter of a maximum of 100m around the reinjection point, the differential may be greater than 3K". This standard adds that *"the nature of the water will be examined in detail in the event that (...) the difference in temperature between the production and the injection points exceeds 10K"*, which implies that a 10K temperature difference can be considered, provided that the ΔT_{max} of 3K to 100m is respected seasonally.

Some cantons, such as Zurich, have a strong differentiation between permits for hot and cold uses. For example, local groundwater cooling of up to 7K for building heating is permitted in view of global anthropogenic warming.

It should be noted that the SIA 384/7 standard explicitly excludes from its scope the seasonal storage of heat or cold and groundwater at temperatures higher than 25°C.

To our knowledge, the legislation is not explicit for aquifers whose temperature is higher than 25°C (i.e., from about 400m below the surface). In its practical instructions of 2004, the FOEN recommends that for *"the exploitation of geothermal energy by deep drilling (...) each case must therefore be examined individually, to determine feasibility, to lay down the conditions to be met and the prescriptions to be applied. It is then necessary to ensure that the equipment used is compliant and that personnel are trained to deal with unforeseen circumstances. "(*OFEFP, 2004). The term "*deep drilling"* is not strictly defined.

5.4.1 Application

To be more specific on the application of these regularity framework in Switzerland, the federal water legislation requires a maximum of 3K ΔT for discharge into surface or reinjection into ground water. The FOEN regulations and SIA 384/7 interpret this 3K value as a maximum variation within a radius of 100m from the point of reinjection (if we consider for instance deep hydrothermal projects). Without further clarification of the duration of the fluctuation from 3K to 100m, it is generally accepted in modelling of the thermal plume propagation withing the that the thermal plume after 30 years of operation should be a maximum of 3K at 100m. The SIA 384/7 standard specifies that "depending on the groundwater flow or the natural groundwater flow, the calculation must be made on a seasonal or long-term basis, i.e., over the entire lifetime of the installation".

The different potential environmental impacts on surface water, shallow groundwater, deep groundwater, climate, and CO_2 are not distinguished in the application of the ΔTmax rule of 3K. There is also no distinction in the law between shallow or medium/large ("deep") geothermal energy for the application of the ΔTmax of 3K rule.

It seems obvious that the basic principle of water legislation is to protect the quality and drinkability of water. As such, deep (>400m) and saline aquifers are of little interest and could quite easily be used with ΔT higher than 3K. Indeed, the thermal recovery of this type of reservoirs would not a priori have a significant impact on the quality of a resource of little interest but would respond favorably to the energy challenges by limiting CO2 emissions (substitution of fossil fuels). However, the question of the reinjection and the assessment of its impacts/risks of modifying the thermal (and therefore potentially chemical) groundwater characteristics remains unresolved.

Finally, certain elements of the legislation are left to the discretion of the cantons, such as the reinjection strategy. For example, in Chapter 5.3 of its recommendations, the FOEN advocates reinjection primarily into the unsaturated zone and secondarily into the saturated zone, thus promoting a buffer effect at the thermal level. For its part, the SIA standard states that "the choice of the type of reinjection strategy depends on local conditions and the requirements of the approval authority". However, the same standard (Annex D) specifies that infiltration must take place into the groundwater, to avoid interaction with the air and in principle avoid physico-chemical problems (precipitation, clogging, etc.). Therefore, both approaches are possible but do not have the same effect on ΔT_{max} at 100m and depend on the assessment of the approval authority. But his applies to shallow applications.

For deeper projects, a strict application of the current value of ΔT_{max} from 3K to 100m may eventually block projects such as those operating in other countries but in very similar geologic/hydrogeologic context such as the Paris Basin.

Let us take as an example a borehole at 1'400m with a wellhead temperature of 60°C and a flow rate of 20 l/s. A ΔT of 25K would provide 2 MWth of geothermal energy on the surface, to be injected into a DHN with suitable temperatures. Injection into a multi-resource thermal network of 5 MWth (10 GWh of annual consumption) would make it possible to substitute about 1,500 tons of CO2/year compared with traditional gas boilers. If the 3K ΔT at 100m were applied, the production would be limited only 0.4 MWth geothermal energy which would have a negative impact not only on the carbon footprint reduction performance but mostly on the economic viability of such project.

It should also be remembered that the Riehen geothermal doublet (drilled in 1989) was carried out within the legislative framework of the ΔT_{max} of 3K and that the temperature difference between the producer well (1'550m) and the injector well (1'250m) can rise up to 40K in winter (http://www.erdwaermeriehen.ch/de/geothermie/index.php). With 15 GWh of geothermal energy recovered annually, the environmental gain in Riehen is high, in the order of 3,000 tones of CO2/year. Current optimizations measures and the development of the CAD network will even make it possible to recover up to 25 GWh/year of geothermal energy, i.e., 5,000 tons of CO2/year, assuming 100% gas substitution.

Since 1994, the connection of geothermal energy to the DHN in Riehen has saved about 50'000 tons of CO2 and to our knowledge, no negative impact on groundwater has been noted.

Nevertheless, a Riehen-type project still represents a potential saving of 1/10'000 of Switzerland's total greenhouse gas emissions.

Within this framework and to enable the development of deep geothermal projects, it might be desirable a certain degree of flexibility to derogate from certain current limits set, and in the case of medium to deep projects in Switzerland, it might be interesting to set up a working group with project leaders, the engineering offices involved, cantons and the Confederation in order to define the limits of the system and to propose management, operating and monitoring solutions for new projects. Ultimately, the elements analysed in this framework could make it possible to draw up guidelines for projects with medium/large depths of heat use.

The comparison of existing regulatory frameworks for HT-ATES systems across several European countries thanks the HEATSTORE project has shown that the following key elements are necessary for an efficient development of HT-ATES projects :

- Clearly and well-defined workflows between project developers and authorities
- Existing legal framework on national level but implemented and adapted on a regional level through local competent authorities
- Well documented, up to date, and easily accessible public databases
- Long term development schemes (masterplans) on a regional level based on a global vision shared and driven by both the authorities and project developers

- Compulsory monitoring of production data (temperature, pressure, pH, water analyses, etc.) coupled to an appropriate history-matching process based on an iteratively updated 3D thermo-hydraulic model of the underground

5.4.2 Conclusion

Swiss environmental legislation aims to protect the local and global environment. The purpose of the Water Act is to protect surface and ground water and to ensure that the various uses of water are sustainable. The energetic use of water can have a negative impact on the immediate environment, but at the same time it allows the substitution of fossil fuels and thus acts against global warming (CO_2). The reduction of electricity consumption thanks to a better efficiency of the systems also makes it possible to reduce the impacts on water (heating of rivers due to nuclear thermal power stations, disturbance of rivers due to the turbining of hydroelectric dams. For instance, a borehole at 1'400m could potentially substitute about 1'500 tons of CO_2/year, equivalent to the consumption of more than 500'000 liters of fuel oil per year.

Moreover, when using groundwater, even if the principle of setting a temperature limit for heating and/or cooling at a defined distance between two wells is not fundamentally bad, the static values often do not consider the particularities of the local hydrogeology (heterogeneity, water flow in the aquifer, thermal conduction, etc.) and the existing thermal impacts (anthropogenic or natural). A certain flexibility in the authorities' approach therefore is necessary, possibly based on a dual legislative approach with specific standards for shallow geothermal energy (<400m) and others for medium or deep geothermal energy (>400m), as practiced in several countries.

In Switzerland, for shallow geothermal energy, the current application of the ΔT_{max} from 3K to 100m is legitimate but a strict application of ΔT_{max} from 3K to 100m could compromise the implementation potential of deep projects for DHC networks.

Within this framework and to enable the development of deep geothermal projects, it might be desirable a certain degree of flexibility to derogate from certain current limits set, and in the case of medium to deep projects in Switzerland, it might be interesting to set up a working group with project leaders, the engineering offices involved, cantons and the Confederation in order to define the limits of the system and to propose management, operating and monitoring solutions for new projects. Ultimately, the elements analysed in this framework could make it possible to draw up guidelines for projects with medium/large depths of heat use.

6 Conclusions

The HEATSTORE project provided a unique opportunity to explore the possibility of implementing HT-ATES solutions in Switzerland, thanks to the continuous collaboration established within the Swiss consortium and with the international partners.

Energy storage is one of the priorities to decarbonize the global energy system, and HT-UTES systems can strongly contribute to the Swiss energy strategy. In the Swiss project, excess heat storage in aquifers has been tackled on two sites in Geneva and Bern, focusing on two main reservoirs: the Cenozoic Molasse sediments and the Upper Mesozoic carbonates. These two geologic units are the main potential reservoirs across the Swiss Molasse Plateau, where most of the excess heat and heat demand are distributed.

HEATSTORE allowed the implementation of a techno-economic assessment framework in Geneva based on integrating subsurface and energy system data. The concept of the Geneva site was to recover excess heat from a waste incineration plant, store it in the Upper Mesozoic carbonates on a seasonal basis and eventually deliver it according to the demand configuration. The framework evolved based on a stepwise approach to produce HT-ATES performance prediction scenarios according to the evolution of the data availability. Data from the literature were initially used to set up the framework and verify how subsurface criteria (e.g., geologic geometries, petrophysics, and hydraulic properties distribution) could have been combined with energy system data focusing on the distribution of excess heat and heat demand (temporal, geographical, temperature ranges of excess heat and operating DHN). 3D static reservoir models were developed at GEo-01 and GEo-02 exploration well locations for the two study sites. Static models picture the 3D architecture of the main geologic features (geologic units and faults). They are populated with a set of petrophysical properties such as porosity and permeability, which control the fluid flow in the reservoir, hence the performance of the HT-ATES system. Based on the initially available data at the two well sites, the focus for the static model was the fault corridors cutting the Upper Mesozoic Carbonates, responsible for locally enhancing porosity and permeability distributions.

Subsequently, dynamic models (TH-HM-THC), computed combining static models and energy system data as inputs, allowing to:

- Identify optimal operating scenarios for efficient heat storage and recovery
- Assess potential soil mechanics effects (ground deformation) due to seasonal cycles of storage
- Assess the activation of water-rock interactions, potentially leading to mineral dissolution and precipitation in the reservoir and proliferation of organic matter

As new data became available from the GEo-01 and GEo-02 exploration wells, the entire set of models was updated and calibrated, resulting in more accurate predictions. The results of the two wells demonstrated the heterogeneous distribution of fault-controlled fractures. The GEo-01 is 744m deep and shows a natural artesian flow (55l/s at 34˚C and 8 bars of wellhead pressure). These conditions represent an extremely interesting hydrothermal resource whose optimal utilization is now under evaluation by SIG. The reservoir produces from fractures mainly from the Lower Cretaceous (~70%) and partially from the Upper Jurassic (~30%). The permeability has been quantified to an average of 300 mD, which, combined with the high flow rate and wellhead pressure, makes this site challenging for thermal storage implementation. The GEo-02, 1456m deep, is characterized by a low natural artesian flow (0.3l/s at 18˚C and 12 bars wellhead pressure), suggesting low natural reservoir transmissivity for thermal storage implementation.

Despite the two wells proving to have challenging hydraulic conditions for storage solutions, they delivered a unique set of data. These data allowed the implementation of a wide variety of subsurface architecture scenarios, which can be considered extreme cases of low favorability for HT-ATES. However, the faulted Mesozoic is widespread across the entire Swiss Plateau in different geometry, architecture, and petrophysics configurations, making these units worth further investigations in Geneva and across the entire Molasse Basin. New potential targets have been identified in other formations, such as in the karstified Top Lower Cretaceous carbonates of the Siderolithic Formation at GEo-02. This formation is spatially discontinuous and heterogeneous, but it is laterally confined by the tight carbonates and on top by the Molasse sediments, making this volume potentially interesting for storage. However, its geometry is not fully constrained and will be defined only after interpreting the 3D seismic data collected by SIG in September 2021. Additionally, its mineralogical composition and petrophysical properties are poorly understood and are now under investigation by the University of Geneva.

To complement the deep boreholes in the Geneva basin and to be able to perform heat storage experiments, the University of Neuchâtel implemented a field lab in Concise (VD - Switzerland) in Upper Mesozoic limestone formation, analogs to the carbonates investigated in Geneva. Three 50 meters deep boreholes drilled into the Lower Cretaceous, and Upper Jurassic fractured and karstified limestones. The objectives of the field lab activities were to characterize the thermo-hydraulic response of the fracture and karstified limestone rock mass to heat storage. A series of hydraulic and thermal tests have been carried out in the boreholes and complemented by image and flow logs. Tracer dilution tests were performed to assess natural flow conditions and were monitored in-situ with pressure and temperature gauges and fiber optic-based distributed temperature sensing. The results show that the system's hydraulics is highly heterogeneous and that a few structures dominate the flow. The intersection between bedding planes and steeply dipping fractures leads to control of the position of the dominant flow paths. Somewhat direct pressure connections link the wells, but the flow paths are complex, as revealed by the difficulty of transmitting heat and tracer between adjacent wells. Distinct piezometric levels also reveal this over a few meters along the wells.

In these conditions, heat storage and recovery are primarily dominated by the dominant flow path geometry. In the case of the Concise test site, channelized planar flow paths drive the heat transport and exchange behavior. This suggests that hydraulic testing is insufficient for characterizing a target reservoir for heat storage. Thus. Thus, tests with tracers (heat or otherwise) are required to assess transport and exchange characteristics. This also suggests that simulators able to include local geometrical heterogeneities are required for assessing the design and sustainability of subsurface heat storage in fractured and karstified limestone aquifers. Appropriate geological conditions to build an HT-ATES system in Geneva were not encountered (either too high permeability in Geo-01 or too low at GEo-02). Eventually, the field laboratory resulted in a partial recovery of the hot water and tracer injected, demonstrating that the Mesozoic carbonates could be suitable for ATES systems.

In addition to the storage-recovery potential predictions via modeling and assessed via the Concise field lab, the availability of new data resulting in updated models served as inputs for economic analysis. The impact of subsurface conditions and energy system configuration on the Levelized Cost of Heat (LCOH) of HT-ATES systems was assessed from a techno-economic perspective. Analysis of the CO_2 intensity was also performed, revealing that HT-ATES systems can play a role in decarbonizing the Geneva energy system. Results show that, subject to subsurface constraints, the nominal capacity ranges from 0.4 MW to 81 MW, with aquifer permeability and thickness being the significant control variables. A minimum transmissivity of $1.5 \cdot 10^{-13}$ m^3 is considered to be the minimal economically viable threshold. However, when looking more in detail at the correlation between subsurface criteria and economics, a transmissivity of $2.5 \cdot 10^{-12}$ m^3 is required to keep the Levelized Cost Of Heat (LCOH) below 200 CHF/MWh.

Additionally, a capacity of 25 MW or higher is needed for the HT-ATES system to become competitive with other large-scale DHN heat sources. The capacity increase from adding Heat Pumps (HP) incurs non-recoverable costs and increases the LCOH. Nonetheless, the addition of HP increases the nominal capacity of the system and results in higher cumulative avoided CO_2 emissions.

The project in Geneva is now finished, and new opportunities for HT storage in the region will be evaluated in the future.

The Bern project aimed to assess the feasibility and eventually implement an HT-ATES storage site to improve the efficiency of the Energiezentrale Forsthaus operated by Energie Wasser Bern (EWB) and contribute to the creation of an Energy Hub. A set of maximum 6 wells at a depth of 500m were planned to be drilled, with the first well serving as a test well for evaluating the reservoir performances. Wells will be distributed on a constellation geometry with one central well acting as the primary push-pull storage/recovery operations. Storage temperature is expected to range between 90-120˚C and recovery between 60-90˚C with circulation flow rates in the range of 25-60 l/s. The drilling site for the project is on the northwest corner of the Forsthaus energy hub.

The subsurface reservoir investigated at this site is the Cenozoic Molasse, where Individual layers of porous and permeable sandstones can take on the function of heat storage. A set of activities to characterize the subsurface was planned and carried out in Bern. Geologic analysis of outcrop reservoir analogs was performed to estimate the configuration of the sandstone layers; thermo-hydraulic models were computed to assess the thermal effect on the near-surface groundwater, and geochemical laboratory experiments were performed.

Modeling results revealed that after 20 years of permanent operation of the geothermal reservoir with 120˚C hot water, a heat plume appears along the natural groundwater flow direction. It has a maximum extension of about 40 m in the flow direction and about 10 m perpendicular to it. The maximum extension of the heat front with a temperature change of 3˚C and more is about 6 m in the flow direction and about 2 m perpendicular to it. Geochemical studies aimed at:

- Understanding which challenges might be encountered during the operation of the Geospeicher Forsthaus based on problems encountered in previous projects.
- Acquiring as much knowledge as possible about the geology and hydrogeology of the target formation (Lower Freshwater Molasse, USM) and the heterogeneity of the properties before drilling starts to judge if (a) the drill cores and groundwater compositions used during the experiments are representative for the USM and (b) find reasonable input values for different parameters to be included in the numerical simulations.
- Assessing potential mineral reactions at the site through experimental work by (a) investigating mineral reactions in the reservoir through core and batch experiments and (b) assessing the potential for carbonate scaling during heating of the formation fluid.
- Conducting numerical modeling simulations of the thermal-hydraulic-chemical (THC) processes expected to occur during the operation of the system to identify potential red flags before drilling starts
- The results of the geochemical study revealed no critical issues in operating an HT-ATES system. However, some cautionary issues have been identified, including:
- Generation of preferential flow paths between the main and supporting wells due to heterogeneous permeability of the sandstones. This could reduce the volume of rock swept by the injected hot water, lowering heat storage efficiency below previous expectations.
- Calcite precipitation is predicted to impact the evolution of the hydraulic performances of the reservoir, with regions clogged by calcite that may become barriers to the injection/extraction flow regimes, and regions of moderate calcite depletion may represent preferential flow paths leaving other regions of the reservoir unswept by the injected hot water.
- Extreme dissolution of calcite cement may induce local mechanical disintegration and compaction of the sandstones and mobilize fines that clog pore throats, reducing permeability and hence further lowering the efficiency of the water injection/extraction cycles.
- Microbes may form biofilms and clog the casings of the supporting wells, where temperatures are < 50 °C. Microbial activity is expected to diminish as the reservoir heats up to 90 °C.
- The evolving thermal plume and the water-rock reaction zone around the main well are predicted to remain within a 50 m radius from the well. However, the influence of the entire heat storage reservoir might be much larger. There is, therefore, a possibility that unwanted chemical compounds are transported over large distances.
- Significant carbonate scaling is expected in the surface installations during the heat-loading cycle. This could impede

The drilling operations were started in 2022.The results of the extensive exploration program conducted with three wells during phase 1 for the Geospeicher Forsthaus project allow the following general conclusions:

- The drilled interval in the USM sediments form ~240 – 520 m prove the existence of up to 15 m thick, laterally continuous and homogeneous fluvial sandstone layers, that are potential reservoir units for the heat storage project.
- These reservoir units are characterized by porosity and permeability values (plug measurements on plugs and first hydrotests) in a range that justify further hydrotesting. They are comparable to values known from other projects in the greater Bern area.

- The mineralogical composition and the geomechanical parameters measured in the sandstone units allow further stimulation measures, such as acidizing or radial drilling to enhance porosity and permeability.
- The data collected with the drilled well sections is adequate for building the next generation of 3D models to assess behavior of heat transfer and rock/water interactions during storage operations.
- The exploration program carried out in these first 3 wells shows that continuous and time-consuming coring can be replaced in the future partially by a high-tech wireline program (FMI, NMR etc.). The calibration of these tools for the Forsthaus project was possible with the acquired data.
- Drilling deviated and large diameter boreholes through the Quaternary section remains an operational challenge. This is related to the combination of conductive gravel layers and mobile clay layers.

Following the drilling phase, the reservoir was hydraulically developed via micro-side-tracks, and a series of hydraulic tests were conducted and evaluated, including cross-hole tests, staged pressure tests (hydraulic jacking), a long-term circulation experiment, and chemical stimulation via CO_2 acidization followed by backflushing.

It was determined that, in principle, the conditions required for a geothermal storage system are mostly met at Forsthaus Bern, except for sufficient permeability of the sandstone layers. The insufficient permeability is currently the showstopper. In contrast to Burgdorf, where the natural transmissivity of USM sandstone is one to two orders of magnitude higher and hence sufficient for heat storage, the sandstones at the ewb Forsthaus site have permeabilities below 600 mD and porosities below 22%.

In the USM, a sufficient number of sandstone layers and sufficient thick sandstone layers for a heat storage system were found at the drilled depth. Within these sandstone layers, there is a large heterogeneity of permeability and porosity in the vertical direction and a moderate heterogeneity in the horizontal direction. The one sandstone layer tested hydraulically has been proven to be hydraulically connected over a horizontal distance of more than 40 m. The hydraulic characterization, in accordance with geological considerations, indicates an anisotropic geometry of the sandstone layers with much greater extents in the direction of flow of the former rivers and limited widths.

The high vertical heterogeneity with sublayers within the sandstone layer is not a fundamental obstacle, but may facilitate stimulation measures, such as the injection of acids into more permeable sublayers or sand as a proppant along horizontal separation surfaces, that act as preferential flow paths. Based on the results and experience of the experiments carried out in 2024 and models calibrated with the data, the necessary procedures and technologies for improved stimulation and development measures can be further developed.

The investigations have shown that the sandstone layers of the USM are hydraulically extremely well insulated from the nearby Quaternary at the Bern Forsthaus site. Although the investigated layer at a depth of 485 m lies only about 250 m below the groundwater of the Quaternary sand, the model age of the formation water was dated to approx. 560,000 years with the ^{81}Kr analysis. The high salinity of about one third of seawater and a formation water pressure of minus 65 m below OK terrain are also clear indications of an extremely good insulation of the sandstone layers of the USM. This property makes the USM a very good host rock for underground storage facilities of all kinds, where it is important to isolate the storage contents hydraulically and chemically from the environment and the atmosphere in the very long term.

Although not studied in detail, the strain measurements with fiber optic cables along the F2 well show that the USM behaves largely deformable during the high-pressure step tests in F2. Induced seismicity therefore represents a very small risk as long as there are no major fault zones in the immediate vicinity. In fact, no micro-seismicity was measured during the injection test. This geomechanical behavior is in turn favorable because potential induced fractures will quickly close again. Conversely, suitable stimulation measures must be dimensioned for such behavior.

From a hydrochemical point of view, the precipitation of calcite and a high risk of iron hydroxides precipitation are to be expected in the surface facilities, but not within the reservoir itself. In addition, problems with corrosion could occur. From today's perspective, all potential hydrogeochemical problems are technically controllable with the use of inhibitors and suitable material selection. The extent to which such technical solutions dominate the profitability of a storage facility operation cannot be estimated at present.

The Bern pilot project demonstrates the potential and the challenges of geological heat storage in USM sandstones. The methods and results provide a valuable foundation for future storage systems across the Swiss Plateau. The USM sandstones offer favorable conditions for seasonal heat and other types of subsurface storage (e.g. CO_2).

The project confirmed that hydraulic connection, circulation, and chemical stimulation are technically feasible. However, the low permeability of fine- to medium-grained sandstones at the Forsthaus site remains a challenge and requires site-specific technical solutions. The technologies applied in Bern can and should be further developed to ensure scalability. Future efforts must also focus on cost reduction to ensure economic viability. Moreover, further investigations on a regional or even Molasse Basin wide scale are needed to obtain a more predictive understanding of the spatial distribution of USM reservoir properties.

All publicly accessible reports for the Geospeicher Forsthaus can be found here: assets.swissgeol.ch – Forsthaus Geospeicher

The original borehole data are available via the following links:

- Borehole Geospeicher Forsthaus 1 (GES-F1): https://boreholes.swissgeol.ch/49502/location
- Borehole Geospeicher Forsthaus 2:
  - GES-F2: https://boreholes.swissgeol.ch/49537/location
  - GES-F2A: https://boreholes.swissgeol.ch/49503/location
- Borehole Geospeicher Forsthaus 3:
  - GES-F3: https://boreholes.swissgeol.ch/49504/location

GES-F3A: https://boreholes.swissgeol.ch/49505/location

Environmental concerns are highly relevant in the perception, acceptance, and development of HT-ATES technologies. Identifying potential effects of HT-ATES systems is, therefore, necessary to optimize their design and ensure the operation's sustainability.

The most significant environmental effects brought about by HT-ATES utilization are 1) surface disturbances, 2) subsurface chemical and 3) physical effects, 4) noise, 5) thermal effects, and 6) emissions in both the atmosphere and in the subsurface. However, ATES systems can also positively affect the environment if considering the potential of reducing the CO2 intensity of heat supply. Previous studies focused on subsurface effects distinguishing between hydrogeological, thermal, chemical, and microbiological.

A set of potential effects related to subsurface, surface, and operations has been identified, described, and classified in terms of risk and opportunities according to the available data from field operations at the study sites.

For the Geneva areas, the focus is directed to the environmental effects identified by SIG as associated with the drilling operations, on the prediction of the water-rock interactions, hence on the effects on the reservoir water chemistry based on Thermo-Hydraulic-Chemical modeling and laboratory experiments, and of the ground deformation effects associated with production/injection cycles predicted via Thermo- Hydraulic-Mechanic modeling. Additionally, ground deformations and micro-seismicity have been monitored by SIG, revealing a quiet natural state for both criteria.

For the Bern site, information available provided by EWB includes the prediction of the water-minerals interaction at the Forsthaus site. Therefore, the focus will be limited to the potential effects on the reservoir water chemistry.

For Geneva, the fast-track assessment revealed that the risk of affecting the air, noise, groundwater, soil occupation, soil mechanics, wastes, nature, and seismicity is low to medium during drilling operations which are limited in time and decrease to low during operations. The water chemistry might be impacted only at the reservoir level but not on the shallow freshwater.

For the Bern project, the study about the prediction of water-rock processes leading to dissolution and precipitation at the reservoir scale revealed a likely occurrence but with limited impacts; therefore, this component has been classified as medium risk.

A spatial multi-criteria play-fairway framework allowed identifying those regions over the entire Swiss Molasse Plateau potentially suitable for HT-ATES in the Cenozoic Molasse and the Upper Mesozoic carbonates. The results show how the Cenozoic has some theoretical potential storage in the southern part of the Plateau, where some major cities are located (Zurich, Bern, Lausanne). According to the data available, fault structures in the Mesozoic can be suitable as targets in Aarau, Biel, and Geneva. However, as demonstrated by the GEo-01 well in Geneva, high permeabilities characterizing fault corridors lead to high wellhead pressure and natural artesian flow, therefore, a limiting factor for storage. A more detailed characterization of the hydraulic properties of the fault structures will be necessary for the future to calibrate such type of assessment.

The Swiss regulatory framework was analyzed to identify potential blockers and improvements to be implemented for HT-ATES applications. Thanks to the collaboration with the international partners, a comparison of existing regulatory frameworks for HT-ATES systems across several European countries revealed that the following key elements are necessary for the efficient development of HT-ATES projects

- Clearly and well-defined workflows between project developers and authorities
- Existing legal framework on a national level but implemented and adapted on a regional level through local competent authorities
- Well documented, up to date, and easily accessible public databases
- Long term development schemes (masterplans) on a regional level based on a global vision shared and driven by both the authorities and project developers

- Compulsory monitoring of production data (temperature, pressure, pH, water analyses, etc.) coupled with an appropriate history-matching process based on an iteratively updated 3D thermo-hydraulic model of the underground

The results of the entire project reveal the main subsurface challenges related to such fractured reservoirs, which are hydraulic heterogeneity and reservoir compartmentalization, requiring more detailed exploration surveys (i.e., 3D seismic) to identify those targets potentially suitable for storage correctly. Additionally, potential storage targets in Geneva should not be limited to the Mesozoic carbonates but could be in the Cenozoic sediments as well.

7 Outlook and next steps

The results of the project clearly reveal the great opportunities for HT-UTES, in particular HT-ATES in Switzerland, but also several challenges must be overcome before implementing in a sustainable way HT-UTES system.
First, an accurate understanding of the configuration of the energy system and the spatial and temporal distribution of excess heat and heat demand are the main priority to identify how HT-UTES systems can be integrated in complex energy systems where the different energy sources are often competing for the energy supply at defined temperature ranges and periods over the year.
To fit HT-UTES systems in the energy system it is important to define a merit order among energy sources not only based on the energy supply capacity but also on economic and environmental performances. In this case HT-UTES systems can play a major role being able to supply energy at economically viable conditions and with low or even beneficial environmental effects.
In addition, specifically with respect to HT-ATES, the accurate characterization, development, and management of the subsurface is the second main pillar that must be considered to an optimal implementation of storage solutions in aquifers. The integration of exploration data leading to the prediction storage/extraction performance constrained by energy data has been demonstrated in the project to be the optimal protocol to implement in the early stages of a project. The results will lead to the accurate wellbore design and drilling, reservoir testing operations that would follow. However, subsurface performances are always affected by the complex and heterogenous subsurface conditions, which, as demonstrated by the Geneva case-study, where the two exploration wells are not fully suitable for HT-ATES systems, therefore alternatives such as HT-BTES should be explored.
The combination of energy and subsurface elements leads to the possibility to assess the economic and environmental performances of a HT-ATES system, highlighting the benefits but also the risks associated with such project, hence support the decision-making process.
The spatial multi-criteria analysis allowed identifying potential favorable areas across the Swiss Plateau, but such regional screening must be applied at more local and project scales, and the applied framework in this project can has the great capability to be adapted to any scale of investigation and target user from project developers, public administration and research community.
Eventually, the need of a clear regulatory framework is a third priority to consider as the lack of it, might discourage project developers in moving from the early stages of a project towards the implementation and market uptake.

Some recommendation for further explore opportunities for HT-ATES in Switzerland are:

- Further explore the Mesozoic fault structures and the Karstified Upper Cretaceous with high resolution geophysical methods and field lab tests
- Consider the Cenozoic sedimentary cover as a potential target for both ATES and BTES solutions
- In situ tests of different smart control set-ups to define the charge/discharge/rest periods and the impact on energy efficiency

- Site analysis during drilling of the well to define well deviation to reach favorable geological conditions
- Compare geochemical site samples with previous laboratory analysis to establish at first order mineral precipitation and their impacts on borehole and surface installations
- Test different well configurations and see the impact on energy efficiency and analyse the impacts on the financial sustainability of the different solutions

8 National and international cooperation

The coordination of the HEATSTORE European consortium occurred on three levels: international consortium, national consortium, and individual partners.

On international consortium level, operational and technical progress was managed by the Executive Board/Project Management Team (EB-PMT) which consisted of the coordinator, the national leads from each country, and the WP leads (note, that 5 of the national leads were also WP lead). The EB-PMT meets regularly every 5-6 weeks or on request for a virtual meeting of 1.5 hours to discuss progress and challenges. Minutes including discussed matters and an action point list were prepared by the coordinator of each meeting.

National lead of the Swiss consortium partners is University of Geneva, Dr. Luca Guglielmetti (luca.guglielmetti@unige.ch).

The entire European consortium is composed by:

Organization	Country	Role
TNO	The Netherlands	Project Coordinator, WP6 lead
IF Technology B.V.	The Netherlands	Partner
KWR Water B.V.	The Netherlands	Partner
ECW Projects B.V.	The Netherlands	Partner
Netherlands Institute of Ecology	The Netherlands	Partner
University of Geneva	Switzerland	National Coordinator
Eidgenössische Technische Hochschule Zürich	Switzerland	Partner, WP2 lead
University of Neuchâtel	Switzerland	Partner
University of Bern	Switzerland	Partner
Services industriels de Geneve	Switzerland	Partner
Energie Wasser Bern	Switzerland	Partner
BRGM	France	Partner
Storengy	France	National Coordinator, WG5 lead
Fraunhofer IEG	Germany	National Coordinator, WP4 lead
Delta-h Engineering GmbH	Germany	Partner
The Geological Survey of Denmark and Greenland	Denmark	National Coordinator, WP1 lead
PlanEnergi	Denmark	Partner
VITO	Belgium	National Coordinator, WP3 lead
SPIE Belgium	Belgium	Partner

Kempens Warmtebedrijf	Belgium	Partner
University of the Azores	Pertugal	National Coordinator
Orkuveita Reykjavíkur SF	Iceland	National Coordinator
Universidad Politécnica de Cataluña	Spain	National Coordinator

In the framework of the European project, Swiss partners have been involved in several activities being WP and task leaders across all the 7 WPs composing the European project (Figure 130).

The European project was set-up on 7 work packages and the Swiss project on 6 work packages.

The correlation between the activities carried out is shown in Table 1.

Table 30 WP structure in the European and Swiss projects. The colours aim at showing the correlation between WPs and Task. For instance, WP4 of the European project corresponds to WP3 of the Swiss project

European Project		
WP1 - Specifications and characterization for UTES concepts	Task 1.1: Analysis of existing UTES projects: lessons learned	UniGe
	Task 1.2: General specification and design for UTES systems	-
	Task 1.3: Screening of national potential for UTES	**UniGe LEADER**, UniNe, UniBe, SIG, EWB
	Task 1.4: Best-practice guideline development for UTES	UniNe
WP2 - Models and tools for subsurface dynamics **ETHZ LEADER**	Task 2.1: Modelling toolsets and workflows for optimal and efficient HT-UTES of different types	ETHZ, UniGe, UniBe
	Task 2.2: Integrating advanced academic simulation codes into diverse geothermal project development workflows	ETHZ, UniGe, UniNe foe GENEVA
		UniBe, EWB for BERN
	Task 2.3: Benchmarking, and improving models of subsurface heat storage dynamics	UniBe, ETHZ
WP3 - Heating system integration and optimisation of desing and operation	Task 3.1 Characterization of existing DHC network / situation regarding (flexibility of) demand, supply and grid operation	-
	Task 3.2: Progressing Models and tools for system integration and optimization	UniGe for GENEVA
	Task 3.3: Design & execution of Business case model	UniGe
WP4 - Demostration and case studies: detailed design and implementation in practice	Task 4.1 Case study feasibility assessment and technical design for Demonstration	**EWB LEADER**, SIG, UniGe, UniNe, UniBe
	Task 4.2 Demonstrator realization & verification for Demonstration	UniGe, UniNe, UniBe, ETHZ, SIG, EWB
	Task 4.3 The Demonstrator synthesis & best practice guidelines for replication	UniGe, UniNe, UniBe, ETHZ, SIG, EWB
WP5 - Monitoring and valiradation to assess system performance and workflow	Task 5.1: Monitoring plan demonstrations and case studies	SIG, UniGe
	Task 5.2: Monitoring results	SIG, UniGe
	Task 5.3: Model validation for Subsurface dynamics	SIG, UniGe, UniNe, UniBe
	Task 5.4: Model validation for system integration and optimization	-
	Task 5.5: Uncertainty management	UniGe
WP6 - Fast-Track market uptake	Task 6.1 Technical future potential for smart heat systems with underground thermal energy storage in Europe	UniGe
	Task 6.2 Regulatory and policy boundary conditions	SIG
	Task 6.3 Evaluation of new business models for flexible energy systems with underground thermal energy storage in Europe	SIG, UniGe
	Task 6.4 Roadmap for flexible energy systems with underground thermal energy storage in Europe	-
	Task 6.5 Stakeholder engagement & dissemination	UniGe
	Task 6.6 Environmental impact	**UniGe LEADER**
WP7 - Project management		UniGe for Switzerland
Swiss Project		
WP1 - Subsurface modelling and well engineering optimisation for ATES implementation	Task 1.1 Specification and characterization for ATES concepts in Geneva	SIG, UniGe, UniNe
	Task 1.2 Design, Project Management & -Engineering in Bern	EWB, ETHZ, UniBe
	Task 5.1 Mapping technical potential and expansion in Switzerland	UniGe
WP2 - Models and tools for subsurface dynamics for optimal/efficient heat storage.	Task 2.1 Mineral reactions experiments using core samples	UniBe
	Task 2.2 1DTHC simulations	UniBe
	Task 2.3 3D THC simulations	UniBe
	Task 2.4 THM numerical model coupling if needed and 2D simulations	ETHZ
	Task 2.5 THM 3D simulations	ETHZ
	Task 2.6 Adaptation of academic THM code for professional use	ETHZ
	Task 2.7 Design and optimization of CSMP++ based reservoir simulation tools	ETHZ
	Task 2.8 Build initial reservoir model, model refinement	ETHZ
	Task 2.9 Geneva Pilot initial and updated scenario modeling	ETHZ
- Heating system integration design and optimization for future commercial implementa	Task 4.1 Progressing Models and tools for system integration and optimisation	UniGe, SIG
	Task 4.2 Design & execution of Business case model	UniGe, SIG
WP3 - Drilling, logging, in-situ & laboratory tests	Task 3.1 Drilling, logging, and laboratory tests in Geneva	SIG, UniGe, UniBe, UniNe
	Task 3.2 Heat Storage Tests (Bern-Forsthaus)	EWB, ETHZ, UniBe
WP5 - Fast-track market uptake and dissemination	Task 5.2 Definition of possible evolutions of the Swiss legal framework	SIG
	Task 5.3 Evaluation of new business models for ATES in Switzerland	UniGe, SIG
	Task 5.4 Roadmap development with national, international stakeholders	UniGe
WP6 - Project management	Task 5.5 Support for workshops and presentations	UniGe
	Task 6.1 Operation and budget management and quality control	UniGe

ETHZ was WP2 leader about Models and tools for subsurface dynamic, also leading Task 2.1 and 2.2. In this work package UniBe was T2.3 leader about benchmarking and improving model of subsurface heat storage dynamics

UniGe was T1.3 about Screening national potential for UTES and T6.6 leader about environmental effects of UTES

EWB was T4.1 leader about case-stud feasibility assessment and technical design for demonstration

SIG T6.2 leader about regulatory and policy boundary conditions

All the activities carried out by the Swiss partners contributed to the production of a set of deliverables, publications, and presentations at international conferences.

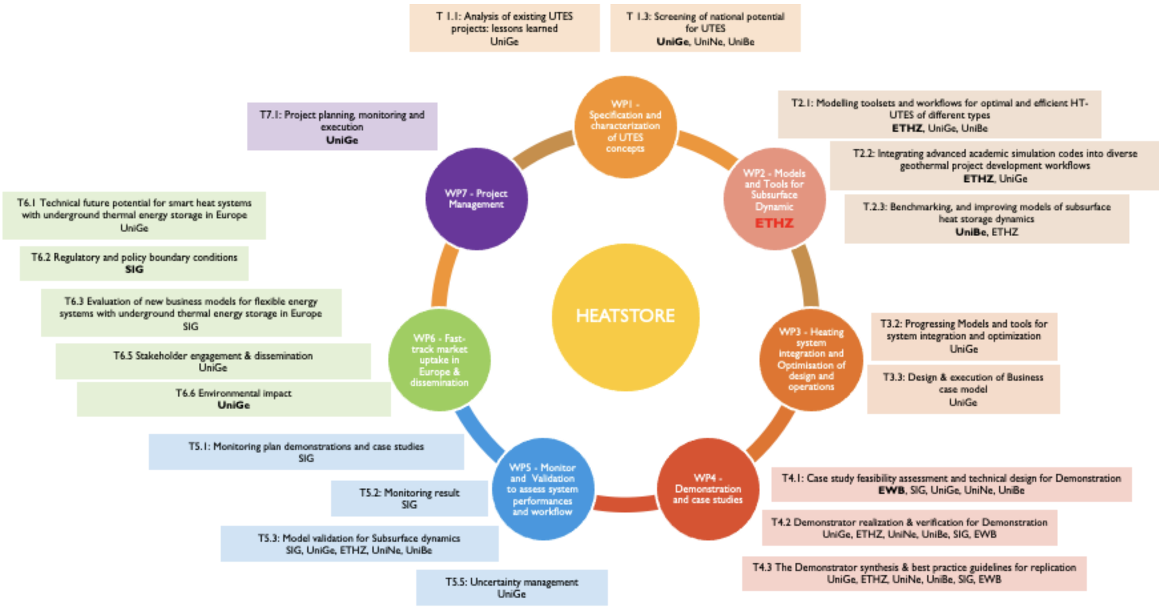

Figure 130 – Implications of the Swiss consortium in the European project

9 Publications

Peer-review journals

Birdsell, D. et al. (2021). Minimum transmissivity and optimal well spacing and flow rate for high-temperature aquifer thermal energy storage. Applied Energy 289. https://doi.org/10.1016/j.apenergy.2021.116658

Giardini, D., Gischig, V., Hertrich, M., Zappone, A., Wenning, Q., Guidati, G., Moscariello, A., Guglielmetti, L., Valley, B., Diamond, L., Lateltin, O., Baumberger, R., (2021). Eight years of geoenergy research in SCCER-SoE. Swiss Bulletin für angewandte Geologie. In press

Mindel, J. et al. (2021). Benchmark study of simulators for thermo-hydraulic modelling of low enthalpy geothermal processes. Geothermics 96. https://doi.org/10.1016/j.geothermics.2021.102130

Conference Proceedings

André M., Valley B., Sohrabi R. (2021). Characterization of fractured and karstified limestone reservoir for Aquifer Thermal Energy Storage (ATES). Swiss Geoscience Meeting 2021, Geneva, Switzerland.

Eruteya O., Guglielmetti L., Makhloufi Y., Moscariello A. (2020). 3-D Static Model to Characterize Geothermal Reservoirs for High-Temperature Aquifer Thermal Energy Storage (HT-ATES) in the Geneva Area, Switzerland. Proceedings World Geothermal Congress 2021, Reykjavik.

Ferreira De Oliveira G., De Haller A., Guglielmetti L., Makhloufi Y., Moscariello A. (2020). Application of Chemostratigraphy and Petrology to Characterize the Reservoirs of the Mesozoic Sequence Crossed by the Geo-01 Well: Potential for Direct Heat Production and Heat-Storage. Proceedings World Geothermal Congress 2021, Reykjavik.

Guglielmetti L., Alt-Epping P., Birdsell D., De Oliveira Filho F., Diamond L., Driesner T., Eruteya O., Hollmuller P., Makhloufi Y., Martin F., Meier P., Meyer M., Mindel J., Moscariello A., Nawratil De Bono C., Quiquerez L., Saar M., Sohrabi R., Spring U., Valley B., Van Den Heuvel D., Wanner C. (2020). HEATSTORE SWITZERLAND: New Opportunities of Geothermal District Heating Network Sustainable Growth by High Temperature Aquifer Thermal Energy Storage Development. Proceedings World Geothermal Congress 2021, Reykjavik.

Guglielmetti L., Eichinger F., Moscariello A (2020). Geochemical Characterization of Geothermal Waters Circulation in Carbonate Geothermal Reservoirs of the Geneva Basin (GB). Proceedings World Geothermal Congress 2021, Reykjavik.

Guglielmetti L., Eichinger F., Moscariello A. 2019. Geochemical Characterization of Deep Geothermal Waters Circulation in Carbonatic Geothermal Reservoirs of the Geneva Basin (GB). Proceedings 17th Swiss Geoscience Meeting. Fribourg. pp. 205.

Kallesoee, A.J., Vangkilde-Pedersen, T., Nielsen, J.E., Bakema, G., Egermann, P., Maragna, C., Hahn, F., Guglielmetti, L., Koornneef, J. (2020). HEATSTORE – Underground Thermal Energy Storage (UTES) – State of the Art, Example Cases and Lessons Learned. Proceedings World Geothermal Congress 2021, Reykjavik.

Koornneef, J., Guglielmetti, L., Hahn, F., Vangkilde-Pedersen, T., Aradottir, E.S., Allaerts, K., Viveiro, F., Saaltink, M. (2020). HEATSTORE Project Update: High Temperature Underground Thermal Energy Storage. Proceedings World Geothermal Congress 2021, Reykjavik.

Koumrouyan M., Sohrabi R., Valley B. (2019). Geomechanical characterisation of geothermal exploration borehole for Aquifer Thermal Energy Storage (ATES) development in Geneva, Switzerland. European Geothermal Congress 2019, Den Haag, The Netherland

Koumrouyan M., Sohrabi R., Valley B. (2019). Rock mechanics properties for fractured limestone hydrothermal system. SCCER-SoE Annual Conference 2019, Lausanne, Switzerland.

Milo A., Valley B., Sohrabi R. (2021). Thermo-Hydraulic behavior in fractured limestone for Aquifer Thermal Energy Storage (ATES). Swiss Geoscience Meeting 2021, Geneva, Switzerland.

Moscariello, A., Guglielmetti, L., Omodeo-Salé, S., De haller, A., Eruteya, O.-E., Lo, H.-Y., Clerc, N., Makhloufi, Y., Do Couto, D., Feereira de Oliveira, G., Perozzi, L., De Oliveira Filho, F., Hollmuller, P., Quiquerez, L., Nawratil de Bono, C., Martin, F., Meyer, M. (2020). Heat production and storage in Western Switzerland: advances and challenges of intense

multidisciplinary geothermal exploration activities, an 8 years progress report. Proceedings World Geothermal Congress 2021, Reykjavik.
Sohrabi R. & Valley B. (2021). Thermo-Hydraulic-Mechanical (THM) experiments and numerical simulations to quantify heat exchange characteristics of fractured limestone reservoir for Aquifer Thermal Energy Storage (ATES). World Geothermal Congress 2020+1, Reykjavik, Iceland.
Sohrabi R. & Valley B. (2018). Thermo-hydraulic testing for fractured rock mass for heat storage projects. SCCER-SoE Annual Conference 2018, Lucerne, Switzerland.
Valley B. & Miller S. M. (2021). Play-fairway analysis for deep geothermal resources in Switzerland. World Geothermal Congress 2020+1, Reykjavik, Iceland.

Thesis and Reports

Andre Ghapgou, M. M. (in prep.) Characterisation of fractured and karstified limestone reservoir for Aquifer Thermal Energy Storage (ATES). Master thesis, Centre for Hydrogeology and Geothermics (CHYN), University of.Neuchâtel, Neuchâtel.
Jaquet, Y. (in prep.) Groundwater modelling for heat storage project management. Master thesis, Centre for Hydrogeology and Geothermics (CHYN), University of.Neuchâtel, Neuchâtel.
Koumrouyan, M. (2019). Geomechanical Characterisation of Geothermal Exploration Borehole: Implication for the GEo-01 Well, in Geneva. M.Sc. thesis, Centre for Hydrogeoogy and Geothermics (CHYN), University of Neuchâtel, Neuchâtel.
Lo, H.Y. (2019). Discrete Fracture Network Modelling in the Geneva Basin (Lower Cretaceous Garbonates): Implication for Geothermal Exploration. MSc Thesis University of Neuchatel 136pp.
Milo, A. (in prep.) Thermo-hydraulic (TH) behavior in a fractured limestone reservoir. Master thesis, Centre for Hydrogeology and Geothermics (CHYN), University of.Neuchâtel, Neuchâtel.
Sohrabi R. & Valley B. (2018). Thermo-hydraulic well testing for characterization and management for heat storage projects. SCCER-SoE Annual Conference 2018, Lucerne, Switzerland.
Sohrabi R. & Valley B. (2019). Experimental Thermo-Hydro-Mechanical site to quantify heat exchange characteristics of fractured limestone aquifers. SCCER-SoE Annual Conference 2019, Lausanne, Switzerland.
Sohrabi R. & Valley B. (2021). Hydrogeological report for the RSBV boreholes, Concise (Vaud). Centre for Hydrogeology and Geothermics (CHYN), University of Neuchâtel, p.20.

HEATSTORE Europe reports

Kallesøe, A.J., et al. (2019). Underground Therma Energy Storage (UTES) – State-of-the-art, examples cases and lessons learned. GEOTHERMICA – ERA NET Cofund Geothermal, unpublished report. HEATSTORE project deliverable number D1.1, 130 pp.
Driesner et al. (2019). Initial report on tools and workflows for simulating subsurface dynamics of different types of High Temperature Underground Thermal Energy Storage. HEATSTORE D2.1, 143 pp.
Tómasdóttir, S., et al. (2019). Interim report on UTES-type/site-specific simulators based on academic/research codes. HEATSTORE project deliverable number D2.2, 55 pp.
Vanschoenwinkel, J., et al. (2019). Design and execution of business case models for the demonstration sites. ERA NET Cofund Geothermal, unpublished report. HEATSTORE project deliverable number D3.4, 41 pp + appendices
Hahn, F., et al. (2019). Monitoring plans: demonstration projects and case studies. ERA NET Cofund Geothermal, unpublished report. HEATSTORE project deliverable number D5.1, 29 pp
Hahn, F., et al. (2019). Feasibility assessment & design for demonstration projects – learnings of an international workshop. ERA NET Cofund Geothermal, unpublished report. HEATSTORE project deliverable number D4.1, 22 pp
Hahn, F., et al. (2019). Report on evaluation of new business models for flexible energy systems with UTES in Europe. ERA NET Cofund Geothermal, unpublished report. HEATSTORE project deliverable number D6.3, 103 pp
Cremer, H., et al. (2019). HEATSTORE Mid-term review report. 36pp

Alt-Epping, P., et al. (2020). Benchmarking and improving models of subsurface heat storage dynamics. GEOTHERMICA – ERA NET Cofund Geothermal, unpublished report. HEATSTORE project deliverable number D2.3, 104 pp

Guglielmetti, L., et al. (2021). Screening of national potential for UTES. GEOTHERMICA – ERA NET Cofund Geothermal, unpublished report. HEATSTORE project deliverable number D1.3, 89 pp

Hamm, V. et al. (2021). Synthesis of demonstrators and case studies - Best practice guidelines for UTES development. ERA NET Cofund Geothermal, unpublished report. HEATSTORE project deliverable number D1.4-D4.2-D4.3, 62 pp.

Driesner et al. (2021). Final report on tools and workflows for simulating subsurface dynamics of different types of High Temperature Underground Thermal Energy Storage. GEOTHERMICA – ERA NET Cofund Geothermal. HEATSTORE project deliverable number D2.1, 348 pp.

Allaerts, K. Et al. (2021). UTES and its integration in the heating system - Defining optimal design and operational strategies for the demonstration cases. ERA NET Cofund Geothermal, unpublished report. HEATSTORE project deliverable number D3.3, 95 pp.

Oerlemans, P., et al. (2021). Monitoring data availability of the UTES demonstration projects and case studies, status 2021. ERA NET Cofund Geothermal, unpublished report. HEATSTORE project deliverable number D5.2, 12 pp

Guglielmetti, L., et al. (2021). Monitoring results for the Geneva HT-ATES case-study. ERA NET Cofund Geothermal, unpublished report. HEATSTORE project deliverable number D5.2, 33 pp

Diaz-Maurin, F., et al. (2021). Model validation for subsurface dynamics. ERA NET Cofund Geothermal, unpublished report. HEATSTORE project deliverable number D5.3, 110 pp

Mirjolet, F., et al. (2021). Regulatory and policy boundary conditions for UTES. ERA NET Cofund Geothermal, unpublished report. HEATSTORE project deliverable number D6.3, 110 pp

Guglielmetti, L., et al. (2021). Environmental effects of UTES tehcnologies in Europe. GEOTHERMICA – ERA NET Cofund Geothermal, unpublished report. HEATSTORE project deliverable number D6.6, 120 pp

References

Alt-Epping, P., Mindel, J. (2020). HEATSTORE - Benchmarking and improving models of subsurface heat storage dynamics.
Altamimi Z, Métivier L, Collilieux X (2012). ITRF2008 plate motion model. J Geophys Res 117(B7) Andre Ghapgou MM (2021) Characterisation of fractured and karstified limestone reservoir for Aquifer Thermal Energy Storage (ATES). MSc thesis, Université de Neuchâtel
Attema E, Cafforio C, Gottwald M, Guccione P, Monti Guarnieri A, Rocca F (2010). Flexible dynamic block adaptive quantization for Sentinel-1 SAR missions. IEEE Geoscience and Remote Sensing Letters 7(4):766-770
Bear, J., Corapcioglu, M.Y., (1981). A mathematical model for consolidation in a thermoelastic aquifer due to hot water injection or pumping. Water Resour. Res. 17, 723–736. https://doi.org/10.1029/WR017I003P00723
Birdsell DT, Saar M.O., (2020). Modeling ground surface deformation at the Swiss HEATSTORE underground thermal energy storage sites. In: World geothermal congress. Reykjavik, Iceland: ETH Zurich, Institute of Geophysics; , p. 1–6. http://dx.doi.org/10.3929/ethz-b-000421353, Originally accepted at WGC 2020, which was postponed to 2021.
Blanton TL, Olson JE (1999) Stress Magnitudes from Logs: Effects of Tectonic Strains and Temperature. SPE Reserv Eval Eng 2:62–68. https://doi.org/10.2118/54653-PA Bleicher, V. (2007). Zukunft Erde, Energie heute und morgen – Ein Ausblick“
Burkhard Sanner, Frank Kabus, Peter Seibt and Jörn Bartels (2005): Underground Thermal Energy Storage for the German Parliament in Berlin, System Concept and Operational Experiences. Proceedings World Geothermal Congress 2005 Antalya, Turkey, 24-29 April
Sibbit B., Mc Clenahan D. (2005). Seasonal Borehole Thermal Energy Storage – Guidelines for design & construction, IEA-Solar Heating & Cooling TECH SHEET 45.B.3.1, page 1 of 15, April. Charollais, J., Wernli, R., Mastrangelo, B., Metzger, J., Granier, B., Martin, M. Saint, & Weidmann, M. (2013). Présentation d'une nouvelle carte géologique du Vuache et du Mont de Musièges. Archives Des Sciences, 66, pp.1–63.
Chelle-Michou, C., Do Couto, D., Moscariello, A., Renard, P., Rusillon, E. (2017). Geothermal state of the deep Western Alpine Molasse Basin, France-Switzerland. Geothermics, vol. 67, pp. 48-65
Clerc, N., Rusillon, E., Moscariello, A., Renard, P., Paolacci, S. and Meyer, M. (2015). Detailed structural and reservoir rock typing characterisation of the Greater Geneva Basin, Switzerland, for geothermal resource assessment. Proceedings of the World Geothermal Congress 2015, Melbourne, Australia, 19-25 April 2015.
Craigie, N. W. (2015). Applications of chemostratigraphy in Cretaceous sediments encountered in the North Central Rub’ al-Khali Basin, Saidi Arabia. Journal of African Earth Sciences, 104, pp. 27–42.
D. Mangold, T. Schmidt, Solites. The next Generations of Seasonal Thermal Energy Storage in Germany
D. Mangold, T. Schmidt, Solites. The next Generations of Seasonal Thermal Energy Storage in Germany
Danish Energy Agency (2014). Udredning vedrørende varmelagringsteknologier og store varmepumper til brug i fjernvarmesystemet
Danish Energy Agency, (2014). Status and recommendations for RD&D on energy storage technologies in a Danish context
DARTS (2021). Delft Advanced Research Terra Simulator (DARTS) [WWW Document]. URL https://darts.citg.tudelft.nl/
Davies, E. J., Ratcliffe, K. T., Montgomery, P., Pomar, L., Ellwood, B. B., & Wray, D. S. (2013). Magnetic susceptibility (X stratigraphy) and chemostratography applied to an isolated carbonate platform reef complex; Llucmajor Platform, Mallorca. SEPM Special Publication dedicated to the deposits, architecture and controls of carbonate margin, slope and basin systems.
De Oliveira Filho, L. Quiquerez, M. Ruegg, M. Monnard, B. Lachal and P. Hollmuller (2020). Évaluation quantitative de scénarios de développement du marché de la chaleur à Genève à

l’horizon 2050 : du fossile aux renouvelables, pistes pour décarboner le système thermique,” Technical report, Université de Genève.
De Zan F, Guarnieri AM (2006). TOPSAR: Terrain Observation by Progressive Scans. Geoscience and Remote Sensing, IEEE Transactions on 44(9)
Dincer, I. & Rosen, M., (2011). Thermal Energy Storage Case Studies. 2nd ed. s.l.:John Wiley & Sons, Ltd.
Driesner, T. et al., (2019). HEATSTORE - Initial report on tools and workflows for simulating subsurface dynamics of different types of High Temperature Underground Thermal Energy Storage. Zurich.
EASE/EERA (2017) Joint EASE-EERA Recommendations for a European Energy Storage Technology Development Roadmap Towards 2030.
Eltom, H., Abdullatif, O. M., Makkawi, M. H., & Eltoum, I. E. (2017). Rare earth element geochemistry of shallow carbonate outcropping strata in Saudi Arabia: Application for depositional environments prediction. Sedimentary Geology, 348, pp.51–68.
Eruteya O, Guglielmetti L, Moscariello A (2021). 3D geologic model of the GEo-01 well area. In: Project GECOS - Geothermal Energy Change of Success.
Evans K (1987) A Laboratory Study of Two Straddle-Packer Systems Under Simulated Hydrofrac Stress-Measurement Conditions. J Energy Resour Technol 109:180–190. https://doi.org/10.1115/1.3231345
Faessler, J., Lachal, B.M. (2017). Géothermie moyenne enthalpie avec valorisation dans les réseaux thermiques : Retours d’expérience sur trois installations et Proposition d’une grille d’analyse. Technical report, Université de Genève.
Fleuchaus, P. et al. (2020) S. Schüppler, M. Bloemendal, L. Guglielmetti, O. Opel and P. Blum, “Risk analysis of High-Temperature Aquifer Thermal Energy Storage (HT-ATES),” Renewable and Sustainable Energy Reviews, vol. 133, no. 110153, 2020.
Ganguly, S., Kumar, M.S.M., (2015). A numerical model for transient temperature distribution in an aquifer thermal energy storage system with multiple wells. Lowl. Technol. Int. 17, 179–188. https://doi.org/10.14247/LTI.17.3_179
Godet, A., Durlet, C., Spangenberg, J. E., and Föllmi, K. B. (2016). Estimating the impact of early diagenesis on isotope records in shallow-marine carbonates: A case study from the Urgonian Platform in western Swiss Jura. Palaeogeography, Palaeoclimatology, Palaeoecology; 454, pp. 125-138.
Gottlieb, P., Wilkie, G., Sutherland, D., Ho-Tun, E., Suthers, S., Perera, K., Jenkins, B., Spencer, S., Butcher, A., Rayner, J. (2000). Using quantitative electron microscopy for process mineralogy applications. Journal of the Minerals, Metals and Materials Society, 52(4), pp 24-25.
Guglielmetti L, Eichinger F, Moscariello A (2020). Geochemical Characterization of Geothermal Waters Circulation in Carbonatic Geothermal Reservoirs of the Geneva Basin (GB). In: World Geothermal Congress 2020. Reykjavik
Guglielmetti, L., Eichinger, F., Moscariello, A., (2020). Geochemical Characterization of Geothermal Waters Circulation in Carbonate Geothermal Reservoirs of the Geneva Basin (GB), in: Proceedings World Geothermal Congress 2020. Reykjavik, Iceland.
Haimson B, Cornet F (2003) ISRM Suggested Methods for rock stress estimation--Part 3: hydraulic fracturing (HF) and/or hydraulic testing of pre-existing fractures (HTPF). Int J Rock Mech Min Sci 40:1011–1020
Heat Roadmap Europe http://www.heatroadmap.eu/
HEATSTORE, “Underground Thermal Energy Storage (UTES) – state-of-the-art, example cases and lessons learned (2019). HEATSTORE project report,” A. J. Kallesøe and T. Vangkilde-Pedersen, Eds., GEOTHERMICA – ERA NET Cofund Geothermal p. 130 + Appendix.
Houlié N, Funning G, Bürgmann R (2016). Use of a GPS-derived troposphere model to improve InSAR deformation estimates in the San Gabriel Valley, California. Trans. Geosc. Rem. Sensing 54(9):5365-5374
Houlié N, Occhipinti G, Blanchard T, Shapiro N, Lognonne P, Murakami M (2011). New approach to detect seismic surface waves in 1Hz-sampled GPS time series. Sci Rep 1:44
Houlié N, Romanowicz B (2011). Asymmetric deformation across the San Francisco Bay Area faults from GPS observations in Northern California. Phys. Earth Planet. Inter. 184(3-4):143-153

Houlié N, Stern TA (2017). Vertical tectonics at an active continental margin. Earth Planet. Sc. Lett. 457:292-301

Houlié N, Woessner J, Giardini D, Rothacher M (2018). Lithosphere strain rate and stress field orientations near the Alpine arc in Switzerland. Sci. Rep. (8)

Hubbert MK, Willis DG (1957) Mechanics Of Hydraulic Fracturing

Huber, M.L., Perkins, R.A., Laesecke, A., Friend, D.G., Sengers, J. V., Assael, M.J., Metaxa, I.N., Vogel, E., Mareš, R., Miyagawa, K., (2009). New international formulation for the viscosity of H2 O. J. Phys. Chem. Ref. Data 38, 101–125. https://doi.org/10.1063/1.3088050

Ito T, Evans K, Kawai K, Hayashi K (1999) Hydraulic fracture reopening pressure and the estimation of maximum horizontal stress. Int J Rock Mech Min Sci 36:811–826

Jamshidi A, Zamanian H, Zarei Sahamieh R (2018) The Effect of Density and Porosity on the Correlation Between Uniaxial Compressive Strength and P-wave Velocity. Rock Mech Rock Eng 51:1279–1286. https://doi.org/10.1007/s00603-017-1379-8

Jarvis, K.E. (1988). Inductively coupled plasma mass spectrometry: A new technique for the rapid or ultra-trace level determination of the rare-earth elements in geological materials. Chemical Geology, 68, pp. 31-39.

Jenner G.A. Longerich, H.P., Jackson S.E. and Fryer B.J. (1990). ICP-MS A powerful tool for high-precision trace-element analysis in Earth sciences: Evidence from analysis of selected. Chemical Geology, 83, pp.133-148.

Jorgensen, N. O. (1986). Chemostartigraphy of Upper Cretaceous chalk in the Danish sub-basin. Bulletin of American Association of Petroleum Geologists, 70, pp. 309–317.

Kabus, F., Wolfgramm, M., Seibt, A., Richlak, U. and Beuster, H. (2009): Aquifer thermal energy storage in Neubrandenburg-monitoring throughout three years of regular operation, Proceedings of the 11th International Conference on Energy Storage.

Khait, M., Voskov, D., (2018). Operator-based linearization for efficient modeling of geothermal processes. Geothermics 74, 7–18. https://doi.org/10.1016/j.geothermics.2018.01.012

Kimball CV, Marzetta TL (1984) Semblance processing of borehole acoustic array data. Geophysics 49:274–281. https://doi.org/10.1190/1.1441659

Koumrouyan M (2019) Geomechanical characterisation of geothermal exploration borehole: implication for the GEo-01 well in Geneva. Msc thesis, Université de Neuchâtel

Lee, K. S., (2013). Underground Thermal Energy Storage, Green Energy and Technology, DOI: https://10.1007/978-1-4471- 4273-7_2

Lichte, H., (1988). Electron holography of atomic structures — Prospect and limitations, Physica B+C, 151, pp. 214-222.

Makhloufi, Y., Rusillon, E., Brentini, M., Moscariello, A., Meyer, M., & Samankassou, E. (2018). Dolomitization of the Upper Jurassic carbonate rocks in the Geneva Basin, Switzerland and France. Swiss Journal of Geosciences, 111(3), pp.475–500.

Mari J-L, Vergniault C (2018) Sismique en forage et diagraphies acoustiques, EDP open book

Mastrangelo, B., Charollais, J., Wernli, R., and Metzger, J. (2013). Accidents longitudinaux dans la Molasse rouge auct. et dans son substratum sur le versant oriental du Salève (Haute-Savoie, France). Swiss Journal of Geosciences, 106 (2), pp. 253–263.

Mesquita, J. et al. (2017). Drake Landing Solar Community: 10 Years of Operation. ISES Solar World Congress.

Mijnwater, B.V., (2015). Report on classification of district heating and cooling networks and control strategies. Deliverable D1.1 - HORIZON 2020 – STORM project (http://storm-dhc.eu/library/)

Mindel, J.E., Driesner, T., (2020). HEATSTORE: Preliminary Design of a High Temperature Aquifer Thermal Energy Storage (HT-ATES) System in Geneva Based on TH Simulations, in: Proceedings World Geothermal Congress 2020. pp. 1–12.

Moscariello, A. (2016). Geothermal exploration in SW Switzerland. European Geothermal Congress 2016, 9, Strasbourg, France.

Moscariello, A. et al. (2020). Heat production and storage in Western Switzerland: advances and challenges of intense multidisciplinary geothermal exploration activities, an 8 years progress report. World Geothermal Congress.

Moscariello, A., Guglielmetti, L., Omodeo-Salé, S., De Haller, A.,Eruteya, O.E., Lo, H.Y., Clerc, N., Makhloufi, Y., Do Couto, D., Ferreira De Oliveira, G., Perozzi, L., De Oliveira, F., Hollmuller, P., Quiquerez, L., Nawratil De Bono, C., Martin, F., Meyer, M. (2020). Heat production and storage in Western Switzerland: advances and challenges of intense multidisciplinary geothermal exploration activities, an 8 years progress report. Proceedings World Geothermal Congress, Reykjavik, Iceland, pp.12.

P. Østergaard, “Reviewing EnergyPLAN simulations and performance indicator applications in EnergyPLAN simulations,” Applied Energy, vol. 154, pp. 921-933, 2015.

Psimoulis P, Houlié N, Michel C, Meindl M, Rothacher M (2014) Long-period surface motion of the multi-patch Mw9.0 Tohoku-Oki earthquake. Geophys J Int. 199:968-980

QGIS Development Team (2009) QGIS Geographic Information System. In,

Quiquerez, L. (2017). “Décarboner le système énergétique à l'aide des réseaux de chaleur: état des lieux et scénarios prospectifs pour le canton de Genève. PhD theses, Université de Genève.

Quiquerez, L., De Oliveira Filho, F., Faÿ, S., Hollmuller, P., Meyer, M. (2020). Scenarios for integration of medium-depth geothermal energy in an evolving district heating system: case study in Geneva (Switzerland) in World Geothermal Congress

Quiquerez, L., Lachal, B. M., Monnard, M., Faessler, J. (2016). The role of district heating in achieving sustainable cities: comparative analysis of different heat scenarios for Geneva. 15th International Symposium on District Heating and Cooling.

Ratcliffe, K.T. Morton, A.C. Ritcey, D.H., Evenchick, C.A. (2007). Whole-rock geochemistry and heavy mineral analysis as petroleum exploration tools in the Bowser and Sustut basins, British Columbia, Canada. Bulletin of Canadian Petroleum Geology, 55 (4), 320–336.

Romera, J.J.G., (2020). Python library for IAPWS standard calculation of water and steam properties. https://doi.org/10.5281/ZENODO.3734292

Rosenbrand, E., Haugwitz, C., Jacobsen P.S.M., Kjøller, C. and Fabricius, I.L., (2014). The Effect of Hot Water Injection on Sandstone Permeability. Geothermics, 50, 155-166.

Rusillon, E. (2018). Characterisation and Rock Typing of Deep Geothermal Reservoirs in the Greater Geneva Basin. Terre & Environnement, 141, pp. 252

Rusillon, E., (2017). Characterisation and rock typing of deep geothermal reservoirs in the Greater Geneva Basin (Switzerland & France). University of Geneva, Geneva. https://doi.org/10.13097/archive-ouverte/unige:105286

Schlumberger (2002) Well test interpreatation

Schmitt DR, Currie CA, Zhang L (2012) Crustal stress determination from boreholes and rock cores: Fundamental principles. Tectonophysics 580:1–26. https://doi.org/10.1016/j.tecto.2012.08.029

Schout, G., et al. (2014). Analysis of recovery efficiency in high-temperature aquifer thermal energy storage: a Rayleigh-based method. Hydrogeology Journal (2014) 22: 281–291 DOI 10.1007/s10040-013-1050-8

Services Inddustriels de Geneve (2020). Projet SECURE, echantillonage GEo-02. Presentation IFPN Energie Nouvelles

Services Industriels de Geneve (2020). Rapport de fin sondage GEo-01. Unpiblished report, pp. 137-170

Sibbitt, B., McClenahan, D., Djebbar, R., Thornton, J., Wong, B., Carriere, J., & Kokko, J. (2012). The Performance of a High Solar Fraction Seasonal Storage District Heating System – Five Years of Operation. Energy Procedia, 30, 856–865. https://doi.org/10.1016/j.egypro.2012.11.097

Signer, C., & Gorin, G. (1995). New geological observations between the Jura and the Alps in the Geneva area, as derived from reflection seismic data. Eclogae Geol. Helv., 88/2, pp.235–265.

Soerensen, P.A., PlanEnergi et al. (2013) Boreholes in Brædstrup. Final Report

Thiercelin MJ, Plumb RA (1994) A Core-Based Prediction of Lithologic Stress Contrasts in East Texas Formations. SPE Form Eval 9:251–258. https://doi.org/10.2118/21847-PA

Todorov, O., Alanne, K., Virtanen, M., Kosonen, R. (2020). A method and analysis of aquifer thermal energy storage (ATES) system for district heating and cooling: A case study in Finland. Sustainable Cities and Society, vol. 53, p. 101977.

Valley B, Sohrabi R (2021) Geomechanical analyses of GEo-01 and GEo-02 explorationboreholes. Centre d’Hydrogéologie et de Géothermie, Université de Neuchâtel

Vangkilde-Pedersen, T., Nielsen, A.M. (2012). REGEOCITIES Deliverable 2.1: Denmark – National Report. Intelligent Energy Europe

Verhoeven, R., Eijdems, H., Wenmecker, M, Harcouet-Menou, V.: (2016). Update (Geo-) Thermal Smart Grid Mijnwater Heerlen, Proceedings European Geothermal Congress

Vishnevskaya, I., Letnikova, E., Pisareva, N., and Proshenkin, (2015). A chemostratigraphy of neoproterozoic carbonate deposits of the Tuva-Mongolian and Dzabkhan continental blocks: constraints on the age, glaciation and sedimentation. Chemostratigraphy: concepts, techniques and applications, 18, pp. 451–487.

Wang, Y., Voskov, D., Khait, M., Bruhn, D., (2020). An efficient numerical simulator for geothermal simulation: A benchmark study. Appl. Energy 264, 114693. https://doi.org/10.1016/j.apenergy.2020.114693

Wells DL, Coppersmith KJ (1994). New empirical relationships among magnitude, rupture length, rupture width, rupture area, and surface displacement. Bulletin of Seismological Society of America 84:974-1002

Willmes, Jens (2014). Nutzung von Grubenwasser zur Wärmeerzeugung – ein Projektbeispiel", bbr Sonderheft Geothermie

Zanoni, G., Šegvić, B. and Moscariello, A. (2016). Clay mineral diagenesis in Cretaceous clastic reservoirs from west African passive margins (the South Gabon Basin) and its impact on regional geology and basin evolution history. Applied Clay Science, 134, pp. 186-209.

Zoback MD, Barton CA, Brudy M, et al (2003) Determination of stress orientation and magnitude in deep wells. Int J Rock Mech Min Sci 40:1049–1076. https://doi.org/10.1016/j.ijrmms.2003.07.001

Appendix

1. Kallesøe, A.J., et al. (2019). *Underground Therma Energy Storage (UTES) – State-of-the-art, examples cases and lessons learned*. GEOTHERMICA – ERA NET Cofund Geothermal, unpublished report. HEATSTORE project deliverable number D1.1, 130 pp.
2. Makhloufi, Y., et al. (2021). *Mineralogical and petrophysical analysis of the GEo-01 and GEo02 cuttings*. Report n. GEG2021008. University of Geneva, 16pp.
3. Eruteya, O., et al. (2021). *3D static models of the GEo-01 and GEo-02 exploration wells*. Report n. GEG2021007. University of Geneva, 34pp.
4. Driesner et al. (2020). *Final report on tools and workflows for simulating subsurface dynamics of different types of High Temperature Underground Thermal Energy Storage.* GEOTHERMICA – ERA NET Cofund Geothermal. HEATSTORE project deliverable number D2.1, 348 pp.
5. Tómasdóttir, S., et al. (2019). Interim report on UTES-type/site-specific simulators based on academic/research codes. HEATSTORE project deliverable number D2.2, 55 pp.
6. Van den Heuvel, D., et al. (2021). *Assessing geochemical issues expected during High Temperature Aquifer Thermal Energy Storage (HT-ATES) in the Mesozoic limestones of the Geneva Basin*. University of Bern, 42 pp.
7. Van den Heuvel, D., et al. (2021). *Van den Heuvel, D., et al. (2021). Pre-study of the geological heat storage and utilisation project Geo- speicher Forsthaus (Bern): Geological and geochemical aspects*. University of Bern, 202 pp.
8. Klee, G. (2020). *Hydraulic fracturing stress measurements in borehole GEo-02. Activity Report including overview plots of test records.* . Solexperts Gmbh report, 8 pp.
9. Klee, G. (2020). *Hydraulic fracturing stress measurements in borehole GEo-02. Activity Report including overview plots of test records.* Solexperts Gmbh report, 36 pp.
10. El-Alfy, A. et al. (2021). *Geospeicher Forsthaus 1 (GES-F-1) – Well Summary. Geoenergie Suisse, 1 pp.*
11. Guglielmetti, L., et al. (2021). *Screening of national potential for UTES*. GEOTHERMICA – ERA NET Cofund Geothermal, unpublished report. HEATSTORE project deliverable number D1.3, 89 pp
12. Alt-Epping, P., et al. (2020). *Benchmarking and improving models of subsurface heat storage dynamics.* GEOTHERMICA – ERA NET Cofund Geothermal, unpublished report. HEATSTORE project deliverable number D2.3, 104 pp
13. Hahn, F., et al. (2019). *Feasibility assessment & design for demonstration projects – learnings of an international workshop*. ERA NET Cofund Geothermal, unpublished report. HEATSTORE project deliverable number D4.1, 22 pp
14. Hahn, F., et al. (2019). *Report on evaluation of new business models for flexible energy systems with UTES in Europe*. ERA NET Cofund Geothermal, unpublished report. HEATSTORE project deliverable number D6.3, 103 pp
15. Hahn, F., et al. (2019). *Monitoring plans: demonstration projects and case studies*. ERA NET Cofund Geothermal, unpublished report. HEATSTORE project deliverable number D5.1, 29 pp
16. Guglielmetti, L., et al. (2021). *Environmental effects of UTES tehcnologies in Europe.* GEOTHERMICA – ERA NET Cofund Geothermal, unpublished report. HEATSTORE project deliverable number D6.6, 120 pp
17. Hamm, V. et al. (2021). *Synthesis of demonstrators and case studies - Best practice guidelines for UTES development.* ERA NET Cofund Geothermal, unpublished report. HEATSTORE project deliverable number D6.3, 62 pp.
18. Allaerts, K. Et al. (2021). *UTES and its integration in the heating system - Defining optimal design and operational strategies for the demonstration cases.* ERA NET Cofund Geothermal, unpublished report. HEATSTORE project deliverable number D3.3, 95 pp.
19. Oerlemans, P., et al. (2021). *Monitoring data availability of the UTES demonstration projects and case studies, status 2021*. ERA NET Cofund Geothermal, unpublished report. HEATSTORE project deliverable number D5.2, 12 pp
20. Guglielmetti, L., et al. (2021). *Monitoring results for the Geneva HT-ATES case-study.* ERA NET Cofund Geothermal, unpublished report. HEATSTORE project deliverable number D5.2, 33 pp
21. Diaz-Maurin, F., et al. (2021). *Model validation for subsurface dynamics.* ERA NET Cofund Geothermal, unpublished report. HEATSTORE project deliverable number D5.3, 110 pp
22. Mirjolet, F., et al. (2021). *Regulatory and policy boundary conditions for UTES*. ERA NET Cofund Geothermal, unpublished report. HEATSTORE project deliverable number D6.3, 110 pp
23. Cremer, H., et al. (2019). *HEATSTORE Mid-term review report*. 36pp
24. Guglielmetti, L. et al. (2020). *Swiss Consortium mid-term review*. 24pp
25. Guglielmetti et al. (2020). *HEATSTORE YEAR2 Meeting.* 31pp
26. Swiss Consortium (2019). *YEAR 1 report and annexes*
27. Swiss Consortium (2020). *YEAR 2 report and annexes*
28. Rapport hydrogéologique Commune de Concise (VD)